Genomics-driven and biochemical approaches to expand the spectrum of natural products

Genomikgestützte und biochemische Ansätze zur Erweiterung des Spektrums natürlicher Produkte

DISSERTATION

zur

Erlangung des Doktorgrades

der Naturwissenschaften

(Dr. rer. nat.)

dem Fachbereich Pharmazie

der Philipps-Universität Marburg

vorgelegt von

Wen Li

aus Zhumadian, China

Marburg/Lahn, 2023

Erstgutachter: **Prof. Dr. Shu-Ming Li**

Zweitgutachter: **Prof. Dr. Raphael Reher**

Eingereicht am 14. August 2023

Tag der mündlichen Prüfung: 13. Oktober 2023

Hochschulkennziffer: 1180

Dedicated to my family

Table of contents

List of publications

Wen Li, Jie Fan, Ge Liao, Wen-Bing Yin and Shu-Ming Li (2021) Precursor supply increases the accumulation of 4-hydroxy-6-(4-hydroxyphenyl)-α-pyrone after NRPS-PKS gene expression. *Journal of Natural Products*, 84, 2380-2384, DOI: 10.1021/acs.jnatprod.1c00120.

Wen Li, Lindsay Coby, Jing Zhou and Shu-Ming Li (2023) Diprenylated cyclodipeptide production by changing the prenylation sequence of the nature´s synthetic machinery. *Applied Microbiology and Biotechnology*, 107, 261–271, DOI: 10.1007/s00253-022-12303-4.

Wen Li, Xiulan Xie, Jing Liu, Huili Yu and Shu-Ming Li (2023) Prenylation of dimeric *cyclo*-L-Trp-L-Trp by the promiscuous *cyclo*-L-Trp-L-Ala prenyltransferase EchPT1. *Applied Microbiology and Biotechnology*, (submitted).

Erklärung zum Eigenanteil

Titel der Publikation und **Journal incl. Jahr, Heft, Seitenzahl + doi** **O: Originalarbeit** **Ü: Übersichtartikel/Review**	Autoren	geschätzter Eigenanteil in %	Datum: ange-nommen	Datum: eingereicht
Precursor supply increases the accumulation of 4-hydroxy-6-(4-hydroxyphenyl)-α-pyrone after NRPS-PKS gene expression. *Journal of Natural Products,* 2021, 84, 2380-2384 DOI: 10.1021/acs.jnatprod.1c00120 Originalarbeit	**Wen Li**, Jie Fan, Ge Liao, Wen-Bing Yin, and Shu-Ming Li	55	9 July, 2021	3 February, 2021
Diprenylated cyclodipeptide production by changing the prenylation sequence of the nature´s synthetic machinery. *Applied Microbiology and Biotechnology*, 2023, 107, 261–271. DOI: 10.1007/s00253-022-12303-4. Originalarbeit	**Wen Li**, Lindsay Coby, Jing Zhou, and Shu-Ming Li	65	18 November, 2022	04 August, 2022
Prenylation of dimeric *cyclo*-L-Trp-L-Trp by the promiscuous *cyclo*-L-Trp-L-Ala prenyltransferase EchPT1. *Applied Microbiology and Biotechnology* Originalarbeit	**Wen Li**, Xiulan Xie, Jing Liu, Huili Yu, and Shu-Ming Li	60		05 May, 2023

---------------------------------   --------------------------------------

   Kandidat(in)   **Unterschrift Betreuer(in)**

V

Academic activities

Wen Li, Jie Fan, Ge Liao, Wen-Bing Yin, and Shu-Ming Li

A nonribosomal peptide synthetase-polyketide synthase hybrid enzyme is responsible for the formation of an α-pyrone derivative

Poster presentation, annual meeting of the German Pharmaceutical Society (DPhG), 30th September 2021, Leipzig (online)

Abbreviations

The international system of units and units derived thereof have been used.

$[M + H]^+$	molecular ion plus hydrogen
$\times$ g	gravitational acceleration
6-DMATS$_{Sa}$	6-dimethylallyl tryptophan synthase from *Streptomyces ambofaciens*
7-DMATS	7-dimethylallyl tryptophan synthase
A domain	A domain
A. fumigatus	*Aspergillus fumigatus*
A. nidulans	*Aspergillus nidulans*
A. niger	*Aspergillu niger*
A. oryzae	*Aspergillus oryzae*
A. ruber	*Aspergillus ruber*
aa	amino acid
aa-tRNA	aminoacyl-tRNA
ACP domain	acyl carrier protein domain
AT domain	acyltransferase domain
BGC	biosynthetic gene cluster
BLAST	basic local alignment search tool
bp	base pair
br	broad (NMR signal)
C domain	condensation domain
CDCl$_3$	deuterated chloroform
CDP	cyclodipeptide
CDPS	cyclodipeptide synthase
CoA	coenzyme A
COSY	correlation spectroscopy
cWA	*cyclo*-L-Trp-L-Ala
cWL	*cyclo*-L-Trp-L-Leu
cWP	*cyclo*-L-Trp-L-Pro
cWW	*cyclo*-L-Trp-L-Trp

d	Doublet
dd	double doublet
DH domain	β-hydroxyacyl-thioester dehydratase domain
DKP	diketopiperazine
DMAPP	dimethylallyl diphosphate
DMATS	dimethylallyl tryptophan synthase
DMSO-*d6*	deuterated dimethyl sulfoxide
DNA	deoxyribonucleic acid
dq	double quartet
dt	double triplet
E. coli	*Escherichia coli*
e.g.	exempli gratia
EIC	extracted ion chromatogram
ER domain	enoyl reductase domain
ETP	epipolythiodioxopiperazine
FPP	farnesyl diphosphate
gDNA	genomic DNA
GGPP	geranylgeranyl diphosphate
GPP	geranyl diphosphate
His_6	hexahistidine
His_8	octahistidine
HMBC	heteronuclear multiple bond correlation
HPLC	high performance liquid chromatography
Hz	Hertz
i.e.	id est
IPP	isopentenyl diphosphate
IPTG	isopropyl β-D-thiogalactopyranoside
k_{cat}	turnover number
kDa	kilo dalton
K_M	Michaelis-Menten constant
KR domain	β-ketoacyl-ACP reductase domain
KS domain	β-ketoacyl-ACP synthase domain

LC-MS	liquid chromatography-mass spectrometry
m	Multiplet
m/z	mass-to-charge ratio
MAT domain	malonyl-CoA-ACP transacylase domain
mAU	Milli absorbance unit
MEP	methylerythritol phosphate
MS	mass spectrometry
MT	methyltransferase
MT domain	methyltransferase domain
MVA	mevalonate acid
multi	multiplicity
N. fischeri	*Neosartorya fischeri*
NADH	nicotinamide adenine dinucleotide (reduced form)
NADPH	nicotinamide adenine dinucleotide phosphate (reduced form)
Ni-NTA	nickel-nitrilotriacetic acid
nm	nanometer
NMR	nuclear magnetic resonance
NOESY	nuclear overhauser effect spectroscopy
NP	natural product
NRP	nonribosomal peptide
NRP-PK	nonribosomal peptide-polyketide
NRPS	nonribosomal peptide synthetase
NRPS-PKS	nonribosomal peptide synthetase-polyketide synthase
A_{600}	absorption at 600 nm
P. crustosum	*Penicillium crustosum*
P_{450}	cytochrome P450
PCP domain	peptidyl carrier protein domain
PEG	polyethylene glycol
PHBA	*para*-hydroxybenzoic acid
PK	polyketide
PK-NRP	polyketide-nonribosomal peptide
PKS	polyketide synthase

PKS-NRPS	polyketide synthase-nonribosomal peptide synthetase
PPi	inorganic pyrophosphate
PT	prenyltransferase
R domain	reductase domain
rpm	revolutions per minute
s	Singlet
S. cerevisiae	*Saccharomyces cerevisiae*
S. coelicolor	*Streptomyces coelicolor*
S. lividans	*Streptomyces lividans*
S. albus	*Streptomyces albus*
SAM	S-adenosyl-L-methionine
SDS-PAGE	sodium dodecyl sulfate polyacrylamide gel electrophoresis
SM	secondary metabolite
t	Triple
T domain	thiolation domain
TB	terrific broth
TC	terpene cyclase
TE domain	thioesterase domain
Tris	tris (hydroxymethyl) aminomethane
UV	ultraviolet
UV-Vis	ultraviolet-visible
v/v	volume per volume
δ_C	chemical shift of carbon
δ_H	chemical shift of proton

Summary

Natural products (NPs) derived from secondary metabolism of living organisms play a pivotal role in drug discovery, especially for the treatment of cancer and infectious diseases. Their versatile skeletons are synthesized by different biosynthetic enzymes including polyketide synthases (PKSs), nonribosomal peptide synthetases (NRPSs), terpene cyclases, and hybrid enzymes. Further modifications by tailoring enzymes such as oxidoreductases, cytochrome P450 enzymes, and prenyltransferases (PTs) increase the structural diversity and improve their biological and pharmacological activities. With the advances in genome sequencing and analytical technologies, many strategies have been applied for exploring the promising categories for drug discovery. Due to low or no expression of the majority of biosynthetic gene clusters (BGCs) in the native genomes, it is of great significance to activate such promiscuous BGCs for new drug leads. In recent years, genome mining of novel BGCs has achieved significant progress in NP discovery.

In addition to secondary metabolite (SM) exploration in microorganisms, the substrate-based enzymatic reactions have also been proven to be a useful tool for enriching the chemical database. The members of dimethylallyl tryptophan synthase (DMATS) superfamily as important biocatalysts were widely used for structural modification of diverse small molecules. Vast of new prenylated structures have been obtained through chemoenzymatic synthesis. In this thesis, we identified an α-pyrone derivative by genome mining of a NRPS-PKS gene in *Penicillium crustosum* and obtained a series of prenylated cyclodipeptide (CDP) analogs through chemoenzymatic synthesis of different DMATSs.

In the first project, a novel NRPS-PKS hybrid gene *pcr10109* from *Penicillium crustosum* PRB-2 was chosen for detailed investigation by Dr. Jie Fan. She cloned the gene into the expression vector for heterologous expression in *Aspergillus nidulans*. Analysis of the SMs and structure elucidation proved its responsibility for 4-hydroxy-6-(4-hydroxyphenyl)-2*H*-pyran-2-one production. Further isotopic feeding experiments revealed its biosynthetic pathway. *Para*-hydroxybenzoic acid (PHBA) as the precursor and two acetate molecules are assembled for final product formation. To increase the product yield, we fed PHBA in the cultures and the product yield reached a maximum of 51 mg/kg rice culture, which is five-fold higher than that obtained without feeding. This provides another method to increase product formation by supplementing of special substrates.

SUMMARY

In the second project, we mainly focused on the production of diprenylated *cyclo*-L-Trp-L-Pro (cWP). At first, we intended to follow the nature′s biosynthetic machinery by utilizing *C2*-PT EchPT1 as the first biocatalyst. However, the *C2*-prenylated cWP could not be accepted by *C4*-, *C5*-, *C6*-, and *C7*-PTs for further prenylation. Dr. Lindsay Coby found that the *C2*-PT EchPT1 can also catalyze prenylations of monoprenylated cyclodipeptides. Then we changed the strategy and firstly obtained the *C4*-, *C5*-, *C6*-, *C7*-monoprenylated cWP in high product yields. After that, the monoprenylated derivatives were incubated with EchPT1 for the reverse *C2*-prenylation. Large scale enzyme assays and NMR analysis proved the products to be *C2,C4*-, *C2,C5*-, *N1,C6*-, and *C2,C7*-diprenylated cWP. This is the first report that EchPT1 can also catalyze the prenylation at the N1 position of the indole ring.

In the third project, a similar method was used for the production of prenylated tryptophan-containing dimeric CDPs. We chose different dimeric CDPs and PTs for the enzyme activity test. *cyclo*-L-Trp-L-Trp (cWW) dimers tetratryptomycins A − C were well accepted by EchPT1 in the presence of DMAPP. Tetratryptomycins A and C are better substrates of EchPT1 for prenylation compared with tetratryptomycin B. Compound isolation and NMR analysis determined the products as *C2*- (and *C2′*-) prenylated tetratryptomycins, which is consistent with EchPT1-catalyzed reactions. Further kinetic parameter determination revealed that the values are in the range of EchPT1-catalyzed reactions toward most CDPs.

Zusammenfassung

Naturstoffe (NP), die aus dem Sekundärstoffwechsel lebender Organismen stammen, spielen eine zentrale Rolle bei der Entdeckung von Arzneimitteln, insbesondere solche zur Behandlung von Krebs und Infektionskrankheiten. Ihr vielseitiges Gerüst wird von verschiedenen Biosyntheseenzymen rekonstruiert, darunter Polyketidsynthasen (PKSs), nichtribosomale Peptidsynthetasen (NRPSs), Terpencyclasen und Hybridenzyme. Weitere Modifikationen durch Enzyme wie Oxidoreduktasen, Cytochrom-P450-Enzyme und Prenyltransferasen (PTs) erhöhen die strukturelle Vielfalt und verbessern ihre biologischen und pharmakologischen Aktivitäten. Mit den Fortschritten bei der Genomsequenzierung und den Analysetechnologien wurden viele Strategien angewandt, um die vielversprechenden Kategorien für die Arzneimittelentdeckung zu erforschen. Da die meisten biosynthetischen Gencluster (BGCs) in den Genomen nur schwach oder gar nicht exprimiert sind, ist es von großer Bedeutung, solche promiskuitiven BGCs für die Suche nach neuen Wirkstoffkandidaten zu aktivieren. In den letzten Jahren hat das Genom-Mining neuartiger BGCs erhebliche Fortschritte bei der Entdeckung von NPs ermöglicht. Neben der Erforschung von Sekundärmetaboliten (SMs) in Mikroorganismen haben sich auch die substratbasierten enzymatischen Reaktionen als nützliches Instrument zur Erweiterung der chemischen Datenbank erwiesen. Die Mitglieder der Dimethylallyl-Tryptophan-Synthase (DMATS)-Superfamilie wurden als wichtige Biokatalysatoren in großem Umfang zur strukturellen Veränderung verschiedener niedermolekularer Moleküle eingesetzt. Zahlreiche neue prenylierte Strukturen wurden durch chemoenzymatische Synthese gewonnen. In dieser Arbeit haben wir ein α-Pyron-Derivat durch Genom-Mining eines NRPS-PKS-Gens in *Penicillium crustosum* identifiziert und eine Reihe von prenylierten Cyclodipeptid (CDP)-Analoga durch chemoenzymatische Synthese verschiedener DMATSs erhalten.

Im ersten Projekt wurde ein neuartiges NRPS-PKS-Hybridgen *pcr10109* aus *Penicillium crustosum* PRB-2 von Dr. Jie Fan für eine eingehende Untersuchung ausgewählt. Sie klonierte das Gen in den Expressionsvektor für die heterologe Expression in *Aspergillus nidulans*. Die Analyse der SMs und die Strukturaufklärung bewiesen, dass das Gen für die Produktion von 4-Hydroxy-6-(4-hydroxyphenyl)-2H-pyran-2-on verantwortlich ist. Weitere Isotopenfütterungsexperimente enthüllten den Biosyntheseweg. *para*-Hydroxybenzoesäure (PHBA) als Vorstufe und zwei Acetatmoleküle werden zur Bildung des Endprodukts zusammengesetzt. Um die Produktausbeute zu erhöhen, fütterten wir die Kulturen mit PHBA,

und die Produktausbeute erreichte ein Maximum von 51 mg/kg Reiskultur, was fünfmal höher ist als die ohne Fütterung. Dies ist eine weitere Möglichkeit, die Produktbildung durch die Zugabe spezieller Substrate zu erhöhen.

Im zweiten Projekt konzentrierten wir uns hauptsächlich auf die Produktion von diprenyliertem *cyclo*-L-Trp-L-Pro (cWP). Zunächst wollten wir der natürlichen Biosynthesemaschinerie folgen, indem wir die *C2*-PT EchPT1 als ersten Biokatalysator einsetzten. Das *C2*-prenylierte cWP konnte jedoch nicht von *C4*-, *C5*-, *C6*-, und *C7*-PTs zur weiteren Prenylierung akzeptiert werden. Dr. Lindsay Coby fand heraus, dass der *C2*-PT EchPT1 auch die Prenylierungen von monoprenylierten Cyclodipeptiden katalysieren kann. Dann haben wir unsere Strategie geändert und zunächst das *C4*-, *C5*-, *C6*-, *C7*-monoprenylierte cWP in hoher Produktausbeute erhalten. Anschließend wurden die monoprenylierten Derivate mit EchPT1 für die reverse *C2*-Prenylierung inkubiert. Enzymtests im großen Maßstab und NMR-Analysen zeigten, dass es sich bei den Produkten um *C2,C4*-, *C2,C5*-, *N1,C6*-, und *C2,C7*-diprenylierte cWP handelt. Dies ist der erste Bericht, dass EchPT1auch die Prenylierung an der N1-Position des Indolrings katalysieren kann.

Im dritten Projekt wurde eine ähnliche Methode für die Bildung von prenylierten Tryptophan-haltigen dimeren CDPs verwendet. Wir wählten verschiedene dimere CDPs und PTs für den Enzymaktivitätstest. Interessanterweise konnten nur die *cyclo*-L-Trp-L-Trp (cWW)-Dimere Tetratryptomycine A − C von EchPT1 in Gegenwart von DMAPP gut akzeptiert werden. Tetratryptomycine A und C sind, verglichen mit Tetratryptomycin B, bessere Substrate für die Prenylierung durch EchPT1. Die Isolierung der Verbindungen und die NMR-Analyse ergaben, dass es sich bei den Produkten um *C2*- (und *C2'*-) prenylierte Tetratryptomycine handelt, was mit EchPT1-katalysierten Reaktionen übereinstimmt. Die weitere Bestimmung der kinetischen Parameter ergab, dass die Werte im Bereich der EchPT1-katalysierten Reaktionen für die meisten CDPs liegen.

1 Introduction

1.1 Diversity of natural products for drug discovery

Natural products (NPs) are highly valuable small molecules derived from widely distributed living organisms.[1-3] They are also known as secondary metabolites (SMs) which are not essential for survival, development and reproduction, but play key roles in defense and cell to cell communication.[4,5] Unlike primary metabolites which are required for growth and are mostly the same across the spectrum of living organisms, SMs vary widely from species to species and encompass a diverse array of complex chemical structures.[6] They exhibit broad range of functions during cell development, such as stress prevention, predation defense, competitiveness, communications, pathogenicity and exposure of other organisms.[7-9]

With the advances in compound isolation and characterization, millions of NPs have been discovered mainly from microorganisms, plants, and animals.[10] Approximately 70 % of them were isolated from plants according to the *Dictionary of Natural Products*, which are higher than that originated from other organisms.[4,11] This can be dated back to the medicinal herbs, which are the first well-studied natural substance sources. For example, morphine was already isolated in 1817. Discovery of the first antibiotic penicillin G from *Penicillium* by Alexander Fleming in 1928 led to an era of NP discovery from microbial sources.[12,13] Numerous novel structures with biological activities have been identified from the typical members over the last decades, such as actinobacteria and filamentous fungi.[14-16] In the history, Natural drugs have been used as agents since thousands of years and still as the most important source of new potential therapeutic drugs.[17]

Normally, NPs are products of secondary metabolism and use a small number of primary metabolism precursors such as acetyl-CoA, malonyl-CoA, pyruvate and amino acids.[18] Differing from the primary metabolites (carbohydrates, proteins, nucleosides, and fats), SMs encompass a diverse array of complex chemical structures (**Figure 1**).[19,20] According to the structural diversity, NPs can be mainly classified into four categories, *i.e.*, polyketides (PKs), peptides including nonribosomal peptides (NRPs), terpenoids, and alkaloids (**Figure 2**). Besides, there are also hybrid molecules like terpenoid-polyketides, polyketide-nonribosomal peptides (PK-NRPs), and nonribosomal peptide-polyketides (NRP-PKs).
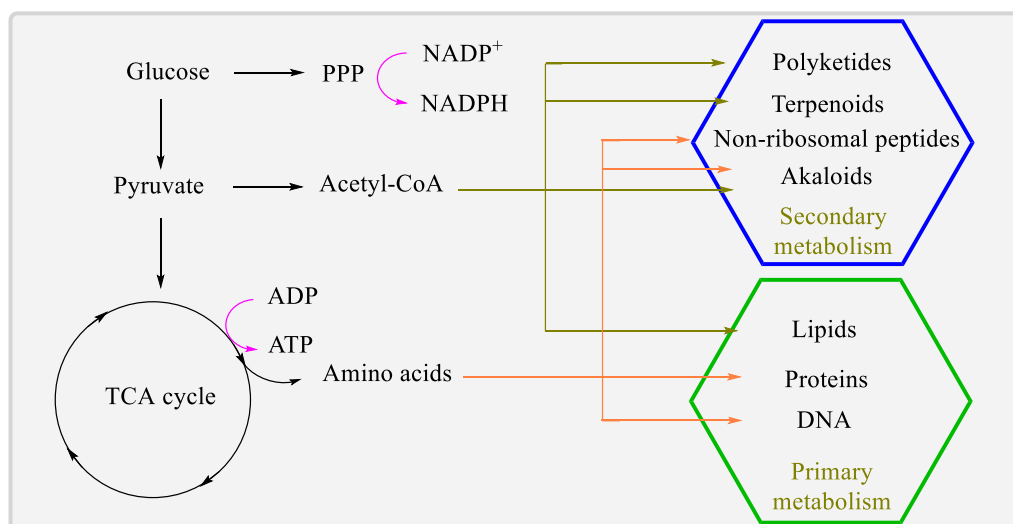
Figure 1. A simple scheme of the connection between primary and secondary metabolism. PPP, pentose phosphate pathway; TCA, tricarboxylic acid.

PKs are a large group of NPs with wide spectrum of biological and pharmacological activities.[21,22] They are produced by bacteria, fungi, plants, and certain marine organisms.[22,23] These compounds often exhibit highly structural diversity, such as macrolides, aromatics and polyenes.[24] Representative PKs from bacteria are macrolide erythromycin obtained from *Saccharopolyspora erythraea*,[25] tetracycline isolated from *Streptomyces aureofaciens*,[26] and rifamycin B from *Streptomyces mediterranei*[27] as well as geldanamycin produced by *Streptomyces hygroscopicus*.[28] They are all antibiotics used clinically. In the meantime, PKs originated from fungi also show strong toxic and some are of pharmacological relevance.[29-31] Aflatoxin B1 is a carcinogenic mycotoxin produced by *Aspergillus flavus*.[32] Lovastatin isolated from *Aspergillus terreus* is used as a blood cholesterol lowing agent.[33,34] Naringenin, which was isolated from plants, has significant antioxidant properties (**Figure 2**).[35]

NRPs belong to another important group of NPs, which are also found in various bacteria and fungi.[36-39] Cyclosporin A, featured with one D-configured alanine and two nonproteinogenic residues, is an immunosuppressant from *Tolypocladium inflatum*.[40] Daptomycin is a cyclic lipopeptide antibiotic produced by *Streptomyces roseosporus* and used in the treatment of systemic and life-threatening infections caused by Gram-positive bacteria.[41,42] Penicillin G from *Penicillium* sp. was the first natural antibiotic, which has been applied to the treatment of bacterial infections.[39,43] Head-to-tail-cyclized peptides enniatin B from *Fusarium* fungi is a mycotoxin with antibacterial, antihelmintic, antifungal, herbicidal, and insecticidal activities.[44] Brevianamide F, a tryptophan-containing cyclodipeptide (CDP) with a 2,5-diketopiperazine

(DKP), is produced by *Aspergillus fumigatus* and has been proved against cardiovascular dysfunction and cognitive disorders.[45,46] Furthermore, the fungal metabolite apicidin is considered as a potential histone deacetylase inhibitor showing antiproliferative activity against various cancer cell lines (**Figure 2**).[47]
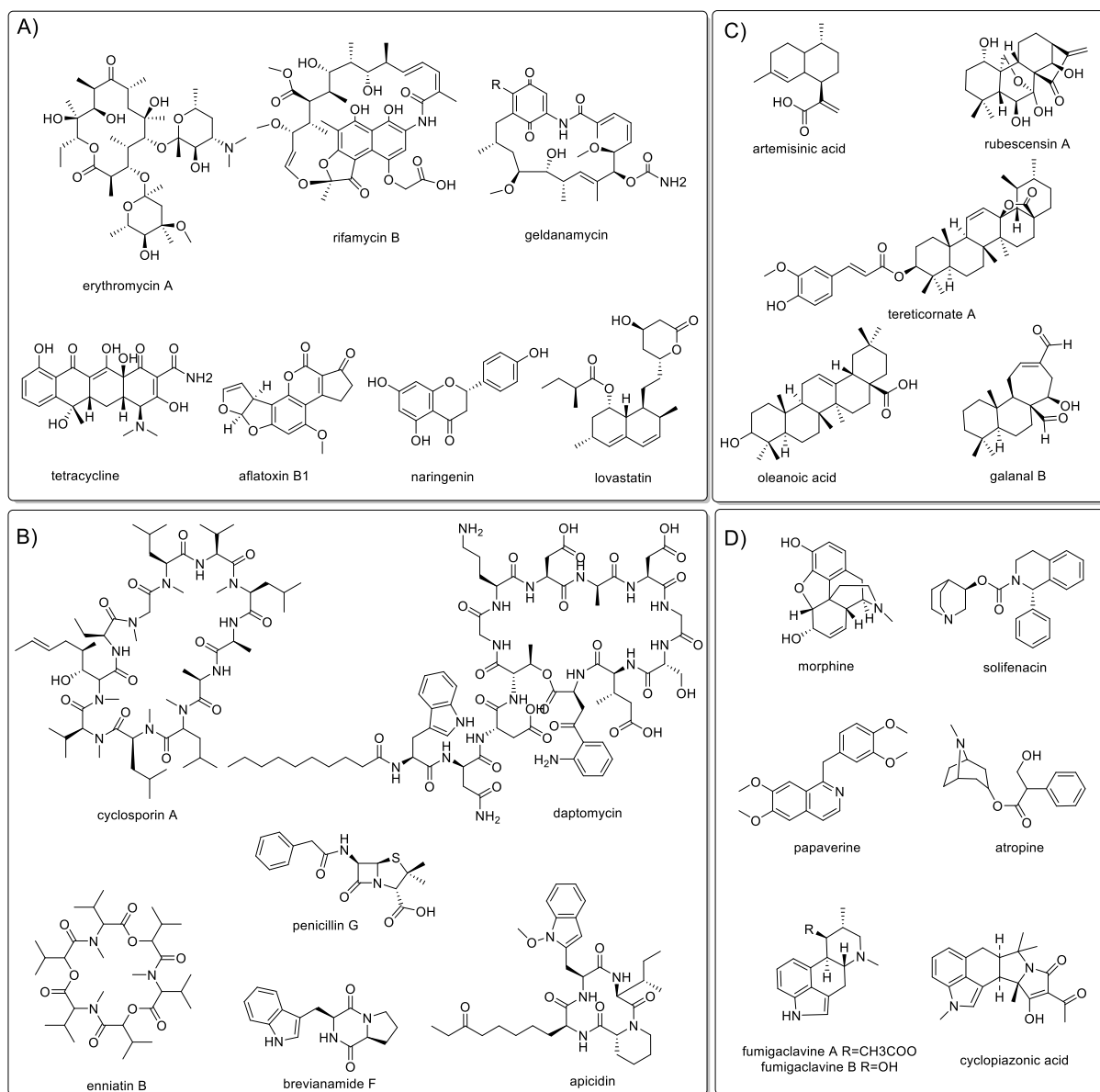

Figure 2. Representative structures of natural products. (A) polyketides, (B) nonribosomal peptides, (C) terpenoids, and (D) alkaloids.

The third major group of NPs is terpenoids including monoterpenes (C10), sesquiterpenes (C15), diterpenes (C20), and triterpenes (C30).[48,49] They are all originated from the C5 units, *i.e.*, dimethylallyl diphosphate (DMAPP) and isopentenyl diphosphate (IPP).[50] Artemisinic acid isolated from *Artemisia annua* L is a key precursor of sesquiterpene lactone artemisinin, which is a typical example of antimalarial drug.[51] Rubescensin A originally found in

Rabdosia[52] and galanal B from flower buds of the myoga plant (*Zingiber mioga* Roscoe)[53] are diterpenoids that exhibit antitumor and antimicrobial activities, respectively.[54,55] Tereticornate A is a triterpene ester compound extracted from the leaves and branches of *Eucalyptus gracilis*, which possesses antiviral, antibacterial, and anti-inflammatory activities.[56] Oleanolic acid is also a ubiquitous pentacyclic triterpene from plants, which is often used as medicinal herbs and as an integral part of the human diet (**Figure 2**).[57]

Besides, alkaloids belong to the largest class of nitrogen-containing NPs (**Figure 2**).[58-60] They can be relative easily purified from crude extracts by acid-base solvent extractions.[23,61,62] This category of NPs has a wide range of pharmacological activities including antimalarial, antitumor, antiarrhythmic, antibacterial, and antihyperglycemic activities.[63-65] Many of them have been use in traditional or modern medicines.[60,66-68] The outstanding represent is analgesic agent morphine, which was isolated from the opium poppy of *Papaver somniferum*.[12,13] Solifenacin isolated from mouse plasma is a muscarinic antagonist used to treat symptoms of an overactive bladder.[69,70] Papaverine is another example found in crude opium, but its major functions are smooth muscle relaxation and coronary and cerebral vasodilation. Now it has been clinically used as an antispasmodic and vasodilator.[71] Atropine belonging to tropane alkaloid is isolated from *Atropa belladonna* and used as a muscarinic acetylcholine receptor antagonist.[72] In addition, fumigaclavine from *Aspergillus fumigatus*[73] and cyclopiazonic acid from *Penicillium cyclopium*[74] are typical mycotoxins of indole alkaloids from fungal source. The various core structures together with multiple modifications extensively increase the structural diversity of NPs, which have huge potential for drug discovery.

1.2 Biosynthesis of natural products

Due to importance of NPs mentioned above, many genetic tools have been developed for better understanding of their biosynthesis in organisms. In the year 1976, the first complete genome sequence from the bacteriophage MS2 was elucidated and published.[75,76] Analysis of the genomic sequence of several microorganisms in the following years revealed that genes are not randomly distributed but organized in close proximity to form biosynthetic gene clusters (BGCs).[77]

The BGCs of NPs usually contain essential genes for backbone enzymes and additional genes for modification of the formed metabolic scaffold. Besides, transporters, specific regulators, and other functional genes are also aligned in the BGCs (**Figure 3**).[78,79] Diverse backbone genes, such as polyketide synthases (PKSs), nonribosomal peptide synthetases (NRPSs), and

8

terpene cyclases (TCs), are responsible for the core structures of PKs, NRPs, and terpenoids, respectively.[20] Different kinds of tailoring enzymes including cytochrome P450 monooxygenases (P450s),[80] prenyltransferases (PTs),[81] nonheme Fe^{II}/2-oxoglutarate (Fe^{II}/2-OG)-dependent oxygenases,[82] and methyltransferases (MTs),[83] contribute to the diverse modification of precursors by oxidation, reduction, rearrangement, and transfer reactions.
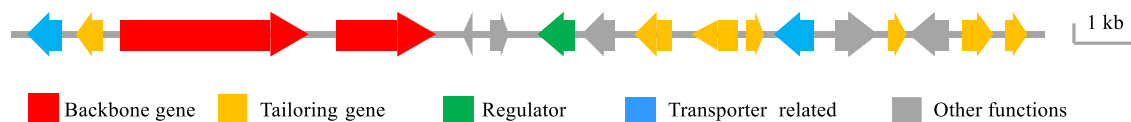

Figure 3. Schematic presentation of typical BGCs.

1.2.1 Biosynthesis of cyclodipeptides

Cyclodipeptides (CDPs) are the smallest cyclic peptides and usually characterized by a 2,5-DKP scaffold. They constitute a large group of SMs from fungi, bacteria, plants, and mammals.[84] The CDP core is generated by the condensation of two α-amino acids.[85] They are named by the three letter code for each of the two amino acids, plus a prefix to designate the absolute configuration, *e.g., cyclo*-L-Xaa-L-Yaa.[86] Normally, they exhibit noteworthy biological activities, such as antibacterial, antimicrobial, antitumor, and immunosuppressive effects.[81,87] The outstanding examples are *cyclo*-L-Pro-L-Pro and *cyclo*-D-Pro-D-Pro. They are useful experimental models for studying Parkinson's disease.[88] *Cyclo*-L-Leu-L-Pro is another CDP displays herbicidal and antibiotic activity.[89] *Cyclo*-L-Leu-Gly is active in memory processes and stimulate muscle to block the narcotic-induced dopamine receptor sensitivity.[90] Three CDPs, *cyclo*-L-Pro-L-Val, *cyclo*-L-Pro-L-Phe, and *cyclo*-L-Pro-L-Tyr, are involved in the quorum-sensing-mediated promotion of plant growth by *Pseudomonas aeruginosa*.[91] Brevianamide F (*cyclo*-L-Trp-L-Pro) mentioned before is a mycotoxin with antibacterial activity.[92] *Cyclo*-L-His-L-Pro is an antihyperglycemic agent and also exerts anti-inflammatory effects.[93] *Cyclo*-L-His-L-Phe and *cyclo*-L-His-L-Tyr act as efficient antiarrhythmic agents.[94]

Recently, significant progress has been achieved in the discovery of CDPs. Many tailoring enzymes were reported to contribute to their biosynthetic pathways, which enlarge the spectrum of the CDP family.[95] Prominent representatives are shown in **Figure 4**. Plinabulin (NPI-2358) with isomerization, hydroxylation, hydration, and oxygenation of *cyclo*-L-His-L-Phe shows an inhibitory effect on the cancer cell.[96] Gliotoxin belongs to the epipolythiodioxopiperazine (ETP) class of cytotoxin with immunosuppressive activity.[97,98] Bicyclomycin modified by six oxidases has been used to treat diarrhea in humans and domestic

animals.[99] The bridged scaffold of nocardioazine A is a noncytotoxic inhibitor of the membrane protein P-glycoprotein.[100,101] What is more, guanitrypmycin D1 has the unique structure containing the guanine nucleobase.[102] Very recently, tryptophan-containing dimeric CDPs coupled with prenyl moieties also found in different species. Interestingly, all these complex structures are *cyclo*-L-Trp-L-Pro (cWP) or *cyclo*-L-Trp-L-Ala (cWA) dimers with different linkages and prenyl moieties at C2 position of the indole rings.[103-105] Brevianamide S as an example shows selective antibacterial activity against Bacille Calmette-Guérin (BCG), suggesting a valuable new lead in the search for next-generation antitubercular drugs.[45,103] Another cWP dimer asperginulin A showed obvious toxicity in inhibiting settlement of the larvae of *Balanus reticulatus* with an adhesive rate of 48.4 % (**Figure 4**).[104]
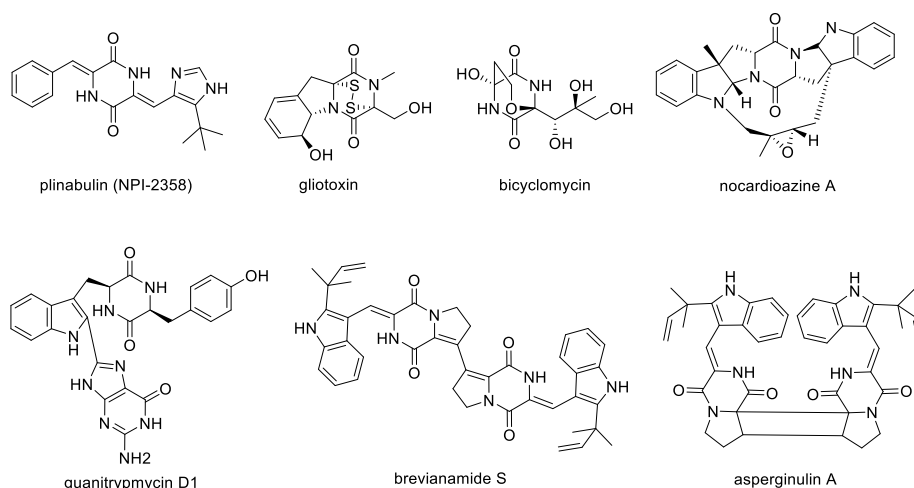

Figure 4. Examples of modified CDPs with biological activities and novel skeletons.

In nature, the CDP scaffold can be synthesized by at least two different types of biosynthetic enzymes, the nonribosomal peptide synthetases (NRPSs) from fungi and the CDP synthases (CDPSs) from bacteria (**Figure 5**).[106,107]

The core NRPS module contains at least three domains, adenylation (A), thiolation or peptidyl carrier protein (T or PCP), and condensation (C) domain.[108] As shown in **Figure 5**, the NRPS FtmPS/FtmA from *Aspergillus fumigatus* is responsible for the formation of the DKP backbone brevianamide F (cWP).[45] Firstly, L-tryptophan and L-proline are recognized and activated by A1 and A2 domains to generate a high-energy aminoacyl-AMP intermediates at the expense of ATP molecules, separately. After that, the activated intermediates are respectively transferred onto the thiol group of T1 and T2 domains. Then the activated L-tryptophan and L-proline are condensed by C1 domain to form the peptide bond. The final product is released by cyclization catalyzed by the terminal C2 domain to form the DKP structure.[46,109]

10

In contrast to the large NRPSs with 2300 – 2500 amino acid residues, CDPSs are smaller enzymes with typical of 200 – 300 amino acid residues which are mostly distributed in *Actinobacteria*, *Proteobacteria*, and *Firmicutes*.[110] Hundreds of CDPSs have been experimentally characterized so far, with an incorporation of total 20 proteinogenic amino acids.[111] They are new family enzymes which hijack the aminoacyl-tRNAs (aa-tRNAs) from the primary metabolism as substrates to biosynthesis the DKP scaffolds. The catalytic mechanism of CDPSs can be described using a ping-pong model.[112] As an example, the precursor of nocardioazines *cyclo*-L-Trp-L-Trp (cWW) is biosynthesized by NozA/NcdA from *Nocardiopsis sp.* CMB-M0232.[100] The CDPS enzyme uses two molecules of tryptophanyl-tRNA as the first and the second substrate. Firstly, the first tryptophanyl-tRNA is attached to the residue of NozA/NcdA, generating a tryptophanyl-enzyme intermediate. After that, the second tryptophanyl-tRNA binds to the intermediate, and its aminoacyl moiety is transferred to the tryptophanyl-enzyme, resulting in the formation of a dipeptidyl-enzyme intermediate. Finally, the dipeptidyl moiety undergoes intramolecular cyclization and generates the tryptophan-containing CDP cWW.[100]
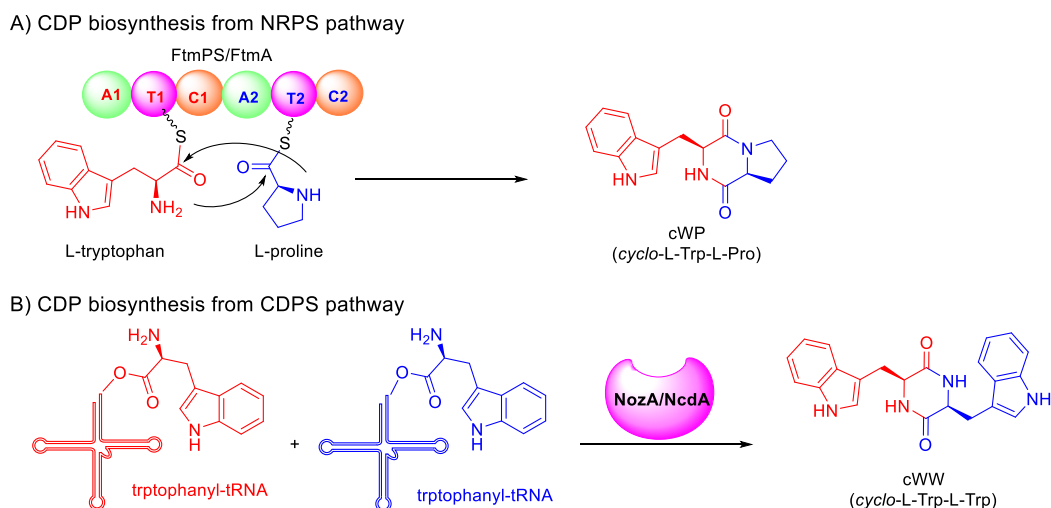

Figure 5. Examples of CDP biosynthesis in the (A) NRPS and (B) CDPS pathways.

1.2.2 PTs in the biosynthesis of prenylated tryptophan-containing cyclodipeptides

PTs are a large family of modification enzymes widely distributed in the secondary metabolism of bacteria, fungi, and plants.[113-115] They catalyze the prenyl transfer reactions of diverse acceptors, such as indole,[116] quinone,[117] xanthone,[118] flavone,[119] and naphthalene.[120] So far, PTs can catalyze both regular and reverse prenylation at C, N or O atoms of the CDP scaffold (**Figure 6**).[121,122] A broad range of prenylated CDPs with important biological activities have been identified.[122,123] The posttranslational modification by PTs shows that they are part of

physiological processes and the prenylated structures often exhibit increased functionality.[124] Therefore, they are always applied for target production of drugs.
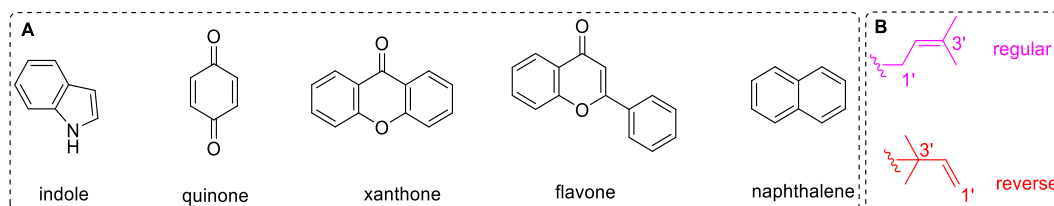

Figure 6. (A) Examples of PT acceptors. (B) The regular and reverse pattern of prenylations.

The prenyl donors of PTs are normally derived from either the mevalonate (MVA) or methylerythritol phosphate (MEP) pathway and consist of n × C5 units, *e.g.*, dimethylallyl diphosphate (DMAPP: n=1), geranyl diphosphate (GPP: n=2), farnesyl diphosphate (FPP: n=3), or geranylgeranyl diphosphate (GGPP: n=4).[125] According to the aromatic substrates, dependency on divalent cations, organism sources, and cell localizations, aromatic PTs can be mainly classified into three categories, *i.e.,* membrane-bound PTs of the UbiA family,[126] soluble PTs as CloQ/NphB group,[127] and dimethylallyl tryptophan synthase (DMATS) superfamily (**Figure 7**).[128]

Membrane-bound PTs are involved in the biosynthesis of ubiquinones, menaquinones, and membrane lipids. They are membrane-bound proteins and divalent ion-dependent.[129] UbiA from *Escherichia coli* with a conserved (N/D) DXXD motif is responsible for an essential biosynthesis step of ubiquinones (known as coenzyme Q).[130] The homologue UBIAD1 involved in the vitamin K biosynthesis was discovered in human cells.[131] The CloQ/NphB group PTs are mostly independent of divalent ions. They demonstrate higher substrate flexibility and mainly catalyze prenylations of naphthalenes, quinones as well as phenolic compounds.[123] These soluble proteins always share structural feature of a five repeating αββα-fold, also known as PT barrel. The first identified enzyme CloQ from *Streptomyces roseochromogenes* catalyzes the prenylation of 4-hydroxyphenylpyruvic acid (**Figure 7**).[132] Another example is NphB from *Streptomyces sp.* which is involved in the biosynthesis of naphterpin and derivatives.[133,134]

The DMATS superfamily are the best studied group of PTs predominantly found in fungi of *Aspergillus*, *Penicillium*, and *Claviceps,* less in bacteria.[113] They mainly attach prenyl moieties onto the indole ring of tryptophan and tryptophan-containing CDPs.[128] Up to date, at least more than 60 representatives of this family have been identified and characterized.[135] Most of these

enzymes show high flexibility toward aromatic substrates with high regioselectivity.[135] These soluble enzymes also have the similar characteristic structure of the PT barrel and the reactions are independent of divalent metal ions as the group of CloQ/NphB. However, the presence of ions like Mg^{2+} and Ca^{2+} can positively increase the reaction activities.[136,137] The reaction mechanism of DMATSs follows the Friedel-Crafts alkylation, *i.e.,* the dimethylallylic cation is nucleophilically attacked by the substrate like the indole nucleus, then the prenylated product is released after rearomatization. Most members of DMATS family are mainly use DMAPP for their prenylations. However, there are also few examples using FPP and GPP as prenyl donors.[138,139]
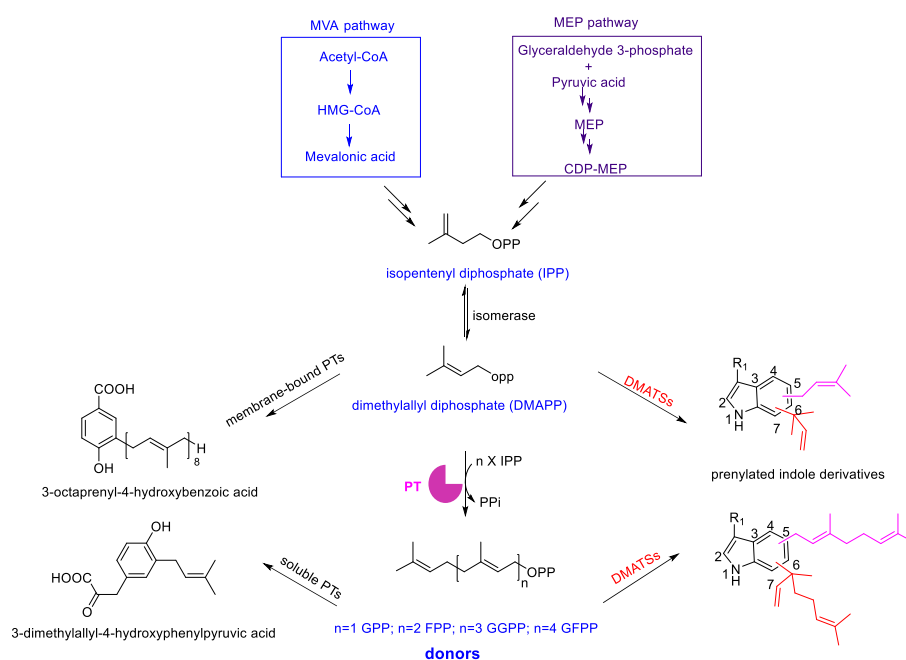

Figure 7. Schematic presentation of prenyl donors and the member of aromatic PTs.

Normally, the prenyl moieties can be attached to position N1, C2, C3, C4, C5, C6, or C7 of the indole ring of tryptophan or tryptophan-containing CDPs in a regular or reverse manner by DMATSs (**Figure 8**). The first identified DMATS is DmaW (4-DMATS) from *Claviceps fusiformis* and catalyzes the prenylation of tryptophan.[140] Since then, several other DMATS enzymes catalyzing prenylations of L-tryptophan have been identified, such as 5-DMATS,[141] 6-DMATSsa,[142] IptA,[143] and 7-DMATS.[144] FtmPT1 is the first identified CDP PT from *Aspergillus fumigatus*, which catalyzes *C2*-prenylation of brevianamide F in the biosynthesis of fumitremorgins.[145] Later, more CDP PTs have been found from fungi and bacteria, such as *N1*-PTs FtmPT2[137] and CTrpPT[146]; *C2*-PTs NotF,[107] BrePT,[92] and CdpC2PT1[147]. SasB,[148] AnaPT,[149] and CdpC3PT[150] are responsible for *C3*-prenylation, FgaPT2[151] for *C4*-prenylation,

EchPT2 for *C4*-, *C5*-, and *C7*-prenylation, and NotC for *C7*-prenylation (**Figure 8**).[152] Furthermore, the DMATS PTs can transfer prenyl moieties onto unnatural structures.[136,153] Elucidation of the crystal structure of FgaPT2 provided a basis for structure-based protein engineering.[142]
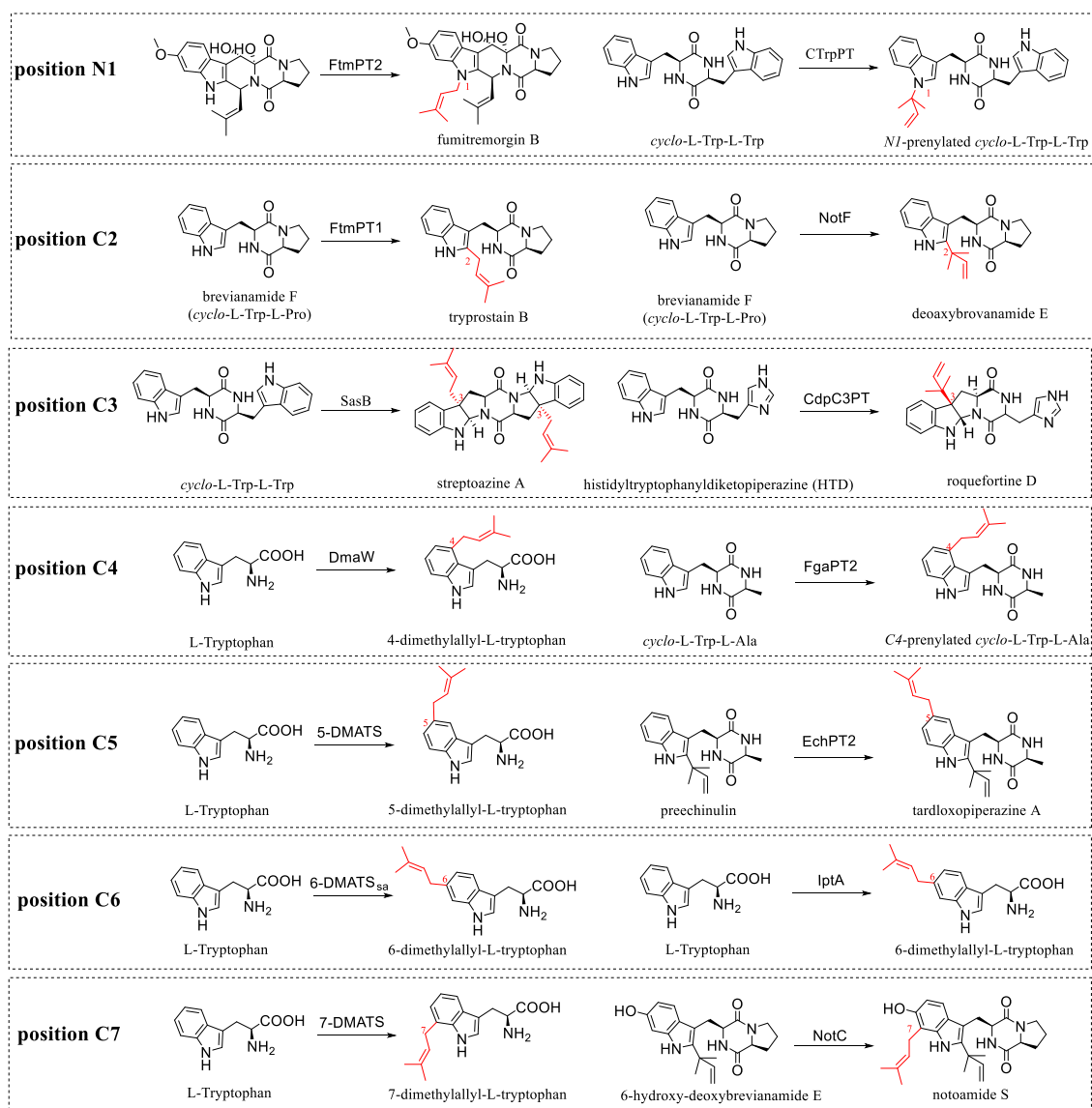

Figure 8. Known examples of prenylation reactions catalyzed by the DMATS superfamily. (Modified from literature[141])

Until now, numbers of multiprenylated tryptophan-containing CDPs from fungal have been identified.[152,154] Interestingly, all these multiprenylated indole DKPs with *C2*-prenyl moieties share similar reaction steps. The CDP core is firstly catalyzed by a *C2*-PT and other PTs later attach the prenyl moieties onto other positions of indole ring (**Figure 9**). Taking notoamide S as an example, the NRPS gene FtmA/FtmPS is responsible for the biosynthesis of

brevianamide F (*cyclo*-L-Trp-L-Pro), which is served as substrate of PTs and firstly prenylated by *C2*-PT NotF and then prenylated at position C7 by *C7*-PT NotC, leading to the pivotal intermediate notoamide S.[155] In the biosynthesis of fumitremorgin A, brevianamide F also as the substrate is catalyzed by FtmPT1 and FtmPT2 for production of *C2,N1*-prenylated fumitremorgin B. Modification by the O-PT FtmPT3 leads to the triprenylated derivative fumitremorgin A.[156] In the studies of tri- and tetraprenylated echnulins, EchPT1 can well accept *cyclo*-L-Trp-L-Ala and EchPT2 afterwards attaches, in a consecutive prenylation cascade, up to two prenyl moieties.[157]
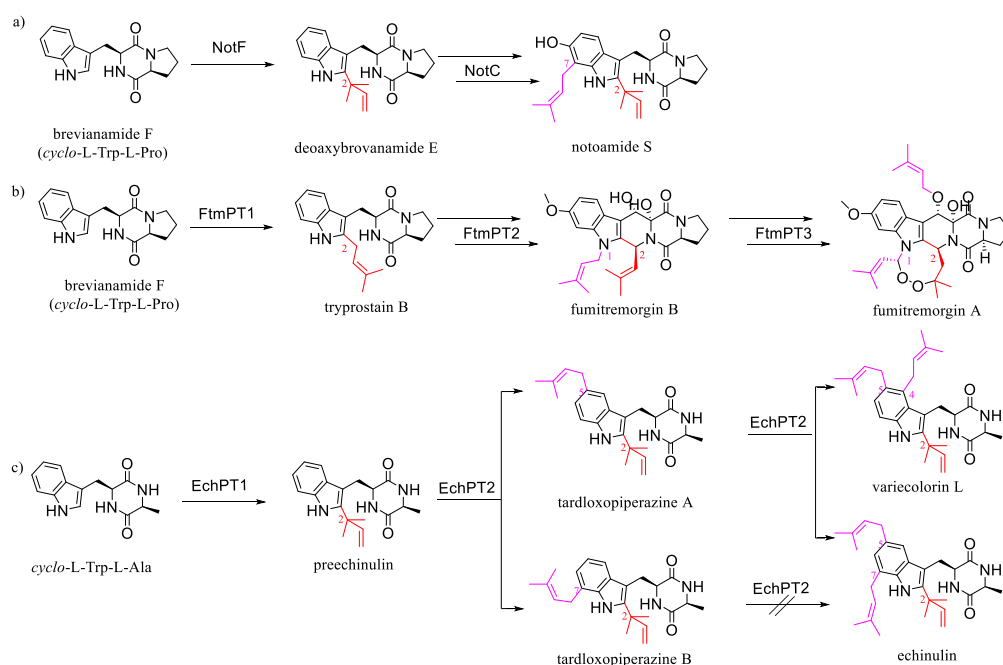

Figure 9. Examples of biosynthetic pathways for multiprenylated CDP derivatives with *C2*-prenylation as the first decoration step.

1.2.3 Biosynthesis of NRP-PKs

PKs and NRPs are two large group of NPs in fungal kingdom.[43,158] Hybrid NPs of the polyketide-nonribosomal peptide (PK-NRP) group have been clearly elucidated in recent years.[159-162] This superfamily of NPs are responsible for the formation of diverse biologically active amide-containing SMs, such as the neurotoxin cyclopiazonic acid,[163] the mycotoxin fusarin C,[164] the cytotoxin aspyridones A[165] and cytochalasin K[166] as a potent actin polymerization inhibitor (**Figure 10**). In comparison, the nonribosomal peptide-polyketide (NRP-PK) hybrids have rarely been reported from fungi.[167] The mycotoxin tenuazonic acid from *Alternaria tenuis* is the first reported fungal NRP-PK product.[168] Later, swainsonine from *Metarhizium robertsii*,[169,170] hispidin from *Neonothopanus nambi*,[171] pyrophen from

Aspergillus niger,[172] and aspcandine from *Aspergillus candidus*[173] were also identified. The indolizidine alkaloid swainsonine is a potent immunomodulator and also exhibits antimetastatic and antiproliferative activities.[170] Hispidin and pyrophen are α-pyrone derivatives, which have been reported to possess a wide range of biological and pharmacological activities (**Figure 10**).[174,175]
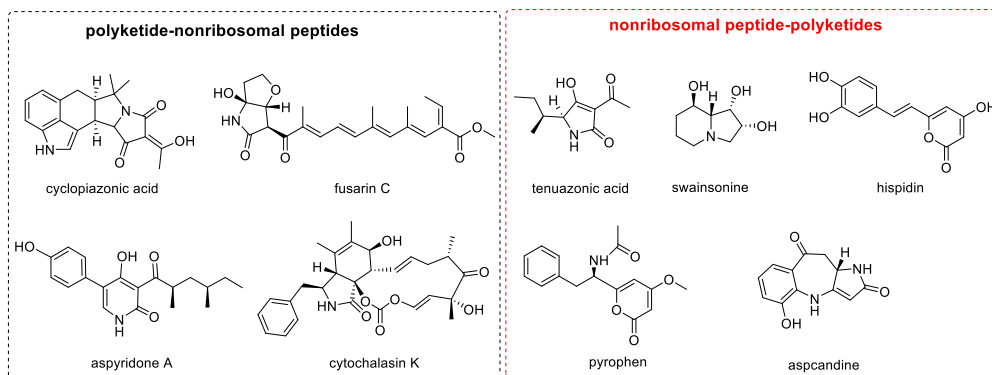

Figure 10. Examples of hybrid NPs of PK-NRPs and NRP-PKs from fungi.

Normally, the PK-NRPs are catalyzed by PKS-NRPSs characterized with PKS domains at N-terminus and NRPS domains at C-terminus. In comparison, the NRPS-PKS hybrid enzymes with NRPS at N- and PKS at the C-terminus are responsible for production of NRP-PKs.[167] Differing from PKS-NRPSs, all these enzymes catalyze C-C bond formation by addition of acetyl units from malonyl-CoA to the precursors.[176]

According to the literatures, the T/PCP domain of upstream NRPS module and the KS domain of downstream PKS module play an important role in the C-C bond formation of NRP-PKs.[177] After receiving the aminoacyl chain from the T domain, the KS domain of PKS catalyze the decarboxylative condensation between the aminoacyl chain and the malonyl-type extender unit. As a result, the C-C bond is formed as an aminoacyl-acyl hybrid chain.[168]

As shown in **Figure 11**, hispidin and pyrophen are biosynthesized by HispS[178] and AnATPKS,[172] respectively. Both of the enzymes share the same domain structure of A-T-KS-MAT-ACP (A: adenylation, T: thiolation, KS: ketosynthase, MAT: malonyl acyl transferase, ACP: acyl carrier protein). In HispS, the minimal PKS module performs two rounds of chain elongation using malonyl-CoA, leading to a triketide intermediate. The intermediate then spontaneously off-loads through lactonization, leading to the α-pyrone hispidin. Interestingly, HispS uses caffeic acid instead of an amino acid as its substrate for activation to form the nitrogen-free product.[178] In contrast, the A domain of AnATPKS recognize L-phenylalanine as

substrate for loading.[172] The other examples are SwnK[170] and AcdB,[173] which are responsible for the formation of swainsonine and aspcandine, respectively. Comparing with HispS and AnATPKS, the two enzymes share additional KR (ketoreductase) and R (reductase) domains before and after the ACP domain. Pipecolic acid[170] originated from L-lysine and 3-hydroxy-L-kynurenine[173] from L-tryptophan were incorporated as a building block for biosynthesis of swainsonine and aspcandine, respectively (**Figure 11**).
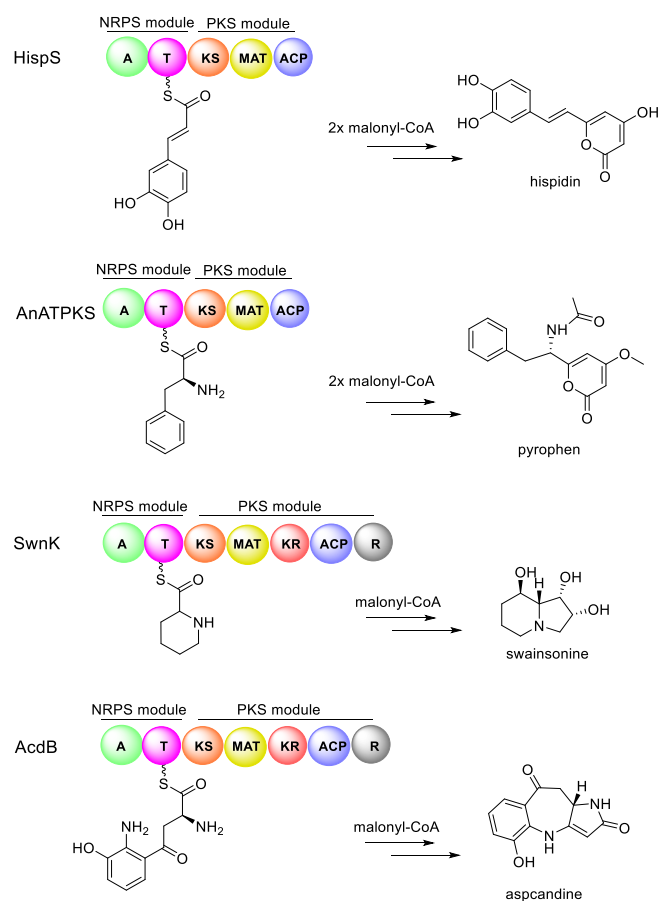
Figure 11. Biosynthesis of representative NRP-PK hybrids from fungi.

In recent years, a series of methods have been applied to mining novel hybrid NPs.[162,179,180] Due to few reported NRP-PKs from fungi, it is of great significance to focus on this less explored group for new structures identification.

1.3 Ascomycota as important source for natural product discovery

Ascomycota is the most diverse and best studied phylum in fungi kingdom, which comprises more than 110,000 species.[23] They are known as sac fungi which produce microscopic spores inside special, elongated cells or sacs with the filaments partitioned by cellular cross-walls.[181] Normally, they can produce sexual spores like ascospores formed in sac-like structures, but

there are also members producing small asexual spores called conidia.[181] Many ascomycetes are pathogens of plants, animals, and humans. Plant-pathogenic ascomycetes cause plant diseases such as apple scab, rice blast, black knot, and the powdery mildews.[182] *Candida albicans* and *Aspergillus niger* can cause skin infections.[183] Even through the ascomycetes are harmful for human life, they are notable for producing huge numbers of antibiotics for treating bacterial infections.[184] *Penicillium* species are widely used for fermenting bread, alcoholic beverages and cheese. Several species of ascomycetes, such as *Saccharomyces cerevisiae* and *Aspergillus* species, are biological model organisms used in genetics and biology studies.[185]

So far, great progress has been achieved for the isolation and chemical characterization of SMs from ascomycetes, especially in members of *Aspergillus* and *Penicillium*. Due to the diversity of SMs and their broad range of biological activities, these fungi have gradually become the main objects for discovery of novel drugs.

1.3.1 *Penicillium crustosum* and its secondary metabolites

Penicillium crustosum is a common foodborne fungus belonging to the genus *Penicillium*. They often cause spoilage in a wide variety of foods, including meat, cheese, and fruits.[186] They are psychrophilic microorganisms which have blue-green or blue-gray conidia and can grow at low temperatures or in low water activity environments.[187] Almost all *P. crustosum* strains produce mycotoxins penitrems A – G.[188] Penitrem G has been shown to have insecticidal activity.[189] Isolation and genetic manipulation suggested *P. crustosum* can produce versatile NPs, including PKs such as xylariolide D,[190] orsellinoxylpropanoic acid,[191] and YWA1,[187] NPRs like viridicatol,[192] cyclopenin,[186] and roquefortine C[193] as well as hybrid SMs, *e.g.,* terrestric acid,[194] penilactones A and D (**Figure 12**).[195]
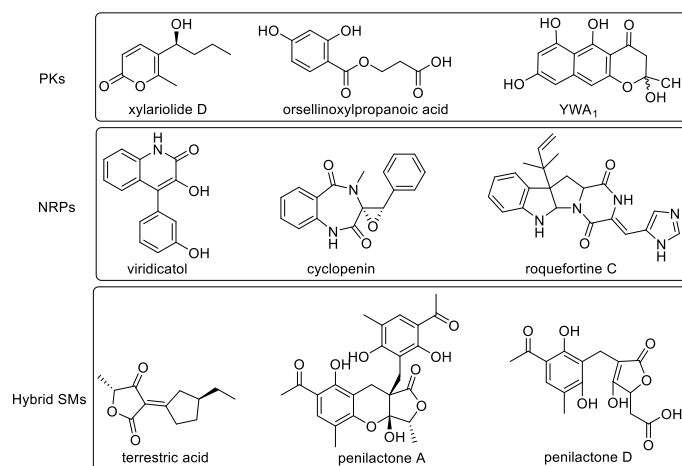

Figure 12. Known secondary metabolites from *Penicillium crustosum*.

The strain *Penicillium crustosum* PRB-2 used in this thesis was isolated from a deep-sea sediment collected in Prydz Bay at a depth of -526 m.[187] The genome was sequenced in 2019 and assembled with a total of 32.4 Mbp length scaffolds.[187] In this thesis, this PhD candidate focused on the novel NRP-PK in *P. crustosum* PRB-2 and elucidated its biosynthetic pathway.

1.3.2 *Aspergillus nidulans* and its application in genetics and biology studies

Aspergillus nidulans, a saprophytic filamentous fungus with green asexual spores, is widespread in nature.[196] It is phylogenetically related to other ascomycetes of economic (*Aspergillus niger* and *Aspergillus oryzae*) or clinical importance (*Aspergillus fumigatus*).[197,198] Due to its haploid genome, simple nutritional requirements, rapid growth and reproduction rates, *A. nidulans* is a well-established model organism for studying genetic regulation, developmental biology, signal transduction and secondary metabolism.[199] This fungus is usually harmless to humans and has been used as a versatile cell factory for industrial production of enzymes such as cellulase, β-glucosidase, laccase, and xylanase[200] as well as NPs, *e.g.,* echinocandin B[201] and anidulafungin.[202] In addition, the studies in *A. nidulans* have developed a platform for heterologous expression of fungal BGCs and represents an alternative for exploration and efficient production of fungal NPs (**Table 1**).

Recently, an engineered strain *A. nidulans* LO8030 has been used as an excellent host for heterologous expression of unknown fungal BGCs.[203] The strain has a low SM background, in which the eight clusters responsible for the biosynthesis of major SMs are deleted: sterigmatocystin, emericellamide, asperfuranone, monodictyphenone, terrequinone, F9775A and B, asperthecin, and austinol.[203] In this thesis, the PhD candidate successfully heterologous expressed the target NRPS-PKS gene into *A. nidulans* LO8030 and proved its function.

Table 1. Examples of biosynthesis of fungal natural products in *A. nidulans*

Natural product	Source of BGC	Titer	Refs
Geodin	*A. terreus*	40–70 mg/plate	[204]
Asperfuranone	*A. terreus*	6.87 mg/L	[205]
Carotenoid	*F. fujikuroi*	125 mg/kg dry mycelial	[206]
Neosartoricin B	*Trichophyton tonsurans*	10 mg/L	[207]
Penicillin V	*P. chrysogenum*	0.7 mg/L	[208]
Olivetolic acid	*Metarhizium anisopliae*	80 mg/L	[209]
Psilocybin	*Psilocybe cubensis*	110 mg/L	[210]

1.4 Strategies to diversify natural products for drug discovery

NPs with biologically active pharmacophores have been widely used as drugs for decades. More than one third of FDA approved molecules are originated from NPs or their analogs,[47,211] especially for antitumor, immunosuppressant, and cholesterol-lowering drugs.[47] These products include unaltered natural compounds, chemically modified derivatives, and synthetic natural mimics, which are meaningful for optimization of the pharmaceutical properties.[211] Therefore, it is of great significance to obtain more diversified structures for drug discovery.

Traditionally, NPs were obtained through bioactivity-guided screening and exploration of organisms from understudied environments.[212] However, the frequently repeated isolation of known compounds make the discovery process much lower. Nowadays, many strategies have been used for discovery of new NPs. One efficient method is growth condition optimization, such as media, UV, temperature, pH values, and chemical mutagenesis.[213,214] Co-cultivation is also proved as a useful tool to increase the chemical diversity.[215] Besides, addition of chemical elicitors and epigenetic perturbations also led to cryptic NPs production.[216,217]

In recent years, development in genomics has revealed that microorganisms have great potential to produce more biologically active SMs.[218] Genome sequence analyzing proved that many BGCs are unknown in the microbials.[176] However, their products cannot be detected under conventional laboratory conditions. Thus, genome mining approaches including genetic manipulation in the native host and heterologous expression[219] have been developed to activate these silent BGCs to obtain the cryptic natural products. In addition, combinatorial synthetic biology and chemoenzymatic approaches offers promising opportunities to access NP analogs, *e.g.,* pathway modification and mutasynthesis, enzymatic and microbial biotransformation.[220,221] Taken together of the strategies, vast of novel NPs with biological activities and new skeletons are expected to be discovered in the future.

1.4.1 Genome mining approaches for novel natural product discovery

Genome mining refers to utilize the genomic information for the discovery of NPs and their biosynthetic pathways.[222] Since the rapid improvement of next generation sequencing technologies, numbers of genome sequences of bacteria and fungi are accessible in the public databases.[223] Thus, a series of computational tools were developed to automatically identify the sets of genes in the genome sequences of many microorganisms. The specialized online tools include prediction databases antiSMASH (https://antismash.secondarymetabolites.org), PRISM (http://magarveylab.ca/prism/), CLUSEAN (https://bitbucket.org/tilmweber/clusean),

and the annotated database MIBiG (https://mibig.secondarymetabolites.org/). For genome mining of targeted BGCs, these computational tools are powerful to analyze each cryptic genes and provide important insights into the structural features of their potential product.[224] The strategies for engineering microbial NP biosynthesis can be mainly divided into two parts, *i.e.,* (i) genetic manipulation in native host and (ii) heterologous expression in well-studied host (**Figure 13**).

Genetic manipulation in the native host is also known as *in situ* activation. This approach includes promotor engineering, transcriptional regulation engineering, as well as ribosome and RNA polymerase engineering.[225] In recent years, the CRISPR-Cas9 technology has been developed as a novel approach to efficiently manipulate genes.[226] Replacement of the native promotors with strong or inducible promotors has also been applied as efficient method for activation the silent BGCs.[227] Transcriptional regulator engineering is also an efficient method, which refers manipulation of global and pathway-specific transcriptional regulators, such as overexpression of the pathway-specific activators and inactivation of the repressors.[228]
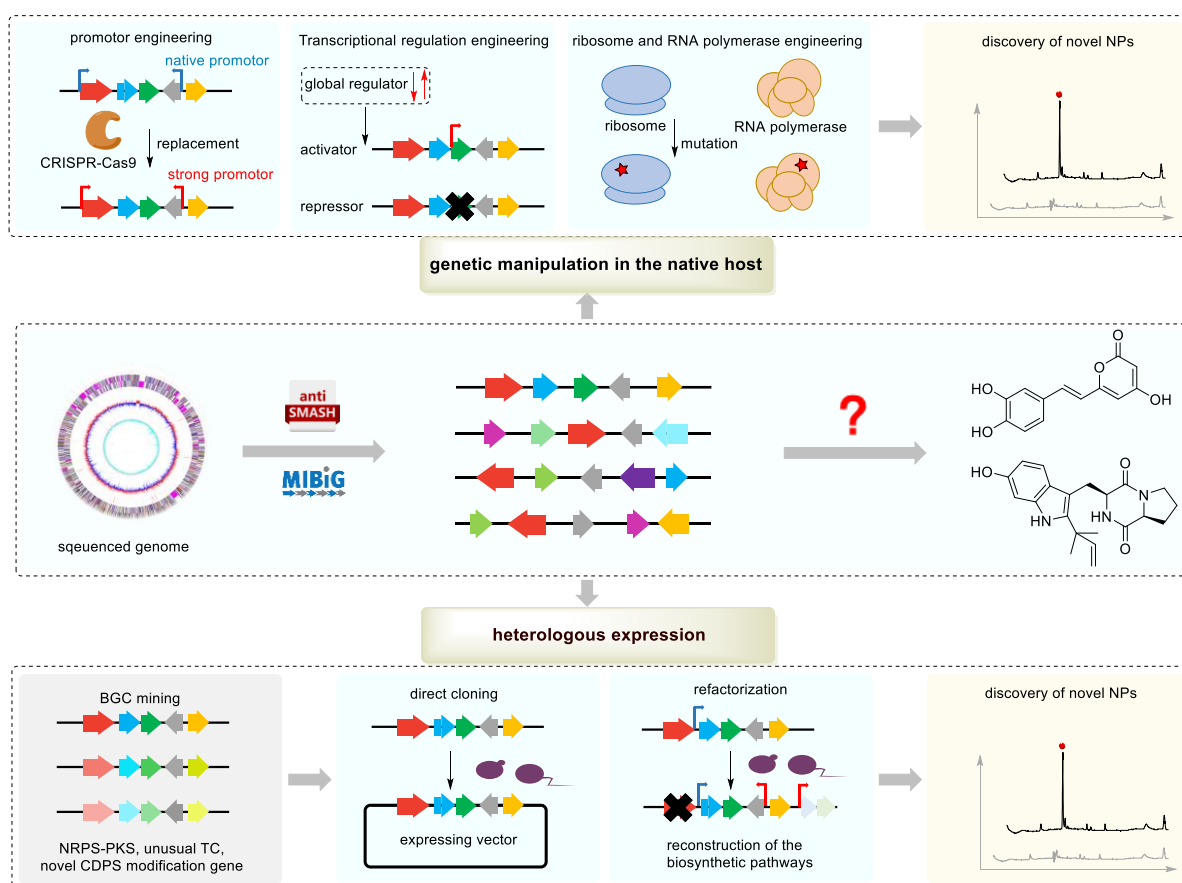
Figure 13. Genome mining for natural product discovery in microorganisms.

Heterologous expression strategy is suitable for the strains, which are difficult to do genetic manipulation. Normally, the heterologous hosts are model strains with well-studied genetic backgrounds and improved growth and expression phenotypes.[229] *Streptomyces coelicolor*, *Streptomyces lividans,* and *Streptomyces albus* from bacteria and *Aspergillus nidulans, Aspergillus oryzae*, and *Aspergillus niger* from fungi are the most widely used heterologous hosts.[230] The target cryptic genes or BGCs, such as NRPS-PKS,[172] unusual TC,[231] novel CDPS modification genes,[232] are assembled and expressed in the heterologous host by direct cloning into a suitable vector with appropriate promotor. After that, the BGC expressing strains were analyzed via untargeted metabolomics. The new metabolites can be elucidated by LC-MS and NMR analysis. In addition, BGC refactoring to reconstruction of the biosynthetic pathways provides additional method for discovery of the new NPs analogs.[230]

1.4.2 Synthetic biology and chemoenzymatic approaches for enhancing natural product titers and producing new unnatural products

Over the past decade, creating pathways is becoming a hot research area to find new NPs. Synthetic biology is based on the biosynthesis and metabolism of NPs at the molecular level, which demonstrates great potential for enhancing the NP titers and producing new unnatural products (**Figure 14**).[233,234] Combinational biosynthesis has been proven to be a promising strategy to obtain target SMs through genetic modification and reorganization of the biosynthetic pathways.[235] In recent years, metabolic engineering, especially engineering the novo biosynthetic pathways have been developed as a powerful biotechnological toolbox to simultaneously improve the access to natural building blocks and their unnatural analogs as well.[236] Another prominent strategy is relied on precursor-directed pathway engineering. [237] Native precursor combining with the downstream pathways provides libraries of desired target compounds. On the other hand, engineering non-native substrates also reveals significant potential for both regio- and chemo-selective diversification of NPs, spurring advancements towards novel drug development.[237]

Recently, protein engineering has emerged as a powerful tool in the development of metabolic engineering, which is normally used to improve enzymatic activities, strengthen enzyme stabilities, and expand product spectra.[238] PTs as the majority tailoring enzymes often improve the interaction of the substance with proteins, leading to the increased biological activities of the prenylated products.[239] The diversity of prenylated compounds has gained increasing attention in pharmaceutical study. Therefore, it is of attractive interest to use chemoenzymatic approach for *in vitro* diversification of prenylated derivatives (**Figure 14**).
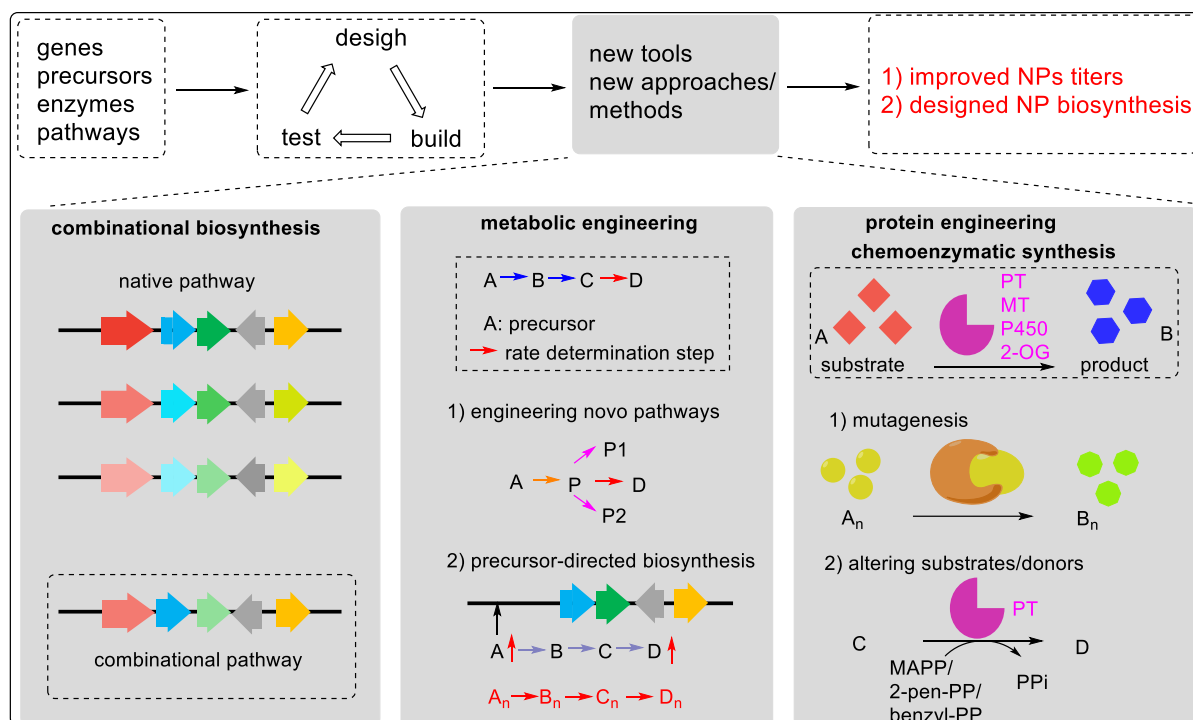
Figure 14. Synthetic biology and chemoenzymatic approaches for discovery of NPs and their unnatural designed analogs.

1.4.3 Chemoenzymatic synthesis of prenylated aromatic compounds by using PTs

Comparing with chemical synthesis, chemoenzymatic synthesis shows broad substrate spectra and mild reaction conditions.[239] Researches show that chemoenzymatic synthesis by PTs has achieved much progress towards pharmacological screening and a series of prenylated products have been successfully synthesized by these enzymes.[240]

The considerable inherent promiscuity of PTs has inspired engineering efforts. Previous studies on the PT engineering showed that site-directed mutagenesis of PTs on some amino acid residues in the prenyl donor binding pocket changed the catalytic activity and improved the acceptance of other substrates.[128,241] One study published in 2015 showed that FgaPT2_K174F altered the substrate preference from L-Trp to L-Tyr.[242] Changing the residue Gly115 and Tyr205 of FtmPT1 led to the altered prenylation position and increased permissiveness towards nonnative acceptors.[243] Outstanding example is the CDP PTs engineering. Mutation of the gatekeeping residues in six PTs to glycine led to the improved acceptance of GPP for *cyclo*-L-Trp-L-Trp (cWW) prenylation with different prenylation positions or patterns (**Figure 15A**).[244]

Due to the relatively open natural active sites of the ABBA-fold, the usage of PT enzymes as biocatalysts demonstrate promiscuity towards both their aromatic substrates and the pyrophosphate alkyl donors.[241] For aromatic acceptors, FgaPT2 natively accepts L-tryptophan,

but can also tolerates tryptophan derivatives, such as indole DKPs and tyrosine.[151] AtaPT also demonstrated unprecedented promiscuity towards aromatic acceptors, such as bioflavonoids, chalcones, and cannabinoids.[245,246] In a previous study, one-step reactions were performed by using eight PTs and the unnatural substrate *cyclo*-L-homotryptophan-D-valine, which produced seven prenylated products with prenyl moieties attached to all nucleophilic reactive positions of the indole ring (**Figure 15B**).[247] In addition to their remarkable high flexibility toward aromatic substrates, recent studies revealed that several members of this family accept not only DMAPP, GPP, and FPP, but also the unnatural DMAPP analogs like monomethylallyl (MAPP), 2-pentenyl (2-pen-PP), and benzyl diphosphate (benzyl-PP) (**Figure 15C**). Indole PTs including FgaPT2 and 5-DMATS as well as CDP PTs as BrePT, FtmPT1, AnaPT, CdpNPT, and CdpC3PT have been demonstrated to well accept the unnatural prenyl donors.[135,248] No doubt the potential application of these enzymes for NP analogs could, in some instances, provide a more efficient and environmentally friendly approach for synthetic modifications.
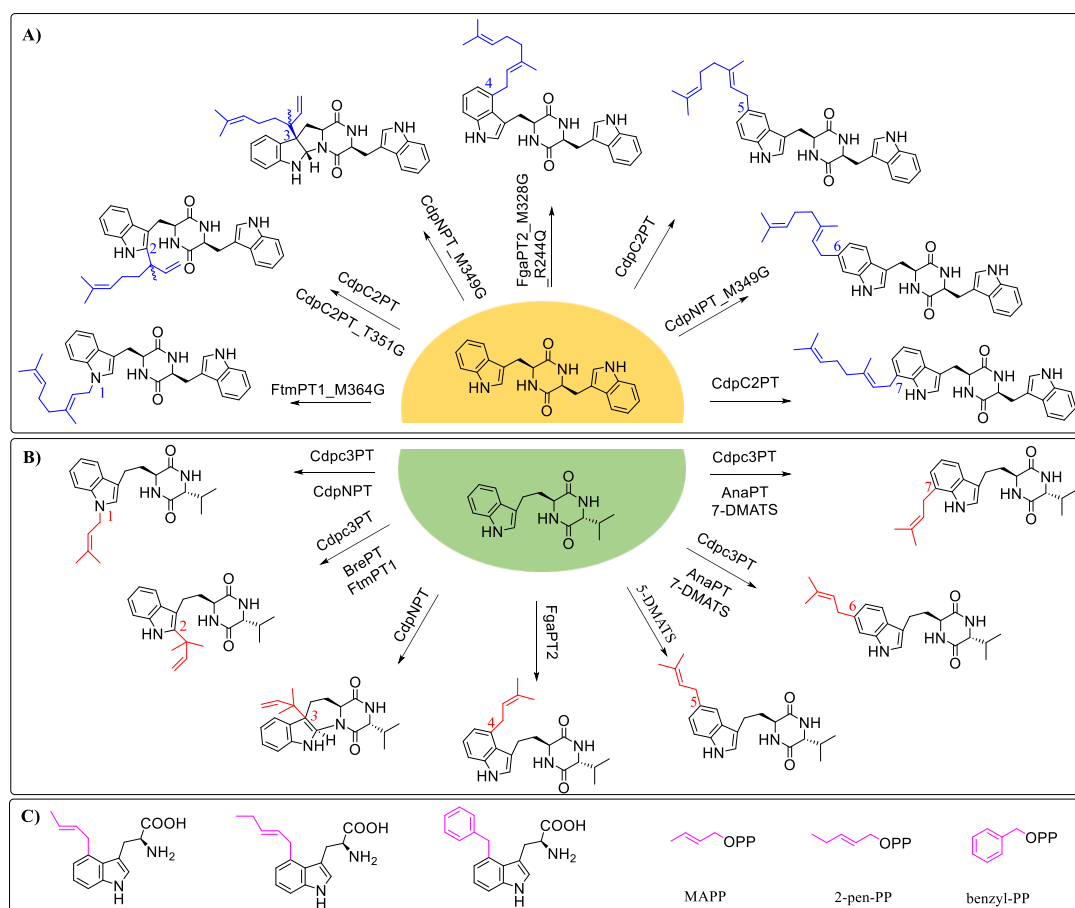
Figure 15. Chemoenzymatic synthesis of prenylated derivatives by using PTs. (A) Decoration of cWW with geranyl moieties, (B) One-step reactions of unnatural substrate *cyclo*-L-homotryptophan-D-valine, (C) Prenylation with unnatural prenyl donors.

2 Aims of this thesis

The overall aim of this thesis was creation of new NPs and derivatives by genome mining and chemoenzymatic synthesis.

The following issues have been addressed in this thesis:

Discovery of 4-hydroxy-6-(4-hydroxyphenyl)-α-pyrone in *Penicillium crustosum* by heterologous expression NRPS-PKS gene and precursor feeding

NPs are crucial for drug discovery and development. However, bioinformatic analysis of genome sequences has revealed that many BGCs remain silent or are only expressed at low levels in their native producer under standard laboratory conditions. Scientists have developed various strategies to activate these silent genes, such as co-cultivation, media composition optimization, cultivation condition optimization, and manipulation of global regulators and transcription factors. One promising technique for discovering new NPs is heterologous expression of the cryptic or silent genes. In recent years, the hybrid genes comprising both PKS and NRPS domains have been identified, primarily in the form of PKS-NRPS hybrids. However, NRPS-PKS hybrid enzymes with the NRPS domain at the N-terminus and the PKS domain at the C-terminus have been rarely reported in fungi. This study focuses on the heterologous expression of the silent NRPS-PKS gene *pcr10109* from *Penicillium crustosum* PRB-2. The project was successfully finished with the help of Dr. Jie Fan and Dr. Ge Liao. Dr. Jie Fan constructed the deletion and heterologous expression strains. Dr. Ge Liao helped with the structure isolation and elucidation. The following experiments were carried out:

➢ Bioinformatic analysis of the NRPS-PKS gene *pcr10109* from the sequenced genomes

➢ Deletion of the gene *pcr10109* in *P. crustosum* PRB-2 wildtype strain

➢ Generating the heterologous expression strain *A. nidulans* JF021 by introduction of the expression construct into *A. nidulans* LO8030

➢ Cultivation of *A. nidulans* JF021 and LC-MS analysis the difference with the control strain harboring empty vector

➢ Isolation and structural elucidation of the new peak as 4-hydroxy-6-(4-hydroxyphenyl)-α-pyrone from *A. nidulans* JF021

➢ Feeding experiments increased the product yield and proved that the unusual NRPS-PKS use PHBA as start unit and two unit of malonyl-CoA to synthesis 4-hydroxy-6-(4-hydroxyphenyl)-α-pyrone

Formation of diprenylated cyclodipeptides by changing the prenylation steps with different DMATSs

Multiprenylated indole DKP alkaloids are metabolites decorated by various indole PTs with prominent agricultural and medicinal applications. Among them, the category of *C2*-prenylated ones normally is formed by first regiospecific *C2*-prenylation at the indole nucleus with DMAPP and later at other positions. Interestingly, in this study, EchPT1 has the reverse reaction order which catalyzed the last prenylation step at C2 position. We firstly obtained *C4*-, *C5*-, C6-, and *C7*-monoprenylated brevianamide F by using four DMATSs. These four products were further accepted by *C2*-prenyltransferase EchPT1 to form four new diprenylated cWP, including the unexpected *N1,C6*-diprenylated derivative. Our study provides an excellent example for production of designed products and increasing structural diversity of metabolites by changing the normal reaction sequences. Dr. Lindsay Coby observed the prenylation reactions for diprenylated derivatives production. The following experiments were carried out:

➢ Overproduction and purification of the recombinant PTs His8-EchPT1, His8-FgaPT2_R244L, His8-FgaPT2_Y398F, 6-DMATSSa-His6, and 7-DMATS-His6

➢ Enzyme reactions of FgaPT2_R244L, FgaPT2_Y398F, 6-DMATSSa, and 7-DMATS with *C2*-prenylated *cyclo*-L-Trp-L-Pro deoxybrevianamide E in the presence of DMAPP

➢ Enzyme assays for production of *C4*-, *C5*-, *C6*-, and *C7*-prenylated *cyclo*-L-Trp-L-Pro by FgaPT2_R244L, FgaPT2_Y398F, 6-DMATSSa, and 7-DMATS

➢ Purification and structure elucidation to confirm the prenylation positions of the monoprenylated products

➢ Prenylation of the *C4*-, *C5*-, *C6*-, and *C7*-prenylated *cyclo*-L-Trp-L-Pro by *C2*-PT EchPT1 and structural elucidation of the diprenylated products

➢ Determination of the kinetic parameters of EchPT1 toward monoprenylated derivatives and DMAPP

Prenylation of dimeric *cyclo*-L-Trp-L-Trp by utilizing the promiscuous *cyclo*-L-Trp-L-Ala prenyltransferase EchPT1

The DMATS superfamily as important biocatalysts usually catalyze metal ion-independent Friedel-Crafts prenylations. They were widely used for structural modification of diverse small molecules. In recent years, several prenylated dimeric CDPs have been identified with wide range of bioactivities. In this study, we intended to get prenylated dimeric CDPs by chemoenzymatic synthesis with a promiscuous known PT EchPT1. One mono- and three

diprenylated *cyclo*-L-Trp-L-Trp (cWW) dimers were obtained in high conversion yields. Our study provides an excellent example for increasing structural diversity by prenylation of complex substrates with known biosynthetic enzymes. The following experiments were carried out:

- Overproduction and purification of the recombinant DMATSs
- Enzyme reactions of EchPT1, FgaPT2_R244L, FgaPT2_Y398F, 6-DMATS$_{Sa}$, and 7-DMATS with cWP dimer apergilazine A and cWA-cWP dimer naseseazine A in the presence of DMAPP
- Enzyme reactions of substrates tetratryptomycin A – C by the five PTs
- Determine the relationship of mono- and diprenylated products in the reaction mixtures of tetratryptomycin A – C with EchPT1
- Isolation and structural elucidation of the mono- and diprenylated cWW dimers in the reaction with EchPT1
- Determination of the kinetic parameters of EchPT1 toward tetratryptomycins and DMAPP

3 Results and discussion

3.1 Discovery of 4-hydroxy-6-(4-hydroxyphenyl)-α-pyrone in *Penicillium crustosum* by heterologous expression of an NRPS-PKS gene and precursor feeding experiments

As mentioned in the introduction, fungal PKSs and NRPSs are two large enzyme groups involved in the biosynthesis of polyketide and nonribosomal peptide, respectively.[43,158,249] Hybrid enzymes of the PKS-NRPS group have been clearly elucidated in recent years.[159-162,250,251] This superfamily enzymes are characterized with PKS domains at N-terminus and NRPS domains at C-terminus. In comparison, the NRPS-PKS hybrid enzymes with NRPS at N- and PKS at the C-terminus have rarely been reported from fungi.[167] The mycotoxin tenuazonic acid from *Alternaria tenuis* is the first reported fungal NRP-PK.[168] Swainsonine,[169,170] hispidin,[171] and pyrophen[172] were identified later and are biosynthesized by SwnK, HispS, and AnATPKS, respectively. The hybrid enzymes HispS and AnATPKS share the same domain structure A-T-KS-MAT-ACP, with the exception for SwnK with additional KR and R domains. Interestingly, the products of HispS and AnATPKS are α-pyrone derivatives, which were reported to possess a wide range of biological and pharmacological activities.[174,175] Therefore, it is of great value to focus on this less explored enzyme group for new structure identification.

We located a NRPS-PKS gene *pcr10109* in *Penicilium crustosum* PRB-2 with the same domain structure A-T-KS-MAT-ACP as HispS and AnATPKS. However, it only shares identities of 33% with HispS (BBH43485.1) and 29% with AnATPKS (EHA27898.1). Such low homology raised our curiosity about its function for product formation.

To prove gene function, Dr. Jie Fan firstly deleted the gene *pcr10109* in *Penicilium crustosum* PRB-2 using split marker strategy. However, LC-MS analysis showed no difference of the SMs in the crude extracts of deletion mutant and wildtype strain. This suggests that the target gene was not expressed under the laboratory conditions. To further verify its function, she changed the method for heterologous expression (**Figure 16**). The 5813 bps fragment was cloned into the expression vector pYH-wA-pyrG under the control of the strong *gpdA* promotor.[252] After PEG-mediated protoplast transformation in *Aspergillus nidulans* LO8030,[252] she obtained the heterologous expressing mutant *Aspergillus nidulans* JF021.
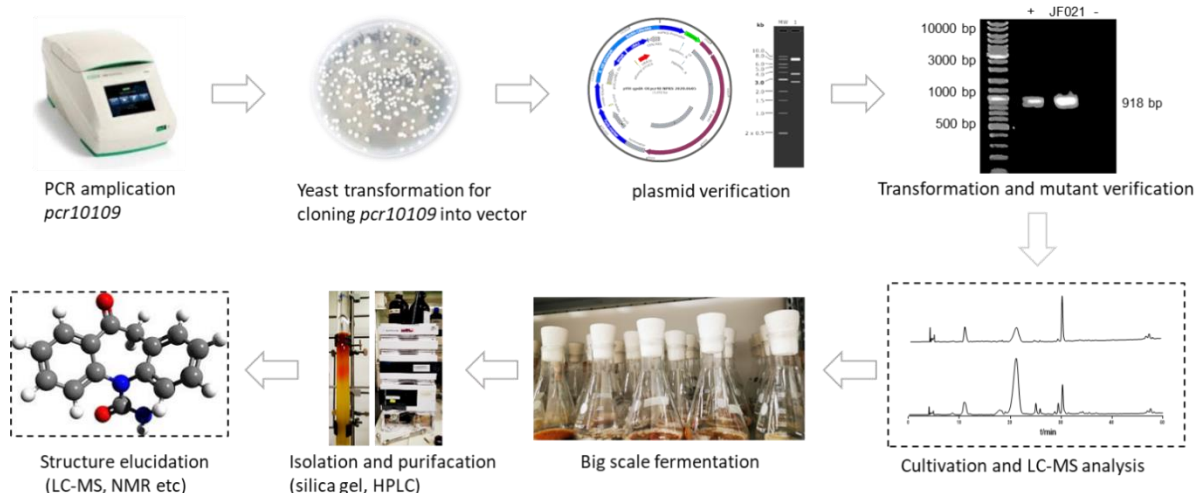
Figure 16. Workflow for heterologous expression the NRPS-PKS gene *pcr10109* from *Penicilium crustosum* PRB-2.

As shown in **Figure 17a**, one additional peak **1** with [M + H]$^+$ ion at *m/z* = 205.0494 was detected in the crude extract of the transformant JF021 in rice media for 5 days, which was absent in the control strain JF010 with empty vector pYH-wA-pyrG. After large scale fermentation, the cultures were extracted by ethyl acetate for three times. Compound **1** was obtained by silica gel column and HPLC purification with the help of Dr. Ge Liao. Further MS and NMR analyses confirmed product **1** to be 4-hydroxy-6-(4-hydroxyphenyl)-2*H*-pyran-2-one (**Figure 18**).[253] The NRPS-PKS encoded by *pcr10109* was therefore termed as hydroxyphenyl pyrone synthase (HppS).

Obviously, the product of *pcr10109* is also an α-pyrone derivative which has similar structure as hispidin and pyrophen. Comparing with the biosynthesis of hispidin and pyrophen, we proposed that the product **1** should also has the similar biosynthetic pathway, *i.e.*, the A domain of HppS recognizes *para*-hydroxybenzoic acid (PHBA) as a starter unit, which is then elongated by decarboxylative condensation with malonyl-CoA in two rounds under the catalysis of the KS domain. Finally, the pyrone product is off-loaded through lactonization (**Figure 18**). To prove this hypothesis, we performed feeding experiments with ^{13}C-labelled PHBA and sodium acetate in the heterologous expressing mutant *A. nidulans* JF021. The isotopic peak of the [M + H]$^+$ ion after [1-^{13}C] PHBA feeding was shifted from *m/z* 205.050 to 206.053 with an incorporation rate of 72%. What's more, the increased intensities of the isotopic peak of the [M + H + 1]$^+$ and [M + H + 2]$^+$ can be obviously observed after feeding with [1-^{13}C] and [2-^{13}C] acetate (**Figure 17b**). These results confirmed the involvement of one PHBA and two units of acetate molecules in the biosynthesis of compound **1** (**Figure 18**).
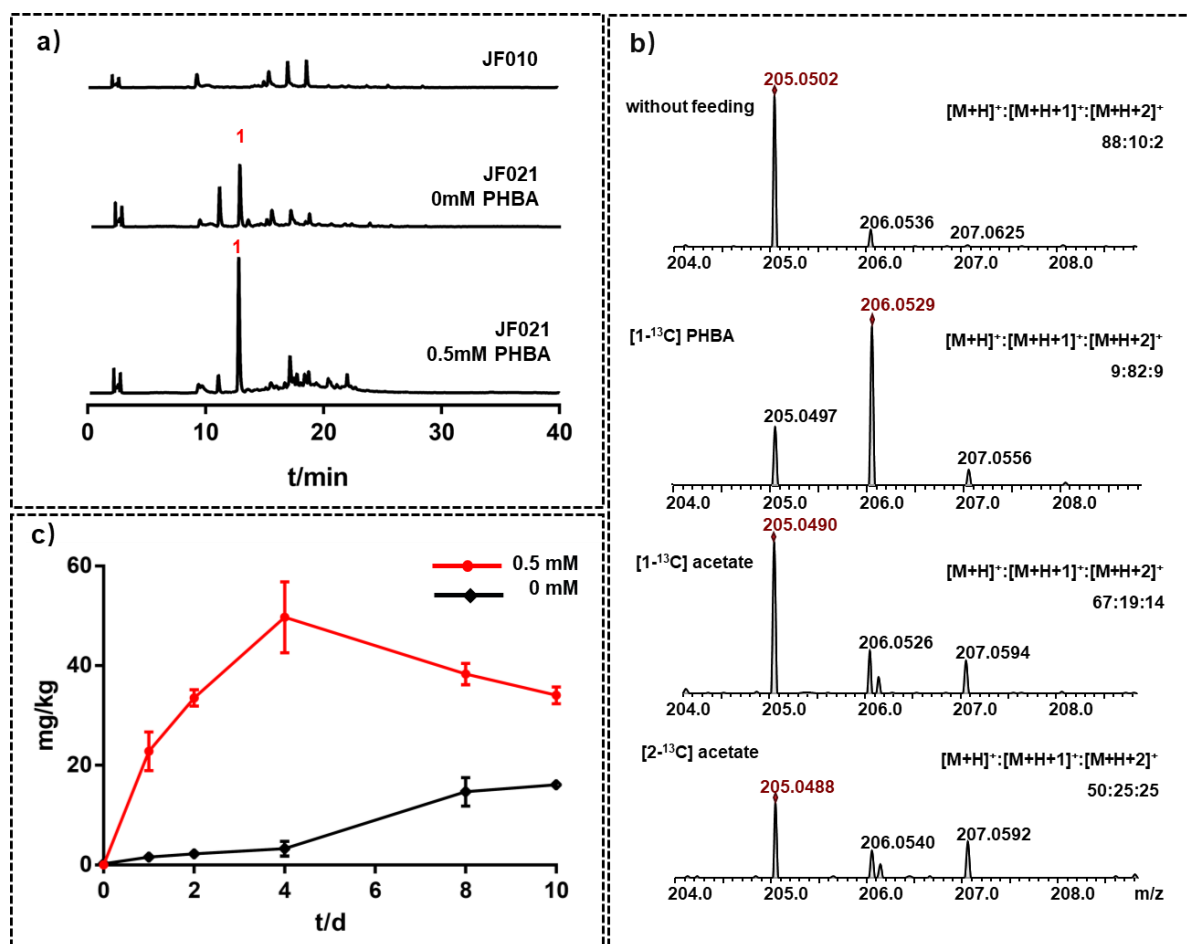
Figure 17. (a) LC-MS analysis of the SM profiles in different *A. nidulans* strains without and with PHBA feeding in rice media for 5 days. Absorptions at 340 nm are illustrated. (b) Isotopic patterns of [M + H]$^+$ ions of **1** from *A. nidulans* JF021 without and with ^{13}C-labelled precursors. (c) Dependence of product yields on cultivation times in *pcr10109*-expression strain without and with 0.5 mM fed PHBA.

To increase the product yield, we cultivated *pcr10109*-expressing strain *A. nidulans* JF021 in rice medium containing 0.5 mM PHBA for different days (**Figure 17c**). The results showed that addition of PHBA led to increasing product yield of **1**, which reached a maximum of 51 mg/kg rice media after 4 days incubation, approximately a five-fold of that without feeding. Cultivation of *A. nidulans* JF021 in the presence of 0.5 mM of cinnamic acid, *para*-coumaric acid or caffeic acid did not lead to accumulation of additional pyrone derivatives, demonstrating the relative high substrate specificity of HppS.

In summary, we successfully expressed the NRPS-PKS gene *pcr10109* from *P. crustosum* in *A. nidulans* and elucidated the biosynthesis of the accumulated product 4-hydroxy-6-(4-hydroxyphenyl)-α-pyrone. This study provides one additional example for the less explored

fungal NRPS-PKS hybrid enzymes. Precursor supply improved the product yield to five-fold of that without feeding. This strategy could be helpful for increasing product formation by supplementing of special substrates.
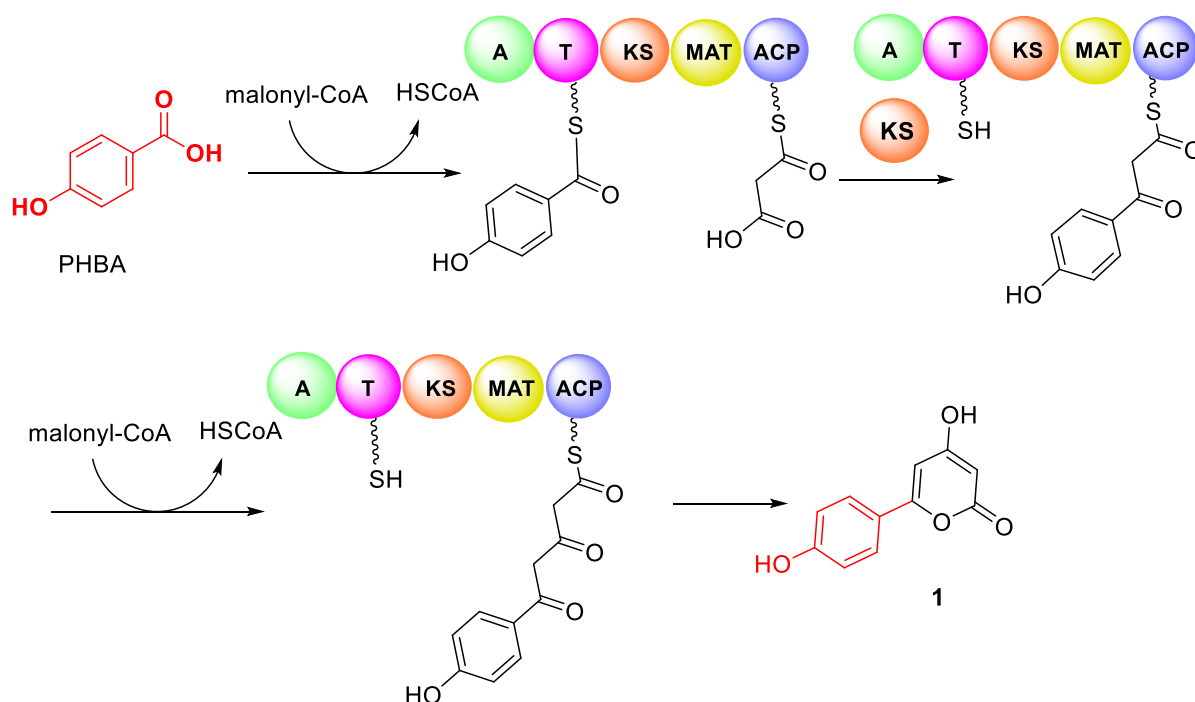
Figure 18. Proposed biosynthesis of the α-pyrone derivative **1**.

For details on this work, please see the publication (section 4.1)

3.2 Formation of diprenylated cyclodipeptides by changing the prenylation order with different prenyltransferases

Prenylated indole alkaloids are hybrid NPs widespread in bacteria, fungi, plants, and marine organisms,[254-256] which are important SMs with prominent agricultural and medicinal applications.[257-259] Prenylated Indole DKPs represent a promising category of them with wide range of biological and pharmacological activities, such as antitumor, antibacterial, immunomodulatory, antioxidant, and insecticidal activities.[137,142,260,261] Biosynthetically, such products are usually assembled by either a NRPS in fungi or a CDPS in bacteria using tryptophan and a second amino acid as substrates. The CDP core is then decorated by different PTs for the hybrid product formation. The PTs from the DMATS superfamily are well-studied members of this enzyme group, which are important biocatalysts and usually catalyze metal ion-independent Friedel-Crafts prenylations.[157,240,262] In nature, CDPs can be prenylated from N1 to C7 of the indole ring by different DMATSs. Therefore, they are usually used for structural modification of natural or unnatural products.[263] Until now, a series of multiprenylated indole DKPs from fungal have been identified and the PTs responsible for their biosynthesis were clearly elucidated. Interestingly, all these multiprenylated indole DKPs with *C2*-prenyl moieties share similar reaction steps. The CDP core is firstly prenylated by a *C2*-PT and later decorated with prenyl moieties at other positions of the indole ring.[152,157,264-266]

In this study, we intent to chemoenzymatic synthesize unnatural *C2,C4*-, *C2,C5*-, *C2,C6*-, and *C2,C7*-diprenylated *cyclo*-L-Trp-L-Pro (cWP) by utilizing different PTs. The five PTs EchPT1, FgaPT2_R244L, FgaPT2_Y398F, 6-DMATS$_{Sa}$, and 7-DMATS were reported to catalyze the prenylations at position C2, C4, C5, C6, C7 of the indole ring of CDPs, respectively.[142,144,157,267,268] Therefore, we selected these five enzymes for production of desired diprenylation *cyclo*-L-Trp-L-Pro (**2**).

At First, we purified these five proteins by Ni-NTA affinity chromatography. SDS-PAGE analysis revealed that all the five recombinant proteins were purified to near homogeneity (**Figure 19**). To get the *C2,C4*-, *C2,C5*-, *C2,C6*-, and *C2,C7*-diprenylated *cyclo*-L-Trp-L-Pro, we first followed the logic of the nature′s biosynthetic strategy mentioned above. The reverse *C2*-PT EchPT1 was selected as the first biocatalyst. After enzyme assays and product purification, we successfully obtained the *C2*-prenylated derivative deoxybrevianamide E (**3**) with a high conversion yield of 70.7 ± 0.5%. To obtain the desired diprenylated derivatives, compound **2** was used as substrate for the second prenylation by FgaPT2_R244L,

FgaPT2_Y398F, 6-DMATS$_{Sa}$, and 7-DMATS, respectively. Unfortunately, LC-MS analysis revealed that no products were detected in the incubation mixtures of FgaPT2_R244L and FgaPT2_Y398F. Formation of diprenylated products in the enzyme assays with 6-DMATS$_{Sa}$ and 7-DMATS was only detected in the extracted ion chromatograms (EICs). Obviously, product **2** was poor substrate for the tested enzymes.
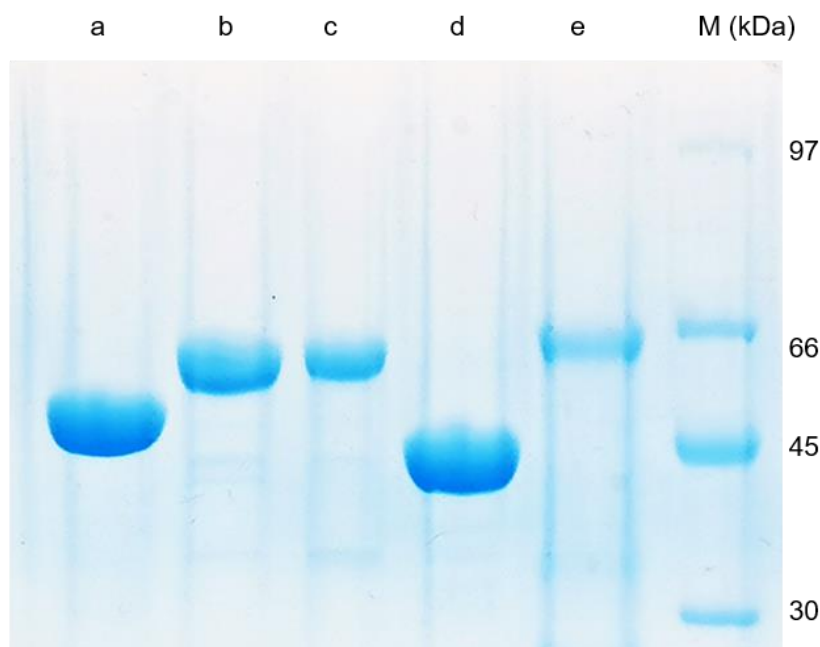

Figure 19. SDS-PAGE analysis of the purified PTs. The proteins were separated on a 12 % polyacrylamide gel. Lanes from left to right: a: EchPT1, b: FgaPT2_R244L, c: FgaPT2_Y398F, d: 6-DMATSSa, e: 7-DMATS, M: protein marker.

The enzyme assays performed by Dr. Lindsay Coby suggested that the *C2*-PT EchPT1 can catalyze the prenylations of monoprenylated cyclodipeptides. Based on the results, we did experiments to obtain the diprenylated derivatives in a reverse reaction order, *i.e.,* first use *C4*-, *C5*-, *C6*-, and *C7*-PTs for prenylation of the indole ring and then the monoprenylated derivatives were incubated with the *C2*-PT EchPT1 as the second prenylation step. To confirm this, substrate **2** was incubated with FgaPT2_R244L, FgaPT2_Y398F, 6-DMATS$_{sa}$, and 7-DMATS in the presence of DMAPP at 37 °C for 16 h. LC-MS analysis revealed that the products with $[M + H]^+$ at *m/z* 352.202 ± 0.005 can be detected in all the four reactions, indicating attachment of a dimethylallyl moiety to their structures (**Figure 20**). In the reaction mixtures with FgaPT2_R244L, 6-DMATS$_{sa,}$ and 7-DMATS, the conversion yields were determined to be 49.7 ± 0.2, 29.9 ± 0.6, and 11.6 ± 1.4%, respectively. There are two product peaks in the reaction mixture of FgaPT2_Y398F with conversion yields of 38.6 ± 0.8% and

28.1 ± 0.4%. They should be the *C4-* and *C5*-prenylated products described in the literature.[142,144,157,267,268] To elucidate the structures of the products, we enlarged the scale of enzyme assays and purified the products by HPLC. The products **6** and **7** were obtained in the reaction with 7-DMATS as a mixtures in a ratio of 0.6:1.0, which was consistent with 7-DMATS reaction for *cyclo*-L-Trp-D-Val.[247] In the ^{1}H NMR spectra of **4** – **7**, the regular dimethylallyl residue signals can be observed at δ_H 3.4 – 3.7 (d or dd, 2H-1′), 5.3 – 5.4 (tsept, H-2′), and 1.7 – 1.8 (one or two br s, 3H-4′ and 3H-5′). The four aromatic proton signals as well as ^{13}C, ^{1}H-^{1}H COSY, HSQC, and HMBC NMR analyses confirmed the products **4**, **5**, **6**, and **7** are *C4-*, *C5-*, *C6-*, and *C7*-prenylated *cyclo*-L-Trp-L-Pro, respectively (**Figure 20**).
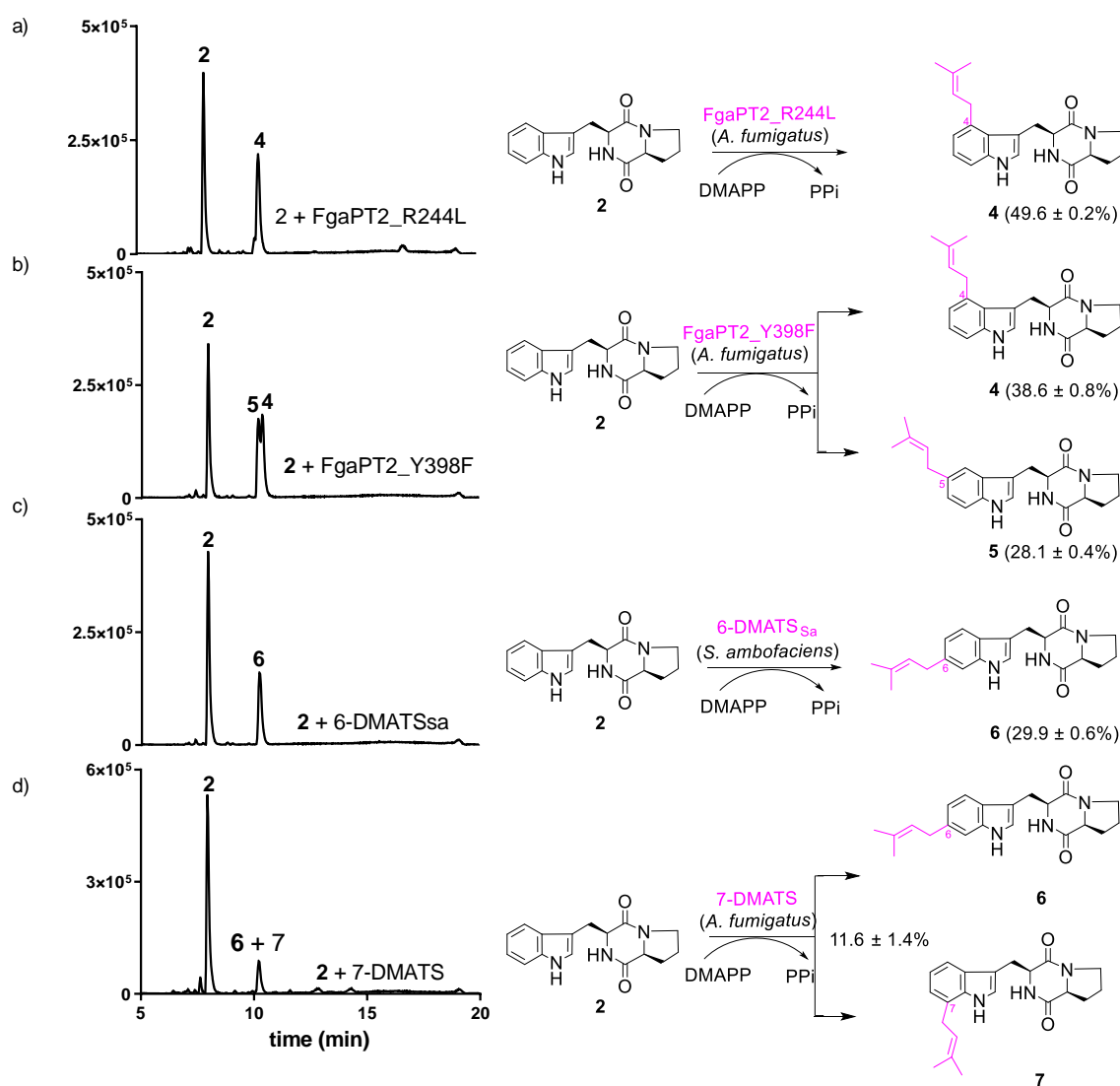
Figure 20. LC-MS analysis of *cyclo*-L-Trp-L-Pro (**2**) prenylation by (a) FgaPT2_R244L, (b) FgaPT2_Y398F, (c) 6-DMATS$_{Sa}$, and (d) 7-DMATS. UV absorptions at 280 nm are illustrated. All the assays were performed in duplicates. The conversion yields are given as mean values.
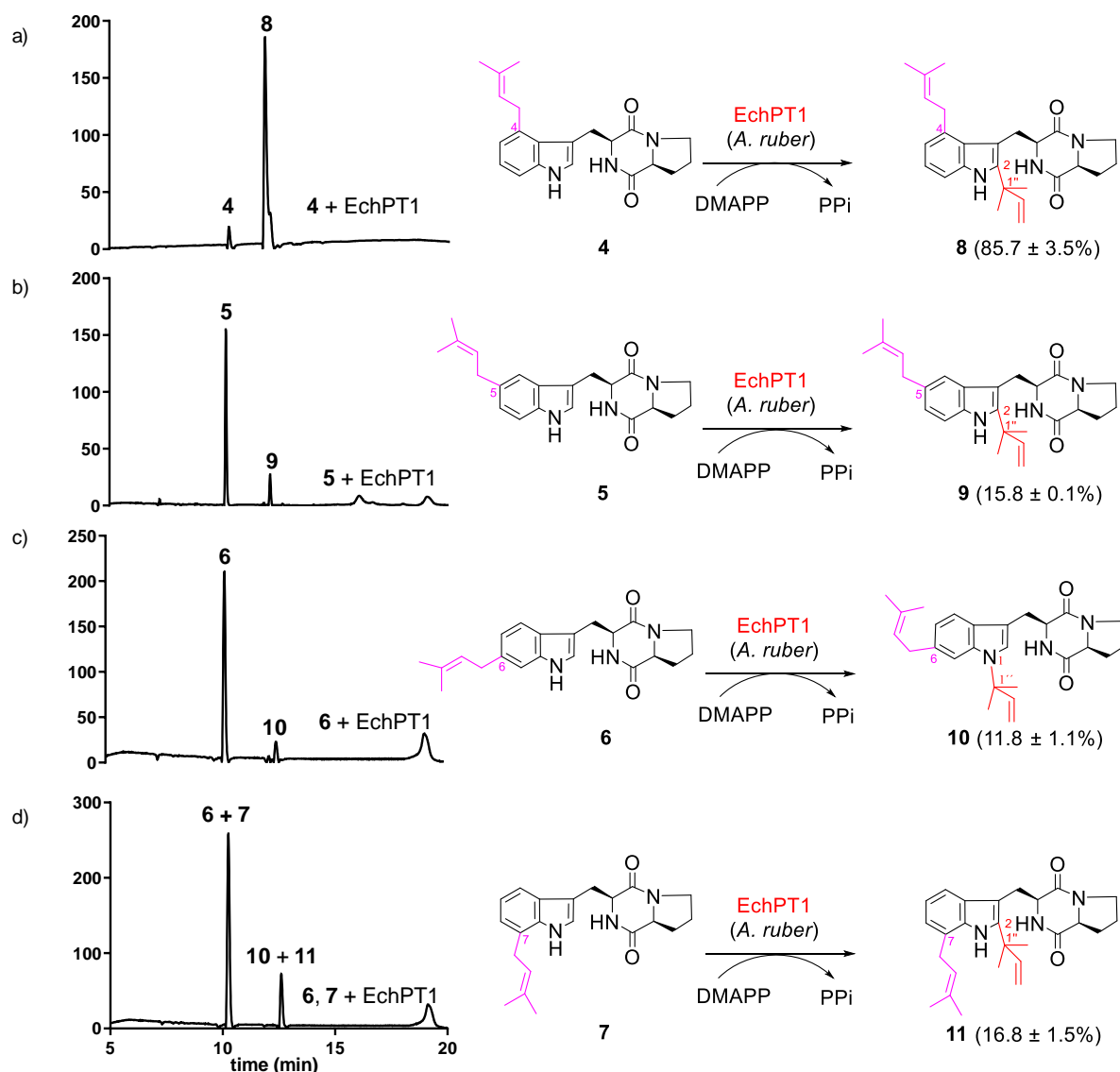
Figure 21. LC-MS analysis of the acceptance of monoprenylated derivatives (**4**, **5**, **6**, and **7**) by EchPT1. Products **10** and **11** were isolated from the incubation mixture of **6** with **7**. UV absorptions at 280 nm are illustrated. All the assays were performed in duplicates. The conversion yields are given as mean values.

After that, the four monoprenylated products were used as substrates for further reverse *C2*-prenylation by EchPT1. LC-MS results showed that all these four substrates were well accepted by EchPT1 with the highest conversion of $85.7 \pm 3.5\%$ for substrate **4** (**Figure 21**). Only one product peak was detected in all the four reactions. As we expected, all these four products have the $[M + H]^+$ ions of diprenylated *cyclo*-L-Trp-L-Pro at *m/z* 420.265 ± 0.005. The isolated products **8** – **11** from the enzyme assays with **4** – **7** were then subjected to MS and NMR analyses. In the ^{1}H NMR spectra of **8**, **9**, and **11**, the signal for H-2 disappeared. Instead,

additional signals for a reverse dimethylallyl moiety were detected at δ_H 6.12 – 6.14 (dd, 17, 10 Hz, H-2″), 5.17 – 5.20 (dd, 17, 0.6 Hz, H-3″), 5.16 – 5.23 (dd, 10, 0.6 Hz, H-3″), and 1.5 – 1.7 (two singlets, 3H-4″ and 3H-5″). In the ^{13}C NMR spectra, the signals of C-2 as well as those of C-1″, C-2″, C-3″, and C-4″/C-5″ of the reverse prenyl residue were observed at δ_c 141.1 – 141.8, 39.1 – 39.2, 145.8 – 145.9, 112.8 – 112.9, and 27.9 – 28.5 ppm, respectively. These data proved **8**, **9**, and **11** to be *C2,C4-*, *C2,C5-*, and *C2,C7-*diprenylated cWP. In the ^{1}H NMR spectra of compound **10**, the signal of NH-1 was disappeared and the signal for H-2 can be still detected at δ_H 7.11 ppm. Further interpretation of the ^{13}C NMR data suggests that the signals of C-2 and C-1″ of product **10** at δ_c 123.9 and 59.1, which differ from the other three compounds. Taken together of the NMR data, the structure of **10** was proven to be *N1,C6-*diprenylated derivative (**Figure 21**). The kinetic parameters of EchPT1 were then determined for the three aromatic substrates **4 – 6** and DMAPP. All the reactions followed the Michaelis – Menten kinetics and the catalytic efficiencies are in good consistence with the observed conversion yields.

In conclusion, we chemoenzymatic synthesized four unnatural *C2,C4-*, *C2,C5-*, *N1,C6-*, and *C2,C7-*diprenylated *cyclo*-L-Trp-L-Pro with significant yields. This is the first report that EchPT1 can also catalyze the unusual *N1-*prenylation at the indole ring other than C2 position.

3.3 Prenylation of dimeric *cyclo*-L-Trp-L-Trp by utilizing the promiscuous *cyclo*-L-Trp-L-Ala prenyltransferase EchPT1

The members of DMATS superfamily are important biocatalysts and used for structural modification of diverse small molecules.[241] Normally, they mainly efficiently prenylate tryptophan and tryptophan containing CDP derivatives, thus produced variety of biologically active prenylated products.[241,263] In addition to the aforementioned prenylated CDPs, several prenylated tryptophan containing dimeric CDPs have been isolated from different species in recent years with significant biological activities (**Figure 22**).[103-105] Interestingly, all these structures are *C2*-prenylated cWP or cWA dimers with different connections and symmetries. Attachment of the prenyl moieties onto the indole nucleus increases the spectrum of bioactivities compared with unprenylated dimeric CDPs. Due to rare examples of prenylating enzymes toward CDP dimers, we intended to get prenylated dimeric CDPs by the soluble DMATS in this study.
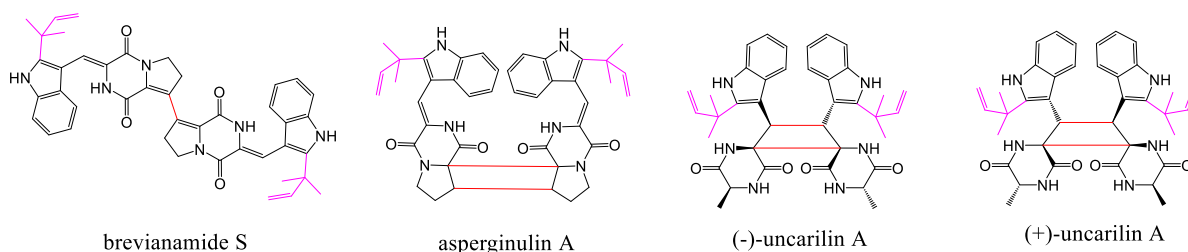
Figure 22. Examples of known prenylated tryptophan-containing dimeric CDPs.

We chose the five PTs EchPT1, FgaPT2_R244L, FgaPT2_Y398F, 6-DMATS$_{Sa}$, and 7-DMATS as tested enzymes.[142,144,157,267,268] Firstly, they were incubated with cWP dimer apergilazine A (**12**) and cWA-cWP dimer naseseazine A (**13**)[269] in the presence of DMAPP at 37 °C for 16h. LC-MS analysis showed that the monoprenylated **12** and **13** was only observed in the EICs of the reaction mixtures with *C2*-PT EchPT1, *C5*-PT FgaPT2_Y398F, and *C7*-PT 7-DMATS. This suggests that cWP-containing dimers were poorly accepted by the tested PTs.

After that, the cWW dimers tetratryptomycins A − C (**14 − 16**) with the symmetrical C3-C3′ and the unsymmetrical C3-N1′ linkage[270] were incubated with the five DMATSs for 16h. LC-MS showed that they were better accepted than substrates **12** and **13**. The C3-C3′ linked **14** and **16** were converted to **14a2** and **16a2** by EchPT1 with the conversion yields at 33.6 ± 0.3 and 14.2 ± 0.2%, respectively. The main product **15a1** accompanied by a second product **15a2** were detected in the reaction mixtures of the C3-N1′ linked **15** by EchPT1 with conversion yields at 12.0 ± 0.2 and 3.7 ± 0.3%, respectively (**Figure 23**). In comparison, the other four

enzymes showed lower conversion than EchPT1. FgaPT2_R244L showed only 8.8 ± 0.1% conversion yields toward **15** and 6.5 ± 2.0% toward **16** for monoprenylated products.
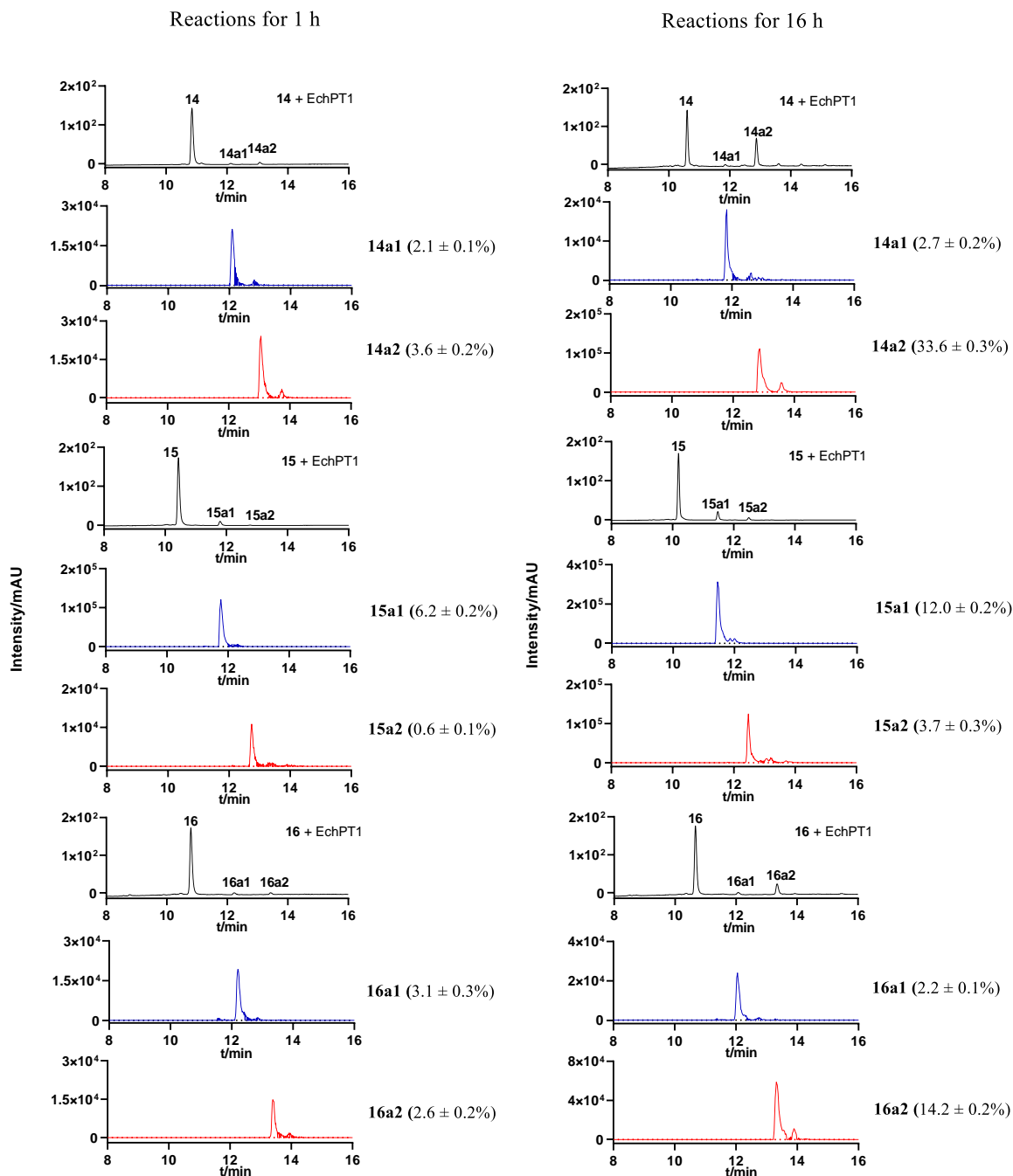

Figure 23. LC-MS analysis of the acceptance of tetratryptomycins A − C (**14 − 16**) by EchPT1 for 1 and 16 h. UV absorptions at 280 nm are illustrated in black. The chromatograms depicted in blue and red refer to EICs of [M + H]$^+$ of the monoprenylated at *m/z* 811.372 ± 0.005 and those of the diprenylated products at *m/z* 879.434 ± 0.005, respectively. All the assays were performed in duplicates. The conversion yields are given as mean values.

In order to detect the monoprenylated tetratryptomycins in the reactions with EchPT1, **14 − 16** were incubated in the presence of DMAPP for 1 h (**Figure 23**). As expected, both monoprenylated (**14a1**, **15a1**, and **16a1**) and diprenylated products (**14a2**, **15a2**, and **16a2**) can be detected with [M + H]$^+$ ions at *m/z* 811.372 ± 0.005 and 879.434 ± 0.005, respectively. The diprenylated product **15a2** with a conversion yield of 0.6 ± 0.1% was the lowest in the reaction mixtures, which proved that **15a1** was poor substrate of EchPT1 for prenylation compared with **14a1** and **16a1** (**Figure 23**). To further figure out the relationship of mono- and diprenylated products in the reaction mixtures of the three cWW dimers with EchPT1, time dependence of their formation was determined. The results correspond well to the results after incubation for 16 h and proved again **14a1** and **16a1** are better substrates of EchPT1 than **15a1**.
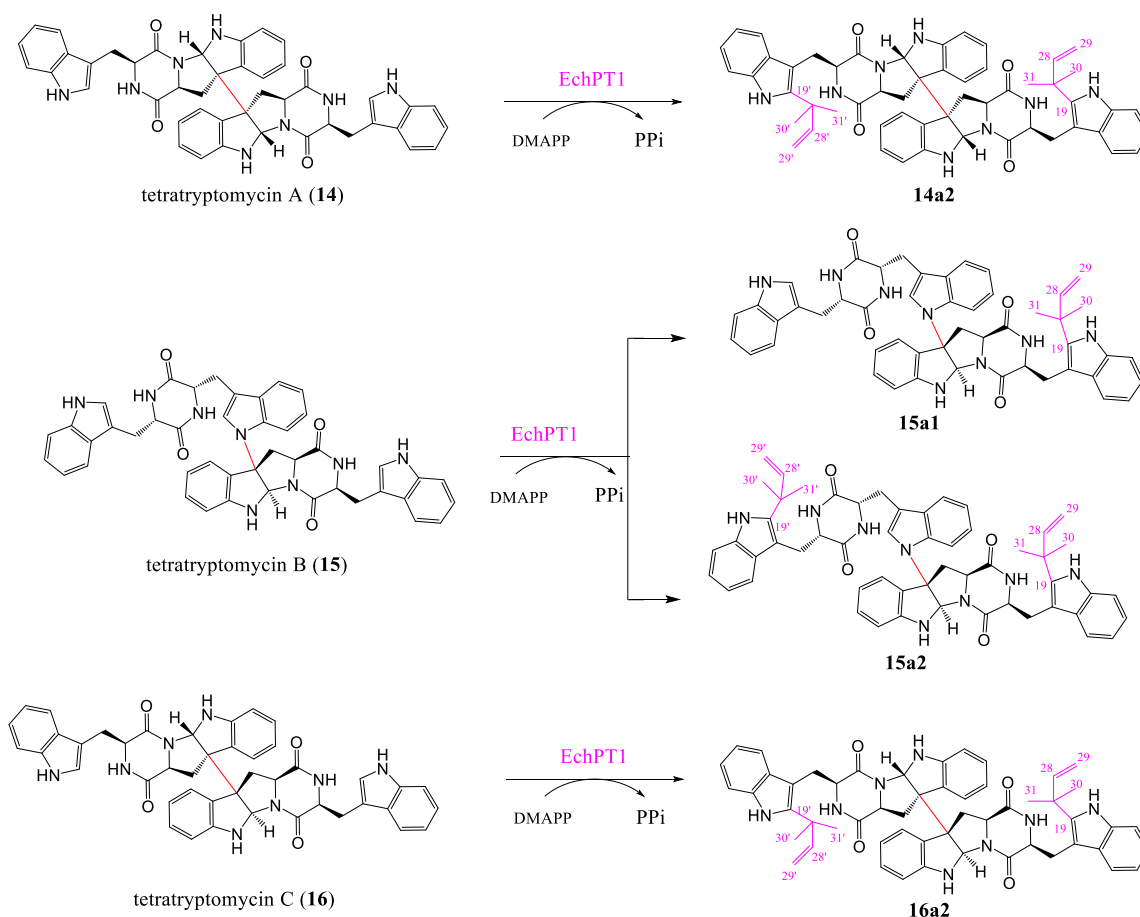
Figure 24. Prenylation of tetratryptomycins A − C by *cyclo*-L-Trp-L-Ala PT EchPT1 in the presence of DMAPP.

For structure elucidation, the enzyme assays were scaled up to 25 ml. After extraction and HPLC purification, we obtained the four prenylated products **14a2**, **15a1**, **15a2**, and **16a2** in high purity. In the ^{13}C NMR spectra, the signals for H-19 (**14a2**, **15a1**, **15a2**, and **16a2**) and H-

19′ (**14a2**, **15a2**, and **16a2**) disappeared. Instead, one (**15a1**) or two (**14a2**, **15a2**, and **16a2**) reverse prenyl moieties can be observed at δ_H 6.15 – 6.23 (dd, H-28/H-28′), 5.00 – 5.11 (d or dd, 2H-29/2H-29′), and 1.46 – 1.52 (s, 3H-30 and 3H-31/3H-30′ and 3H-31′) comparing with those of **14** − **16**.[270] In the ^{13}C NMR spectra, the signals of C-19/C-19′ at the indole ring were observed at δc 141.4 – 141.5ppm. Clear long-range correlations between H-28 (H-30/H-31) and C-19 (**14a2**, **15a1**, **15a2**, and **16a2**) as well as H-28′ (H-30′/H-31′) and C-19′ (**14a2**, **15a2**, and **16a2**) were observed in the HMBC spectra, proving the attachment of one or two reverse prenyl moieties at C-19 and C-19′. Taken together of the NMR data, the structure of **15a1** was proven to be *C19*-prenylated tetratryptomycin B and **14a2**, **15a2**, and **16a2** are *C19,C19′*-diprenylated tetratryptomycins A, B, and C, respectively (**Figure 24**), which is consistent with the EchPT1-catalyzed *C2*-prenylation for its natural substrate *cyclo*-L-Trp-L-Ala.

Finally, kinetic parameters including K_M and k_{cat} of EchPT1 were calculated toward DMAPP and the three dimeric CDPs. The results indicated that the K_M values toward DMAPP for the formation of the four products are slightly lower than that of *cyclo*-L-Trp-L-Ala. The k_{cat}/K_M values were also determined in the range of EchPT1 reactions toward most CDPs.[152]

The results presented in this project expanded the spectrum of prenylated dimeric CDPs. Furthermore, due to the remarkable biological activities of prenylated cyclodipeptides, these prenylated dimetric products could be of significant importance for drug discovery and development process.

<u>For details on this work, please see the publication (section 4.3)</u>

Wen Li, Xiulan Xie, Jing Liu, Huili Yu and Shu-Ming Li (2023) Prenylation of dimeric *cyclo*-L-Trp-L-Trp by the promiscuous *cyclo*-L-Trp-L-Ala prenyltransferase EchPT1. *Applied Microbiology and Biotechnology*, (submitted).

4 Publications

4.1 Discovery of 4-hydroxy-6-(4-hydroxyphenyl)-α-pyrone in *Penicillium crustosum* by heterologous expression of an NRPS-PKS gene and precursor feeding experiments

Note

Precursor Supply Increases the Accumulation of 4-Hydroxy-6-(4-hydroxyphenyl)-α-pyrone after NRPS−PKS Gene Expression

Wen Li, Jie Fan, Ge Liao, Wen-Bing Yin, and Shu-Ming Li*

Cite This: *J. Nat. Prod.* 2021, 84, 2380−2384

Read Online

ACCESS | Metrics & More | Article Recommendations | SI Supporting Information

ABSTRACT: Expression of a nonribosomal peptide synthetase-nonreducing polyketide synthase hybrid gene *pcr10109* from *Penicillium crustosum* PRB-2 in *Aspergillus nidulans* led to the accumulation of 4-hydroxy-6-(4-hydroxyphenyl)-α-pyrone (**1**). Adding *para*-hydroxybenzoic acid into the medium in which the overexpressing mutant is growing increased the product yield up to 5-fold. This strategy could be helpful for heterologous gene expression experiments requiring special substrates for product formation.
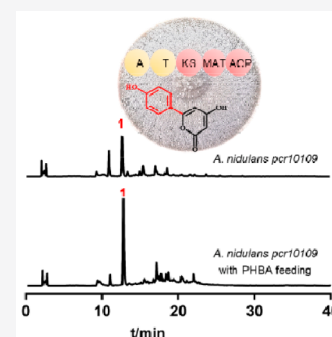
Fungal polyketide synthases (PKSs) and nonribosomal peptide synthetases (NRPSs) are multidomain enzymes involved in the biosynthesis of two large natural product groups.[1−3] Hybrid enzymes with PKS domains at the N-terminus and NRPS domains at the C-terminus (PKS−NRPS hybrid) also frequently exist in microorganisms, including fungi, and are responsible for the formation of diverse biologically active amide-containing secondary metabolites.[4,5] In comparison, NRPS−PKS hybrid enzymes with NRPS at the N- and PKS at the C-terminus have rarely been reported from fungi.[6] Representative examples are SwnK from *Metarhizium robertsii*,[7,8] HispS from *Neonothopanus nambi*,[9] and AnATPKS from *Aspergillus niger*,[10] which assemble swainsonine, hispidin, and pyrophen, respectively (Figure 1). All three enzymes, SwnK, HispS, and AnATPKS, share a domain structure A-T-KS-MAT-ACP (A: adenylation, T: thiolation, KS: ketosynthase, MAT: malonyl acyl transferase, ACP: acyl carrier protein). In the case of SwnK, an additional KR (ketoreductase) and R (reductase) domain are placed before and after the ACP domain, respectively. Differing from PKS−NRPS hybrid enzymes, all these enzymes catalyze C−C bond formation by addition of acetyl units from malonyl-CoA to the starter units. The products of HispS and AnATPKS are α-pyrone derivatives. α-Pyrone natural products are usually formed by pure polyketide synthases.[11] Pyrone derivatives were reported to possess a wide range of biological and pharmacological activities.[12,13] 4-Hydroxyphenyl pyrone was reported as a useful lead structure for the development of new anticancer agents.[14] More interestingly, HispS uses caffeic acid instead of an amino acid as its substrate for activation and catalyzes the formation of a nitrogen-free product. Obviously,

the enzymes from this less explored group have great potential for new structures.

We identified a putative gene, *pcr10109*, from the genome sequence of *Penicillium crustosum* PRB-2,[15] coding for an NRPS−PKS hybrid enzyme with the same domain structure A-T-KS-MAT-ACP as in the cases of HispS and AnATPKS. *pcr10109*, comprising 5270 bps, differs from PCG10_010218 of another *P. crustosum* strain, G10, only in four positions. T445, T1179, A1269, and A1997 in Pcr10109 are replaced by A, C, G, and G, respectively. However, these mutations caused only one difference in the deduced 1710 amino acid length polypeptide. The cysteine residue at position 149 of the gene product from PRB-2 is changed to threonine in KAF7528682 (GenBank) of strain G10. KAF7528682 shares sequence similarities/identities of 50%/33% and 46%/29% with HispS (BBH43485.1) and AnATPKS (EHA27898.1), respectively. This low homology raised our curiosity about its function and our decision to delete *pcr10109* from the genome of *P. crustosum* PRB-2.

For this purpose, the genomic sequence of *pcr10109* was replaced by a hygromycin B resistance cassette using a split-marker strategy [Figure S1, in the Supporting Information (SI)], as reported previously.[15,16] PRB-2 and the obtained deletion mutant strain JF019 (Table S1, SI) were cultivated in various media for different times, as established for production
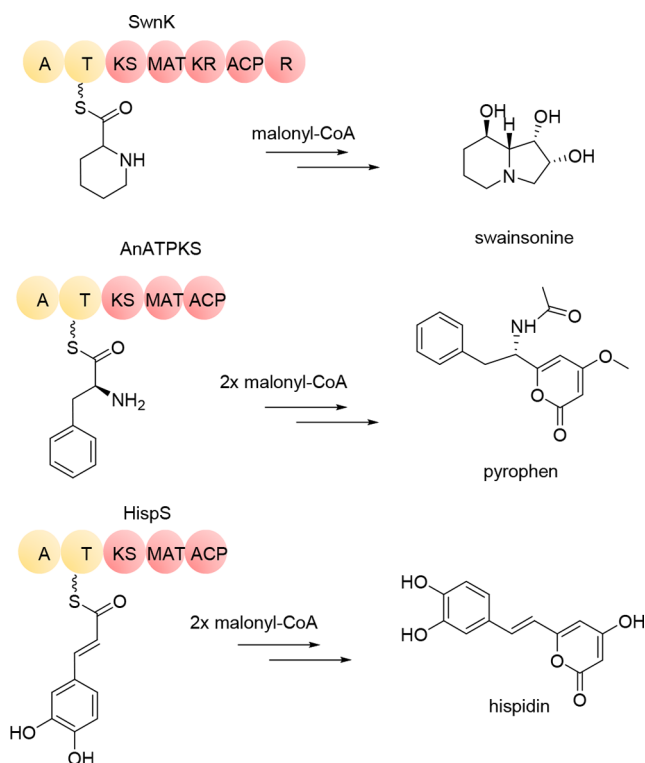
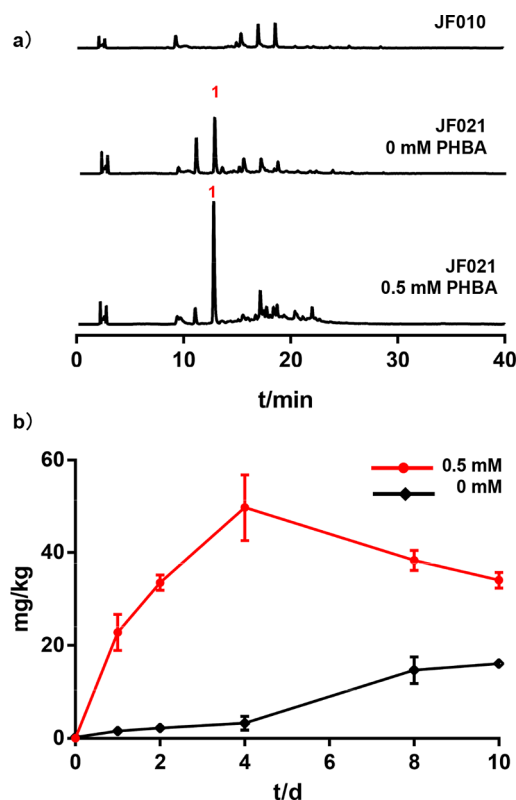**Figure 1.** Examples of NRP−PK hybrids from fungi.

Figure 2. (a) LC-MS analysis of the secondary metabolite profiles in different *A. nidulans* strains without and with PHBA feeding in rice media for 5 days. Absorptions at 340 nm are illustrated. (b) Dependence of product yields on cultivation times in *pcr10109*-expression strain without and with 0.5 mM PHBA.

of other metabolites from this fungus.[15,16] LC-MS analysis of the ethyl acetate extracts revealed, however, no obvious difference in secondary metabolite profiles (Figure S2, in rice medium as an example), indicating no or very low expression of *pcr10109* in the wild-type strain under the cultivation conditions used.

To explore the function of *pcr10109*, we changed our strategy to heterologous expression. The whole genomic sequence of the target gene and its downstream sequence of 543 bps were amplified by PCR using primers listed in Table S2 (SI) and cloned as a 5813 bps fragment into the expression vector pYH-wA-pyrG under the control of the strong *gpdA* promoter through homologous recombination in *Saccharomyces cerevisiae* to create the expression construct pJF84 (Table S3, SI).[17] The obtained construct pJF84 was introduced into *Aspergillus nidulans* LO8030 via PEG-mediated protoplast transformation.[17] The potential transformants were selected by uridine/uracil autotrophy and verified by PCR amplification (Figure S3). The resulted transformant *A. nidulans* JF021 was cultivated in rice medium for secondary metabolite production. *A. nidulans* JF010 containing the empty vector pYH-wA-pyrG was used as a negative control.

The 5-day-old cultures were extracted with ethyl acetate and analyzed on LC-MS. As shown in Figure 2a, one additional peak, **1**, was detected in the extract of the transformant JF021, which was absent in the control strain. Detailed inspection of this peak revealed a [M + H]⁺ ion at *m/z* = 205.0494 and a distinct UV absorption at 340 nm (Figure S4). For structure elucidation, **1** was isolated from a large-scale fermentation and subjected to NMR analysis. Two coupling systems at δ_H 7.68 (d, 8.8, 2H) and 6.87 (d, 8.8, 2H) as well as 5.28 (d, 1.9, 1H) and 6.53 (d, 1.9, 1H) were observed in the ¹H NMR spectrum of compound **1** (Table S4, Figure S5). The UV and MS data are consistent with those of 4-hydroxy-6-(4-hydroxyphenyl)-

2*H*-pyran-2-one.[18] However, our ¹H NMR data differ slightly from material obtained by chemical synthesis.[18] Additional NMR spectra including ¹³C, COSY, HSQC, and HMBC (Figures S6−S9) confirmed **1** to be 4-hydroxy-6-(4-hydroxyphenyl)-2*H*-pyran-2-one. The NRPS−PKS encoded by *pcr10109* was therefore termed as hydroxyphenyl pyrone synthase (HppS).

According to the structural similarities with hispidin and pyrophen,[9,10] **1** is very likely biosynthesized in a similar way. We propose that the A domain of HppS recognizes *para*-hydroxybenzoic acid (PHBA) as a starter unit, which is elongated by decarboxylative condensation with malonyl-CoA in two rounds under the catalysis of the KS domain. The pyrone product is then off-loaded through lactonization (Figure 3). Differing from the substrate preference of HispS for caffeic acid and AnATPKS for L-phenylalanine, HppS uses an aromatic acid with a shorter side chain as substrate.

To prove this hypothesis, we performed feeding experiments with ¹³C labeling PHBA and sodium acetate in *A. nidulans* JF021 (Figure 4). In comparison to that of **1** in *A. nidulans* JF021 without feeding, the dominant isotopic peak of the [M + H]⁺ ion after [1-¹³C] PHBA feeding was shifted from *m/z* 205.050 to 206.053, proving the involvement of one molecule of [1-¹³C] PHBA with a incorporation rate of 72%. Correspondingly, incorporation of up to two ¹³C atoms was observed after feeding with [1-¹³C] and [2-¹³C] acetate, with clearly increased intensities of the [M + H + 2]⁺ peaks in both cases (Figure 4). These results confirmed the involvement of one PHBA and two acetate molecules in the biosynthesis of **1** (Figure 3).
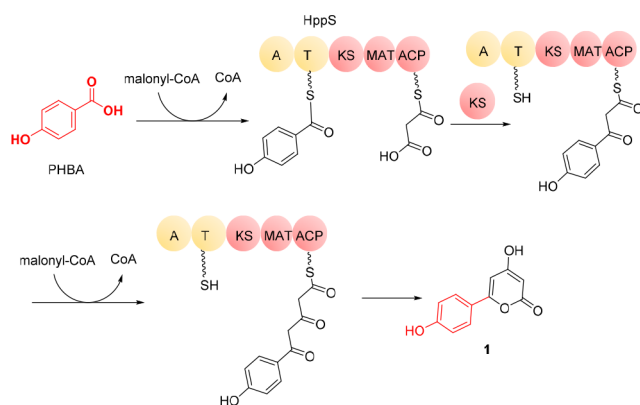
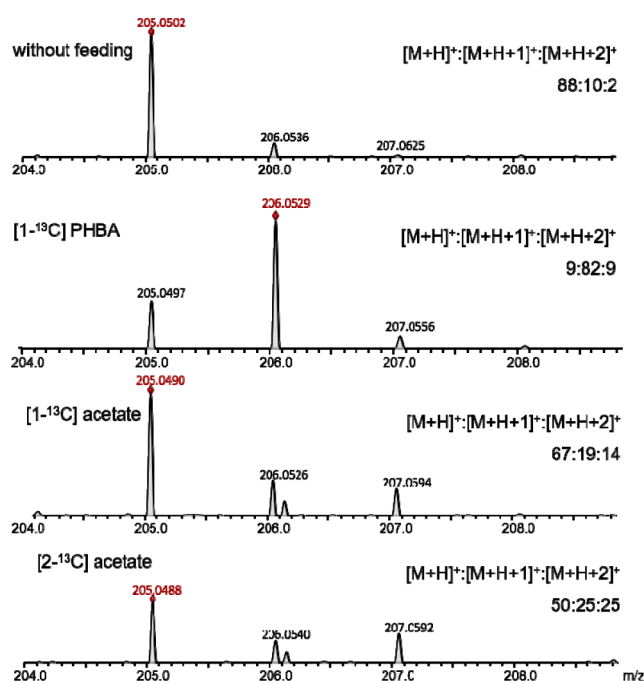**Figure 3.** Proposed biosynthesis of the pyrone derivative **1**.

Figure 4. Isotopic patterns of [M + H]⁺ ions of **1** from *A. nidulans* JF021 without and with ¹³C-labeled precursor feeding.

In comparison to yields of some PKS genes,[19,20] productivity was low, with 10 mg of **1** being produced per kg of rice medium after 1 week of cultivation (Figure 2b). This could indicate a substrate limitation, since no PHBA-forming enzyme has been reported for *A. nidulans*. PHBA is a common degradation product of *para*-coumaric acid in plants and plant biomass,[21] but relatively rare in fungi. We speculate that PHBA for the formation of **1** is supplied from the rice medium. No candidate genes for PHBA formation could be found in the genome of *P. crustosum*. To increase the product yield, we cultivated *pcr10109*-expressing strain JF021 in rice medium containing 0.5 mM PHBA for different times (Figure 2b). Addition of PHBA led to an increase of **1** accumulation, which reached a maximum of 51 mg per kg rice after 4 days of incubation, approximately 5-fold of that obtained, without feeding, after 8 days. Cultivation of *A. nidulans* JF021 in the presence of 0.5 mM cinnamic acid, *para*-coumaric acid, or caffeic acid did not lead to accumulation of additional pyrone derivatives (data not shown), demonstrating the relative high

substrate specificity of HppS, in comparison to the relaxed one of AnATPKS.[10]

Our results provide one additional example for the less explored fungal NRPS−PKS hybrid enzymes. The strategy used in this study could also be helpful for the discovery of products encoded by cryptic genes.

■ EXPERIMENTAL SECTION

General Experimental Procedures. NMR spectra were recorded on a JEOL ECA-500 MHz spectrometer (JEOL, Tokyo, Japan), and all spectra were processed with MestReNova 6.1.0 (Metrelab). Chemical shifts are referred to those of the solvent signals. High-resolution mass spectrometric analysis was performed on an Agilent 1260 HPLC system equipped with a microTOF-Q III spectrometer (Bruker, Bremen, Germany) using a Multospher 120 RP18-5 μ column (250 × 2 mm, 5 μm) (CS-Chromatographie Service GmbH). Electrospray positive ionization mode was selected for determination of the exact masses. The capillary voltage was set to 4.5 kV and a collision energy of 8.0 eV. Sodium formate was used in each run for mass calibration. The masses were scanned in the range of m/z 100−1500. Data were evaluated with the Compass DataAnalysis 4.2 software (Bruker Daltonik, Bremen, Germany). Semipreparative HPLC was performed on the same HPLC equipment with an Agilent Eclipse XDB-C$_{18}$ column (9.4 × 250 mm, 5 μm). Silica gel 60 (230−400 meshes, Carl Roth, Karlsruhe, Germany) was used for column chromatography and precoated TLC silica gel 60 F$_{254}$ plates (Merck, Darmstadt, Germany) for detection of the desired substance in the fractions.

Fungal Strains and Culture Media. *Penicillium crustosum* PRB-2 was cultivated on PDA medium at 25 °C for sporulation. *Aspergillus nidulans* LO8030 was grown at 37 °C on GMM medium (1.0% glucose, 50 mL/L salt solution, 1 mL/L trace element solution, 1.6% agar) with 50 mg/L riboflavin, 20 mg/L pyridoxine, 1.2 g/L uridine, and 1.0 g/L uracil as supplements for sporulation and transformation. *Saccharomyces cerevisiae* BJ5464-NpgA was grown in YPD media (1.0% yeast extract, 1.0% peptone, 2.0% glucose, 1.6% agar) at 30 °C for constructing the plasmid of heterologous expression. *Escherichia coli* DH5α was grown in LB medium for standard DNA propagation. Carbenicillin (50 μg/mL) was supplemented for cultivation of recombinant *E. coli* strains.

Gene Cloning and Transformation. Primers and plasmids used for PCR are given in Tables S2 and S3. Primers were synthesized by Seqlab GmbH (Göttingen, Germany). PCR amplification was carried out using Phusion High-Fidelity DNA polymerase.

To identify if *pcr10109* is expressed in the wild-type strain, we deleted the whole gene *pcr10109* using a split-marker approach.[22] Around 1.5 kb upstream and downstream fragments were amplified from *P. crustosum* genomic DNA using the designed primers listed in Table S2. The two fragments were then inserted into linear vector p5HY and p3YG using an *E. coli* recombination system.[23]

To construct the plasmid for heterologous expression, *pcr10109* including its terminator region of 543 bps, was amplified from genomic DNA of *P. crustosum* using primers An-pcr10109-F and An-pcr10109-R (Table S2) and inserted into pYH-wA-pyrG with flanking sequences of the *wA* gene of *A. nidulans* through homologous recombination in *S. cerevisiae* BJ5464-NpgA.[17] Transformations of *P. crustosum* and *A. nidulans* were followed by PEG-mediated protoplast transformation as reported previously.[15,19,20]

Extraction and Isolation of Secondary Metabolites. To monitor the metabolite profile, *P. crustosum* PRB-2 and JF019 as well as *A. nidulans* JF021 and JF010 were cultivated on 10 g of long-grain rice in 15 mL of H$_2$O, with or without 0.06 mg of riboflavin and 125 mg of yeast extract as supplements, at 25 °C for 5 days. The rice cultures were extracted with ethyl acetate and analyzed by LC-MS described below.

To isolate **1** for structure elucidation, *A. nidulans* JF021 was cultivated in 4 kg of rice supplemented with 25 mg of riboflavin and 50 g of yeast extract at 25 °C for 5 days. After extraction of the culture with ethyl acetate, the organic extracts were concentrated under

45

reduced pressure to afford an extract (50 g), which was subjected to silica gel column chromatography using stepwise gradient elution with mixtures of petroleum ether—ethyl acetate (5:1, 3:1, to 1:1, v/v). Fractions 22−26 eluted with petroleum ether—ethyl acetate (1:1) was further purified on semipreparative HPLC (acetonitrile—H_2O, 50:50 with 0.1% trifluoroacetic acid) to yield 4-hydroxy-6-(4-hydroxyphenyl)-2H-pyran-2-one (**1**) (3 mg). For ^{13}C NMR, COSY, HMQC, and HMBC spectra, 7 mg of **1** was isolated again from cultures of *A. nidulans* JF021 in 2 kg of rice media after feeding with 22 mg of PHBA via a similar procedure.

4-Hydroxy-6-(4-hydroxyphenyl)-2H-pyran-2-one (1): yellow powder; ^1H (500 MHz) and ^{13}C (125 MHz) NMR in DMSO-d_6, see Table S4; HRESIMS *m/z* 205.0494 [M + H]$^+$ (calcd for $C_{11}H_9O_4$, 205.0495).

Feeding Experiments. For precursor feeding experiments, *A. nidulans* JF021 was cultivated in 25 mL flasks each containing 4 g of rice in 6 mL of H_2O with 0.03 mg riboflavin, 50 mg yeast extract, and 0.5 mM PHBA for 1, 2, 4, 8, and 10 days. The ethyl acetate extracts were analyzed on HPLC. Product yields were calculated from three independent replicates.

For labeling experiments, appropriate amounts of *A. nidulans* JF021 spores were transferred from plates into 25 mL flasks containing 5 mL of PDB medium and cultivated at 230 rpm and 25 °C. Two milligrams of sodium [1-^{13}C] acetate, sodium [2-^{13}C] acetate, and [1-^{13}C] PHBA were fed 30 h after inoculation. After cultivation for another 48 h, the cultures were extracted with ethyl acetate and analyzed on LC-MS.

LC-MS and HPLC Analysis of Secondary Metabolites. For LC-MS analysis, water (A) and acetonitrile (B), both with 0.1% (v/v) formic acid, were used as solvents at a flow rate of 0.25 mL/min. The substances were eluted with a linear gradient from 5% to 100% B in 40 min, then washed with 100% (v/v) solvent B for 5 min and equilibrated with 5% (v/v) solvent B for 10 min. HPLC was performed using water (A) and acetonitrile (B) at a flow rate of 0.5 mL/min with the same elution conditions.

■ ASSOCIATED CONTENT

Ⓢ Supporting Information

The Supporting Information is available free of charge at https://pubs.acs.org/doi/10.1021/acs.jnatprod.1c00120.

Supplementary tables and figures (PDF)

■ AUTHOR INFORMATION

Corresponding Author

    Shu-Ming Li − *Institut für Pharmazeutische Biologie und Biotechnologie, Fachbereich Pharmazie, Philipps-Universität Marburg, 35037 Marburg, Germany;* ⓘ orcid.org/0000-0003-4583-2655; Email: shuming.li@staff.uni-marburg.de

Authors

    Wen Li − *Institut für Pharmazeutische Biologie und Biotechnologie, Fachbereich Pharmazie, Philipps-Universität Marburg, 35037 Marburg, Germany*

    Jie Fan − *Institut für Pharmazeutische Biologie und Biotechnologie, Fachbereich Pharmazie, Philipps-Universität Marburg, 35037 Marburg, Germany; State Key Laboratory of Mycology, Institute of Microbiology, Chinese Academy of Sciences, 100101 Beijing, People's Republic of China;* ⓘ orcid.org/0000-0003-4720-8581

    Ge Liao − *Institut für Pharmazeutische Biologie und Biotechnologie, Fachbereich Pharmazie, Philipps-Universität Marburg, 35037 Marburg, Germany; Present Address: Institute of Tropical Bioscience and Biotechnology, Chinese Academy of Tropical Agricultural Sciences, 571101 Haikou, People's Republic of China*

Wen-Bing Yin − *State Key Laboratory of Mycology, Institute of Microbiology, Chinese Academy of Sciences, 100101 Beijing, People's Republic of China;* ⓘ orcid.org/0000-0002-9184-3198

Complete contact information is available at:
https://pubs.acs.org/10.1021/acs.jnatprod.1c00120

Notes

The authors declare no competing financial interest.

■ ACKNOWLEDGMENTS

■ REFERENCES

(1) Horsman, M. E.; Hari, T. P.; Boddy, C. N. *Nat. Prod. Rep.* **2016**, *33*, 183−202.

(2) Cox, R. J. *Org. Biomol. Chem.* **2007**, *5*, 2010−2026.

(3) Süssmuth, R. D.; Mainz, A. *Angew. Chem., Int. Ed.* **2017**, *56*, 3770−3821.

(4) Miyanaga, A.; Kudo, F.; Eguchi, T. *Nat. Prod. Rep.* **2018**, *35*, 1185−1209.

(5) Boettger, D.; Hertweck, C. *ChemBioChem* **2013**, *14*, 28−42.

(6) Theobald, S.; Vesth, T. C.; Andersen, M. R. *BMC Genomics* **2019**, *20*, 847.

(7) Luo, F. F.; Hong, S.; Chen, B.; Yin, Y.; Tang, G.; Hu, F. L.; Zhang, H. Z.; Wang, C. S. *ACS Chem. Biol.* **2020**, *15*, 2476−2484.

(8) Cook, D.; Donzelli, B. G. G.; Creamer, R.; Baucom, D. L.; Gardner, D. R.; Pan, J.; Moore, N.; Krasnoff, S. B.; Jaromczyk, J. W.; Schardl, C. L. *G3: Genes, Genomes, Genet.* **2017**, *7*, 1791−1797.

(9) Kotlobay, A. A.; Sarkisyan, K. S.; Mokrushina, Y. A.; Marcet-Houben, M.; Serebrovskaya, E. O.; Markina, N. M.; Gonzalez, S. L.; Gorokhovatsky, A. Y.; Vvedensky, A.; Purtov, K. V. *Proc. Natl. Acad. Sci. U. S. A.* **2018**, *115*, 12728−12732 and others.

(10) Hai, Y.; Huang, A.; Tang, Y. *J. Nat. Prod.* **2020**, *83*, 593−600.

(11) Schäberle, T. F. *Beilstein J. Org. Chem.* **2016**, *12*, 571−588.

(12) Cooney, J. M.; Vanneste, J. L.; Lauren, D. R.; Hill, R. A. *Lett. Appl. Microbiol.* **1997**, *24*, 47−50.

(13) Zhao, Q.; Wang, C. X.; Yu, Y.; Wang, G. Q.; Zheng, Q. C.; Chen, G. D.; Lian, Y. Y.; Lin, F.; Guo, L. D.; Gao, H. *J. Asian Nat. Prod. Res.* **2015**, *17*, 567−575.

(14) Dong, Y. Z.; Shi, Q.; Nakagawa-Goto, K.; Wu, P. C.; Morris-Natschke, S. L.; Brossi, A.; Bastow, K. F.; Lang, J. Y.; Hung, M. C.; Lee, K. H. *Bioorg. Med. Chem.* **2010**, *18*, 803−808.

(15) Fan, J.; Liao, G.; Kindinger, F.; Ludwig-Radtke, L.; Yin, W.-B.; Li, S.-M. *J. Am. Chem. Soc.* **2019**, *141*, 4225−4229.

(16) Fan, J.; Liao, G.; Ludwig-Radtke, L.; Yin, W.-B.; Li, S.-M. *Org. Lett.* **2020**, *22*, 88−92.

(17) Yin, W. B.; Chooi, Y. H.; Smith, A. R.; Cacho, R. A.; Hu, Y.; White, T. C.; Tang, Y. *ACS Synth. Biol.* **2013**, *2*, 629−634.

(18) Weber, V.; Coudert, P.; Duroux, E.; Leal, F.; Couquelet, J.; Madesclaire, M. *Arzneim. Forsch.* **2001**, *51*, 877−884.

(19) Xiang, P.; Ludwig-Radtke, L.; Yin, W.-B.; Li, S.-M. *Org. Biomol. Chem.* **2020**, *18*, 4946−4948.

(20) Zheng, L.; Yang, Y.; Wang, H.; Fan, A.; Zhang, L.; Li, S.-M. *Org. Lett.* **2020**, *22*, 7837−7841.

(21) Tinikul, R.; Chenprakhon, P.; Maenpuen, S.; Chaiyen, P. *Biotechnol. J.* **2018**, *13*, No. e1700632.

(22) Rahnama, M.; Forester, N.; Ariyawansa, K. G. S. U.; Voisey, C. R.; Johnson, L. J.; Johnson, R. D.; Fleetwood, D. J. *J. Microbiol. Methods* **2017**, *134*, 62−65.

(23) Jacobus, A. P.; Gross, J. *PLoS One* **2015**, *10*, No. e0119221.

47

Supporting Information

Precursor supply increases the accumulation of 4-hydroxy-6-(4-hydroxyphenyl)-α-pyrone after NRPS-PKS gene expression

Wen Li,[†] Jie Fan,[†,‡] Ge Liao,[†,§] Wen-Bing Yin,[‡] Shu-Ming Li*,[†]

[†] Institut für Pharmazeutische Biologie und Biotechnologie, Fachbereich Pharmazie, Philipps-Universität Marburg, Robert-Koch Straße 4, 35037 Marburg, Germany

[‡] State Key Laboratory of Mycology, Institute of Microbiology, Chinese Academy of Sciences, 100101 Beijing, People's Republic of China

[§] Present address: Institute of Tropical Bioscience and Biotechnology, Chinese Academy of Tropical Agricultural Sciences, 571101 Haikou, People's Republic of China

Corresponding to Shu-Ming Li, E-mail: shuming.li@staff.uni-marburg.de

Table S1. Fungal strains used in this study

Strains	Genotype	Source/Ref.
Penicillium crustosum		
PRB-2	Wildtype	Fan *et al*[1]
JF019	Δ*pcr10109::hph* in *P. crustosum* PRB-2	This study
Aspergillus nidulans		
LO8030	*pyroA*4, *riboB*2, *AfpyrG*89, *nkuA::argB*, deletion of secondary metabolite clusters: (AN7804-AN7825)Δ, (AN2545-AN2549)Δ, (AN1039-AN1029)Δ, (AN10023-AN10021)Δ, (AN8512-AN8520)Δ, (AN8379-AN8384)Δ, (AN9246-AN9259)Δ, (AN7906-AN7915)Δ, (AN6000-AN6002)Δ.	Chiang *et al*[2]
JF010	gpdA*::AfpyrG* in *A. nidulans* LO8030	This study
JF021	gpdA*::pcr10109::AfpyrG* in *A. nidulans* LO8030	This study
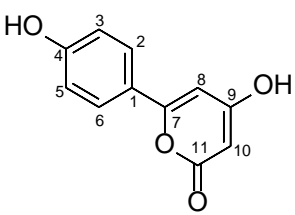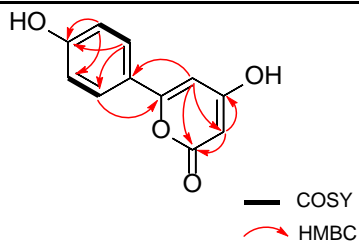
Table S2. Primers used in this study

Primers	Sequence of oligonucleotides (5´-3´)	Description
p5HYpcr10109-F	GAAGAATTGTTAATTAAGAGCTCAGATCTCTCTGGAGTCGTTGATGCG	For PCR amplification of a 1312 bp upstream fragment of *pcr10109* from *P. crustosum* PRB-2 to construct plasmid pJF11
p5HYpcr10109-R	CCCTCACTAAAGGGCGGCCGCACTAGCAAAAACATACAACAGTGAGGAT	
p3YGpcr10109-F	GACTCACTATAGGGCCCGGGCGTCGACGATTAGCGCAGGATGTTTTGG	For PCR amplification of 1260 bp downstream fragment of *pcr10109* from *P. crustosum* PRB-2 to construct plasmid pJF12
p3YGpcr10109-R	GCTAGCCGCGGTACCAAGCTTACTCGAGGCACGGAAAATGATGAACTGG	
Dele-1-F	CTCTTGATTTGAGAATACAAC	For PCR amplification of 1854 bp upstream of *hph* to verify deletion mutant *P. crustosum* JF019
5F-scr-R	GCTGAAGTCGATTTGAGTCCAC	
3F-scr-F	GCATTAATGCATTGgACcTcGC	For PCR amplification of 1661 bp downstream of *hph* to verify deletion mutant *P. crustosum* JF019
Dele-2-R	CGGTGATATAAAATCCCCACCG	
KOc pcr10109-F	GCATCCCAGGCAGAACTAACC	For PCR amplification of 918 bp partial fragment of *pcr10109* to verify strains JF019 and JF021
KOc pcr10109-R	GTATCCAAGCATGAAGCTTGGG	
An-pcr10109-F	cccatccaagaacctttaatcgctagcATGGCTGAGATCTACTCAGTGG	For PCR amplification of 5270 bp of *pcr10109* and 543 bp of its terminator from *P. crustosum* PRB-2 to construct plasmid pJF84
An-pcr10109-R	atttcgtcagacacagaataactctcCTGGTCTAACCAATCTTGGAAGG	

Table S3. Plasmids used and constructed in this study

Plasmids	Description	Source/Ref
p5HY	Two-third of the *hph* resistance gene at the 5´-end, originated from the pUChph and inserted into pESC-URA. For gene replacement using *hph* as selection marker	Fan *et al*[1]
p3YG	Two-third of the *hph* resistance gene at the 3´-end, originated from the pUChph and inserted into pESC-URA. For gene replacement using *hph* as selection marker	Fan *et al*[1]
pJF11	Derived from p5HY by inserting 1312 bp upstream sequence of *pcr10109* obtained with the primers p5HYpcr10109-F and p5HYpcr10109-R	This study
pJF12	Derived from p3YG by inserting 1260 bp downstream sequence of *pcr10109* obtained with the primers p3YGpcr10109-F and p3YGpcr10109-R	This study
pYH-wA-pyrG	*URA3*, *wA flanking*, *AfpyrG*, *Amp*	Yin *et al*[β]
pJF84	Derived from pYH-wA-pyrG by inserting 5270 bp *pcr10109* and 543 bp of its terminator obtained with the primers An-pcr10109-F and An-pcr10109-R	This study

Table S4. The chemical structure of **1** and its ^{1}H NMR data in DMSO-d_6 (500 MHz, δ in ppm, J in Hz).

Position	$\delta_{H,}$ (multi. J)	δ_C	HMBC
1	-	121.9	
2	7.68, d, 8.8	127.3	C-4, C-6, C-7
3	6.87, d, 8.8	115.8	C-1, C-4, C-5
4	-	160.0	
5	6.87, d, 8.8	115.8	C-1, C-3, C-4
6	7.68, d, 8.8	127.3	C-2, C-4, C-7
7	-	160.7	
8	6.53, d, 1.9	96.0	C-1, C-7, C-10, C-11
9	-	163.2	
10	5.28, d, 1.9	88.3	C-8, C-9, C-11
11	-	170.9	
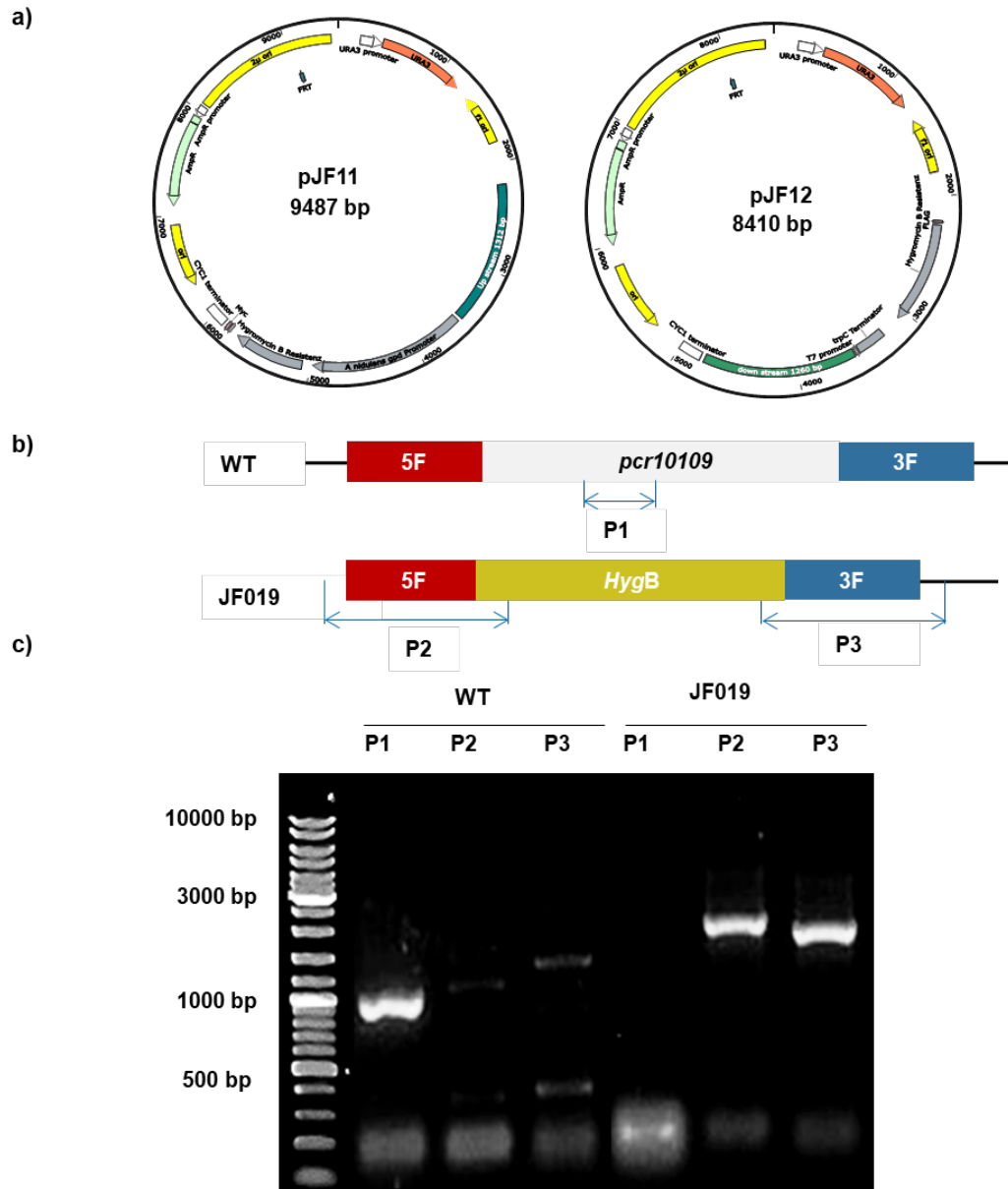
Figure S1. (a) Plasmids for *pcr10109* deletion. (b) Schematic presentation of sequence regions for PCR verification of *Penicillium crustosum* JF019. (c) PCR results for verification of JF019. M: DNA marker; P1: expected size of 918 bp with primers KOc pcr10109-F/ KOc pcr10109-R; P2: expected size of 1854 bp with primers Dele-1-F/ 5F-scr-R; P3: expected size of 1661 bp with primers 3F-scr-F/ Dele-2-R.

6
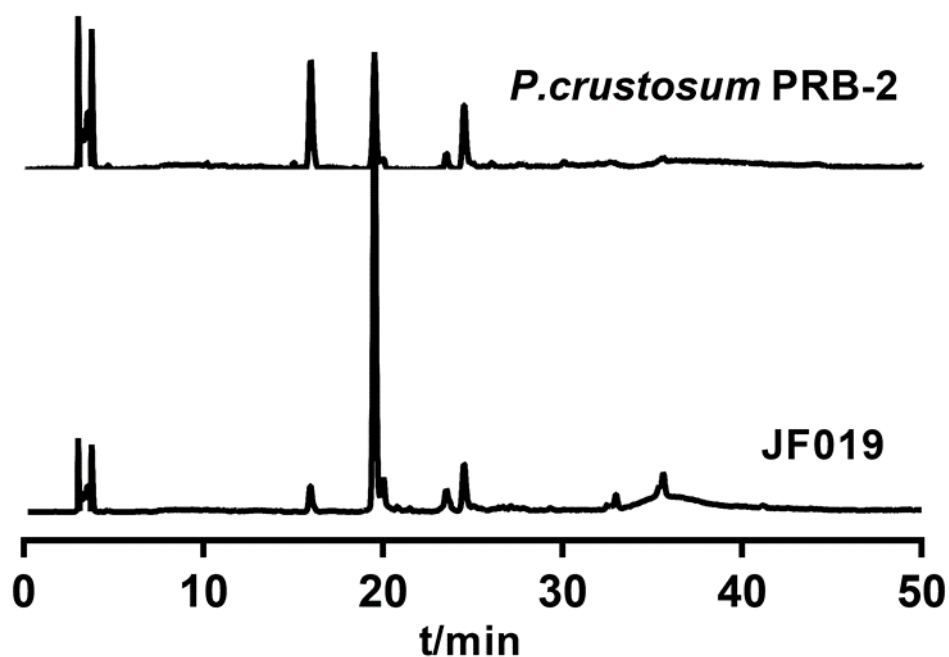
Figure S2. HPLC analysis of the secondary metabolites from *Penicillium crustosum* wild type and JF019 in rice media for 5 days. Absorption at UV 340 nm are illustrated.
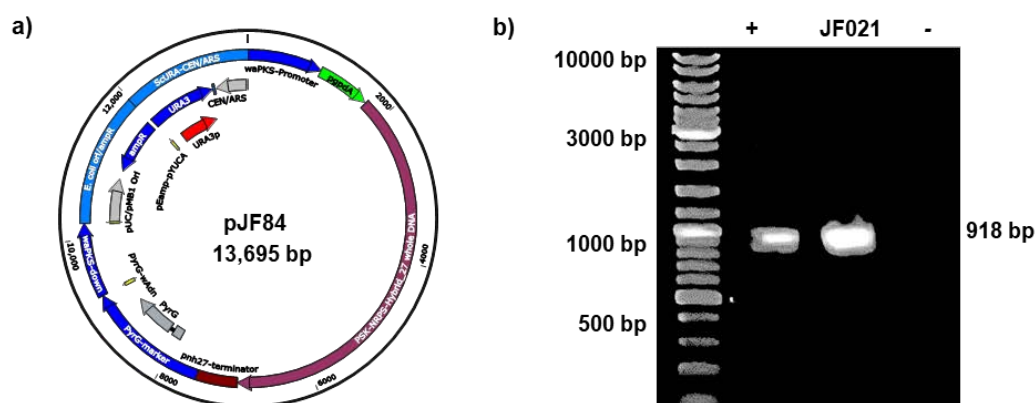
Figure S3. (a) Construct for *pcr10109* expression. (b) Verification of the expression mutant JF021 by PCR amplification with primers KOc pcr10109-F/ KOc pcr10109-R. M: DNA marker; +: Construct pJF84 as template; -: genomic DNA of *A. nidulans* LO8030 as template. The expected PCR product was calculated for 918 bp.

7
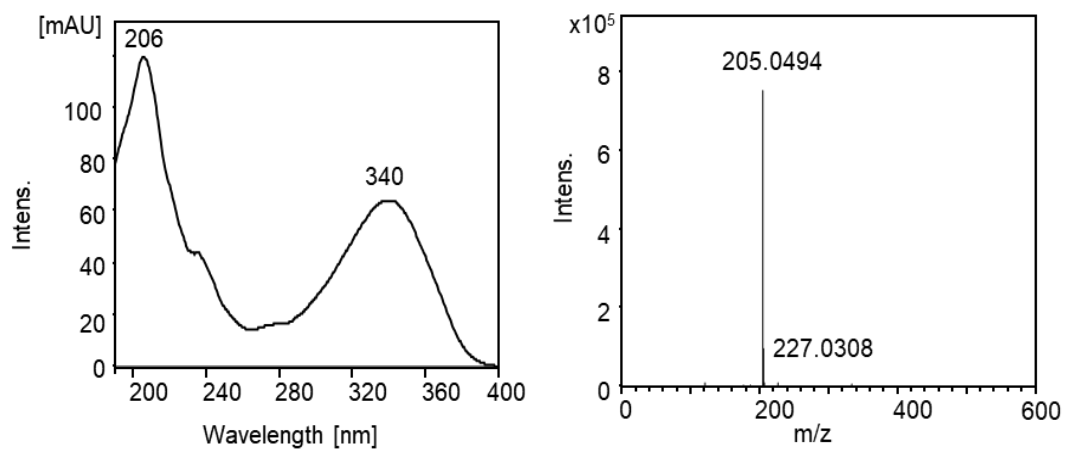
Figure S4. The UV-Vis spectrum and HR-ESI-MS data of **1**
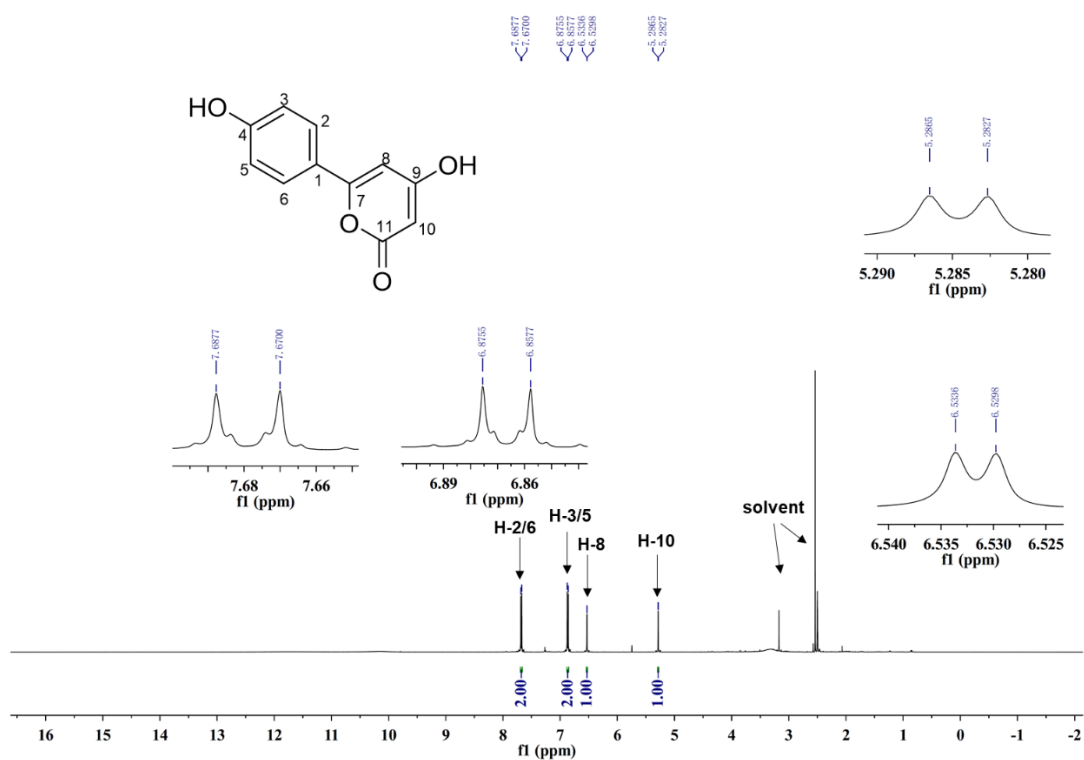
Figure S5. ^{1}H NMR spectrum of **1** in DMSO-d_6 (500 MHz).

8

56
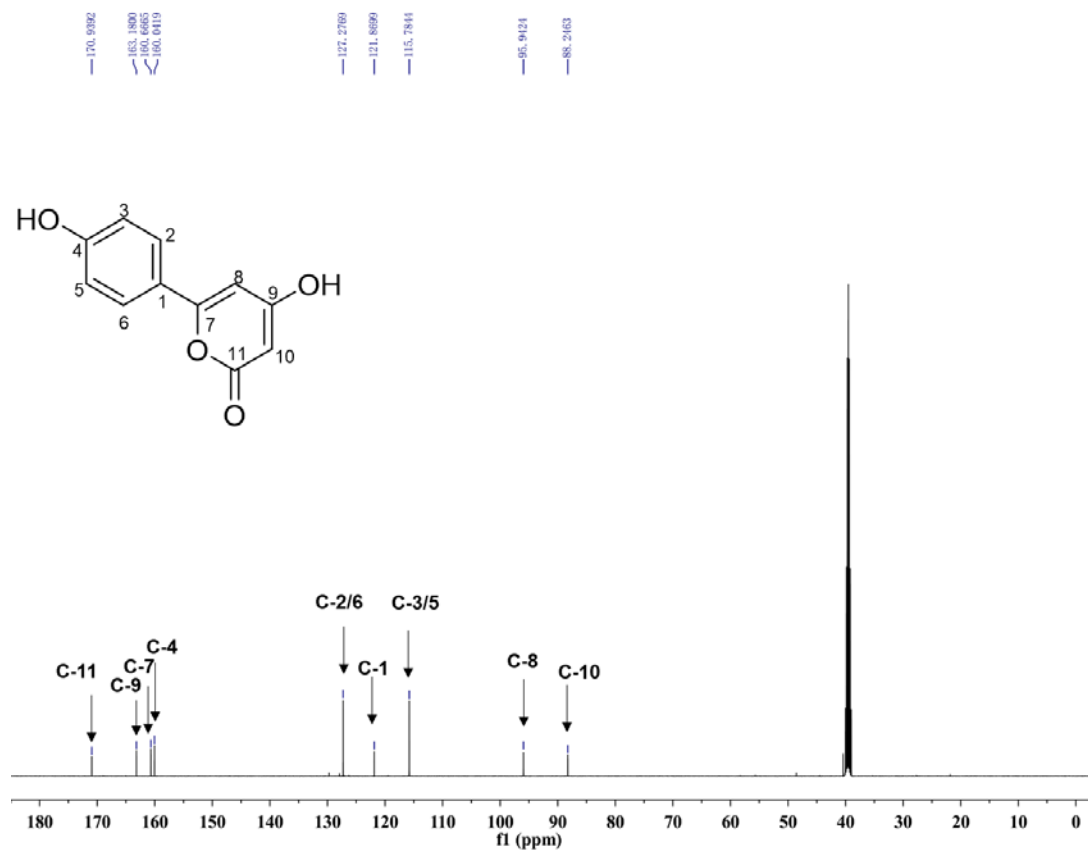
Figure S6. $^{13}C\{^{1}H\}$ NMR spectrum of **1** in DMSO-d_6 (125 MHz).
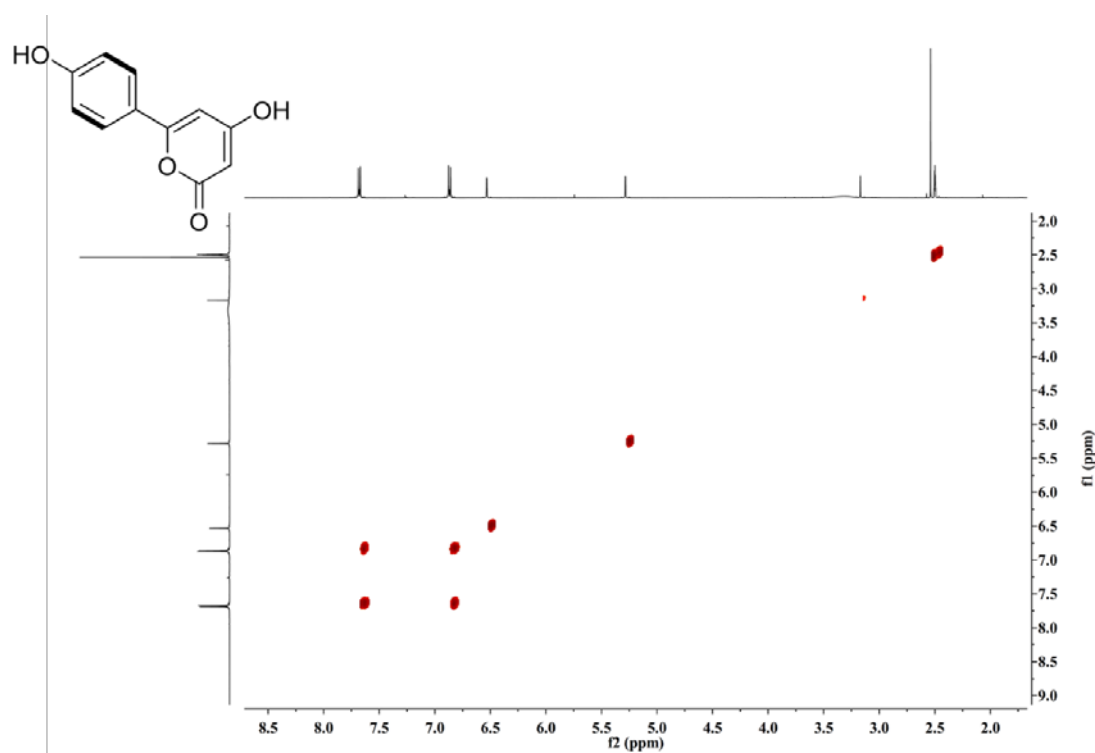
Figure S7. COSY spectrum of **1** in DMSO-d_6.

9
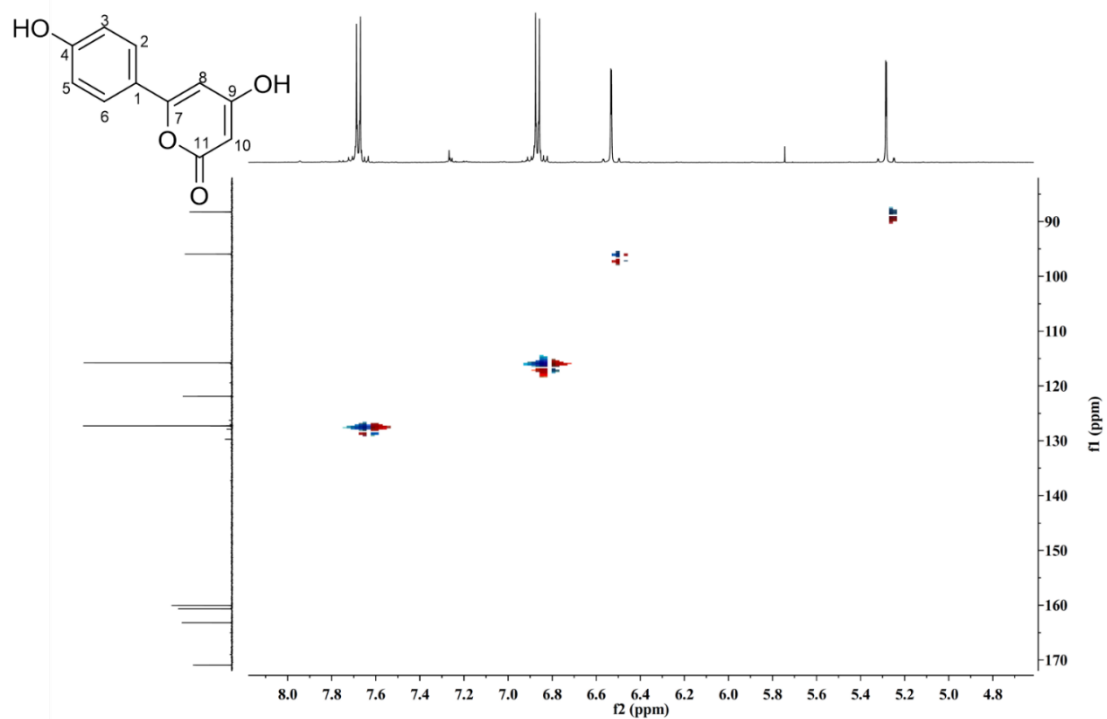
Figure S8. HSQC spectrum of **1** in DMSO-*d₆*.
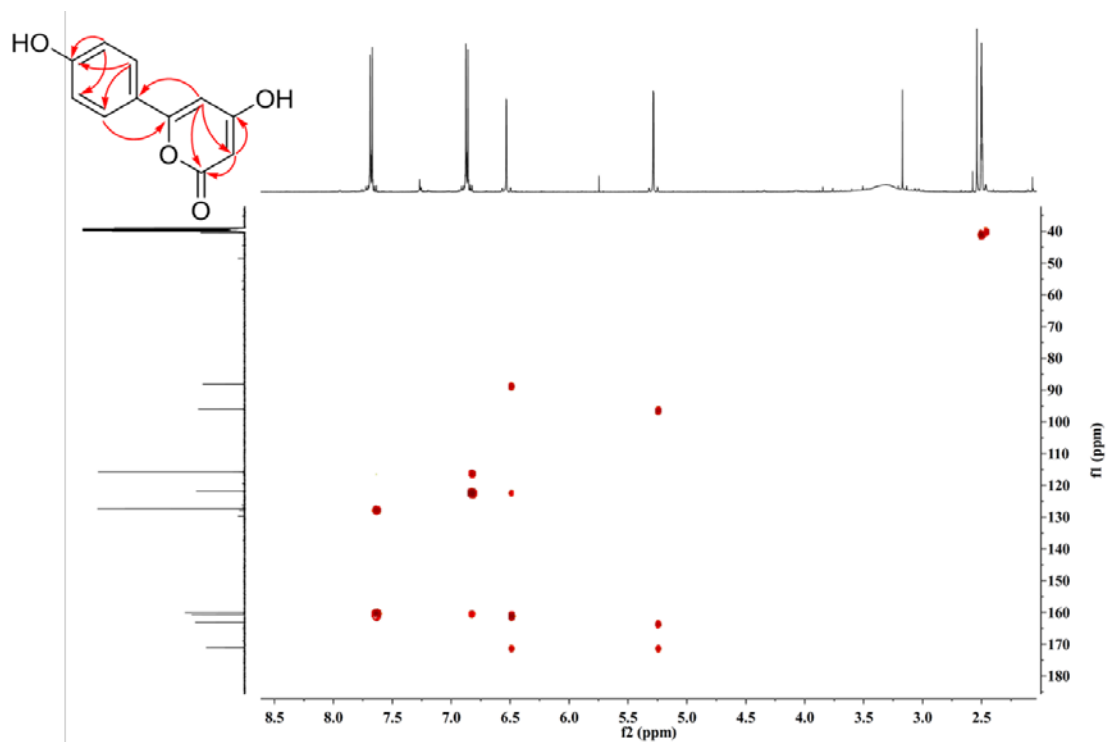
Figure S9. HMBC spectrum of **1** in DMSO-*d₆*.

10

Supplementary References

(1) Fan, J.; Liao, G.; Kindinger, F.; Ludwig-Radtke, L.; Yin, W.-B.; Li, S.-M. *J. Am. Chem. Soc.* **2019**, *141*, 4225-4229.

(2) Chiang, Y. M.; Ahuja, M.; Oakley, C. E.; Entwistle, R.; Asokan, A.; Zutz, C.; Wang, C. C.; Oakley, B. R. *Angew. Chem. Int. Ed. Engl.* **2016**, *55*, 1662-1665.

(3) Yin, W. B.; Chooi, Y. H.; Smith, A. R.; Cacho, R. A.; Hu, Y.; White, T. C.; Tang, Y. *ACS Synth. Biol.* **2013**, *2*, 629-634.

11

4.2 Formation of diprenylated cyclodipeptides by changing the prenylation order with different prenyltransferases

BIOTECHNOLOGICALLY RELEVANT ENZYMES AND PROTEINS

Diprenylated cyclodipeptide production by changing the prenylation sequence of the nature's synthetic machinery

Wen Li[1] · Lindsay Coby[1] · Jing Zhou[1] · Shu-Ming Li[1]

Abstract

Ascomycetous fungi are often found in agricultural products and foods as contaminants. They produce hazardous mycotoxins for human and animals. On the other hand, the fungal metabolites including mycotoxins are important drug candidates and the enzymes involved in the biosynthesis of these compounds are valuable biocatalysts for production of designed compounds. One of the enzyme groups are members of the dimethylallyl tryptophan synthase superfamily, which mainly catalyze prenylations of tryptophan and tryptophan-containing cyclodipeptides (CDPs). Decoration of CDPs in the biosynthesis of multiple prenylated metabolites in nature is usually initiated by regiospecific *C2*-prenylation at the indole ring, followed by second and third ones as well as by other modifications. However, the strict substrate specificity can prohibit the further prenylation of unnatural *C2*-prenylated compounds. To overcome this, we firstly obtained *C4*-, *C5*-, *C6*-, and *C7*-prenylated *cyclo*-L-Trp-L-Pro. These products were then used as substrates for the promiscuous *C2*-prenyltransferase EchPT1, which normally uses the unprenylated CDPs as substrates. Four unnatural diprenylated *cyclo*-L-Trp-L-Pro including the unique unexpected *N1,C6*-diprenylated derivative with significant yields were obtained in this way. Our study provides an excellent example for increasing structural diversity by reprogramming the reaction orders of natural biosynthetic pathways. Furthermore, this is the first report that EchPT1 can also catalyze *N1*-prenylation at the indole ring.

Key points

- *Prenyltransferases as biocatalysts for unnatural substrates.*
- *Chemoenzymatic synthesis of designed molecules.*
- *A cyclodipeptide prenyltransferase as prenylating enzyme of already prenylated products.*

Keywords Cyclodipeptides · Multiple prenylation · Indole prenyltransferases · EchPT1 · Chemoenzymatic synthesis

Introduction

Microorganisms, especially ascomycetous fungi, are often found in contaminated agricultural products like food crops including corns, grain, fruits, and vegetables as well as poorly conserved foods. They produce diverse mycotoxins which are hazardous to human and animal health (Dey et al. 2022; Nan et al. 2022; Pallares et al. 2022). On the other hand, the microbial natural products including mycotoxins are important drug candidates (Newman 2021) and the

enzymes involved in the biosynthesis of these compounds are valuable biocatalysts for structural modification and construction of new biosynthetic pathways (Yi et al. 2021). Among them, tailoring enzymes for modification of the backbone skeletons play key roles in increasing structural diversity and biological activities (Harken and Li 2021; Yang et al. 2022). Prenyltransferases belong to one of the important modification enzyme groups and catalyze transfer of nxC_5 moieties onto different accepters (Winkelblech et al. 2015). Members of the dimethylallyl tryptophan synthase (DMATS) superfamily are most investigated prenyltransferases in the last years. They mainly catalyze prenylations of tryptophan and tryptophan-containing cyclodipeptides (CDPs) by using dimethylallyl diphosphate (DMAPP) as prenyl donor and are involved in the biosynthesis of a large number of prenylated indole alkaloids including mycotoxins (Winkelblech et al. 2015).

✉ Shu-Ming Li
shuming.li@staff.uni-marburg.de

1   Institut Für Pharmazeutische Biologie Und Biotechnologie,
     Fachbereich Pharmazie, Philipps-Universität Marburg,
     Robert-Koch Straße 4, 35037 Marburg, Germany

Prenylated indole alkaloids are widespread in bacteria, fungi, plants, and marine organisms (Klas et al. 2018; Li 2010; Yazaki et al. 2009) and exhibit clearly distinct biological activities from their nonprenylated precursors (Botta et al. 2005; Wollinsky et al. 2012). Prenylated tryptophan-containing cyclodipeptides and derivatives thereof represent an important category within the prenylated indole alkaloids. As examplified in Fig. 1, the cytotoxic notoamides from *Penicillium* and *Aspergillus* species are derivatives of *C2*,*C7*-diprenylated and *C6*-hydroxylated brevianamide F (*cyclo*-L-Trp-L-Pro) (Klas et al. 2018). Fumitremorgins as di- and triprenylated brevianamide F products were identified as tremorgenic metabolites in *Aspergillus fumigatus*, *Neosartorya fischeri*, and other fungi (Li 2010; Mundt et al. 2012). Di- and triprenylated *cyclo*-L-Trp-L-Ala and congeners also occur frequently in the fungal genera of *Aspergillus* and *Eurotium* with echinulin as the important representative (Chen et al. 2015; Du et al. 2017; Kamauchi et al. 2016; Li 2010; Nies and Li 2021; Wohlgemuth et al. 2017).

Biosynthetically, the skeletons of such CDPs in fungi are usually assembled by nonribosomal peptide synthases using tryptophan and a second amino acid as substrates. The CDP core is then decorated by different tailoring enzymes including prenyltransferases from the DMATS superfamily (Li 2010; Wohlgemuth et al. 2017; Xu et al. 2014). In nature, CDPs are mostly monoprenylated at positions C-2 and C-3, and occasionally at positions C-4 to C-7. In contrast, prenylation of the free amino acid tryptophan takes place more frequently at C-4 to C-7 of the benzene ring than other positions (Winkelblech et al. 2015). As shown in Fig. 1, the biosynthesis of multiple prenylated CDPs is usually initiated by the regiospecific *C2*-prenylation at the indole ring, followed directly by the second prenyltransferase as in the case of echinulins or after decoration with other enzymes, e.g., in the biosynthesis of notoamides and fumitremorgins (Klas et al. 2018; Li 2011; Wohlgemuth et al. 2017). Remarkably, the members of the DMATS superfamily show high substrate flexibility toward their aromatic substrates and accept not only structurally similar, but also distinct compounds as prenyl acceptors. For example, the brevianamide F *C2*-prenyltransferases FtmPT1 and BrePT as well as the *cyclo*-L-Trp-L-Ala *C2*-prenyltransferase EchPT1 (Fig. 1)
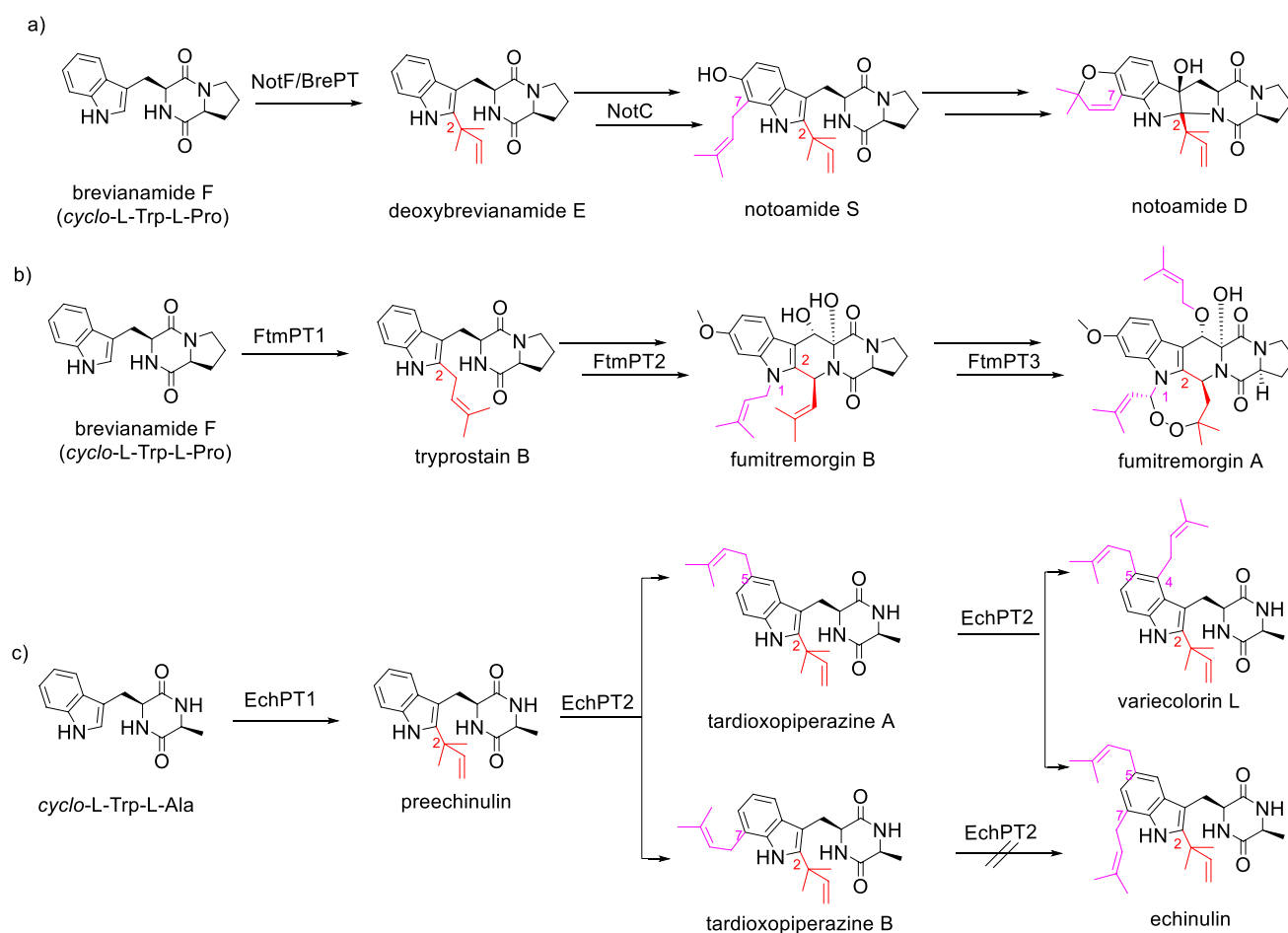
Fig. 1 Examples of biosynthetic pathways for multiprenylated CDP derivatives with *C2*-prenylation as the first decoration step

accept well other CDPs for *C2*-prenylation (Grundmann and Li [2005](); Wohlgemuth et al. [2017](); Wollinsky et al. [2012](); Yin et al. [2013]()). EchPT2 from the echinulin biosynthetic pathway (Fig. [1]()) converts *C2*-prenylated *cyclo*-Trp-Ala and *cyclo*-Trp-Pro isomers to tri- and tetraprenylated derivatives (Wohlgemuth et al. [2018]()). Diprenylated products, e.g., tardioxopiperazines A and B, were only detected as minor products. Furthermore, the tryptophan *C6*-prenyltransferase from *Streptomyces ambofaciens* and 7-DMATS from *Aspergillus fumigatus* can also prenylate CDPs at positions C-6 and C-7, respectively (Kremer et al. [2007](); Liu et al. [2020](); Winkelblech and Li [2014]()). In addition, protein engineering of the tryptophan *C4*-prenyltransferase from *Aspergillus fumigatus* led to the mutant FgaPT2_R244L with increased acceptance for CDPs (Fan and Li [2016]()). As a proof of concept, we decided in this study to produce unnatural *C2,C4*-, *C2,C5*-, *C2,C6*-, and *C2,C7*-diprenylated *cyclo*-L-Trp-L-Pro by combination of different prenyltransferases.

Materials and methods

Chemicals

DMAPP was chemically prepared according to the method published previously (Woodside et al. [1988]()). *cyclo*-L-Trp-L-Pro was synthesized as described in literature (Caballero et al. [1998]()).

Bacterial strains, plasmids, and culture conditions

Escherichia coli strains M15 [pREP4] (Qiagen, Hilden, Germany) and BL21 (DE3) pLysS (Invitrogen, Karlsruhe, Germany) harboring the plasmids pVW90, pALF49, pPM37, pJW12, and pLW40 were used for overproduction of the recombinant proteins EchPT1, FgaPT2_R244L, FgaPT2_Y398F, 6-DMATS$_{Sa}$, and 7-DMATS, respectively (Fan and Li [2016](); Kremer et al. [2007](); Mai et al. [2016](); Winkelblech and Li [2014](); Wohlgemuth et al. [2017]()). Terrific broth (TB) medium supplemented with 50 μg/mL carbenicillin or 25 μg/mL kanamycin was used for cultivation of recombinant *E. coli* strains.

Protein overproduction and purification as well as enzyme assays

Culture conditions and purification of His$_6$-EchPT1, His$_8$-FgaPT2_R244L, His$_8$-FgaPT2_Y398F, 6-DMATS$_{Sa}$-His$_6$, and 7-DMATS-His$_6$ were carried out by Ni–NTA affinity chromatography (Qiagen, Hilden) as described previously (Fan and Li [2016](); Kremer et al. [2007](); Mai et al. [2016](); Winkelblech and Li [2014](); Wohlgemuth et al. [2017]()).

SDS-PAGE analysis revealed that all the five recombinant proteins were purified to near homogeneity (Fig. [2]()).

To determine the enzyme activity, standard assays (50 μL) contained Tris–HCl (50 mM, pH 7.5), aromatic substrate (1 mM), DMAPP (1 mM), glycerol (0.5–5%, v/v), DMSO (2.5%, v/v), and the purified protein (4 μg). CaCl$_2$ at a final concentration of 5 mM was added to the reaction mixtures to enhance the reaction velocity (Li [2009](); Sasaki et al. [2008]()). After incubation at 37 °C for 16 h, the reaction mixtures were terminated by addition of 50 μL methanol. The precipitated proteins were removed by centrifugation at $13,000 \times g$ for 20 min and analyzed on liquid chromatography coupled with mass spectrometer (LCMS) as described below.

The linearity of the EchPT1 reactions toward monoprenylated derivatives was determined up to 240 min with 4 μg protein. The assays for determination of the kinetic parameters of EchPT1 toward monoprenylated CDPs **3**, **4**, and **5** contained 1 mM DMAPP, 4 μg EchPT1 and the aromatic substrate at final concentrations of 0.01, 0.02, 0.05, 0.1, 0.2, 0.5, 1.0, and 2.0 mM. The reaction mixtures containing **3**, **4**, and **5** were incubated at 37 °C for 30, 35, and 30 min, respectively. For kinetic parameters toward DMAPP of EchPT1 in the presence of the monoprenylated compound **3**, the reaction mixture contained 4 μg EchPT1, **3** (1 mM), CaCl$_2$ (5 mM), and DMAPP at final concentrations from 0.01 to 2.0 mM, which was incubated at 37 °C for 30 min. All the assays were performed as triplicates and subsequently terminated with methanol, and analyzed on high performance liquid chromatography (HPLC) as described below. The conversion yields were calculated
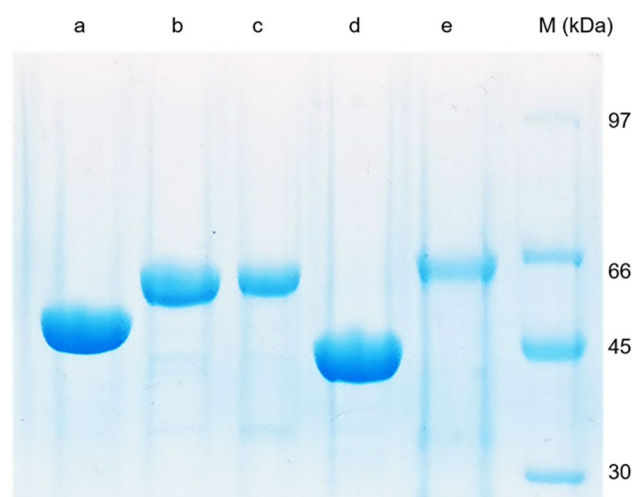

Fig. 2 SDS-PAGE analysis of the purified prenyltransferases. The proteins were separated on a 12% polyacrylamide gel and stained with Coomassie brilliant blue R-250. Lanes from left to right: a, EchPT1; b, FgaPT2_R244L; c, FgaPT2_Y398F; d, 6-DMATS$_{Sa}$; e, 7-DMATS; M, protein marker

by using the isolated products as standards or by ratio of the peak areas of product and substrate in HPLC chromatograms. The data were fitted to the Michaelis–Menten equation in Prism 4.0 (GraphPad Software).

Preparation and isolation of the enzyme products for structure elucidation

Enzyme assays for product isolation were scaled up to a volume of 12 mL, containing Tris–HCl (50 mM, pH 7.5), DMAPP (1.5 mM), the respective aromatic substrate (1 mM), and 1–5 mg purified recombinant proteins. The reaction mixtures were incubated at 37 °C for 16 h and extracted three times with two volumes of ethyl acetate each. The resulting organic phases were combined and concentrated on a rotating vacuum evaporator at 35 °C to dryness and dissolved in 1 ml methanol for isolation.

LCMS and HPLC conditions for analysis and isolation of the enzyme products

LCMS analysis was performed as described previously (Zhou and Li 2021). The substances were eluted at a flow rate of 0.25 mL/min with a linear gradient from 5 to 100% ACN in 10 min. Semi-preparative HPLC was performed with an Agilent Eclipse XDB-C18 (250 × 9.4 mm, 5 μm) column. Water (A) and acetonitrile (B) were used as solvents at flow rate of 2 mL/min. Compounds **2**, **3**, **4**, **5**, and **6** were isolated with 55% B, **10** with 60% B and **7**, **8**, and **9** with 65% B.

Nuclear magnetic resonance analysis

NMR spectra were recorded on a JEOL ECA-500 MHz spectrometer (JEOL, Tokyo, Japan) and processed with MestReNova 6.1.0 (Metrelab). Chemical shifts were referred to those of the solvent signals. The NMR data are provided in Tables S1–S4 and spectra in Figs. S1–S25.

Results

Attempts to produce diprenylated derivatives by prenylation of already *C2*-prenylated cyclo-L-Trp-L-Pro

To get *C2,C4*-, *C2,C5*-, *C2,C6*-, and *C2,C7*-diprenylated *cyclo*-L-Trp-L-Pro, we first followed the logic of the nature's biosynthetic strategy by using the reverse *C2*-prenyltransferase EchPT1 from *A. ruber* (Wohlgemuth et al. 2017) as the first biocatalyst for prenylation of *cyclo*-L-Trp-L-Pro (**1**).

The obtained *C2*-prenylated derivative deoxybrevianamide E (**2**) should be then used as substrate for prenylation at *C4*-, *C5*-, *C6*-, and *C7* of the benzene ring with other prenyltransferases. The results of the enzyme assay are shown in Fig. 3. LCMS analysis revealed that **1** was well converted to **2** having a $[M+H]^+$ ion at *m/z* 352.2023 by EchPT1 with a conversion yield of $70.7 \pm 0.5\%$ (Fig. 3a). Isolation on HPLC and comparison of its ^{1}H NMR data (Fig. S1) with those published previously (Schkeryantz et al. 1999) confirmed **2** to be the expected deoxybrevianamide E.

To obtain the desired diprenylated derivatives, **2** was used as substrate for the second prenylation. As mentioned in the introduction, FgaPT2_R244L, 6-DMATS$_{Sa}$, and 7-DMATS catalyze *C4*-, *C6*-, and *C7*-prenylation of CDPs, respectively (Fan and Li 2016; Kremer et al. 2007; Winkelblech and Li 2014). In a previous study, we have demonstrated that the mutant FgaPT2_Y398F catalyzed the *C4*- and *C5*-penylations at the indole ring of the tripeptide derivative ardeemin FQ (Mai et al. 2016). These four enzymes were chosen for prenylation of **2** at the positions of C-4, C-5, C-6, and C-7 of the benzene ring, respectively. Unfortunately, LCMS analysis revealed that no products were detected in the incubation mixtures of FgaPT2_R244L and FgaPT2_Y398F. Formation of diprenylated products with $[M+H]^+$ ions at *m/z* 420.265 ± 0.005 was observed in the assays with 6-DMATS$_{Sa}$ and 7-DMATS, but only detected in the extracted ion chromatograms (EICs) (Fig. 3b–e). Obviously, prenylation at C-2 of **1** prohibited its acceptance by the tested enzymes. Such low yields make almost impossible to get enough products for structural elucidation. Therefore, we changed our strategy and tested the possibility with first prenylation at the benzene ring by FgaPT2_R244L, FgaPT2_Y398F, 6-DMATS$_{Sa}$, and 7-DMATS, followed by the *C2*-prenylation of the monoprenylated products with EchPT1.

Prenylation of cyclo-L-Trp-L-Pro at the benzene ring by indole prenyltransferases

To obtain diprenylated derivatives in a different way from nature, substrate **1** was incubated with FgaPT2_R244L, FgaPT2_Y398F, 6-DMATS$_{Sa}$, and 7-DMATS in the presence of DMAPP at 37 °C for 16 h. LCMS analysis of the reaction mixtures revealed the conversion of **1** to monoprenylated products with $[M+H]^+$ ions at *m/z* 352.202 ± 0.005 in all the four assays. One product peak each was detected in the reaction mixtures of FgaPT2_R244L, 6-DMATS$_{Sa}$, and 7-DMATS with conversion yields of 49.6 ± 0.2, 29.9 ± 0.6, and $11.6 \pm 1.4\%$, respectively (Fig. 4). Two peaks with a total conversion yield of $66.7 \pm 0.8\%$ were observed in the assay with FgaPT2_Y398F. Isolation and structural elucidation proved the product of FgaPT2_R244L to be *C4*-prenylated derivative **3** (see below for structural
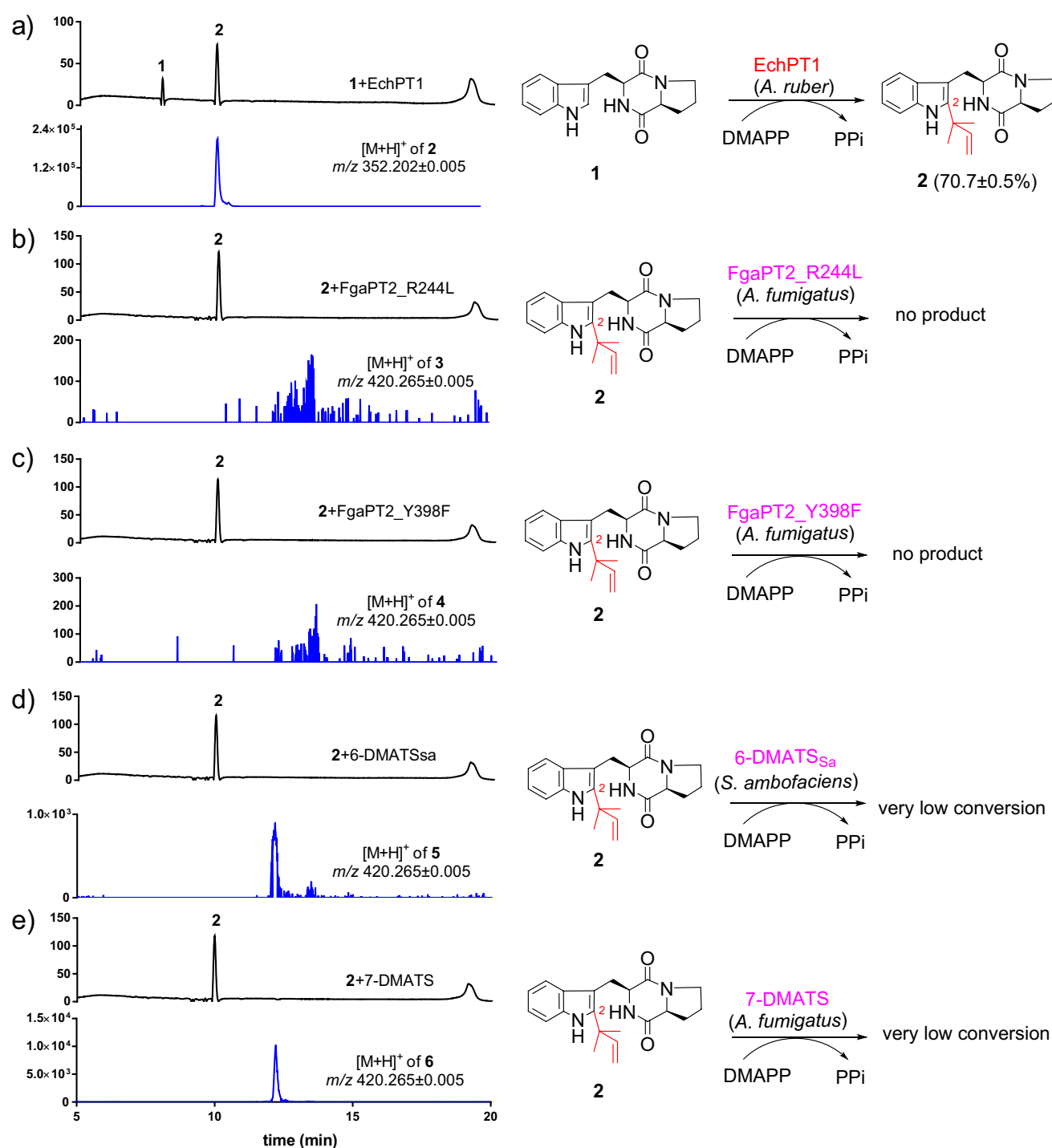
Fig. 3 **a** LCMS analysis of the acceptance of *cyclo*-L-Trp-L-Pro (**1**) by EchPT1. **b–e** LCMS analysis of the acceptance of deoxybrevianamide E (**2**) by FgaPT2_R244L, FgaPT2_Y398F, 6-DMATS$_{Sa}$, and 7-DMATS. UV absorptions at 280 nm are illustrated. All the assays were performed in duplicates. The conversion yield with EchPT1 is given as the mean value

elucidation). Both *C4*- (**3**) and *C5*-prenylated derivative **4** were isolated and identified from the reaction mixture of FgaPT2_Y398F. The sole product of 6-DMATS$_{Sa}$ was the expected *C6*-prenylated *cyclo*-L-Trp-L-Pro (**5**). NMR analysis of the product peak of the enzyme assay with 7-DMATS proved the presence of both **5** and the *C7*-prenylated product **6** in a ratio of 0.6:1.0. Prenylation by 7-DMATS at positions C-6 and C-7 of the benzene ring was already described for *cyclo*-L-Homotrp-D-Val (Fan and Li 2013). Due to their similar physiochemical
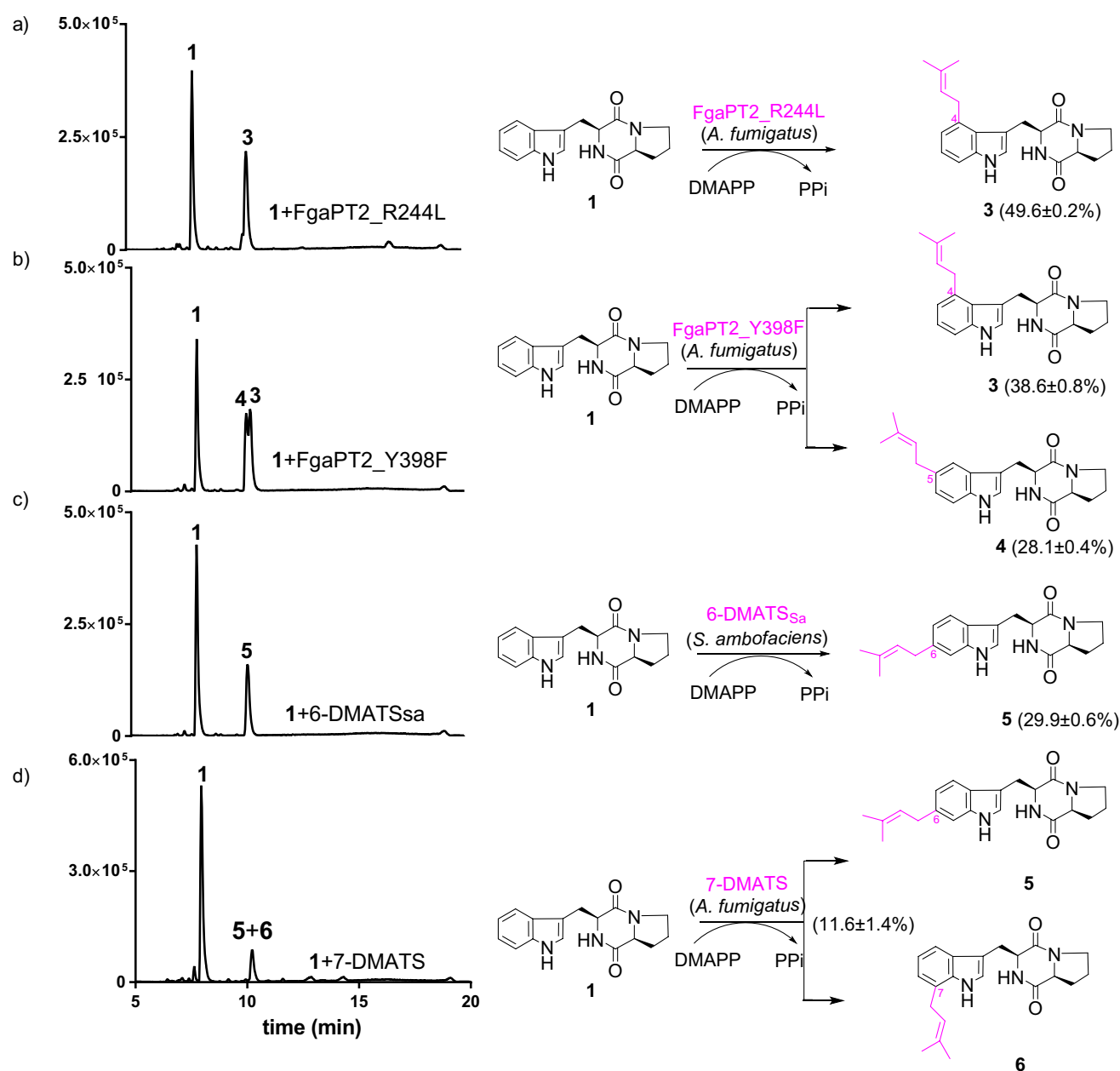
Fig. 4 LCMS analysis of *cyclo*-L-Trp-L-Pro (**1**) prenylation by **a** FgaPT2_R244L, **b** FgaPT2_Y398F, **c** 6-DMATS$_{Sa}$, and **d** 7-DMATS. Only absorptions at 280 nm are illustrated. All the assays were performed in duplicates. The conversion yields are given as mean values

properties, **5** and **6** could not be separated from each other. Nevertheless, their structures can be unequivocally elucidated by NMR analysis, because of the availability of the spectrum for **5** in high purity obtained from the enzyme assay with 6-DMATS$_{Sa}$.

Confirmation of the prenylation positions of the monoprenylated products

For structural elucidation, the enzyme products were isolated on a preparative scale and their structures were elucidated by MS and NMR analyses. ESI–MS proved that the products of **1** with FgaPT2_R244L, FgaPT2_Y398F, 6-DMATS$_{Sa}$, and 7-DMATS had [M + H]$^+$ ions at *m/z* 352.202 ± 0.005, 68 Dalton larger than that of **1**, indicating attachment of a dimethylallyl moiety to their structures. This hypothesis was confirmed by appearance of signals for a regular dimethylallyl residue each at δ_H 3.4–3.7 (d or dd, 2H-1′), 5.3–5.4 (tsept, H-2′), and 1.7–1.8 (one or two br s, 3H-4′ and 3H-5′) (Figs. S2–S4 and S9). The ^{1}H NMR spectra of the isolated compounds showed in the aromatic region signals for four instead of

five protons in that of **1**. The signal for H-2 was detected in all of the spectra of the isolated products **3–6**, indicating the prenylation at the benzene ring. Three vicinal aromatic protons were found in the spectra of **3** and **6**, suggesting for the *C4-* and *C7*-prenylation. Coupling pattern of the three aromatic protons in **4** and **5**, *i.e.*, one at *meta-* and two at *ortho*-position, is consistent with *C5-* and *C6*-prenylations. The structure of compound **5** was unequivocally determined as *C6*-prenylated *cyclo*-L-Trp-L-Pro by interpretation of its ^{1}H, ^{13}C, ^{1}H-^{1}H COSY, HSQC, and HMBC NMR data (Figs. S4–S8). Clear long-range correlations between H-5 and C-9 as well as H-7 and C-9 were observed in the HMBC spectrum, proving the attachment of the prenyl moiety at C-6 of the indole ring (Fig. 4). Comparison of the NMR data of **3** and **6** with those published previously proved their structures to be *C4-* and *C7*-prenylated derivatives, respectively (Fig. 4) (Liu et al. 2020; Steffan and Li 2009).

Prenylation of the C4-, C5-, C6-, and C7-prenylated cyclo-L-Trp-L-Pro by EchPT1 and structural elucidation of the diprenylated products

The isolated monoprenylated samples from the enzyme assays of **1** with FgaPT2_R244L, FgaPT2_Y398F, 6-DMATS$_{Sa}$, and 7-DMATS, *i.e.*, **3**, **4**, and **5** in high purity and **6** in a mixture with **5**, were used for incubation with the *cyclo*-L-Trp-L-Ala reverse *C2*-prenyltransferase EchPT1 in the presence of DMAPP. LCMS analysis showed all these substrates were accepted by EchPT1 with the highest conversion of $85.7 \pm 3.5\%$ for **3** (Fig. 5). Only one product peak each was detected, even in the assay with the mixture of **5** and **6** (Fig. 5d). Isolation and structural elucidation confirmed the presence of one product each in the incubation mixtures of **3–5**. As expected, the single product peak of the incubation mixture of **5** and **6** comprised two products, which can be separated from each other under optimized conditions.

The isolated products **7–10** from the enzyme assays with **3–6** were then subjected to MS and NMR analyses. ESI–MS proved that all these new products were diprenylated *cyclo*-L-Trp-L-Pro with [M + H]$^+$ ions at *m/z* 420.265 ± 0.005. In the ^{1}H NMR spectra of **7**, **8**, and **10**, the signal for H-2 disappeared. Instead, additional signals for a reverse dimethylallyl moiety were detected at δ_H 6.12–6.14 (dd, 17, 10 Hz, H-2″), 5.17–5.20 (dd, 17, 0.6 Hz, H-3″), 5.16–5.23 (dd, 10, 0.6 Hz, H-3″), and 1.5–1.7 (two singlets, 3H-4″ and 3H-5″) (Figs. S10, S15, and S24). These data suggested **7**, **8**, and **10** to be *C2,C4-*, *C2,C5-*, and *C2,C7*-diprenylated *cyclo*-L-Trp-L-Pro by attachment of a reverse dimethylallyl moiety to position C-2 of **3**, **4**, and **6**, respectively. This is expected for the

EchPT1 reactions and also confirmed by intensive interpretation of their ^{13}C, ^{1}H-^{1}H COSY, HSQC, and HMBC spectra. In the ^{13}C NMR spectra of **7**, **8**, and **10**, the signals of C-2 at the indole ring as well as those of C-1″, C-2″, C-3″, and C-4″/C-5″ of the reverse prenyl residue were observed at δ_c 141.1–141.8, 39.1–39.2, 145.8–145.9, 112.8–112.9, and 27.9–28.5 ppm, respectively (Figs. S11, S16, and S25). Inspection of the ^{1}H and ^{13}C NMR spectra of compound **9** revealed the presence of the signals for H-2 at δ_H 7.11 ppm and for C-2 at δ_c 123.9 ppm, suggesting that the additional prenyl residue is attached to another position than C-2. Remarkably, the signal of C-1″ in **9** at δ_c 59.1 ppm was downfield shifted for approximate 20 ppm, in comparison to those of **7**, **8**, and **10**. This indicates its attachment to a hetero such as nitrogen than carbon atom (Fig. S20). Correspondingly, the signal of NH-1 was disappeared in the ^{1}H NMR of **9**. Together with HSQC and HMBC data (Table S4), compound **9** was proven to be *N1,C6*-diprenylated derivative (Fig. 5).

Determination of the kinetic parameters of EchPT1 toward monopernylated cyclo-L-Trp-L-Pro

To better understand the behavior of EchPT1, kinetic parameters including Michaelis–Menten constant K_M and turnover number k_{cat} were determined for the three aromatic substrates **3–5** and DMAPP in the presence of the best accepted **3**. Kinetic parameters for **6** could not be obtained due to the impurity with **5**. All the reactions followed the Michaelis–Menten kinetics (Fig. 6). Similar affinities with K_M values between 0.05 and 0.08 mM were determined for **3–5**, comparable to that of *cyclo*-L-Trp-L-Ala, the natural substrate of EchPT1 at 0.09 mM (Wohlgemuth et al. 2017). The highest k_{cat} at 0.21 s^{-1} was calculated for **3**, followed by those of **4** and **5** at 0.03 and 0.007 s^{-1}, respectively. These values are much lower than that of *cyclo*-L-Trp-L-Ala at 6.63 s^{-1} (Wohlgemuth et al. 2017). The catalytic efficiencies were calculated for **3**, **4**, and **5** to be 3500, 375, and 140 s^{-1} mM^{-1}, respectively, being in good consistence with the observed conversion yields depicted in Fig. 5. The K_M value for DMAPP was determined in the presence of the best *C4*-prenylated *cyclo*-L-Trp-L-Pro **3** at 0.10 mM, slightly lower than in the presence of *cyclo*-L-Trp-L-Ala at 0.18 mM (Wohlgemuth et al. 2017) (Table 1).

Discussion

In nature, cyclodipeptides are assembled by nonribosomal peptide synthases, mostly in fungi, or by cyclodipeptide synthases, mainly in bacteria (Canu et al. 2020; Mishra et al. 2017). They are then modified by different tailoring enzymes
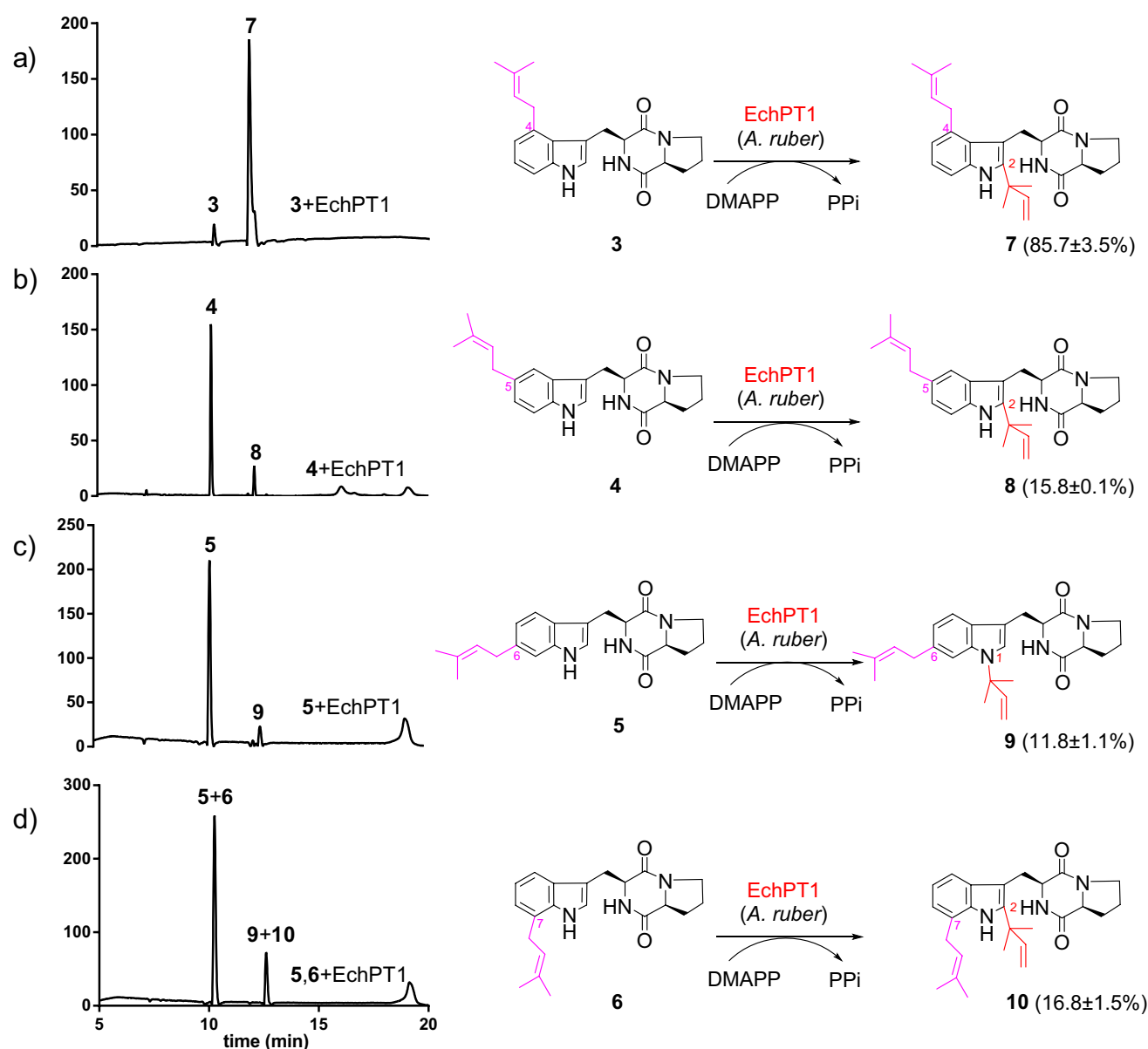
Fig. 5 LCMS analysis of acceptance of monoprenylated derivatives (**3**, **4**, **5**, and **6**) by EchPT1. Products **9** and **10** with a total conversion yield of $23.6 \pm 1.4\%$ were isolated from the incubation mixture of **6** with **5**. Absorptions at 280 nm are illustrated. All the assays were performed in duplicates. The conversion yields are given as mean values

such as prenyltransferases, methyltransferases, cytochrome P450 enzymes and 2-oxoglutarate-dependent monooxygenases (Harken and Li 2021; Winkelblech et al. 2015). Cyclodipeptide prenylation is usually initiated at position C-2 by reverse or regular prenyltransferases (Fig. 1) (Winkelblech et al. 2015). Further prenylations take place thereafter at the benzene ring, as demonstrated in the biosynthesis of the triprenylated *cyclo*-L-Trp-L-Ala derivative echinulin (Wohlgemuth et al. 2017).

In this study, we first followed the nature´s biosynthetic strategy for production of diprenylated *cyclo*-L-Trp-L-Pro, *i.e.*, at *C2,C4*-, *C2,C5*-, *C2,C6*-, and *C2,C7*-diprenylated

derivatives. We first prepared deoxybrevianamide E by prenylation of *cyclo*-L-Trp-L-Pro at position C-2 with EchPT1. Unfortunately, the four prenyltransferases FgaPT2_R244L, FgaPT2_Y398F, 6-DMATS$_{Sa}$, and 7-DMATS used in this study showed strict substrate specificity and did not accept deoxybrevianamide E as substrate for further prenylation (Fig. 3). We therefore changed our strategy by first prenylation of *cyclo*-L-Trp-L-Pro at the benzene ring with the four enzymes FgaPT2_R244L, FgaPT2_Y398F, 6-DMATS$_{Sa}$, and 7-DMATS. As expected, three different monoprenylated derivatives, i.e., *cyclo*-L-Trp-L-Pro with dimethylallyl moieties at the positions C-4, C-5, and
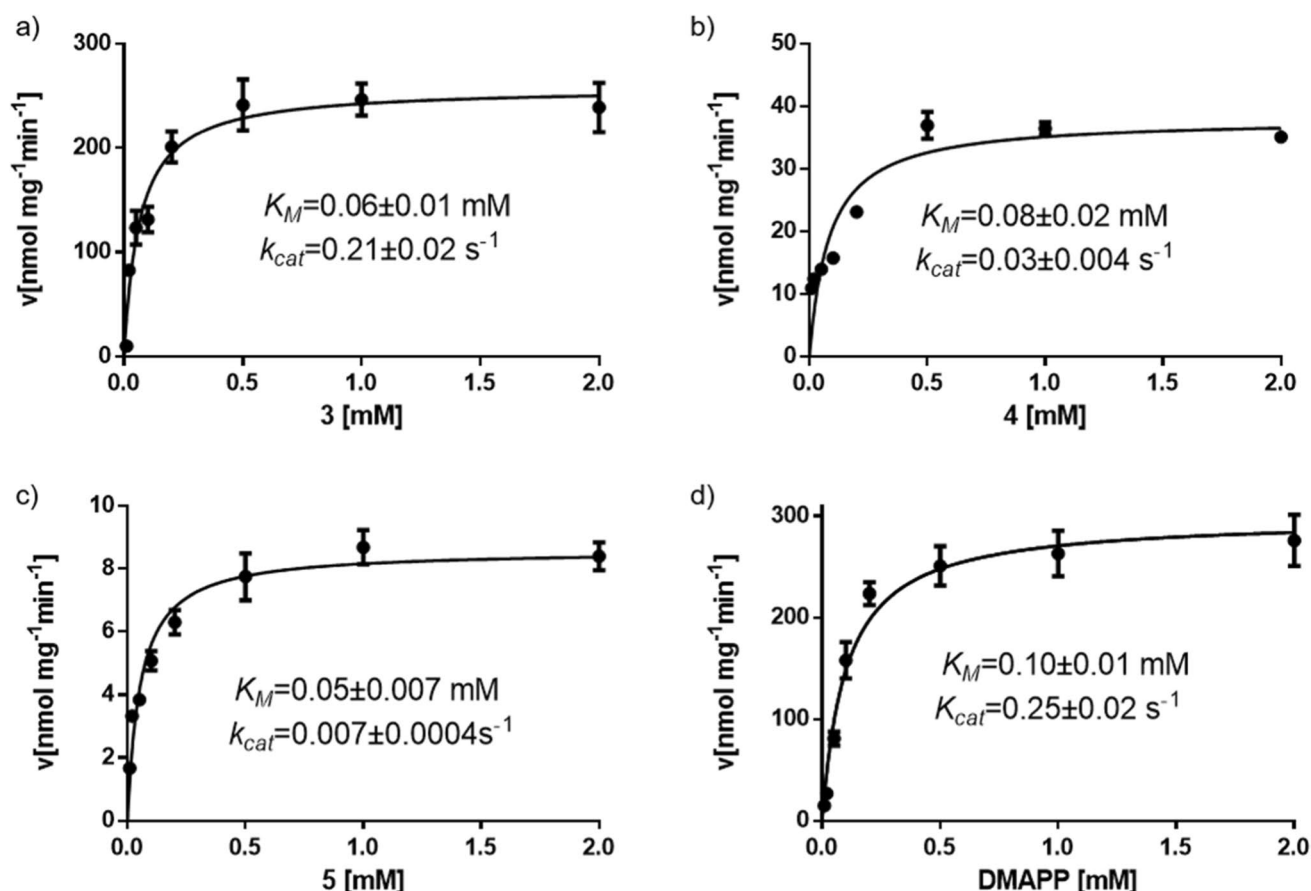
Fig. 6 Determination of kinetic parameters of EchPT1 toward **3–5** and DMAPP with **3**

C-7, were then successfully converted by EchPT1 to the designed diprenylated products (Fig. 5). However, to our surprise, EchPT1 catalyzed the unique *N1*-reverse prenylation of *C6*-prenylated *cyclo*-L-Trp-L-Pro and produced *N1,C6*-diprenylated product. This is the first example for an *N1*-prenylation catalyzed by EchPT1. This study expands therefore significantly our knowledge on prenyltransferases of the DMATS superfamily. It is obvious that their catalytic potential is far away from exhausted, even a large number of biochemical works have been carried out and published in the last decade (Fan et al. 2015; Mori 2020). Furthermore, our results provide a new strategy for production of designed products and increasing structural diversity by changing the normal reaction sequences.

Declarations

Table 1 Kinetic parameters of EchPT1 toward **3–5** and DMAPP

Substrates	K_M (mM)	k_{cat} (s^{-1})	k_{cat}/K_M (s^{-1} M^{-1})
3	0.06 ± 0.01	0.21 ± 0.02	3500
4	0.08 ± 0.02	0.03 ± 0.004	375
5	0.05 ± 0.007	0.007 ± 0.0004	140
DMAPP with **3**	0.10 ± 0.01	0.25 ± 0.02	2500

Three independent experiments were carried out and standard deviations are given as $\pm$ values

References

Botta B, Vitali A, Menendez P, Misiti D, Delle MG (2005) Prenylated flavonoids: pharmacology and biotechnology. Curr Med Chem 12:717–739

Caballero E, Avendaño C, Menéndez JC (1998) Stereochemical issues related to the synthesis and reactivity of pyrazino[2',1'-5,1] pyrrolo[2,3-b]indole-1,4-diones. Tetrahedron: Asymmetry 9:967–981

Canu N, Moutiez M, Belin P, Gondry M (2020) Cyclodipeptide synthases: a promising biotechnological tool for the synthesis of diverse 2,5-diketopiperazines. Nat Prod Rep 37:312–321

Chen X, Si L, Liu D, Proksch P, Zhang L, Zhou D, Lin W (2015) Neoechinulin B and its analogues as potential entry inhibitors of influenza viruses, targeting viral hemagglutinin. Eur J Med Chem 93:182–195

Dey DK, Kang JI, Bajpai VK, Kim K, Lee H, Sonwal S, Simal-Gandara J, Xiao J, Ali S, Huh YS, Han YK, Shukla S (2022) Mycotoxins in food and feed: toxicity, preventive challenges, and advanced detection techniques for associated diseases. Crit Rev Food Sci Nutr. https://doi.org/10.1080/10408398.2022.2059650

Du FY, Li X, Li XM, Zhu LW, Wang BG (2017) Indolediketopiperazine alkaloids from Eurotium cristatum EN-220, an endophytic fungus isolated from the marine alga Sargassum thunbergii. Mar Drugs 15:24

Fan A, Li S-M (2013) One substrate - seven products with different prenylation positions in one-step reactions: prenyltransferases make it possible. Adv Synth Catal 355:2659–2666

Fan A, Li S-M (2016) Saturation mutagenesis on Arg244 of the tryptophan C4-prenyltransferase FgaPT2 leads to enhanced catalytic ability and different preferences for tryptophan-containing cyclic dipeptides. Appl Microbiol Biotechnol 100:5389–5399

Fan A, Winkelblech J, Li S-M (2015) Impacts and perspectives of prenyltransferases of the DMATS superfamily for use in biotechnology. Appl Microbiol Biotechnol 99:7399–7415

Grundmann A, Li S-M (2005) Overproduction, purification and characterization of FtmPT1, a brevianamide F prenyltransferase from Aspergillus fumigatus. Microbiology 151:2199–2207

Harken L, Li S-M (2021) Modifications of diketopiperazines assembled by cyclodipeptide synthases with cytochrome P450 enzymes. Appl Microbiol Biotechnol 105:2277–2285

Kamauchi H, Kinoshita K, Sugita T, Koyama K (2016) Conditional changes enhanced production of bioactive metabolites of marine derived fungus Eurotium rubrum. Bioorg Med Chem Lett 26:4911–4914

Klas KR, Kato H, Frisvad JC, Yu F, Newmister SA, Fraley AE, Sherman DH, Tsukamoto S, Williams RM (2018) Structural and stereochemical diversity in prenylated indole alkaloids containing the bicyclo[2.2.2]diazaoctane ring system from marine and terrestrial fungi. Nat Prod Rep 35:532–558

Kremer A, Westrich L, Li S-M (2007) A 7-dimethylallyltryptophan synthase from Aspergillus fumigatus: overproduction, purification and biochemical characterization. Microbiology 153:3409–3416

Li S-M (2009) Evolution of aromatic prenyltransferases in the biosynthesis of indole derivatives. Phytochemistry 70:1746–1757

Li S-M (2010) Prenylated indole derivatives from fungi: structure diversity, biological activities, biosynthesis and chemoenzymatic synthesis. Nat Prod Rep 27:57–78

Li S-M (2011) Genome mining and biosynthesis of fumitremorgin-type alkaloids in ascomycetes. J Antibiot 64:45–49

Liu R, Zhang H, Wu W, Li H, An Z, Zhou F (2020) C7-Prenylation of tryptophan-containing cyclic dipeptides by 7-dimethylallyl tryptophan synthase significantly increases the anticancer and antimicrobial activities. Molecules 25:3676

Mai P, Zocher G, Ludwig L, Stehle T, Li S-M (2016) Actions of tryptophan prenyltransferases toward fumiquinazolines and their potential application for the generation of prenylated derivatives by combining chemical and chemoenzymatic syntheses. Adv Synth Catal 358:1639–1653

Mishra AK, Choi J, Choi SJ, Baek KH (2017) Cyclodipeptides: an overview of their biosynthesis and biological activity. Molecules 22:E1796

Mori T (2020) Enzymatic studies on aromatic prenyltransferases. J Nat Med 74:501–502

Mundt K, Wollinsky B, Ruan HL, Zhu T, Li S-M (2012) Identification of the verruculogen prenyltransferase FtmPT3 by a combination of chemical, bioinformatic and biochemical approaches. ChemBioChem 13:2583–2592

Nan M, Xue H, Bi Y (2022) Contamination, detection and control of mycotoxins in fruits and vegetables. Toxins 14:309

Newman DJ (2021) Natural product based antibody drug conjugates: clinical status as of November 9, 2020. J Nat Prod 84:917–931

Nies J, Li S-M (2021) Prenylation and dehydrogenation of a C2-reversely prenylated diketopiperazine as a branching point in the biosynthesis of echinulin family alkaloids in Aspergillus ruber. ACS Chem Biol 16:185–192

Pallares N, Tolosa J, Ferrer E, Berrada H (2022) Mycotoxins in raw materials, beverages and supplements of botanicals: a review of occurrence, risk assessment and analytical methodologies. Food Chem Toxicol 165:113013

Sasaki K, Mito K, Ohara K, Yamamoto H, Yazaki K (2008) Cloning and characterization of naringenin 8-prenyltransferase, a flavonoid-specific prenyltransferase of Sophora flavescens. Plant Physiol 146:1075–1084

Schkeryantz JM, Woo JCG, Siliphaivanh P, Depew KM, Danishefsky SJ (1999) Total synthesis of gypsetin, deoxybrevianamide E, brevianamide E, and tryprostatin B: novel constructions of 2,3-disubstituted indoles. J Am Chem Soc 121:11964–11975

Steffan N, Li S-M (2009) Increasing structure diversity of prenylated diketopiperazine derivatives by using a 4-dimethylallyltryptophan synthase. Arch Microbiol 191:461–466

Winkelblech J, Fan A, Li S-M (2015) Prenyltransferases as key enzymes in primary and secondary metabolism. Appl Microbiol Biotechnol 99:7379–7397

Winkelblech J, Li S-M (2014) Biochemical investigations of two 6-DMATS enzymes from Streptomyces revealing novel features of L-tryptophan prenyltransferases. ChemBioChem 15:1030–1039

Wohlgemuth V, Kindinger F, Li S-M (2018) Convenient synthetic approach for tri- and tetraprenylated cyclodipeptides by consecutive enzymatic prenylations. Appl Microbiol Biotechnol 102:2671–2681

Wohlgemuth V, Kindinger F, Xie X, Wang BG, Li S-M (2017) Two prenyltransferases govern a consecutive prenylation cascade

in the biosynthesis of echinulin and neoechinulin. Org Lett 19:5928–5931

Wollinsky B, Ludwig L, Hamacher A, Yu X, Kassack MU, Li SM (2012) Prenylation at the indole ring leads to a significant increase of cytotoxicity of tryptophan-containing cyclic dipeptides. Bioorg Med Chem Lett 22:3866–3869

Woodside AB, Huang Z, Poulter CD (1988) Trisammonium Geranyl Diphosphate Org Synth 66:211–215

Xu W, Gavia DJ, Tang Y (2014) Biosynthesis of fungal indole alkaloids. Nat Prod Rep 31:1474–1487

Yang K, Tian J, Keller NP (2022) Post-translational modifications drive secondary metabolite biosynthesis in Aspergillus: a review. Environ Microbiol 24:2857–2881

Yazaki K, Sasaki K, Tsurumaru Y (2009) Prenylation of aromatic compounds, a key diversification of plant secondary metabolites. Phytochemistry 70:1739–1745

Yi D, Bayer T, Badenhorst CPS, Wu S, Doerr M, Hohne M, Bornscheuer UT (2021) Recent trends in biocatalysis. Chem Soc Rev 50:8003–8049

Yin S, Yu X, Wang Q, Liu XQ, Li S-M (2013) Identification of a brevianamide F reverse prenyltransferase BrePT from *Aspergillus versicolor* with a broad substrate specificity towards tryptophan-containing cyclic dipeptides. Appl Microbiol Biotechnol 97:1649–1660

Zhou J, Li S-M (2021) Conversion of viridicatic acid to crustosic acid by cytochrome P450 enzyme-catalysed hydroxylation and spontaneous cyclisation. App Microbiol Biotechnol 105:9181–9189

Diprenylated Cyclodipeptide Production by Changing the Prenylation Sequence of the Nature´s Synthetic Machinery

Wen Li, Lindsay Coby, Jing Zhou, Shu-Ming Li*

Institut für Pharmazeutische Biologie und Biotechnologie, Fachbereich Pharmazie, Philipps-Universität Marburg, Robert-Koch Straße 4, 35037 Marburg, Germany

Corresponding to Shu-Ming Li, E-mail: shuming.li@staff.uni-marburg.de

Table of Contents

2

Table S1 NMR data of compounds **2−4** in CDCl$_3$

Pos.	δ$_H$ (ppm) multi. J (Hz)	δ$_H$ (ppm) multi. J (Hz)	δ$_H$ (ppm) multi. J (Hz)
	2	**3**	**4**
1	8.07 br s	8.25 br s	8.06 br s
2	-	7.07 s	7.08 d (1.6)
4	7.49 d (8.0)	-	7.35 s
5	7.11 ddd (8.0, 7.1, 1.4)	6.93 d (7.2)	-
6	7.18 ddd (8.0, 7.1, 1.4)	7.14 t (7.4)	7.07 dd (8.3, 1.6)
7	7.33 dd (8.0, 1.4)	7.24 d (8.0)	7.31 d (8.3)
10a	3.75 dd (15.5, 4.3)	3.98 dd (15.4, 3.0)	3.76 dd (15.0, 3.5)
10b	3.19 dd (15.5, 11.7)	2.98 dd (15.4, 11.3)	2.92 dd (15.0, 11.3)
11	4.44 dd (11.7, 4.3)	4.29 dd (11.3, 3.0)	4.37 dd (11.3, 3.5)
12	5.69 br s	5.84 br s	5.72 br s
14	4.07 t (7.7)	4.09 t (8.3)	4.09 t (8.2)
17	3.68 ddd (12.0, 9.5, 3.1)	3.67[a] m	3.67 dt (11.9, 8.5)
	3.60 ddd (12.0, 9.5, 3.1)	3.61 ddd (11.8, 8.9, 3.1)	3.60 ddd (11.8, 8.5, 3.1)
18	2.08 m	2.08 m	2.04 m
	1.92 m	1.92 m	1.91 m
19	2.35 m	2.35 m	2.34 m
	2.08 m	2.08 m	2.04 m
1′	-	3.75 dd (16.1, 6.8)	3.43 d (7.2)
	-	3.67[a] m	
2′	6.14 dd (17.7, 10.4)	5.32 tsept (6.8, 1.4)	5.37 tsept (7.2, 1.4)
3′	5.20 dd (17.7, 0.8)	-	-
	5.18 dd (10.4, 0.8)	-	-
4′	1.56 s	1.74 br s	1.75 br s
5′	1.56 s	1.74 br s	1.75 br s

[a] Signals overlapping with each other.

The NMR data of **2** and **3** correspond well to those published previously (Schkeryantz et al. 1999; Steffan and Li 2009).
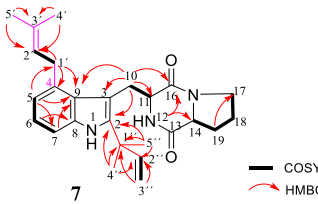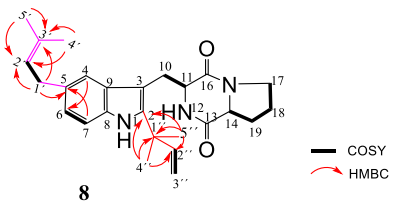
Table S2 NMR data of compounds **5** and **6** in CDCl₃

Pos.	δ_H (ppm) multi. J (Hz)	δ_C	HMBC	δ_H (ppm) multi. J (Hz)
1	8.23 br s	-		8.13 br s
2	7.05 s	123.1	C-3, C-8, C-9	7.10 s
3	-	109.9		-
4	7.49 d (8.1)	118.5	C-3, C-6	7.44 d (7.6)
5	6.99 d (8.1)	121.3	C-7, C-9, C-1′	7.07 t (7.7)
6	-	137.0		7.04 d (7.7)
7	7.20 br s	110.9	C-5, C-9, C-1′	-
8	-	137.3		-
9	-	125.0		-
10a	3.75 dd (15.0, 3.6)	27.1	C-9	3.76 dd (15.0, 3.8)
10b	2.92 dd (15.0, 11.1)			2.93 dd (15.0, 11.1)
11	4.36 dd (11.1, 3.6)	54.7		4.37 dd (11.1, 3.8)
12	5.79 br s	-	C-14, C-16	5.71 br s
13	-	169.5		-
14	4.07 t (8.0)	59.4	C-12	4.07 t (8.0)
16	-	165.7		-
17	3.66 dt (11.9, 8.5)	45.6		3.65 dt (11.8, 8.5)
	3.59 ddd (11.9, 8.5, 3.2)			3.60 ddd (11.8, 8.5, 3.1)
18	2.03 m	22.8		2.03 m
	1.91 m			1.91 m
19	2.33 m	28.5		2.34 m
	2.03 m			2.03 m
1′	3.45 d (7.2)	34.7	C-5, C-6, C-7, C-2′, C-3′	3.57 d (7.1)
2′	5.38 t (7.2)	123.9	C-1′, C-4′, C-5′	5.38 tsept (7.1, 1.4)
3′	-	132.4		-
4′	1.76 br s	18.0	C-2′, C-3′	1.79 br s
5′	1.75 br s	26.0	C-2′, C-3′	1.83 br s

Note: Compound **5** was isolated as the sole product from the enzyme assay of **1** with 6-DMATS_Sa. Both **5** and **6** were isolated as a mixture in a ratio of 0.6:1 from the reaction mixture of **1** with 7-DMATS.
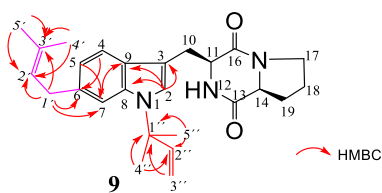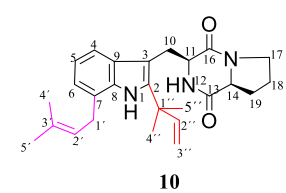
The NMR data of **6** correspond to those of *cyclo*-L-7-dimethylallyl-Trp-L-Pro reported previously (Liu et al. 2020).

4

Table S3 NMR data of compounds **7** and **8** in CDCl$_3$

Pos.	δ$_H$ (ppm) multi. J (Hz)	δ$_C$	HMBC	δ$_H$ (ppm) multi. J (Hz)	δ$_C$	HMBC
1	8.12 br s	-		7.96 br s	-	
2	-	141.5[c]		-	141.8	C-4″, C-5″
3	-	105.4		-	104.4	
4	-	133.9		7.25 br s	117.1	C-6
5	6.89 d (7.2)	121.5	C-7, C-9, C-1′	-	133.8	
6	7.08 t (7.7)	122.4	C-8	7.00 dd (8.3, 1.4)	123.2	
7	7.18 d (8.0)	109.1	C-5, C-9	7.23 d (8.3)	110.9	C-5
8	-	135.2		-	133.0	
9	-	126.9[c]		-	129.4	
10a	3.78 dd (15.7, 4.3)	26.5	C-2, C-3, C-9, C-11, C-16	3.72 dd (15.3, 4.2)	26.1	
10b	3.41 dd (15.7, 11.3)			3.17 dd (15.3, 11.2)		
11	4.35 dd (11.3, 4.3)	55.7[c]		4.44 dd (11.2, 4.2)	54.9	
12	5.66 br s	-	C-14, C-16	5.72 br s	-	
13	-	169.2		-	169.3	
14	4.04 t (7.9)	59.4		4.08 t (8.0)	59.4	
16	-	166.0		-	166.1	
17	3.67[a] m	45.4		3.67 m	45.5	
	3.58 ddd (11.6, 9.0, 2.9)			3.60 ddd (11.8, 8.9, 3.1)		
18	2.06[b] m	22.8		2.08 m	22.8	
	1.92 m			1.92 m		
19	2.35 m	28.5	C-17	2.36 m	28.5	
	2.06[b] m			2.08 m		
1′	3.67[a] m	32.3	C-4, C-5, C-9, C-2′	3.41 d (7.2)	34.8	C-5, C-2′, C-3′
2′	5.28 tsept (6.8, 1.4)	123.7		5.35 tsept (7.2, 1.4)	124.5	C-1′, C-4′, C-5′
3′	-	132.7		-	131.9	
4′	1.72 br s	18.2	C-2′, C-3′	1.74 br s	18.1	C-2′, C-3′
5′	1.69 br s	25.9	C-2′, C-3′	1.73 br s	26.0	C-2′, C-3′
1″	-	39.2		-	39.2	
2″	6.14 dd (17.4, 10.5)	145.9	C-1″, C-4″, C-5″	6.12 dd (17.5, 10.5)	145.8	C-4″, C-5″
3″	5.19 dd (17.4, 0.6)	112.8	C-1″, C-2″	5.17 d (17.5)	112.9	
	5.16 dd (10.5, 0.6)			5.18 d (10.5)		
4″	1.57 s	28.2	C-2, C-1″, C-2″	1.55 s	28.5	C-2
5″	1.56 s	28.1	C-2, C-1″, C-2″	1.54 s	28.1	C-2

[a, b] Signals overlapping with each other; [c] Signals were only detected in HSQC.

5

Table S4 NMR data of compounds **9** and **10** in CDCl$_3$

Pos.	δ$_H$ (ppm) multi. *J* (Hz)	δ$_C$	HMBC	δ$_H$ (ppm) multi. *J* (Hz)	δ$_C$
1	-	-		8.13 br s	-
2	7.11 br s	123.9	C-3, C-8, C-9	-	141.1
3	-	107.7[a]		-	104.7
4	7.45 d (8.1)	118.4	C-6	7.34 d (7.9)	116.1
5	6.94 dd (8.1, 1.3)	120.4	C-7	7.03 t (7.8)	120.4
6	-	135.4		6.97 dd (7.2, 0.8)	122.0
7	7.33 br s	113.5	C-5, C-9, C-1′	-	123.8
8	-	136.6		-	133.8
9	-	126.8		-	129.2
10	3.75 dd (15.0, 3.6)	27.1		3.72 dd (15.2, 4.1)	26.2
	2.87 dd (15.0, 11.3)			3.17 dd (15.2, 11.2)	
11	4.35 dd (11.3, 3.6)	54.8		4.44 dd (11.2, 4.1)	55.0
12	5.72 br s	-		5.69 br s	-
13	-	169.5		-	169.4
14	4.07 t (7.9)	59.3		4.05 t (8.4)	59.4
16	-	165.7		-	166.0
17	3.67 m	45.5		3.68 m	45.5
	3.59 ddd (11.7, 8.8, 2.9)			3.60 m	
18	2.03 m	22.7		2.07 m	22.8
	1.91 m			1.93 m	
19	2.34 m	28.4		2.34 m	28.5
	2.03 m			2.07 m	
1′	3.41 d (7.4)	34.8	C-6, C-7, C-2′, C-3′	3.57 d (7.4)	31.4
2′	5.36 tsept (7.4, 1.5)	124.0	C-1′, C-4′, C-5′	5.43 tsept (7.4, 1.5)	122.9
3′	-	132.3		-	133.2
4′	1.75 br s	17.9	C-2′, C-3′	1.88 br s	18.1
5′	1.75 br s	25.9	C-2′, C-3′	1.81 br s	25.9
1″	-	59.1		-	39.1
2″	6.13 dd (17.5, 10.7)	144.2	C-4″, C-5″	6.12 dd (17.6, 10.4)	145.8
3″	5.20 dd (17.5, 0.5)	113.6	C-4″, C-5″	5.18 dd (17.6, 0.8)	112.8
	5.23 dd (10.7, 0.5)			5.17 dd (10.4, 0.8)	
4″	1.74 s	27.9	C-1″, C-2″	1.55 s	28.0
5″	1.73 s	27.8	C-1″, C-2″	1.53 s	27.9

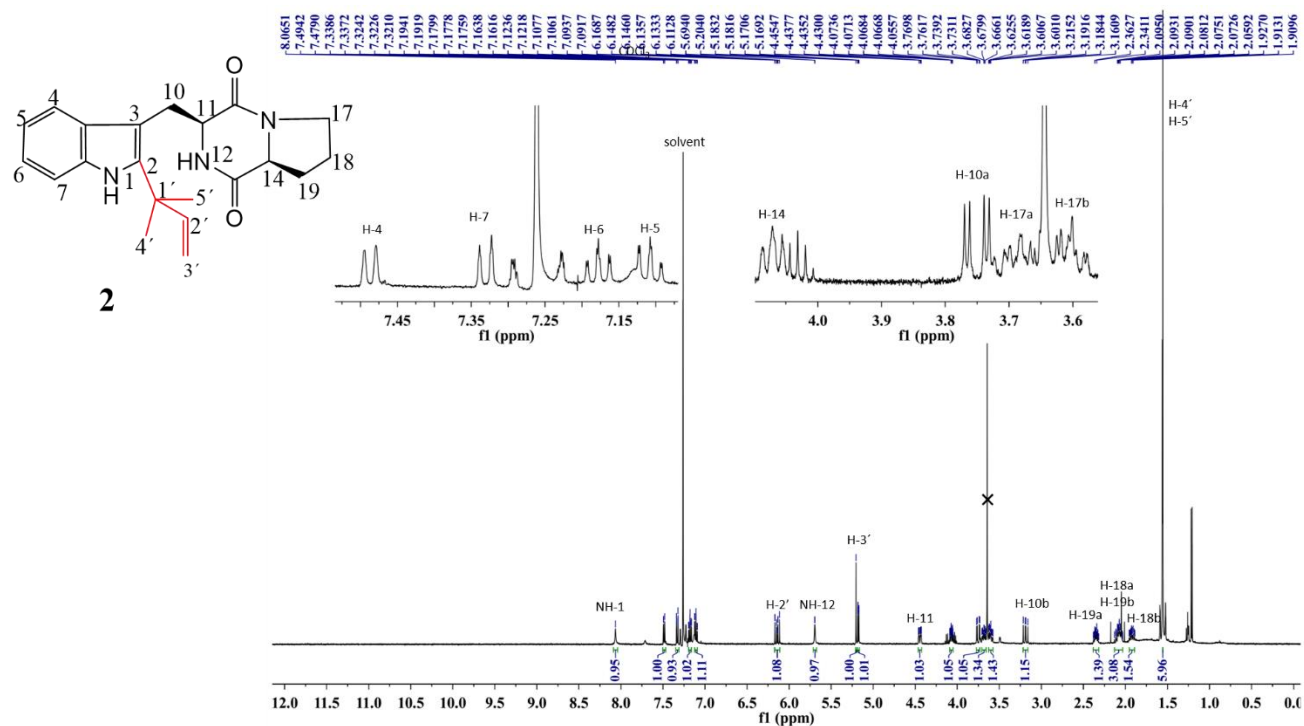[a] Signal was only detected in HSQC.

6

Supplementary Figures

Fig. S1 ^{1}H NMR spectrum of **2** in CDCl$_3$ (500 MHz).
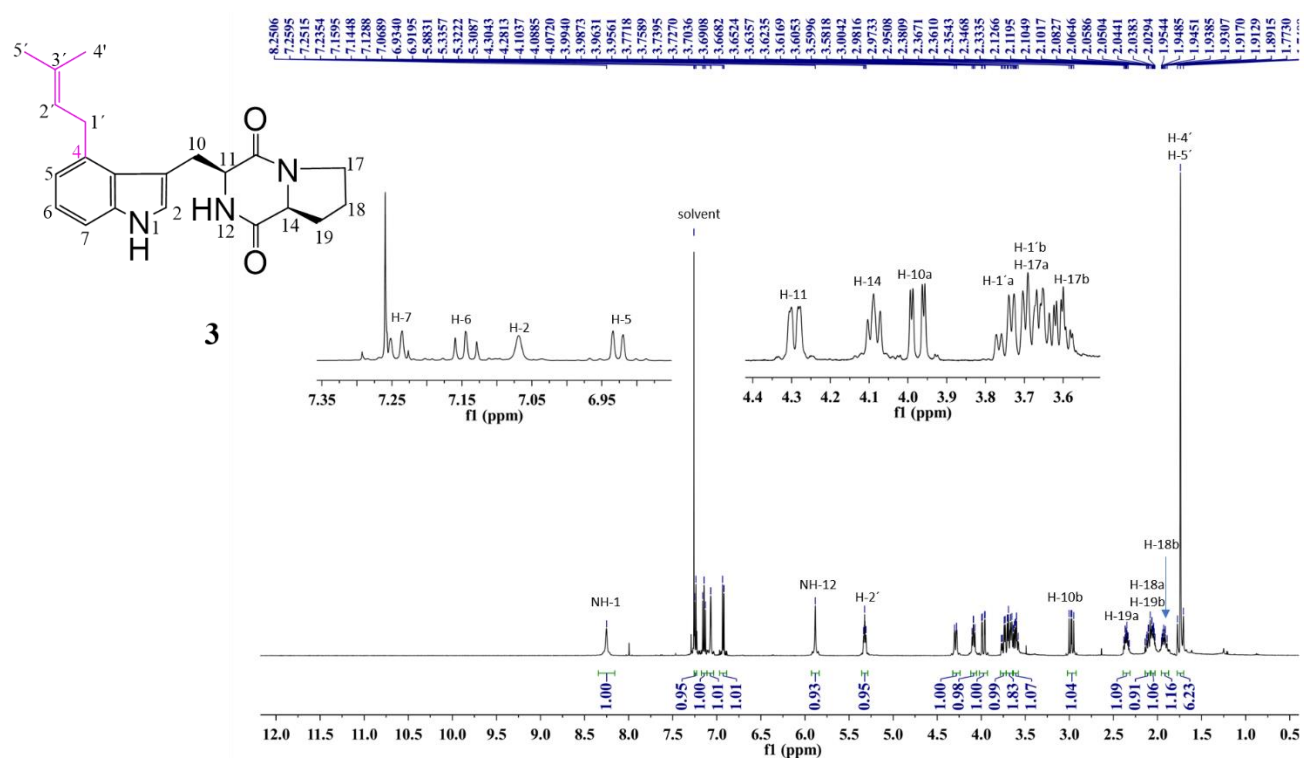

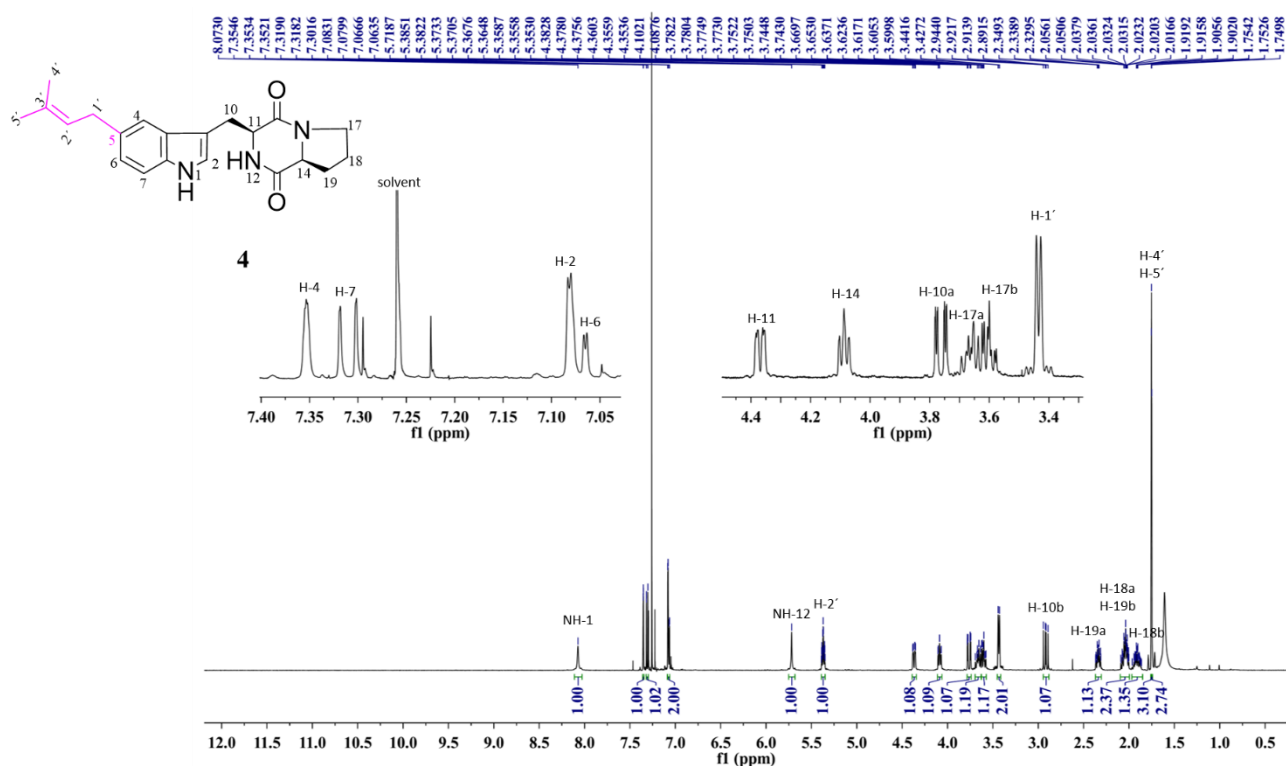Fig. S2 ^{1}H NMR spectrum of **3** in CDCl$_3$ (500 MHz).

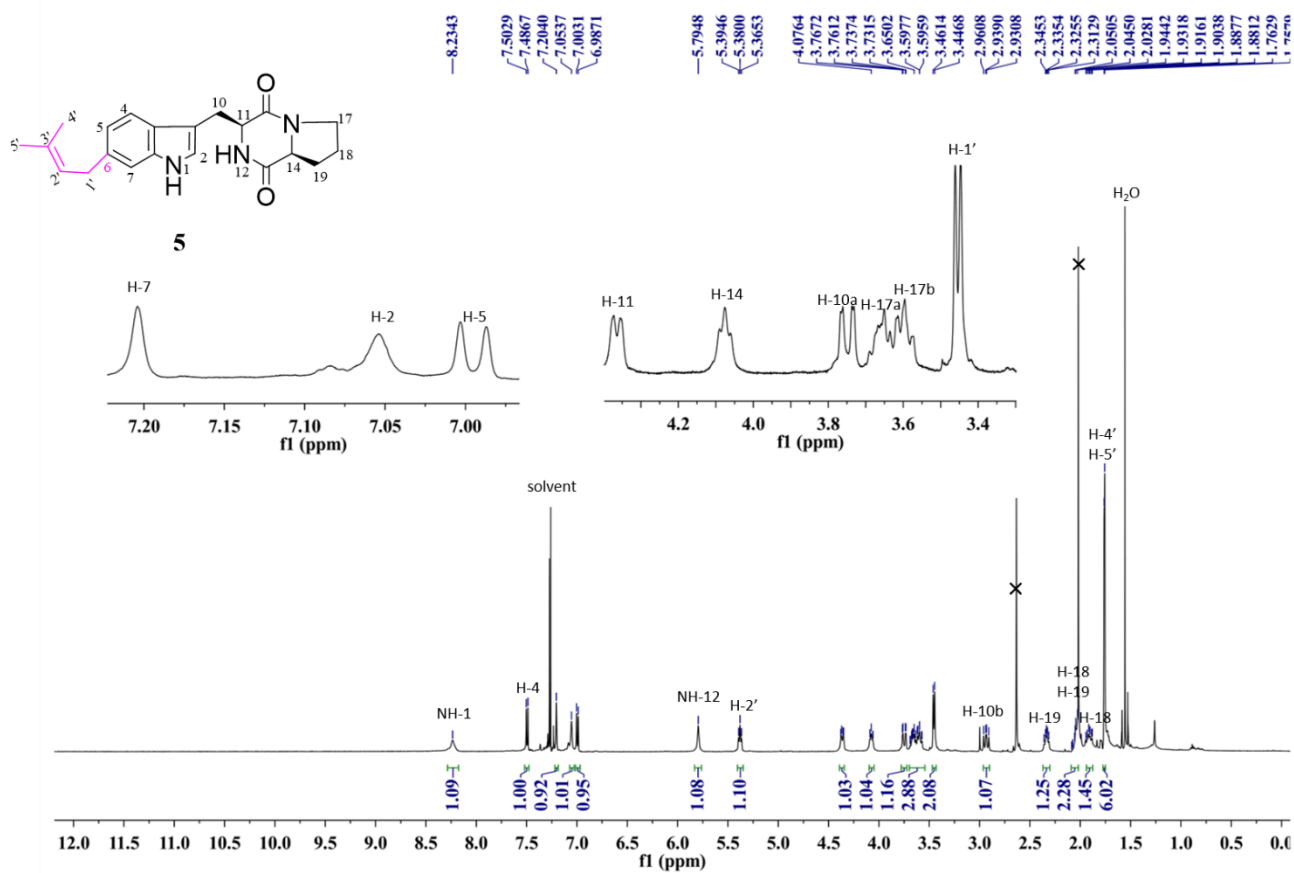**Fig. S3** ¹H NMR spectrum of **4** in CDCl₃ (500 MHz).
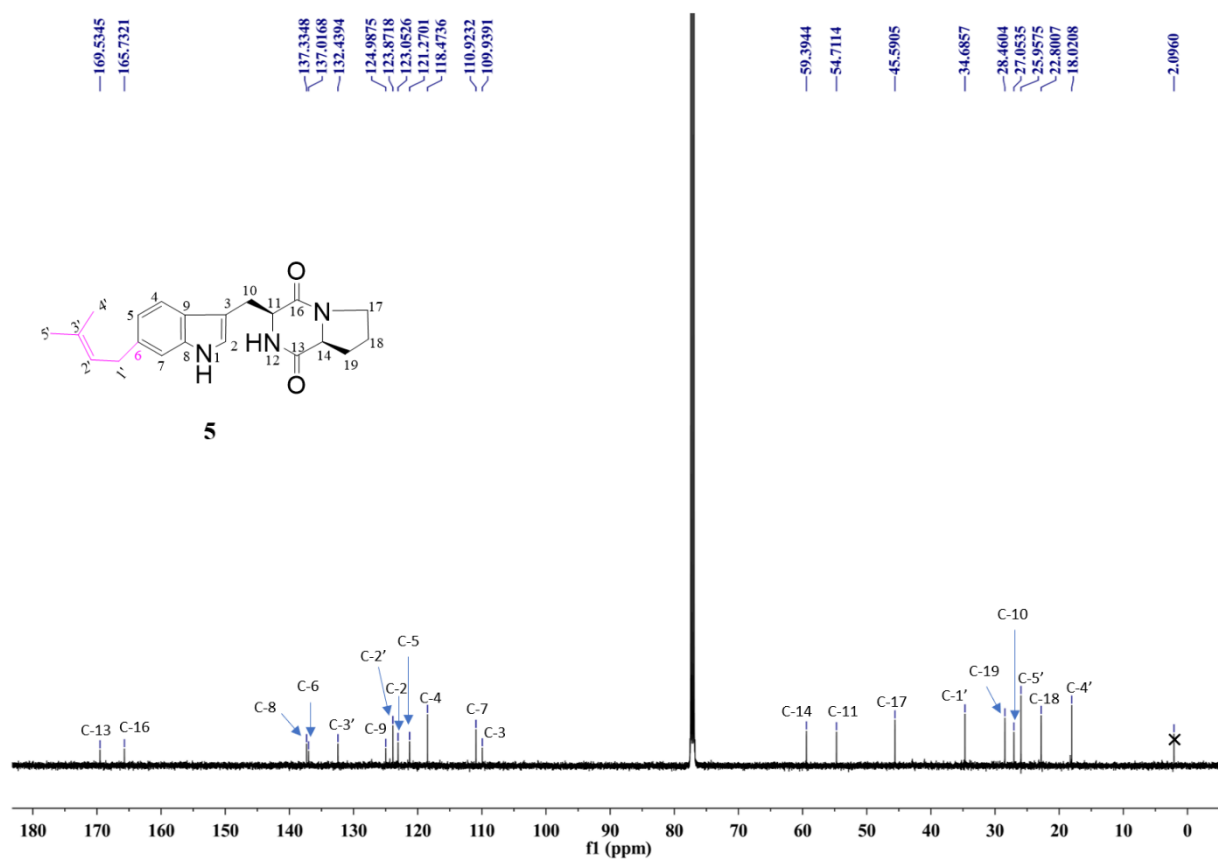

Fig. S4 ¹H NMR spectrum of **5** in CDCl₃ (500 MHz).
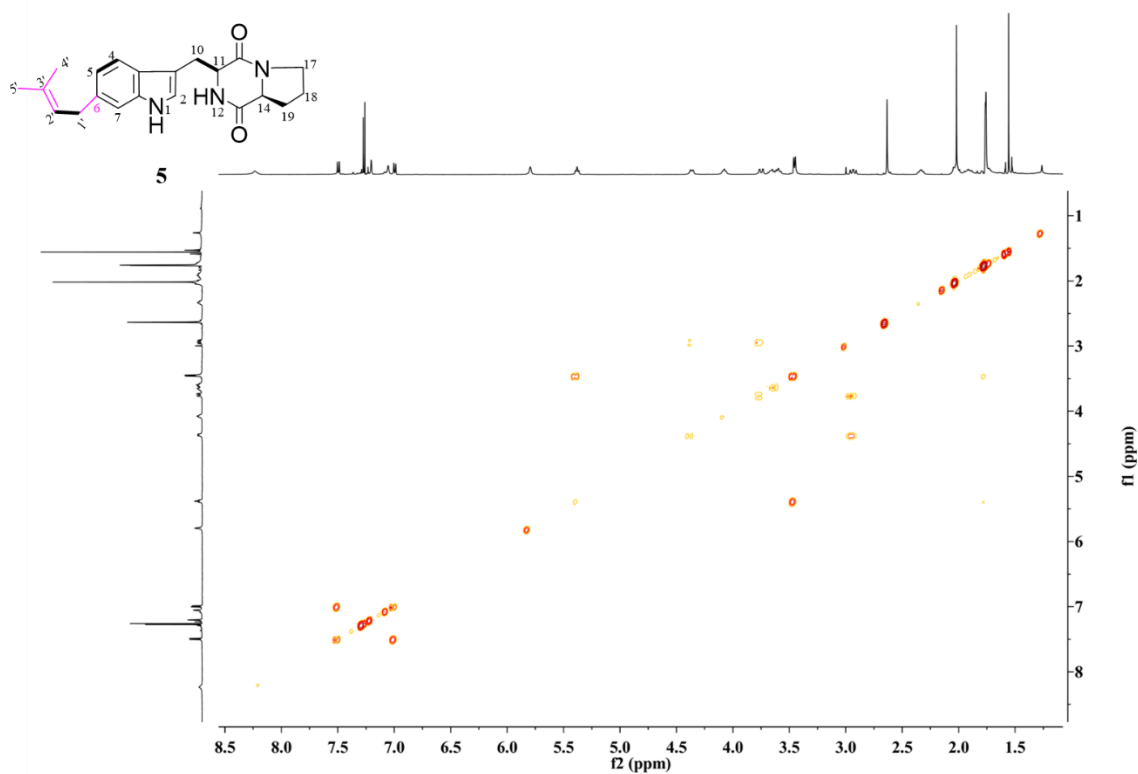
Fig. S5 ¹³C NMR spectrum of **5** in CDCl₃ (125 MHz).

Fig. S6 ¹H-¹H COSY spectrum of **5** in CDCl₃.

Fig. S7 HSQC spectrum of **5** in CDCl₃.
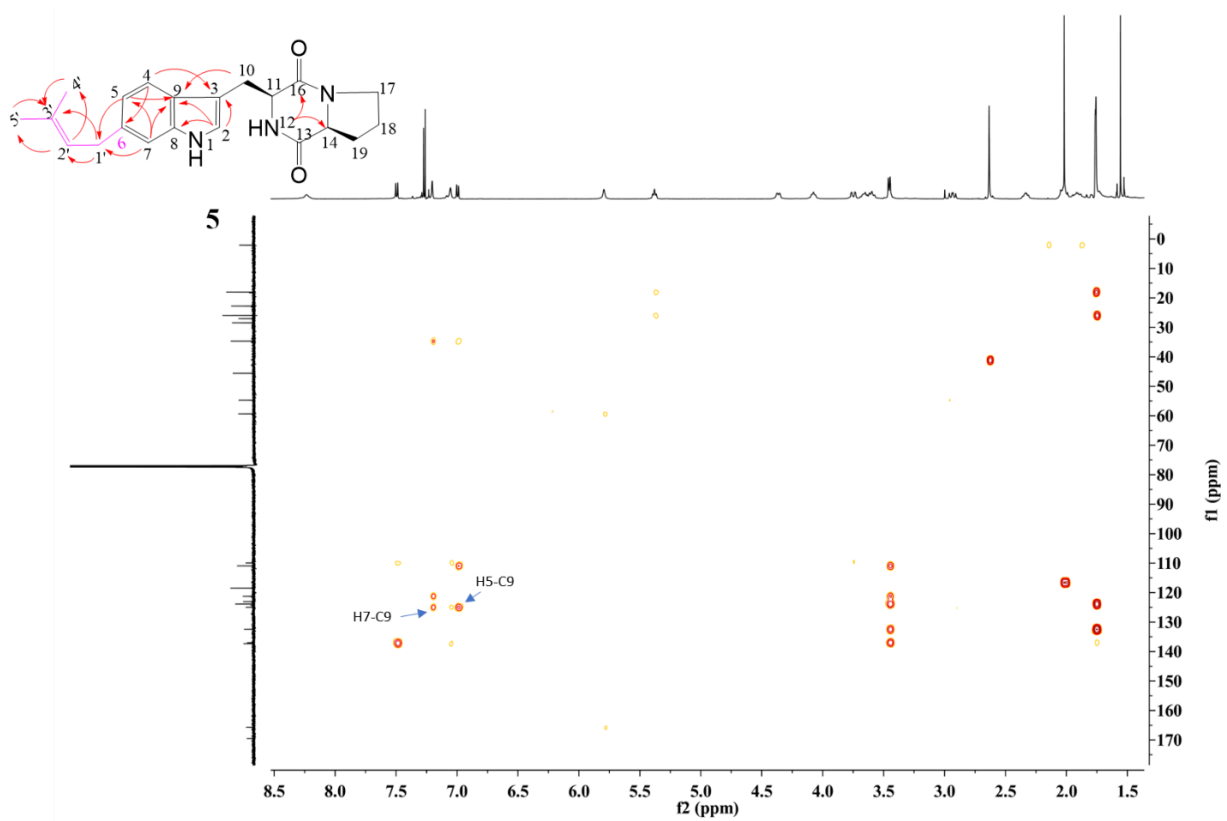
Fig. S8 HMBC spectrum of **5** in CDCl₃.

10

84
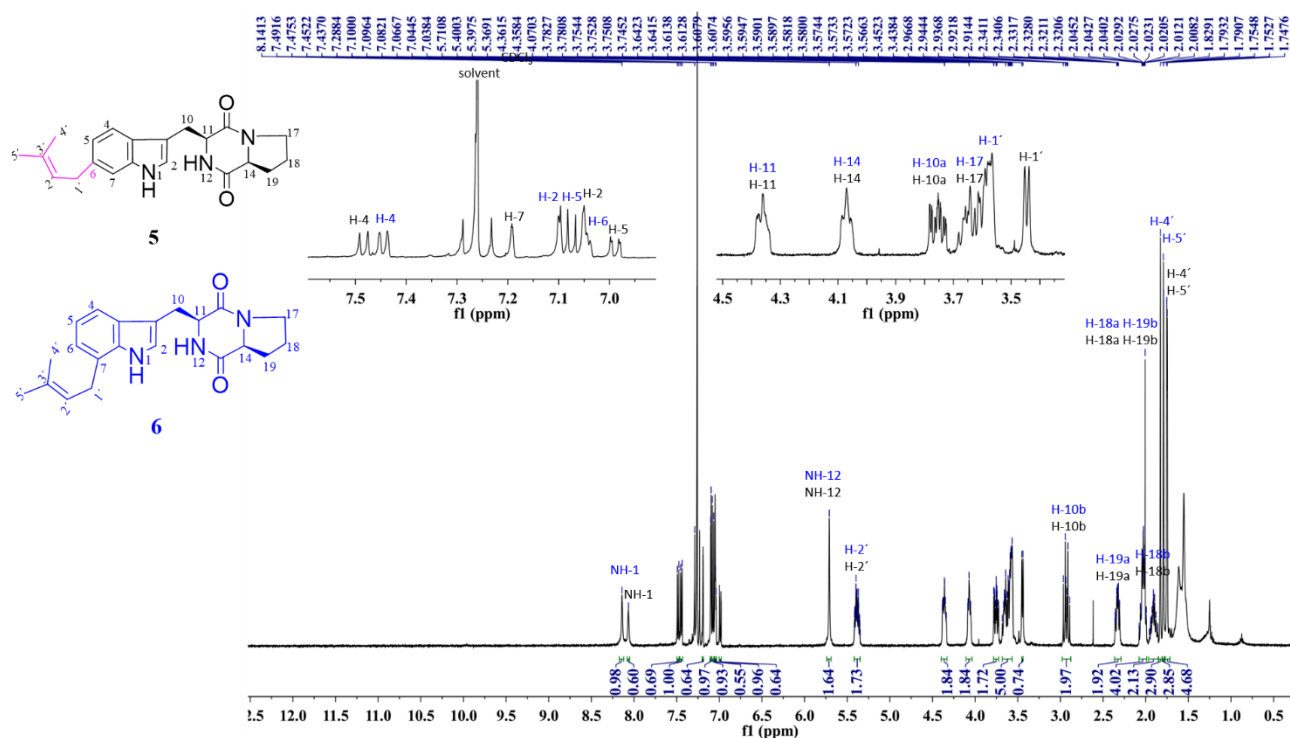
Fig. S9 ¹H NMR spectrum of **6** (mixture with **5**) in CDCl₃ (500 MHz).
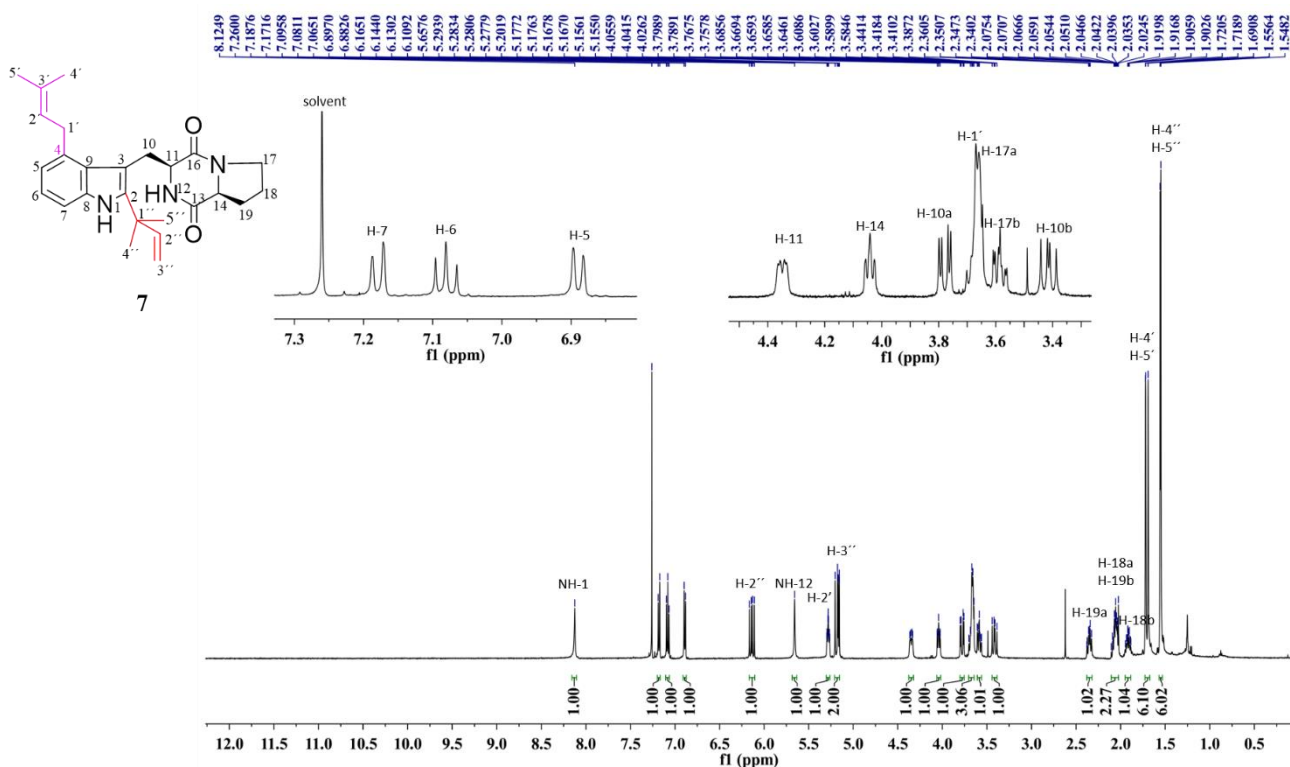
Fig. S10 ¹H NMR spectrum of **7** in CDCl₃ (500 MHz).
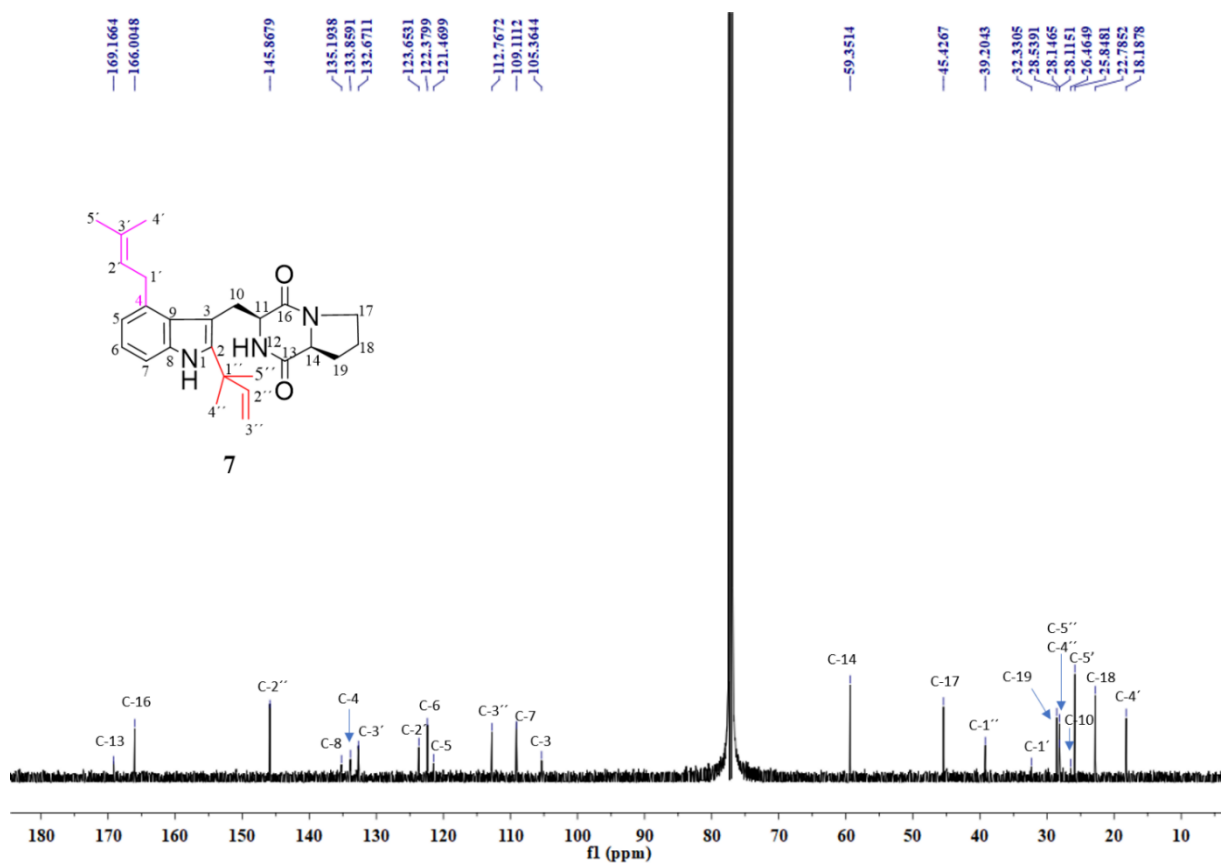
Fig. S11 ^{13}C NMR spectrum of **7** in CDCl$_3$ (125 MHz).

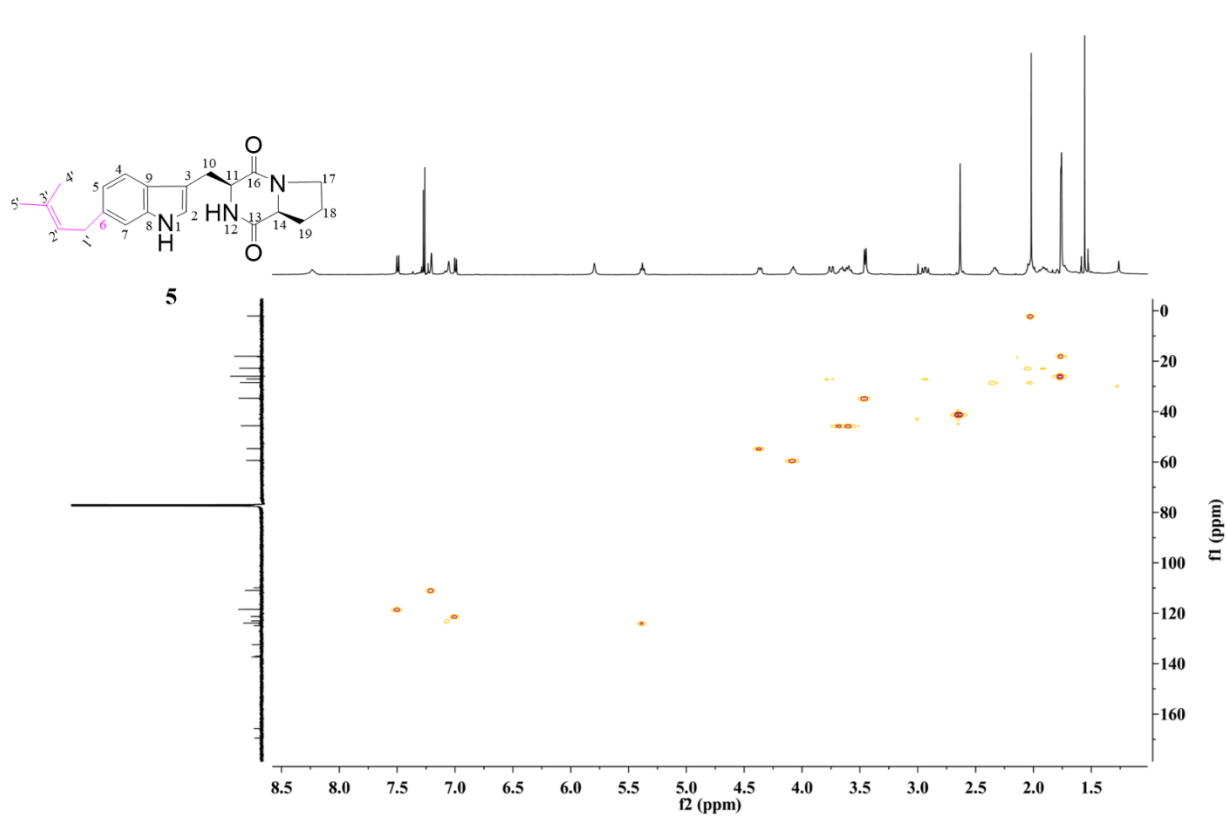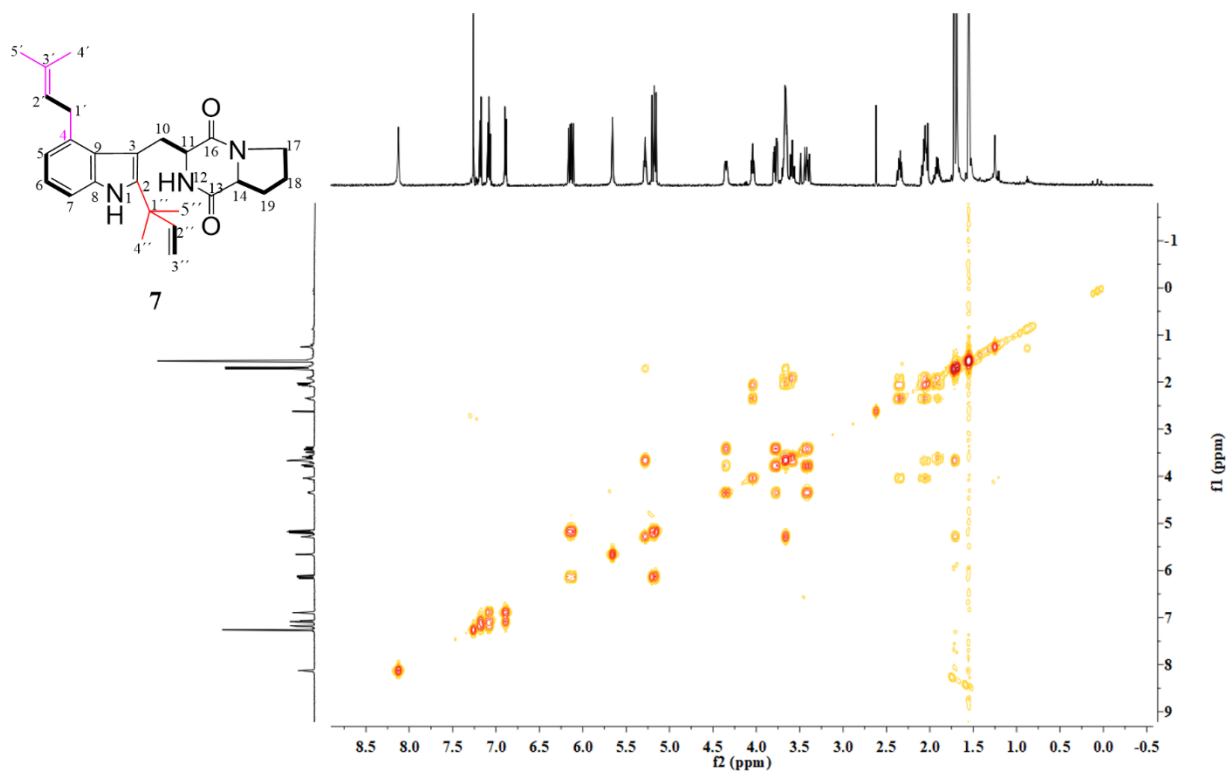**Fig. S12** ^{1}H-^{1}H COSY spectrum of **7** in CDCl$_3$.
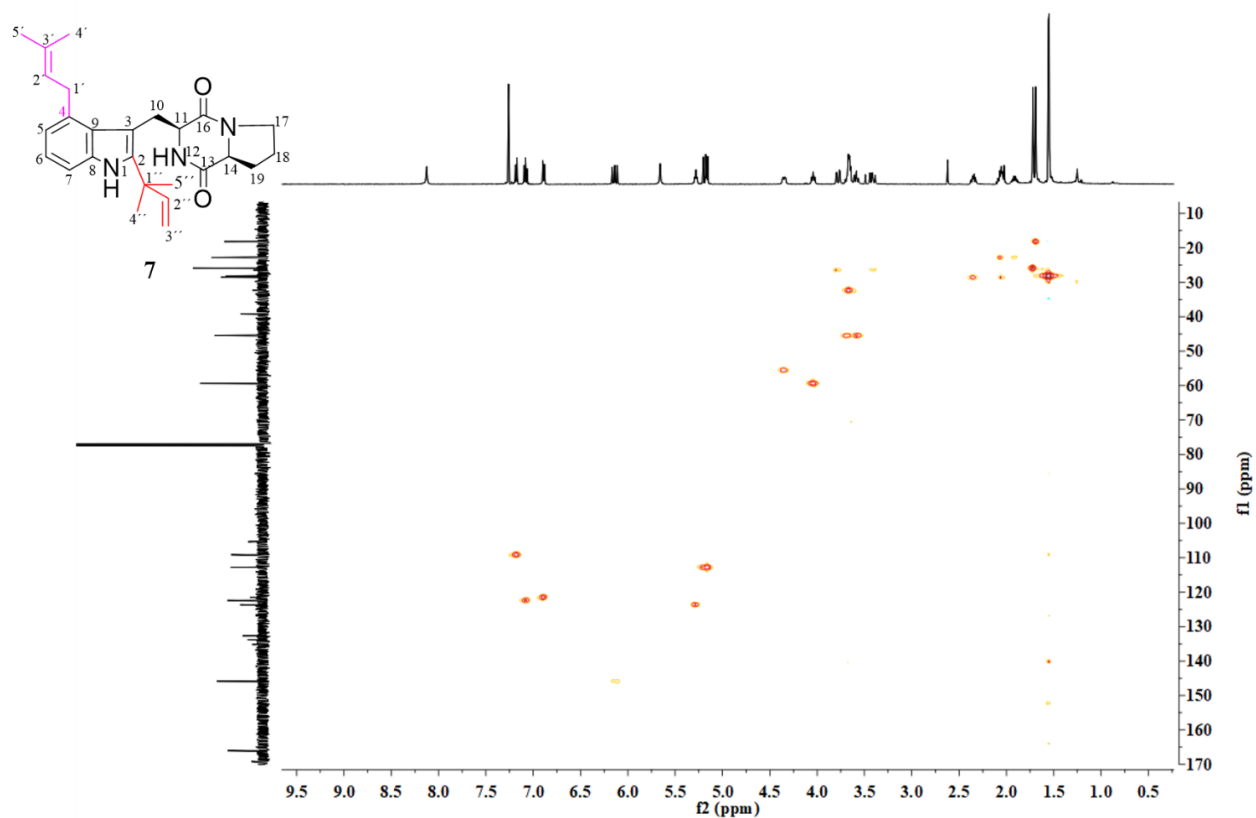
Fig. S13 HSQC spectrum of **7** in CDCl₃.
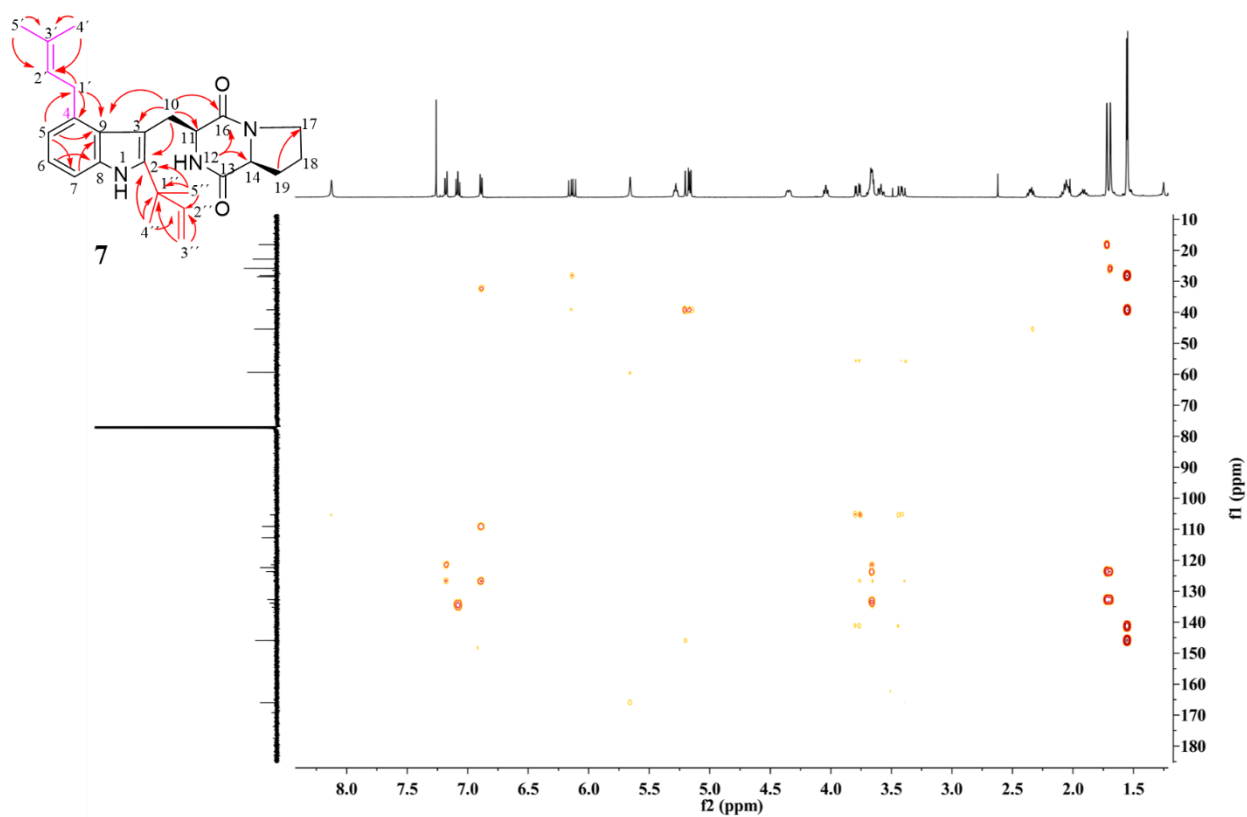
Fig. S14 HMBC spectrum of **7** in CDCl₃.

13

Fig. S15 ^{1}H NMR spectrum of **8** in CDCl$_3$ (500 MHz).

Fig. S16 ^{13}C NMR spectrum of **8** in CDCl$_3$ (125 MHz).
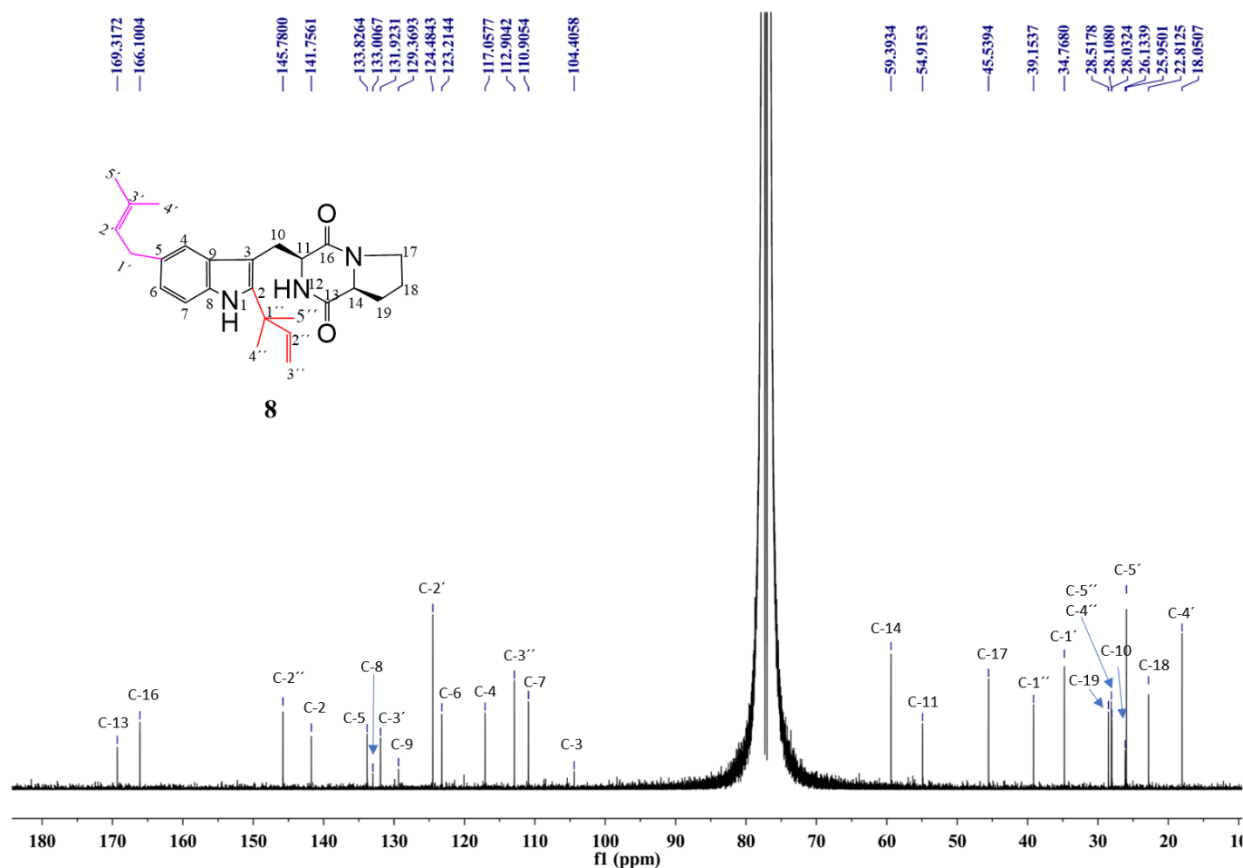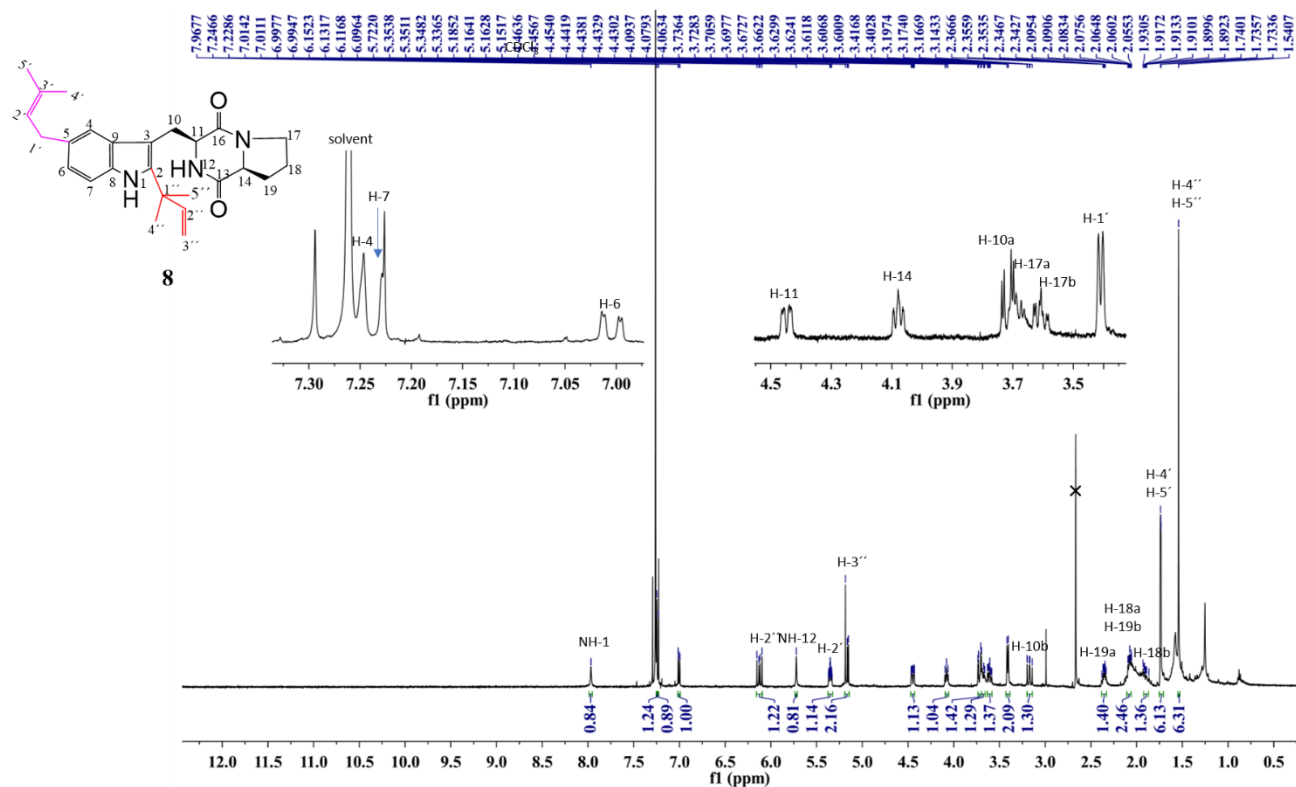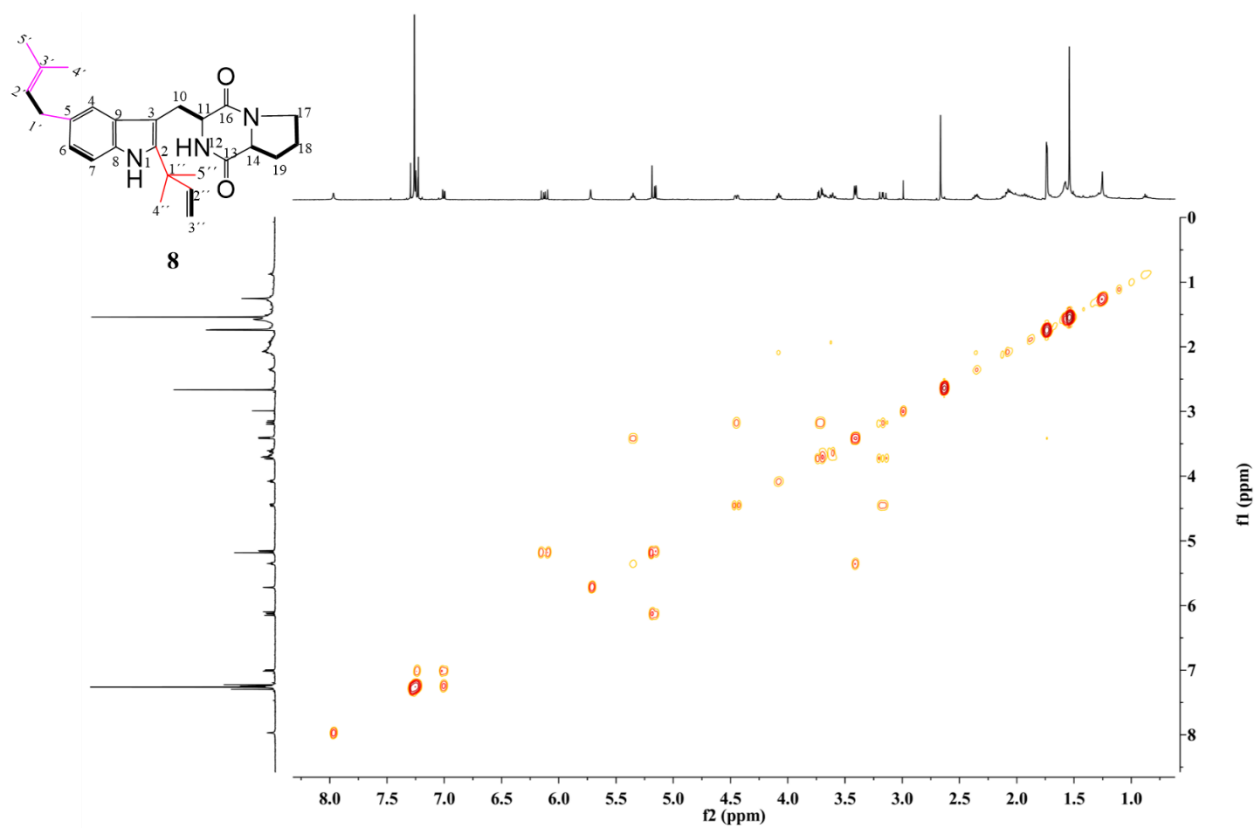
Fig. S17 ^{1}H-^{1}H COSY spectrum of **8** in CDCl$_3$.
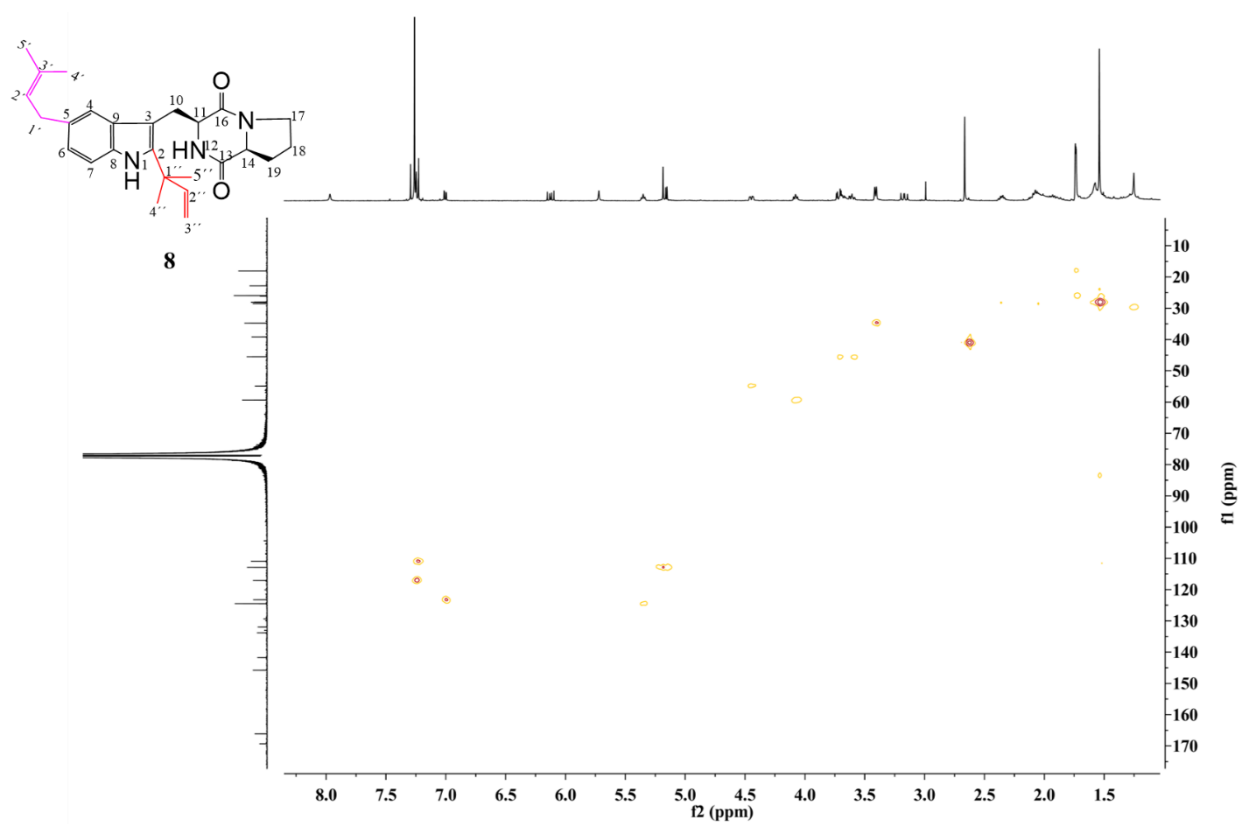
Fig. S18 HSQC spectrum of **8** in CDCl$_3$.

15
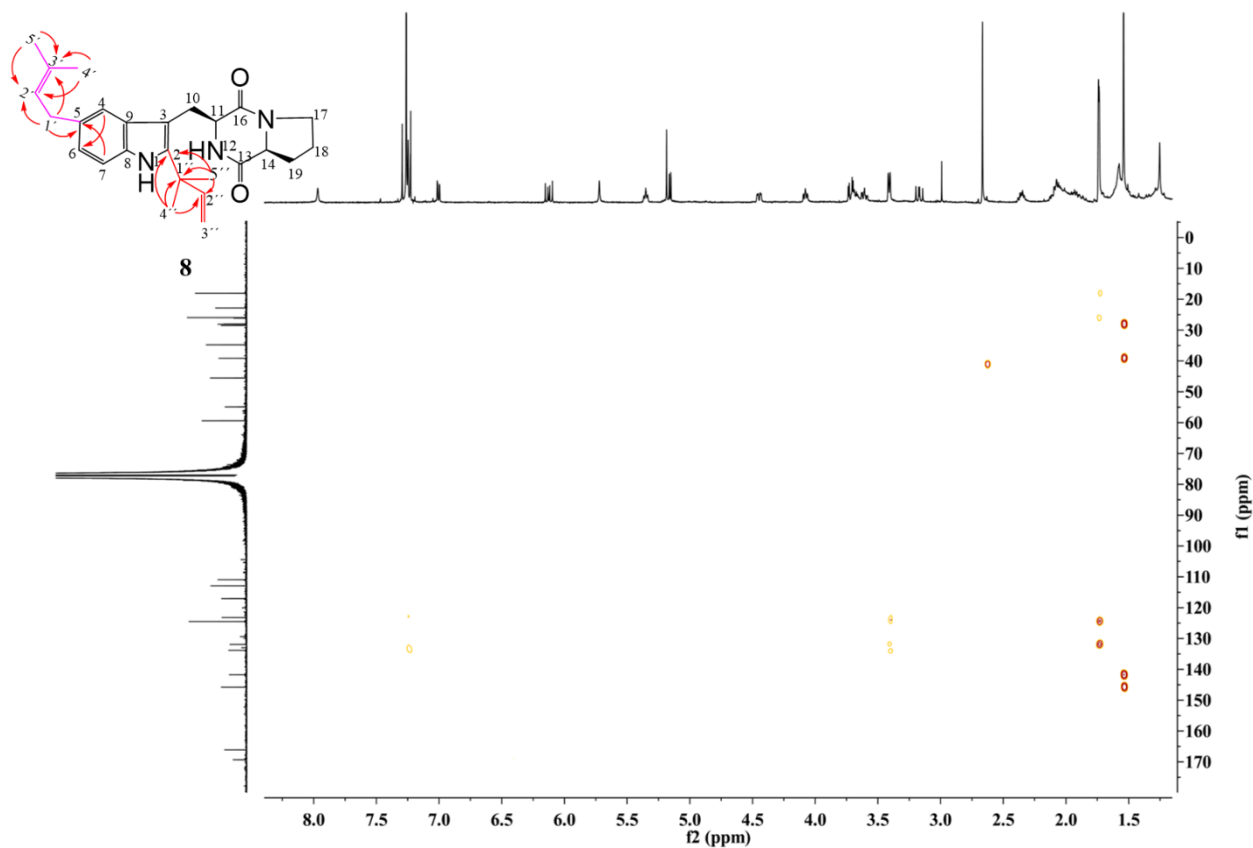
Fig. S19 HMBC spectrum of **8** in CDCl$_3$.
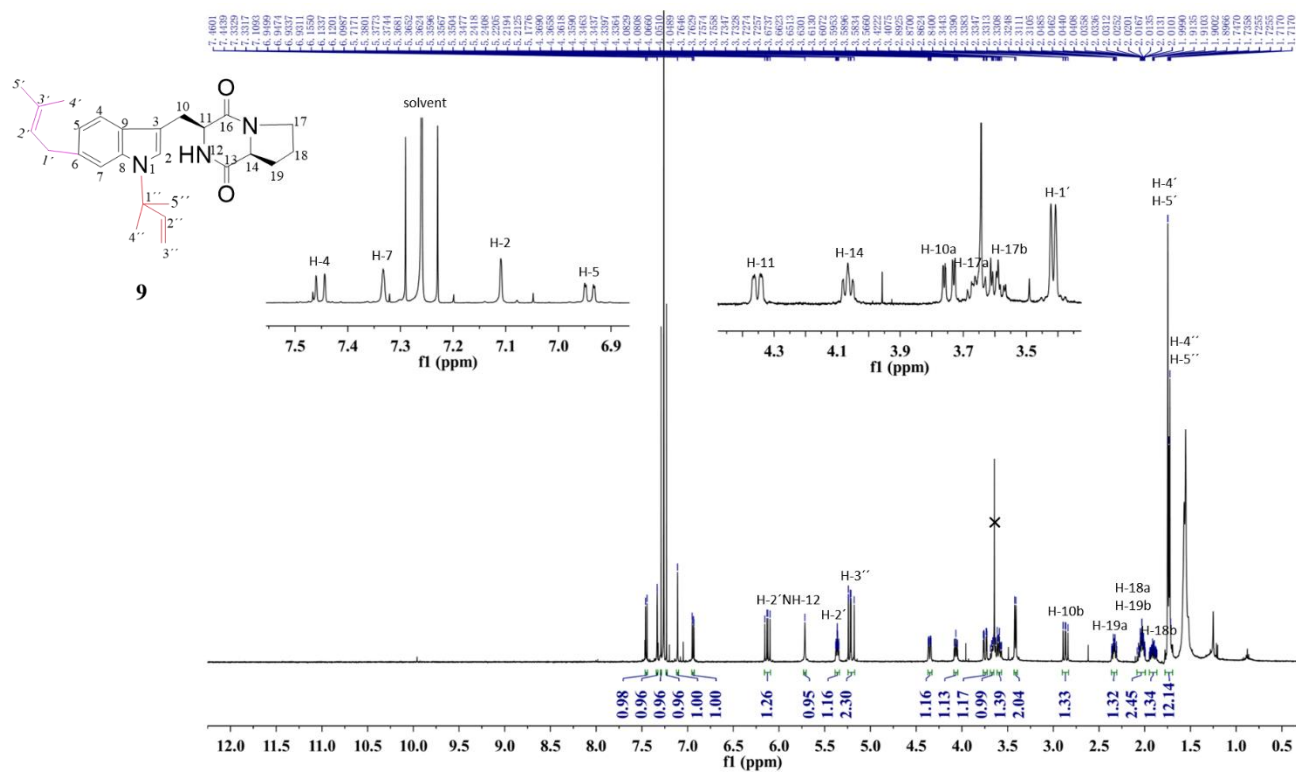
Fig. S20 ^{1}H NMR spectrum of **9** in CDCl$_3$ (500 MHz).

90

16
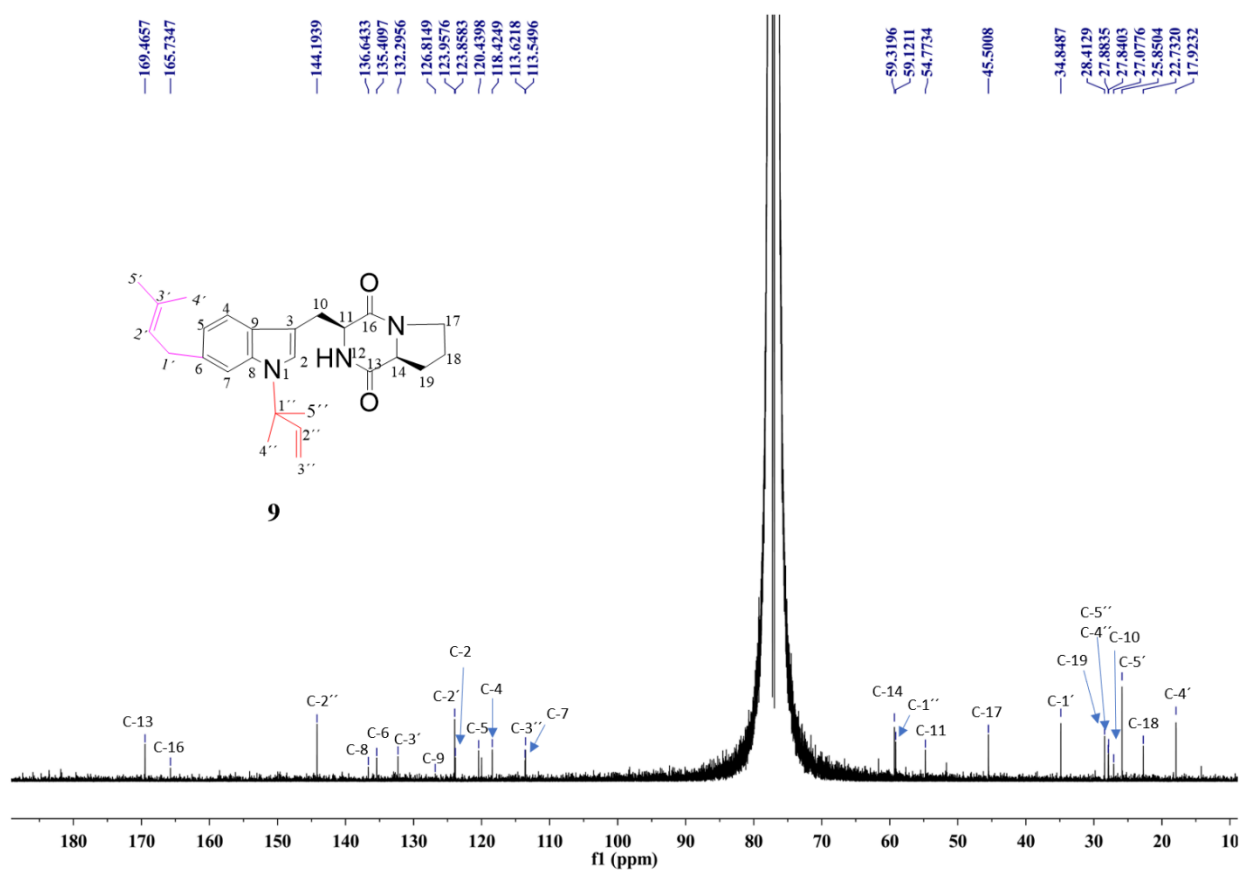
Fig. S21 ^{13}C NMR spectrum of **9** in CDCl$_3$ (125 MHz).
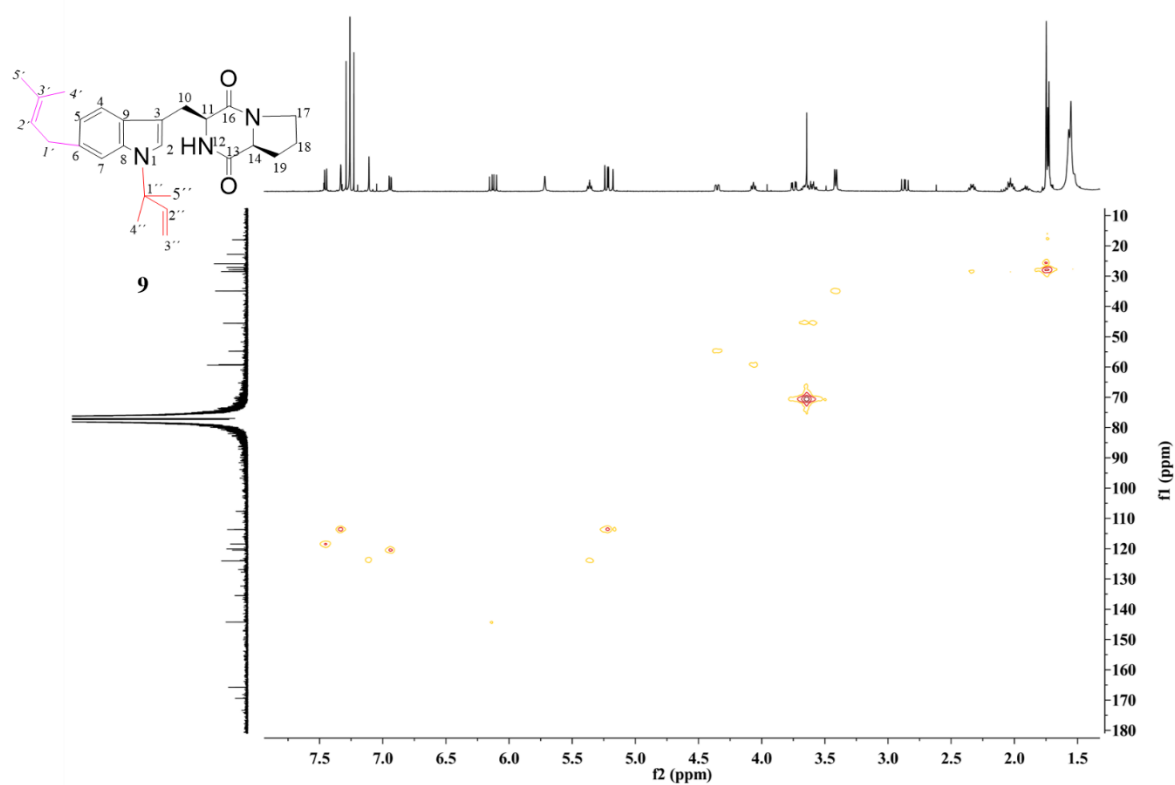
Fig. S22 HSQC spectrum of **9** in CDCl$_3$.

17

91
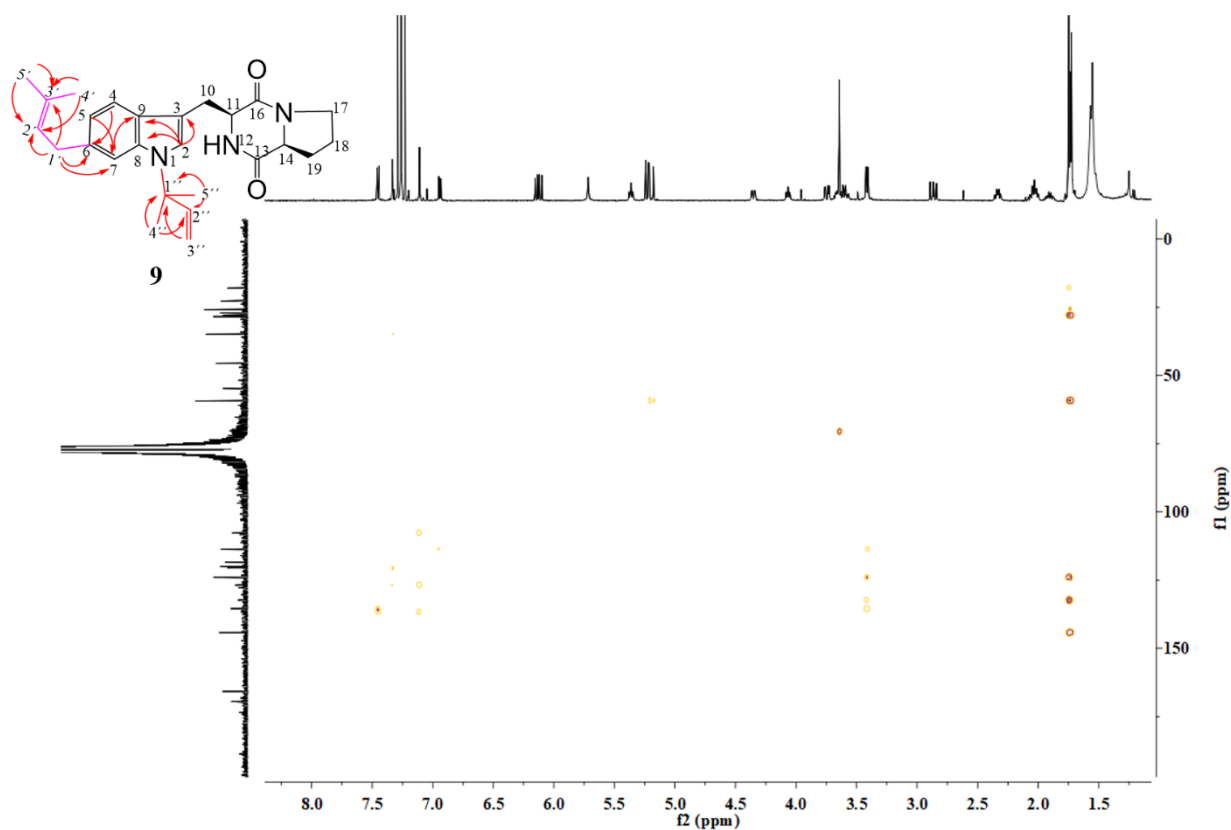
Fig. S23 HMBC spectrum of **9** in CDCl₃.
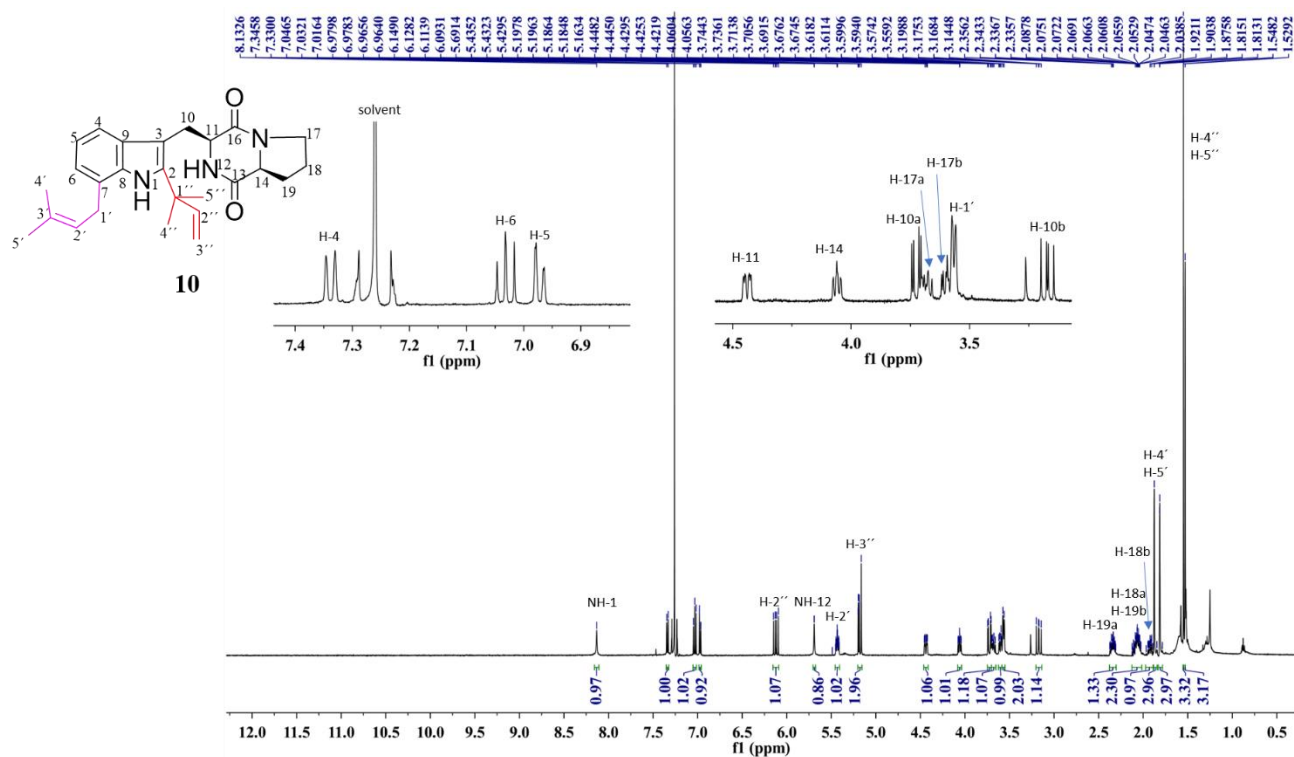
Fig. S24 ¹H NMR spectrum of **10** in CDCl₃ (500 MHz).

18
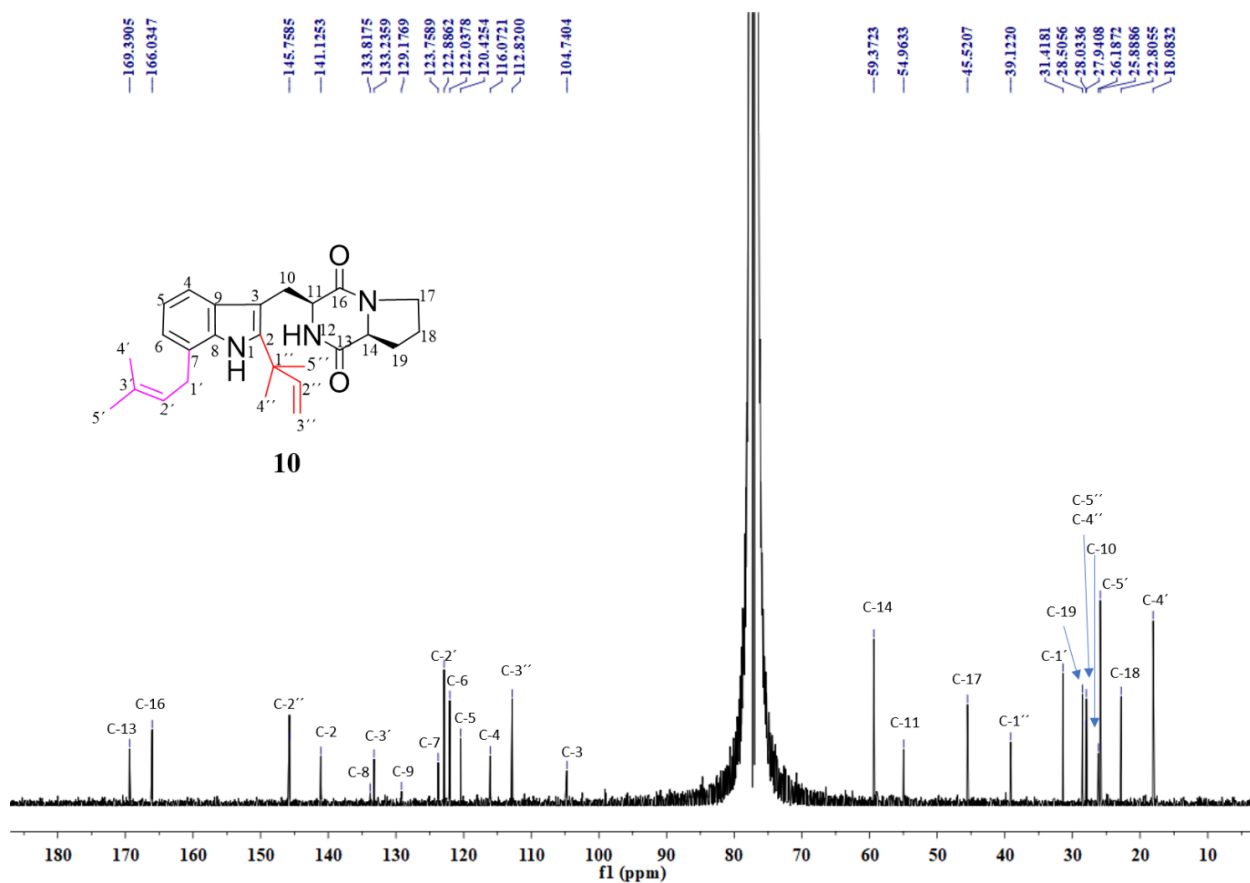
Fig. S25 ^{13}C NMR spectrum of **10** in CDCl$_3$ (125 MHz).

References

Liu R, Zhang H, Wu W, Li H, An Z, Zhou F (2020) C7-Prenylation of tryptophan-containing cyclic dipeptides by 7-dimethylallyl tryptophan synthase significantly increases the anticancer and antimicrobial activities. Molecules 25:3676.

Schkeryantz JM, Woo JCG, Siliphaivanh P, Depew KM, Danishefsky SJ (1999) Total synthesis of gypsetin, deoxybrevianamide E, brevianamide E, and tryprostatin B: novel constructions of 2,3-disubstituted indoles. J Am Chem Soc 121:11964-11975.

Steffan N, Li S-M (2009) Increasing structure diversity of prenylated diketopiperazine derivatives by using a 4-dimethylallyltryptophan synthase. Arch Microbiol 191:461-466.

4.3 Prenylation of dimeric *cyclo*-L-Trp-L-Trp by utilizing the promiscuous *cyclo*-L-Trp-L-Ala prenyltransferase EchPT1

Prenylation of dimeric *cyclo*-L-Trp-L-Trp by the promiscuous *cyclo*-L-Trp-L-Ala prenyltransferase EchPT1

Wen Li,[a] Xiulan Xie,[b] Jing Liu,[a] Huili Yu[a] and Shu-Ming Li*[a]

[a] Institut für Pharmazeutische Biologie und Biotechnologie, Fachbereich Pharmazie, Philipps-Universität Marburg, Robert-Koch-Straße 4, 35037 Marburg, Germany.

[b] Fachbereich Chemie, Philipps-Universität Marburg, Hans-Meerwein-Straße 4, 35032 Marburg, Germany.

Corresponding Author

*Tel/Fax: + 49-6421-28-22461/25365. E-mail: shuming.li@staff.uni-marburg.de.

ORCID Shu-Ming Li: 0000-0003-4583-2655

Abstract

Prenyltransferases (PTs) from the dimethylallyl tryptophan synthase (DMATS) superfamily are known as efficient biocatalysts and mainly catalyze regioselective Friedel-Crafts alkylation of tryptophan and tryptophan-containing cyclodipeptides (CDPs). They can also use other non-natural aromatic compounds as substrates and play therefore a pivotal role in increasing structural diversity and biological activities on a broad range of natural and unnatural products. In recent years, several prenylated dimeric CDPs have been identified with wide range of bioactivities. In this study, we demonstrate the production of prenylated dimeric CDPs by chemoenzymatic synthesis with a promiscuous known PT EchPT1, which uses *cyclo*-L-Trp-L-Ala as natural substrate for reverse *C2*-prenylation. High product yields were achieved with EchPT1 for C3-N1´ and C3-C3´ linked dimers of *cyclo*-L-Trp-L-Trp. Isolation and structural elucidation confirmed the product structures to be reversely C2/C2´-mono- and diprenylated *cyclo*-L-Trp-L-Trp dimers. Our study provides an excellent example for increasing structural diversity by prenylation of complex substrates with known biosynthetic enzymes.

Key points

- Chemoenzymatic synthesis of prenylated *cyclo*-L-Trp-L-Trp dimers.
- Same prenylation pattern and position for cyclodipeptides and their dimers.
- Indole prenyltransferases such as EchPT1 can be widely used as biocatalysts.

Keywords

Dimeric cyclodipeptides, prenylation, dimethylallyl tryptophan synthase, EchPT1, biocatalyst

98

Introduction

Indole alkaloids derived from tryptophan-containing cyclodipeptides (CDPs) with a 2,5-diketopiperazine skeleton were isolated from various microorganisms and plants and are well-known for their structural diversity and pharmaceutical utility (Goetz et al. 2011; Li 2010; Lindel et al. 2012; Vinokurova et al. 2003; Xu et al. 2014). Among them, tryptophan-based dimeric diketopiperazine alkaloids have been identified in recent years and their biosynthetic pathways have been elucidated (Gerken and Walsh 2013; Harken and Li 2021; Kim and Movassaghi 2011; Kim and Movassaghi 2015). Typically, these natural products are biosynthesized from tryptophan and another amino acid such as tryptophan, proline, alanine or valine. The two amino acids are mainly condensed by either a nonribosomal peptide synthetase in fungi or a cyclodipeptide synthase in bacteria, resulting in the formation of the two peptide bonds. The CDP core is then modified by cytochrome P450 to generate the homo- or heterodimer with unique bond connection (Gomes et al. 2019; Harken and Li 2021; Malit et al. 2021). Examples are the C6-N1′ linked aspergilazine A (**1**), the C3-C6′ linked naseseazine A (**2**) and tetratryptomycins A−C (**3−5**) with the symmetrical C3-C3′ and unsymmetrical C3-N1′ linkage (Fig. 1a) (Liu et al. 2020; Yu and Li 2019). The C3-C3′ linked (+)-WIN 64821 was isolated from *Aspergillus versicolor* and exhibits potential analgesic and anti-inflammatory activities for inhibition of substance P receptor (Fig. 1a) (Movassaghi et al. 2008; Tadano et al. 2013).

Recently, several tryptophan-containing dimeric CDPs carrying prenyl moieties were also isolated from different species (Cai et al. 2019; Geng et al. 2017; Song et al. 2012). Interestingly, all these complex structures are *C2*-prenylated *cyclo*-L-Trp-L-Pro (cWP) or *cyclo*-L-Trp-L-Ala (cWA) dimers with different connections and symmetries. The cWP dimer brevianamide S exhibits selective antibacterial activity against Bacille Calmette-Guérin (BCG), which serves as a valuable lead for next-generation antitubercular drugs (Song et al. 2012). Another cWP dimer asperginulin A with an unprecedented 6/5/4/5/6 pentacyclic skeleton showed obvious toxicity in inhibiting settlement of the larvae of *Balanus reticulatus* (Cai et al. 2019). (+)/(-)-Uncarilin A, a pair of dimeric isoechinulin-type enantiomers with a symmetric four-membered core, were isolated from *Uncaria rhynchophyl* as a new type of melatonin receptors (Fig. 1b) (Geng et al. 2017). Attachment of prenyl moieties onto the indole nucleus usually increases the spectrum of the biological activities. However, in sharp contrast to the structural diversity of dimeric CDPs and CDP prenyltransferases (PTs), there are rare examples of prenylating enzymes toward CDP dimers.

3

The members of the dimethylallyl tryptophan synthase (DMATS) superfamily as important biocatalysts usually catalyze metal ion-independent Friedel-Crafts prenylations. They use predominantly tryptophan and other indole derivatives as prenyl acceptors, but can also accept a broad spectrum of aromatic compounds for prenylation. They were therefore already used for structural modification of diverse small molecules (Fan et al. 2015). By using the fungal PT CdpC3PT and its mutants, Xu successfully obtained prenylated biflavonoids (Xu et al. 2021). In this study, we intended to get prenylated dimeric CDPs by these soluble PTs. Our previous studies demonstrated that the *cyclo*-L-Trp-L-Ala (cWA) *C2*-prenyltransferase EchPT1 is involved in the biosynthesis of echinulin (Fig. 2) (Wohlgemuth et al. 2017) and shows a high flexibility toward different substrates (Li et al. 2023; Wohlgemuth et al. 2018). Accordingly, we selected this enzyme and four additional DMATS PTs for prenylation of dimeric CDPs. One mono-and three diprenylated *cyclo*-L-Trp-L-Trp (cWW) dimers were obtained in high conversion yields.

Materials and Methods

Chemicals

Dimethylallyl diphosphate (DMAPP) was chemically synthesized according to the method published previously (Woodside et al. 1988). Aspergilazine A (**1**), naseseazine A (**2**) and tetratryptomycins A−C (**3−5**) were isolated as described before (Liu et al. 2020; Yu and Li 2019).

Strains, plasmids and culture conditions

Escherichia coli strain BL21 (DE3) pLysS (Invitrogen, Karlsruhe, Germany) and M15 [pREP4] (Qiagen, Hilden, Germany) were used for gene expression and cultivated at 37 °C in Terrific broth (TB) medium. The plasmids pVW90, pALF49, pPM37, pJW12 and pLW40 were used for overproduction of the proteins EchPT1, FgaPT2_R244L, FgaPT2_Y398F, 6-DMATS$_{Sa}$ and 7-DMATS, respectively (Fan and Li 2016; Kremer et al. 2007; Mai et al. 2016; Winkelblech and Li 2014; Wohlgemuth et al. 2017). To select the recombinant strains, ampicillin (50 μg/mL) and kanamycin (25 μg/mL) were added to the medium.

Protein purification and enzyme assays

The proteins of EchPT1, FgaPT2_R244L, FgaPT2_Y398F, 6-DMATS$_{Sa}$ and 7-DMATS were purified by Ni-NTA affinity chromatography (Qiagen, Hilden) as described previously (Fan

4

100

105 and Li 2016; Kremer et al. 2007; Mai et al. 2016; Winkelblech and Li 2014; Wohlgemuth et al.

106 2017). The purity of the five recombinant proteins was proven with 12% (w/v) SDS-PAGE (Li

107 et al. 2023).

108 For enzyme reaction, standard assays (50 µL) contained Tris-HCl (50 mM, pH 7.5), $CaCl_2$ (5

109 mM), dimeric substrate (1 mM), DMAPP (1 mM), glycerol (0.5−5%, v/v), DMSO (2.5%, v/v)

110 and the purified protein (7 µg). The reaction mixtures were incubated at 37 °C for 1 or16 h and

111 subsequently terminated with 50 µL MeOH. After centrifugation at 17,000 x g for 20 min, the

112 enzyme reaction mixtures were analyzed on LCMS as described below.

113 Enzyme assays for product isolation were scaled up to a volume of 25 mL, containing Tris-HCl

114 (50 mM, pH 7.5), $CaCl_2$ (5 mM), DMAPP (1.5 mM), the respective dimeric substrate (1 mM)

115 and 5 mg purified EchPT1. The reaction mixtures were incubated at 37 °C for 16 h and extracted

116 three times with two volumes of ethyl acetate each. The resulting organic phases were

117 evaporated and dissolved in 1 ml MeOH for isolation.

118 The linearity of the EchPT1 reactions towards **3**–**5** was determined up to 360 min with 7 µg

119 protein. To determine the kinetic parameters of EchPT1 toward three cWW dimers, the enzyme

120 assays (50 µL) contained Tris-HCl (50 mM, pH 7.5), $CaCl_2$ (5 mM), DMAPP (1 mM), 7 µg

121 EchPT1 and the cWW dimers at final concentrations of 0.01, 0.02, 0.05, 0.1, 0.2, 0.5, 1.0 and

122 2.0 mM. The reaction mixtures containing **3**, **4** and **5** were incubated at 37 °C for 30, 30 and 20

123 min, respectively. For the kinetic parameters of EchPT1 toward DMAPP in the presence of **3**,

124 **4** and **5**, the reaction mixtures contained Tris-HCl (50 mM, pH 7.5), $CaCl_2$ (5 mM), the

125 respective dimeric substrate (1 mM), 7 µg EchPT1 and DMAPP at final concentrations from

126 0.01 to 2.0 mM, which were incubated at 37 °C for 30, 30 and 20 min; respectively. The

127 reactions were terminated with 50 µL MeOH and analyzed on HPLC as described below. All

128 the assays were performed as duplicates. The conversion yields were calculated by comparing

129 with the isolated products as standard or by the ratio of the peak areas in HPLC chromatograms.

130 The data were analyzed by using Prism 8.01 (GraphPad Software).

131

132 **LCMS and HPLC analysis of the enzyme products**

133 LCMS analysis was performed as described previously (Zhou and Li 2021). The enzyme

134 products were eluted at a flow rate of 0.25 mL/min with a linear gradient from 5 to 100% MeCN

135 in 10 min. LCMS data were evaluated with DataAnalysis 4.2 software (Bruker Daltonik,

136 Bremen, Germany).

137 For isolation of the target substances, semi-preparative HPLC was performed with an Agilent

138 Eclipse XDB-C_{18} (250 × 9.4 mm, 5 µm) column. H_2O (A) and MeCN (B) were used as solvents

at a flow rate of 2 mL/min. Compounds **3a2** and **5a2** were isolated with 80% B, **4a1** and **4a2** with 75% B. To determine the enzyme activities, an Agilent HPLC 1260 series equipped with a Multosphere 120 RP-C$_{18}$ (250 × 2 mm, 5μ) column was used. H$_2$O (A) and MeCN (B) were used as mobile phase at a flow rate of 0.5 mL/min. The substances were eluted using a linear gradient from 5−100% B within 20 min.

Structural elucidation of the enzyme products by NMR analysis

NMR spectra were recorded on a 500 MHz Bruker AVIII spectrometer and processed with MestReNova 6.1.0 (Metrelab). All the samples were dissolved in DMSO-d_6 for measurement. Chemical shifts were referred to those of the solvent signals at δ$_H$ 2.50 ppm and δ$_C$ 39.5 ppm. The NMR data are provided in Tables S1−S4 and spectra in Figs. S7−S26.

Results

Acceptance of five dimeric CDPs by DMATS PTs with different activities

To prove the acceptance of the tryptophan-containing dimeric CDPs by the five PTs EchPT1, FgaPT2_R244L, FgaPT2_Y398F, 6-DMATS$_{Sa}$ and 7-DMATS, which are responsible for the prenylation at C2, C4, C5, C6 and C7 of indole ring of tryptophan and/or tryptophan-containing CDPs, respectively, we overproduced the recombinant proteins and first incubated them with cWP dimer apergilazine A (**1**) and cWA-cWP dimer naseseazine A (**2**) in the presence of DMAPP. LCMS analysis showed that formation of monoprenylated **1** with [M + H]$^+$ ions at *m/z* 635.789 ± 0.005 and **2** at 607.735 ± 0.005 was only observed in the extracted ion chromatograms (EICs) of the reaction mixtures with EchPT1, FgaPT2_Y398F and 7-DMATS (Figs. S1 and S2). Obviously, cWP-containing dimers are poor substrates of the tested PTs. In comparison, cWW dimers like tetratryptomycins A−C (**3−5**) with the symmetrical C3-C3′ and the unsymmetrical C3-N1′ linkage were much better accepted, at least by two of the tested PTs. Incubation of **3−5** with the aforementioned five enzymes at 37 °C for 16 h and LCMS analysis showed that the C3-C3′ linked **3** and **5** were well consumed by EchPT1 with conversion yields for the sole products **3a2** and **5a2** at 33.6 ± 0.3 and 14.2 ± 0.2%, respectively. In the reaction mixture of the C3-N1′ linked **4** with EchPT1, the main product **4a1** with a conversion yield of 12.0 ± 0.2% was accompanied by the second product **4a2** with a conversion yield of 3.7 ± 0.3% (Fig. 3). Other four enzymes showed clearly lower catalytic activities toward **3−5** than EchPT1. FgaPT2_R244L showed a conversion yield of 8.8 ± 0.1% toward **4** and 6.5 ± 2.0% toward **5** for monoprenylated products. Almost no conversion of **3** and **4** was observed with FgaPT2_Y398F and 6-DMATS$_{Sa}$ under the same conditions (Figs. S3−S5).

6

102

To detect monoprenylated products, we carried out incubations of **3−5** with EchPT1 in the presence of DMAPP for 1 h. As shown in Fig. 3, both monoprenylated (**3a1**, **4a1** and **5a1**) with $[M + H]^+$ ions at m/z 811.372 ± 0.005 and diprenylated products (**3a2**, **4a1** and **5a2**) with $[M + H]^+$ ions at m/z 879.434 ± 0.005 were clearly detected. Comparable product yields were calculated for the products of **3** and **5** in the range of 2.0−3.8%. The monoprenylated product **4a1** with a yield of 6.2 ± 0.2% was more accumulated in the reaction mixture of **4** than the diprenylated product **4a2** at 0.6 ± 0.1%. These results suggested that **3a1** and **5a1** were better accepted by EchPT1 than **4a1** for further prenylation.

To determine the relationship of mono- and diprenylated products in the reaction mixtures of the three cWW dimers with EchPT1, time dependence of their formation was determined. As shown in Fig. 4a, formation of **3a1** reached its maximum already in 5 min with the same conversion yield as **3a2** and decreased slightly after that. In comparison, the formation of **3a2** increased continuously during the whole incubation process. Similar results were obtained for the formation of **5a1** and **5a2** with lower conversion yields than those for **3a1** and **3a2** (Fig. 4c). The product yield of **4a1** reached its maximum after 30 min, approximately ten-folds of that of **4a2** and then decreased slightly, while the formation of **4a2** started at a lower level and kept steady increasing. The amount of **4a1** is about two-folds of that of **4a2** after incubation for 6 h (Fig. 4b). These results correspond well to the results after incubation for 16 h (Fig. 3) and proved again **3a1** and **5a1** are much better substrates for EchPT1 than **4a1**.

Prenylation of cWW dimers by EchPT1 and structural elucidation of the prenylated derivatives

To verify the structures of the four prenylated cWW dimers **3a2**, **4a1**, **4a2** and **5a2** by EchPT1 mentioned above, the assays of **3−5** and DMAPP were scaled up to 25 ml and incubated for 16 h. After extraction with ethyl acetate and isolation on HPLC, these products with UV absorption maxima at approximately 224 and 284 nm were obtained in high purity (Fig. S9). High-resolution mass spectrometric data proved again the monoprenylation in **4a1** by detection of the $[M + H]^+$ ion at m/z 811.3713, which is 68 dalton larger than that of the substrate **4**. In comparison, **3a2**, **4a2** and **5a2** with $[M + H]^+$ ions at m/z 879.434 ± 0.005 are diprenylated cWW dimers (Table S5).

The presence of the attached prenyl moieties in **3a2**, **4a1**, **4a2** and **5a2** was also confirmed by comparing their NMR data (Table S1−S4) with those of **3−5** (Liu et al. 2020). In the ^{1}H NMR spectra, the signals for indole H-19 (**3a2**, **4a1**, **4a2** and **5a2**) and H-19′ (**3a2**, **4a2** and **5a2**) disappeared. Instead, one (**4a1**) or two (**3a2**, **4a2** and **5a2**) reverse prenyl moieties can be

7

observed by the characteristic chemical shifts and coupling patterns. A doublet of doublets with a chemical shift between 6.23 and 6.15 ppm were observed for H-28/H-28´. The coupling constants with the two protons at H-29/H-29´ also found as a doublet of doublets with a chemical shift around 5.11 to 5.00 ppm. The signals of the two methyl groups were detected at approximately 1.50 ppm (Figs. S7, S12, S17 and S22). These data indicate the attachment of the reverse prenyl moiety at C-19 (and C-19´) of the indole ring, which is also consistent with the EchPT1-catalyzed *C2*-prenylation for its natural substrate cWA.

In the ^{13}C NMR spectra, the signals of C-19/C-19´ at the indole ring were observed at δ_c 141.4–141.5ppm (Figs. S8, S13, S18 and S23), which were comparable with the NMR data of the *C2*-prenylated CDPs in the literature (Li et al. 2023). Clear long-range correlations between H-28 (H-30/H-31) and C-19 (**3a2**, **4a1**, **4a2** and **5a2**) as well as H-28´ (H-30´/H-31´) and C-19´ (**3a2**, **4a2** and **5a2**) were observed in the HMBC spectra, proving the attachment of one or two reverse prenyl moieties at C-19 and C-19´ (Figs. S11, S16, S21 and S26). Taken together, their NMR data including ^{1}H, ^{13}C, ^{1}H-^{1}H COSY, HSQC and HMBC proved unequivocally **4a1** as *C19*-prenylated tetratryptomycin B and **3a2**, **4a2** and **5a2** as *C19,C19´*-diprenylated tetratryptomycins A, B and C, respectively (Fig. 5).

Determination of the kinetic parameters of EchPT1 toward tetratryptomycins and DMAPP

To further compare the catalytic efficiency of EchPT1 toward the dimeric derivatives **3−5** and DMAPP, kinetic parameters including Michaelis-Menten constants (K_M) and turnover numbers (k_{cat}) were determined for the enzyme. The most reactions followed the Michaelis-Menten kinetics, with the exception for **4a1** formation towards DMAPP and **4a2** formation towards **4** (Figs. S27−S30). Both of them fit well to a typical velocity equation with substrate inhibition (Figs. S28−S29). For the reactions of EchPT1 toward the prenyl acceptors **3−5**, the highest K_M at 0.25 mM was calculated for the formation of **4a1**, significantly higher than that of the natural substrate cWA at 0.09 mM. Interestingly, the Michaelis-Menten constants for the formation of **3a2**, **4a2** and **5a2** at 0.06, 0.01 and 0.05 mM, respectively, are somewhat lower than that of cWA (Table 1). The K_M values of EchPT1 reaction toward DMAPP for the formation of the four products between 0.05 and 0.08 mM are also slightly lower than 0.18 mM in the presence of cWA. The turnover numbers from 0.002 to 0.14 s^{-1} and the k_{cat}/K_M values from 286 to 1286 s^{-1} M^{-1} were determined in the range of EchPT1 reactions toward most CDPs (Wohlgemuth et al. 2018). The lowest k_{cat}/K_M value of **4a2** at 25 s^{-1} M^{-1} is also in good consistence with the observed conversion yield depicted in Fig. 3.

104

Discussion

In nature, PTs of the DMATS superfamily are known to be flexible toward aromatic prenyl acceptors. This enzyme family contributes to the structural diversity of small molecules, since they can efficiently prenylate various substrates including indole, xanthone, flavonoid and cyclodipeptide derivatives (Fan et al. 2015; Winkelblech et al. 2015). Prenylated products often exhibit improved interactions with proteins and biological membranes compared with the original precursors (Botta et al. 2009; Wollinsky et al. 2012). Numerous studies in the last years have demonstrated that PTs can be utilized as biocatalysts for the target structures (Chen et al. 2017; Mori et al. 2016; Ostertag et al. 2020).

As proof of concept, our main object in this study was chemoenzymatic synthesis of prenylated dimeric CDPs *in vitro*. Four new cWW dimers with C2/C2´-prenylations on the indole ring were successfully obtained by prenylation of tetratryptomycins A−C with the promiscuous cWA prenyltransferase EchPT1 in the presence of DMAPP. Our results demonstrated that even complex molecules can be modified by known enzymes. For designed small molecule modification, it is worth to test other available biocatalysts. However, cWP-containing dimers were poor substrates of the tested PTs. It would be interesting to test other available PTs or to get mutants of the known enzymes as demonstrated by Xu for prenylation of biflavonoids (Xu et al. 2021).

Author contributions

SL planned this project and WL carried out the experiments. XX did NMR analysis. JL and HY contributed to the substrate isolation. The manuscript was written through contributions of all authors. The authors have given approval to the final version of the manuscript.

Funding

Data availability

272   All data generated during this study are included in this published article and its supplementary

273   information file.

274

275   **Declarations**

276

277   **Ethics approval** This article does not contain any studies with human participants or animals

278   performed by any of the authors.

279

280   **Conflict of Interest**   All the authors declare that they have no conflict of interest

281

106

282   References

284   Botta B, Menendez P, Zappia G, de Lima RA, Torge R, Monachea GD (2009) Prenylated isoflavonoids:
285   Botanical distribution, structures, biological activities and biotechnological studies. An update
286   (1995-2006). Curr Med Chem 16:3414-3468.
287   Cai R, Jiang H, Xiao Z, Cao W, Yan T, Liu Z, Lin S, Long Y, She Z (2019) (-)- and (+)-Asperginulin
288   A, a pair of indole diketopiperazine alkaloid dimers with a 6/5/4/5/6 pentacyclic skeleton from the
289   mangrove endophytic fungus *Aspergillus* sp. SK-28. Org Lett 21:9633-9636.
290   Chen R, Gao B, Liu X, Ruan F, Zhang Y, Lou J, Feng K, Wunsch C, Li S-M, Dai J, Sun F (2017)
291   Molecular insights into the enzyme promiscuity of an aromatic prenyltransferase. Nat Chem Biol
292   13:226-234.
293   Fan A, Li S-M (2016) Saturation mutagenesis on Arg244 of the tryptophan C4-prenyltransferase
294   FgaPT2 leads to enhanced catalytic ability and different preferences for tryptophan-containing
295   cyclic dipeptides. Appl Microbiol Biotechnol 100:5389-5399.
296   Fan A, Winkelblech J, Li S-M (2015) Impacts and perspectives of prenyltransferases of the DMATS
297   superfamily for use in biotechnology. Appl Microbiol Biotechnol 99:7399-7415.
298   Geng CA, Huang XY, Ma YB, Hou B, Li TZ, Zhang XM, Chen JJ (2017) (+/-)-Uncarilins A and B,
299   dimeric isoechinulin-type alkaloids from *Uncaria rhynchophylla*. J Nat Prod 80:959-964.
300   Gerken T, Walsh CT (2013) Cloning and sequencing of the chaetocin biosynthetic gene cluster.
301   Chembiochem 14:2256-2258.
302   Goetz KE, Coyle CM, Cheng JZ, O'Connor SE, Panaccione DG (2011) Ergot cluster-encoded catalase
303   is required for synthesis of chanoclavine-I in *Aspergillus fumigatus*. Curr Genet 57:201-211.
304   Gomes NGM, Pereira RB, Andrade PB, Valentão P (2019) Double the chemistry, double the fun:
305   Structural diversity and biological activity of marine-derived diketopiperazine dimers. Mar Drugs
306   17:551.
307   Harken L, Li S-M (2021) Modifications of diketopiperazines assembled by cyclodipeptide synthases
308   with cytochrome P450 enzymes. Appl Microbiol Biotechnol 105:2277-2285.
309   Kim J, Movassaghi M (2011) Concise total synthesis and stereochemical revision of (+)-naseseazines
310   A and B: regioselective arylative dimerization of diketopiperazine alkaloids. J Am Chem Soc
311   133:14940-14943.
312   Kim J, Movassaghi M (2015) Biogenetically-inspired total synthesis of epidithiodiketopiperazines and
313   related alkaloids. Acc Chem Res 48:1159-1171.
314   Kremer A, Westrich L, Li S-M (2007) A 7-dimethylallyltryptophan synthase from *Aspergillus
315   fumigatus*: overproduction, purification and biochemical characterization. Microbiology 153:3409-
316   3416.
317   Li S-M (2010) Prenylated indole derivatives from fungi: structure diversity, biological activities,
318   biosynthesis and chemoenzymatic synthesis. Nat Prod Rep 27:57-78.
319   Li W, Coby L, Zhou J, Li SM (2023) Diprenylated cyclodipeptide production by changing the
320   prenylation sequence of the nature's synthetic machinery
321   1. Appl Microbiol Biotechnol 107:261-271.
322   Lindel T, Marsch N, Adla SK (2012) Indole prenylation in alkaloid synthesis. Top Curr Chem 309:67-
323   129.
324   Liu J, Xie X, Li S-M (2020) Increasing cytochrome P450 enzyme diversity by identification of two
325   distinct cyclodipeptide dimerases. Chem Commun 56:11042-11045.
326   Mai P, Zocher G, Ludwig L, Stehle T, Li S-M (2016) Actions of tryptophan prenyltransferases toward
327   fumiquinazolines and their potential application for the generation of prenylated derivatives by
328   combining chemical and chemoenzymatic syntheses. Adv Synth Catal 358:1639-1653.
329   Malit JJL, Liu W, Cheng A, Saha S, Liu LL, Qian PY (2021) Global genome mining reveals a
330   cytochrome P450-catalyzed cyclization of crownlike cyclodipeptides with neuroprotective activity.
331   Org Lett 23:doi: 10.1021/acs.orglett.1c01022.
332   Mori T, Zhang L, Awakawa T, Hoshino S, Okada M, Morita H, Abe I (2016) Manipulation of
333   prenylation reactions by structure-based engineering of bacterial indolactam prenyltransferases. Nat
334   Commun 7: 10849.

11

335   Movassaghi M, Schmidt MA, Ashenhurst JA (2008) Concise total synthesis of (+)-WIN 64821 and (-)-
336   ditryptophenaline. Angew Chem Int Ed Engl 47:1485-1487.
337   Ostertag E, Zheng L, Broger K, Stehle T, Li S-M, Zocher G (2020) Reprogramming substrate and
338   catalytic promiscuity of tryptophan prenyltransferases. J Mol Biol 433:166726.
339   Song F, Liu X, Guo H, Ren B, Chen C, Piggott AM, Yu K, Gao H, Wang Q, Liu M, Liu X, Dai H,
340   Zhang L, Capon RJ (2012) Brevianamides with antitubercular potential from a marine-derived
341   isolate of *Aspergillus versicolor*. Org Lett 14:4770-4773.
342   Tadano S, Mukaeda Y, Ishikawa H (2013) Bio-inspired dimerization reaction of tryptophan derivatives
343   in aqueous acidic media: three-step syntheses of (+)-WIN 64821, (-)-ditryptophenaline, and (+)-
344   naseseazine B. Angew Chem Int Ed Engl 52:7990-7994.
345   Vinokurova NG, Khmel'nitskaia II, Baskunov BP, Arinbasarov MU (2003) Occurrence of indole
346   alkaloids among secondary metabolites of soil *Aspergillus*. Appl Biochem Microbiol 39:192-196.
347   Winkelblech J, Fan A, Li S-M (2015) Prenyltransferases as key enzymes in primary and secondary
348   metabolism. Appl Microbiol Biotechnol 99:7379-7397.
349   Winkelblech J, Li S-M (2014) Biochemical investigations of two 6-DMATS enzymes from
350   *Streptomyces* revealing novel features of L-tryptophan prenyltransferases. Chembiochem 15:1030-
351   1039.
352   Wohlgemuth V, Kindinger F, Li S-M (2018) Convenient synthetic approach for tri- and tetraprenylated
353   cyclodipeptides by consecutive enzymatic prenylations. Appl Microbiol Biotechnol 102:2671-2681.
354   Wohlgemuth V, Kindinger F, Xie X, Wang BG, Li S-M (2017) Two prenyltransferases govern a
355   consecutive prenylation cascade in the biosynthesis of echinulin and neoechinulin. Org Lett
356   19:5928-5931.
357   Wollinsky B, Ludwig L, Hamacher A, Yu X, Kassack MU, Li SM (2012) Prenylation at the indole ring
358   leads to a significant increase of cytotoxicity of tryptophan-containing cyclic dipeptides. Bioorg
359   Med Chem Lett 22:3866-3869.
360   Woodside AB, Huang Z, Poulter CD (1988) Trisammonium geranyl diphosphate. Org Synth 66:211-
361   215.
362   Xu W, Gavia DJ, Tang Y (2014) Biosynthesis of fungal indole alkaloids. Nat Prod Rep 31:1474-1487.
363   Xu Y, Li D, Tan G, Zhang Y, Li Z, Xu K, Li S-M, Yu X (2021) A single amino acid switch alters the
364   prenyl donor specificity of a fungal aromatic prenyltransferase toward biflavonoids. Org Lett
365   23:497-502.
366   Yu H, Li S-M (2019) Two cytochrome P450 enzymes from *Streptomyces* sp. NRRL S-1868 catalyze
367   distinct dimerization of tryptophan-containing cyclodipeptides. Org Lett 21:7094-7098.
368   Zhou J, Li S-M (2021) Conversion of viridicatic acid to crustosic acid by cytochrome P450 enzyme-
369   catalysed hydroxylation and spontaneous cyclisation. App Microbiol Biotechnol 105:9181-9189.
370
371

Table 1. Kinetic parameters of EchPT1 toward **3−5** and DMAPP

Substrates	Products	Protein amount and incubation time	K_M [mM]	k_{cat} [s^{-1}]	k_{cat}/K_M [s^{-1} M^{-1}]
3	**3a2**	7μg, 30min	0.06 ± 0.007	0.05 ± 0.0003	833
4	**4a1**	7μg, 30min	0.25 ± 0.03	0.14 ± 0.01	560
4	**4a2**	7μg, 30min	0.01 ± 0.001	0.006 ± 0.0006	600
5	**5a2**	7μg, 20min	0.05 ± 0.005	0.03 ± 0.001	600
DMAPP with **3**	**3a2**	7μg, 30min	0.05 ± 0.007	0.03 ± 0.002	600
DMAPP with **4**	**4a1**	7μg, 30min	0.07 ± 0.01	0.09 ± 0.01	1286
DMAPP with **4**	**4a2**	7μg, 30min	0.08 ± 0.008	0.002 ± 0.0002	25
DMAPP with **5**	**5a2**	7μg, 20min	0.07 ± 0.008	0.02 ± 0.001	286

Three independent experiments were carried out and standard deviations are given as ± values

Figure legends

Fig. 1 Examples of known dimeric tryptophan-containing cyclodipeptides (a) and prenylated ones (b)

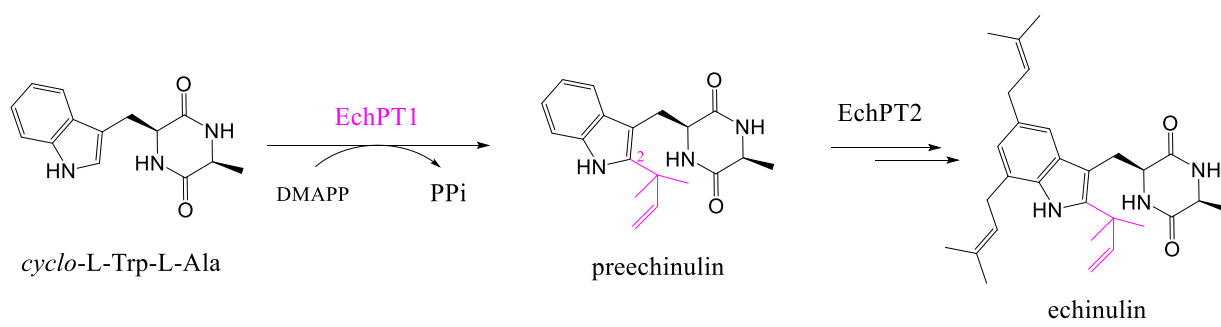**Fig. 2** Prenylation of *cyclo*-L-Trp-L-Ala by EchPT1 in the biosynthesis of echinulin

Fig. 3 LCMS analysis of the acceptance of tetratryptomycins A−C (**3**−**5**) by EchPT1 for 1 and 16 h. UV absorptions at 280 nm are illustrated in black. The chromatograms depicted in blue and red refer to EICs of $[M+H]^+$ of the monoprenylated at *m/z* 811.372 and those of the diprenylated products at *m/z* 879.434, respectively. A tolerance range of ± 0.005 was used for ion detection. All the assays were performed in duplicates. The conversion yields in percent are given in parenthesis after the product number as mean values

Fig. 4 Time dependence of the mono- and diprenylated products formation in the EchPT1 reactions with **3**, **4**, and **5** and DMAPP. UV absorptions at 280 nm are illustrated

Fig. 5 Prenylation of tetratryptomycins A−C by EchPT1 in the presence of DMAPP. See SI for carbon numbering
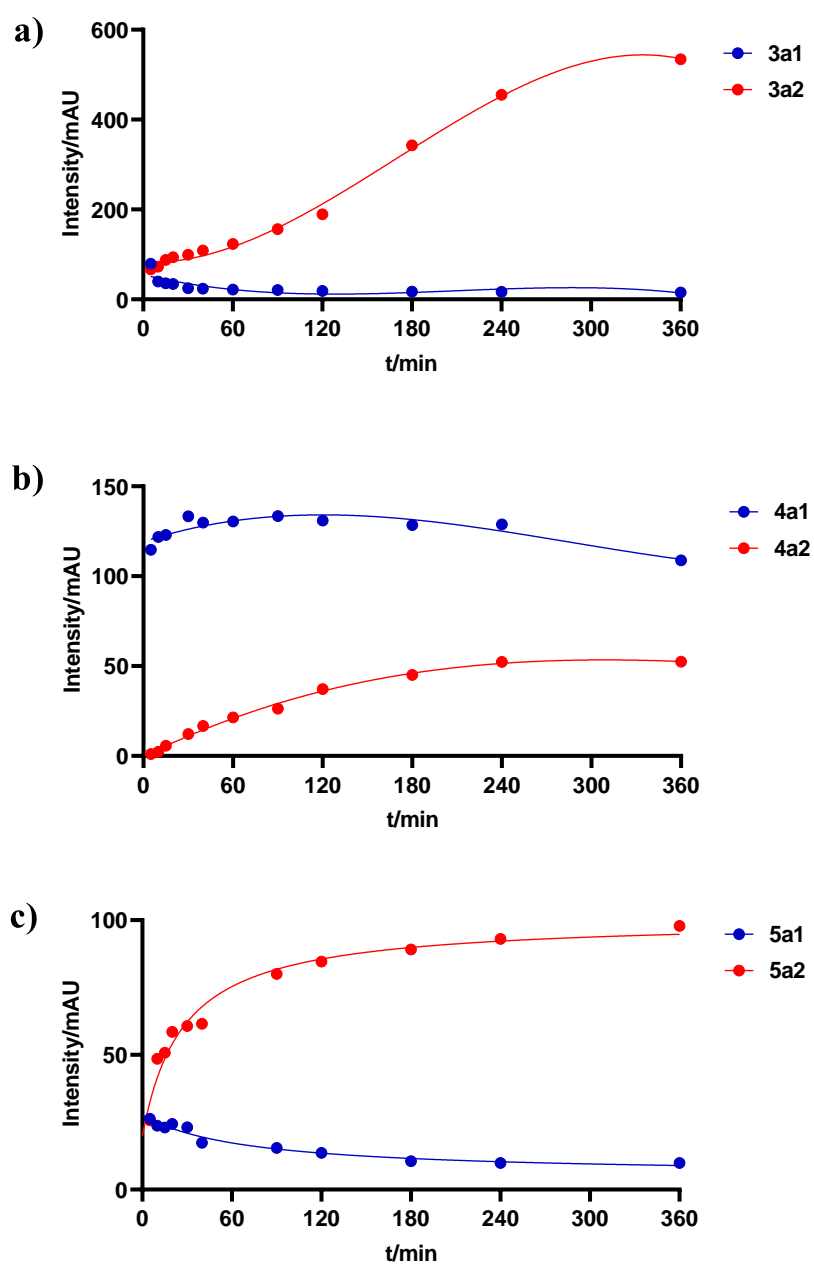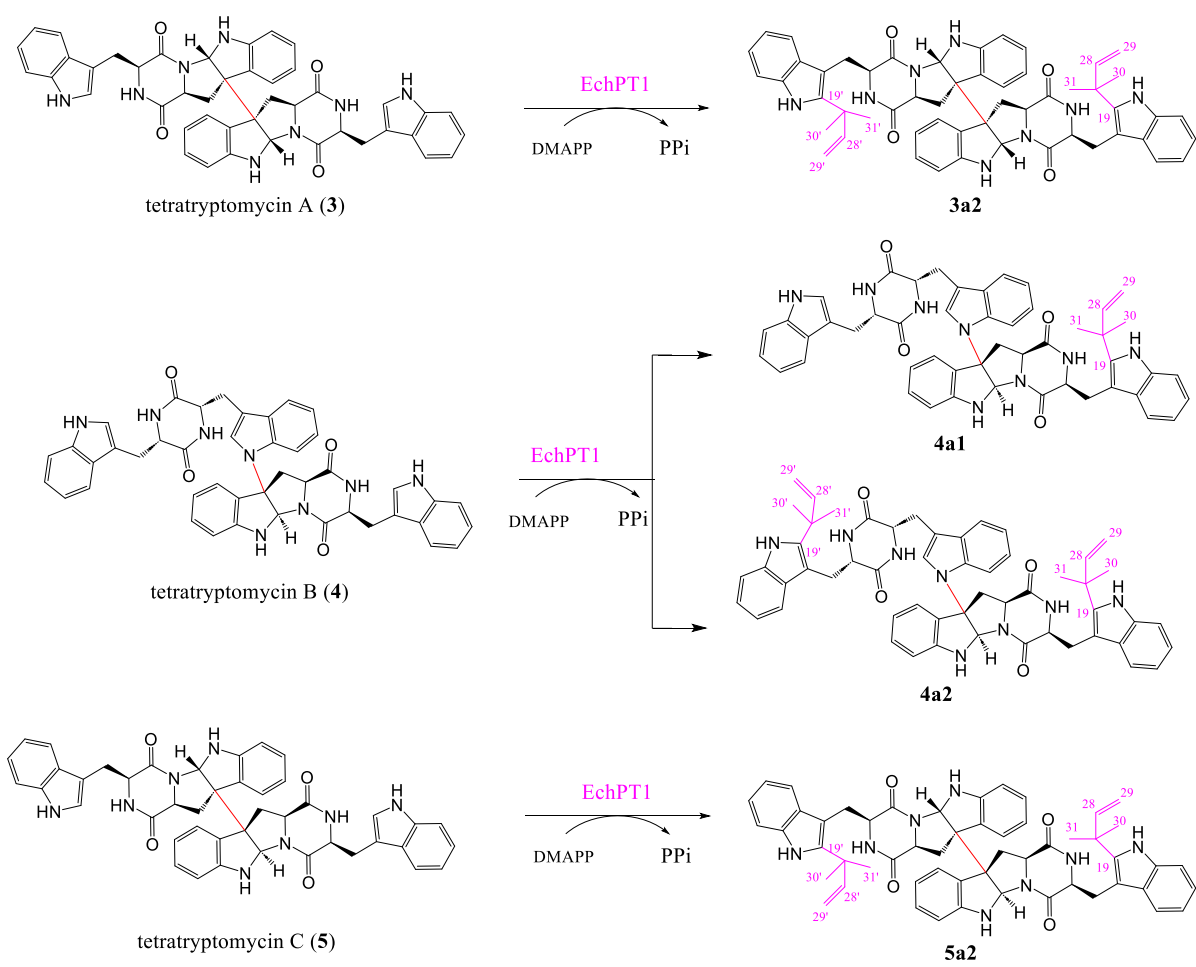
Fig. 1

a)

aspergilazine A (**1**)   naseseazine A (**2**)   (+)-WIN 64821

tetratryptomycin A (**3**)   tetratryptomycin B (**4**)   tetratryptomycin C (**5**)

b)

brevianamide S   asperginulin A   (-)-uncarilin A   (+)-uncarilin A

Fig. 2

cyclo-L-Trp-L-Ala   preechinulin   echinulin

398   **Fig. 3**

Reactions for 1 h
Reactions for 16 h

399

400

Fig. 4

18

114

Fig. 5

tetratryptomycin A (**3**)

EchPT1

DMAPP   PPi

3a2

tetratryptomycin B (**4**)

EchPT1

DMAPP   PPi

4a1

4a2

tetratryptomycin C (**5**)

EchPT1

DMAPP   PPi

5a2
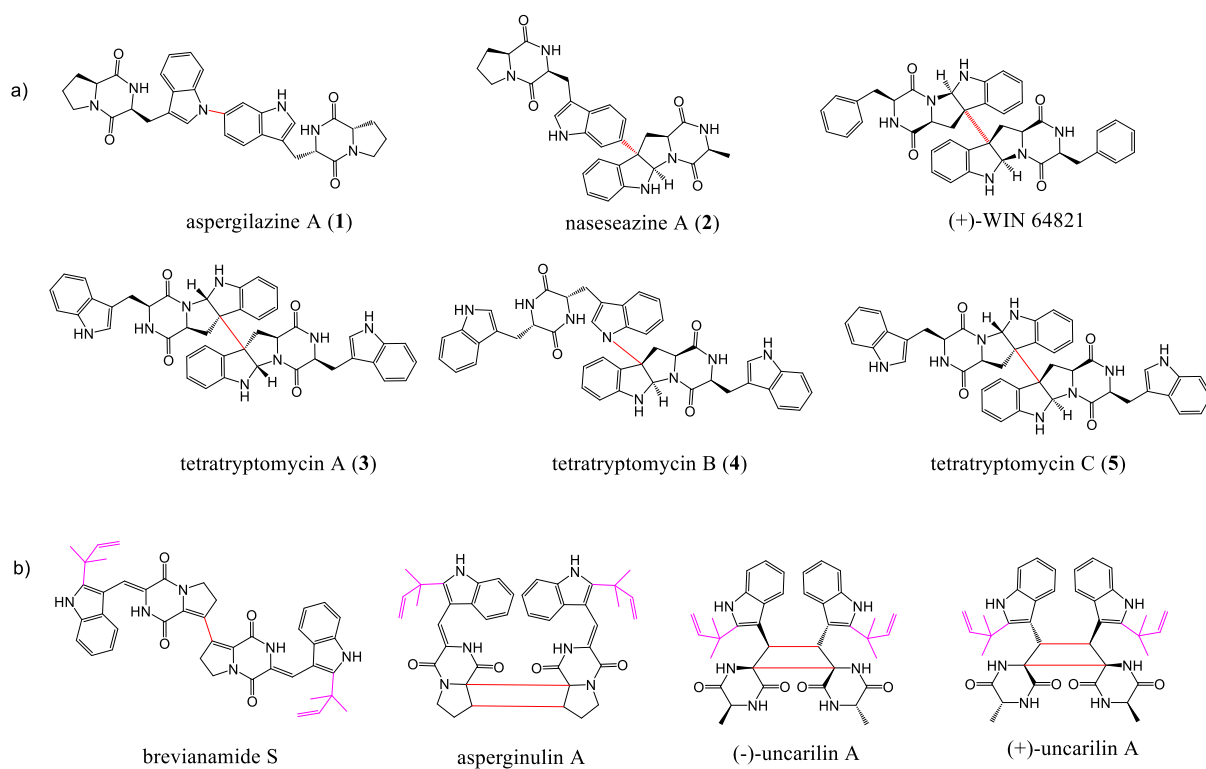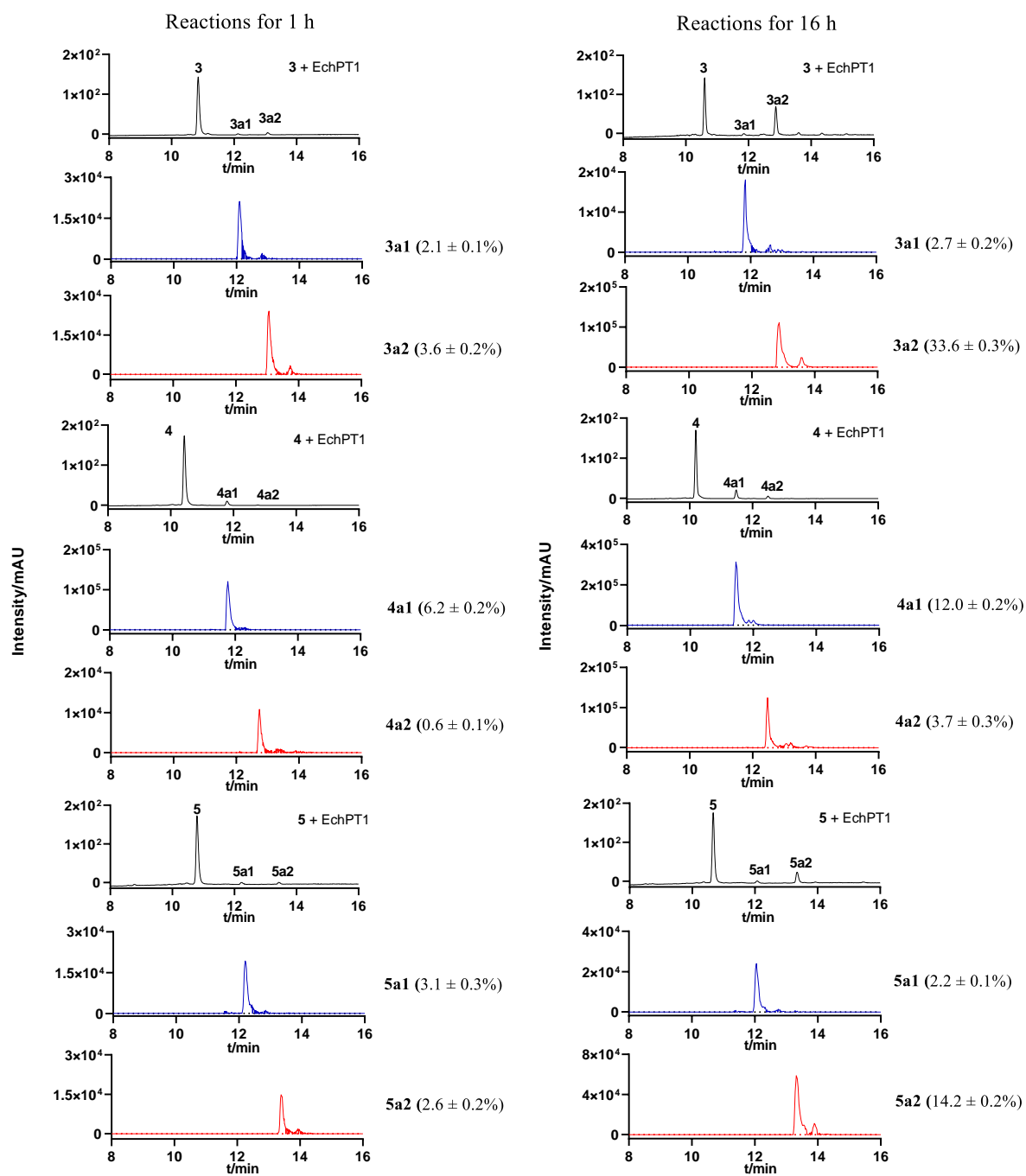
Supporting Information

Prenylation of dimeric *cyclo*-L-Trp-L-Trp by the promiscuous *cyclo*-L-Trp-L-Ala prenyltransferase EchPT1

Wen Li,[a] Xiulan Xie,[b] Jing Liu,[a] Huili Yu[a] and Shu-Ming Li*[a]

[a] Institut für Pharmazeutische Biologie und Biotechnologie, Fachbereich Pharmazie, Philipps-Universität Marburg, Robert-Koch-Straße 4, 35037 Marburg, Germany.

[b] Fachbereich Chemie, Philipps-Universität Marburg, Hans-Meerwein-Straße 4, 35032 Marburg, Germany.

Corresponding to Shu-Ming Li, E-mail: shuming.li@staff.uni-marburg.de
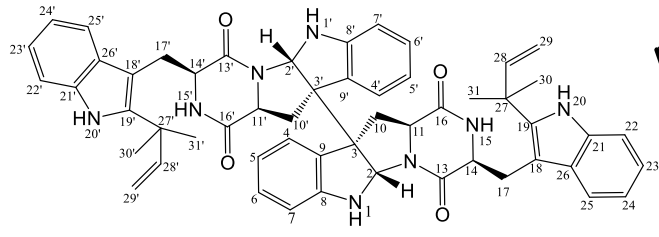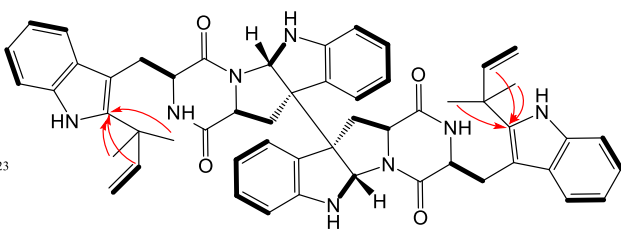
Table of Contents

Supplementary Tables

Table S1. NMR data of compound **3a2** in DMSO-d_6

3a2

Pos.	δ_H (ppm) multi. J (Hz)	δ_C	COSY	HMBC
1	6.74 s	-	H-2	C-2, C-3, C-8, C-9
2	5.13 s	77.3		C-8
3	-	58.7		
4	7.26 d (7.6)	124.8	H-5	C-3, C-5, C-6
5	6.66 t (7.6)	117.4	H-4, H-6	C-7, C-9
6	7.03 t (7.6)	129.2	H-5	C-4, C-5, C-8
7	6.61 d (7.6)	109.0	H-6	C-5, C-9
8	-	151.2		
9	-	127.1		
10	2.53 m	38.9	H-11	C-2, C-3, C-9
	2.47 m			
11	3.88 dd (9.6, 6.8)	57.8	H-10	C-10, C-16
13	-	165.5		
14	4.29 dd (8.9, 4.7)	55.1	H-17	C-13, C-17
15	6.24 s	-		C-11, C-13, C-14, C-16
16	-	168.3		
17	3.42 dd (14.9, 4.7)	25.7	H-14	C-13, C-14, C-18, C-19, C-26
	2.89 (14.9, 8.9)			
18	-	104.3		
19	-	141.4		
20	10.65 s	-		C-18, C-19, C-26
21	-	134.8		
22	7.32 d (8.0)	111.3	H-23	C-24, C-26
23	7.06 t (7.4)	120.7	H-22	C-21, C-25
24	6.94 t (7.4)	118.6	H-25	C-22, C-26
25	7.43 d (8.0)	117.8	H-24	C-18, C-21, C-23, C-26
26	-	128.7		
27	-	40.4		
28	6.17 dd (17.4, 10.5)	146.4	H-29	C-19, C-27, C-30, C-31

(Continued on next page)

S4

120

Pos.	δ_H (ppm) multi. *J* (Hz)	δ_C	COSY	HMBC
29	5.05 dd (17.4, 1.3)	111.3	H-28	C-27, C-28, C-30, C-31
	5.02 dd (10.5, 1.3)			
30	1.48 s	27.9		C-19, C-27, C-28, C-29, C-31
31	1.47 s	27.8		C-19, C-27, C-28, C-29, C-30
1′	6.74 s	-	H-2′	C-2′, C-3′, C-8′, C-9′
2′	5.13 s	77.3		C-8′
3′	-	58.7		
4′	7.26 d (7.6)	124.8	H-5′	C-3′, C-5′, C-6′
5′	6.66 t (7.6)	117.4	H-4′, H-6′	C-7′, C-9′
6′	7.03 t (7.6)	129.2	H-5′	C-4′, C-5′, C-8′
7′	6.61 d (7.6)	109.0	H-6′	C-5′, C-9′
8′	-	151.2		
9′	-	127.1		
10′	2.53 m	38.9	H-11′	C-2′, C-3′, C-9′
	2.47 m			
11′	3.88 dd (9.6, 6.8)	57.8	H-10′	C-10′, C-16′
13′	-	165.5		
14′	4.29 dd (8.9, 4.7)	55.1	H-17′	C-13′, C-17′
15′	6.24 s	-		C-11′, C-13′, C-14′, C-16′
16′	-	168.3		
17′	3.42 dd (14.9, 4.7)	25.7	H-14′	C-13′, C-14′, C-18′, C-19′, C-26′
	2.89 (14.9, 8.9)			
18′	-	104.3		
19′	-	141.4		
20′	10.65 s	-		C-18′, C-19′, C-26′
21′	-	134.8		
22′	7.32 d (8.0)	111.3	H-23′	C-24′, C-26′
23′	7.06 t (7.4)	120.7	H-22′	C-21′, C-25′
24′	6.94 t (7.4)	118.6	H-25′	C-22′, C-26′
25′	7.43 d (8.0)	117.8	H-24′	C-18′, C-21′, C-23′, C-26′
26′	-	128.7		
27′	-	40.4		
28′	6.17 dd (17.4, 10.5)	146.4	H-29′	C-19′, C-27′, C-30′, C-31′
29′	5.05 dd (17.4, 1.3)	111.3	H-28′	C-27′, C-28′, C-30′, C-31′
	5.02 dd (10.5, 1.3)			
30′	1.48 s	27.9		C-19′, C-27′, C-28′, C-29′, C-31′
31′	1.47 s	27.8		C-19′, C-27′, C-28′, C-29′, C-30′

Table S2. NMR data of compound **4a1** in DMSO-d_6

4a1

Pos.	δ_H (ppm) multi. J (Hz)	δ_C	COSY	HMBC
1	7.27 d (3.9)	-	H-2	C-2, C-3, C-4, C-9
2	5.78 d (3.9)	81.5	H-1	C-3, C-8, C-10, C-11
3	-	73.5		
4	6.71 d (8.3)	110.1	H-5, H-6	C-5, C-8, C-9
5	6.53 t (7.5)	118.0	H-4, H-6	C-4, C-7, C-9
6	7.12 t (7.5)	129.7	H-4, H-5	C-4, C-7, C-8
7	6.71 d (8.3)	122.2	H-6	C-5, C-8, C-9
8	-	148.0		
9	-	128.6		
10	3.45 dd (14.3, 5.8)	38.9	H-11	C-2, C-3, C-9, C-11, C-16
	2.22 dd (14.3, 12.2)			
11	4.65 dd (11.5, 5.8)	57.5	H-10	C-10, C-16
12	-	-		
13	-	167.9		
14	4.41 dd (8.3, 5.5)	55.5	H-17	C-13, C-17, C-18
15	6.67 s	-		C-11, C-13, C-14, C-17
16	-	169.2		
17	3.50 dd (15.3, 5.5)	24.7	H-14	C-13, C-14, C-18, C-19, C-26
	3.02 m			
18	-	104.4		
19	-	141.5		
20	10.68 s	-		C-18, C-19, C-21, C-26, C-a
21	-	136.0		
22	7.33 d (8.1)	111.6	H-23	C-24, C-26
23	7.11 t (7.8)	120.7	H-22	C-21, C-25
24	6.97 t (7.8)	118.7	H-25	C-22, C-26
25	7.54 d (8.1)	118.2	H-24	C-18, C-21, C-23, C-26
26	-	128.7		
27	-	40.4		
28	6.23 dd (17.4, 10.5)	146.3	H-c	C-19, C-a, C-d, C-e

(Continued on next page)

Pos.	δ_H (ppm) multi. J (Hz)	δ_C	COSY	HMBC
29	5.11 d (17.4)	111.5	H-b	C-a, C-b
	5.08 d (10.5)			
30	1.52 s	27.8		C-a, C-b, C-c, C-e, C-19
31	1.50 s	27.9		C-a, C-b, C-c, C-d, C-19
1′	-	-		
2′	6.41 s	124.7		C-3, C-3′, C-7′, C-8′, C-9′, C-10′
3′	-	109.1		
4′	7.19 d (8.2)	118.7	H-5′	C-3′, C-6′, C-8′, C-9′
5′	6.93 t (7.6)	119.1	H-4′	C-6′, C-7′, C-9′
6′	6.87 t (7.6)	120.9	H-7′	C-5′, C-8′
7′	6.49 d (8.2)	111.8	H-6′	C-5′, C-9′
8′	-	134.8		
9′	-	129.2		
10′	2.61 dd (14.1, 2.8)	30.3	H-11′	C-2′, C-3′, C-9′, C-11′, C-16′
	1.16 dd (14.1, 9.9)			
11′	3.67 td (9.7, 2.8)	54.5	H-10′	C-3′, C-13′
12′	7.59 d (2.1)		H-11′	C-14′, C-16′
13′	-	166.6		
14′	4.05 d (2.3)	55.5	H-17′	C-16′, C-18′
15′	8.13 d (1.6)		H-14′	C-11′, C-13′
16′	-	166.9		
17′	3.02 m	29.8	H-14′	C-13′, C-14′, C-16′, C-18′, C-19′, C-22′
	2.87 dd (14.2, 4.3)	-		
18′	-	108.6		
19′	6.89 d (1.9)	124.9	H-20′	C-18′, C-21′, C-26′
20′	10.98 s	-	H-19′	C-18′, C-19′, C-21′, C-26′
21′		135.1		
22′	7.36 d (8.1)	111.0	H-23′	C-23′, C-26′
23′	7.04 t (7.1)	118.5	H-22′, H-24′	C-21′, C-22′
24′	7.03 t (7.1)	121.0	H-25′	C-21′, C-22′, C-23′, C-26′
25′	7.52 d (8.1)	119.2	H-24′	C-18′, C-21′, C-22′, C-24′, C-26′
26′	-	127.7		

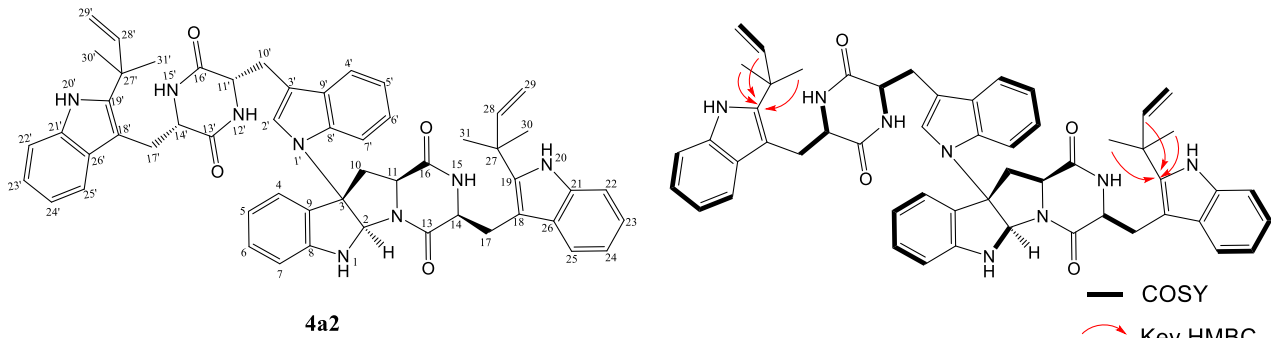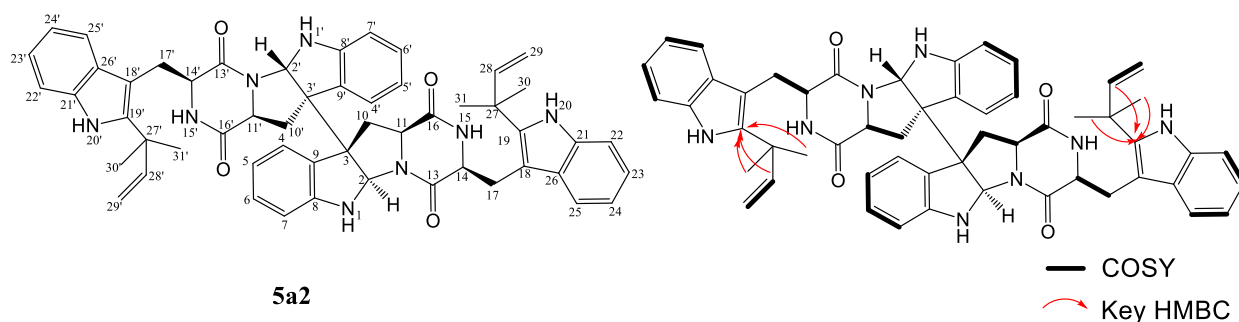**Table S3.** NMR data of compound **4a2** in DMSO-d_6

4a2

COSY
Key HMBC

Pos.	δ_H (ppm) multi. J (Hz)	δ_C	COSY	HMBC
1	7.30 d (4.0)	-	H-2	C-2, C-3, C-5, C-9
2	5.82 d (4.0)	81.6	H-1	C-3, C-8, C-10, C-11
3	-	73.6		
4	6.69 d (8.2)	122.3	H-5	C-3, C-6, C-8
5	6.45 td (7.6, 1.3)	118.2	H-4, H-6	C-4, C-7, C-9
6	7.11 td (7.6, 1.3)	129.7	H-5, H-7	C-4, C-5, C-7, C-8
7	6.72 d (8.2)	110.1	H-6	C-5, C-9
8	-	148.0		
9	-	128.6		
10	3.55 dd (14.5, 6.2)	39.0	H-11	C-2, C-3, C-9, C-11, C-16
	2.26 dd (14.5, 11.8)			
11	4.76 dd (11.8, 6.2)	57.5	H-10	C-10, C-16
12	-			
13	-	167.9		
14	4.44 dd (8.6, 5.3)	55.4	H-17	C-13, C-17, C-18
15	6.64 s	-		C-11, C-13, C-14, C-17
16	-	169.1		
17	3.50 dd (14.8, 5.3)	24.7	H-14	C-13, C-14, C-18, C-19, C-26
	3.02 dd (14.8, 9.3)			
18	-	104.9		
19	-	141.5		
20	10.51 s	-		C-18, C-19, C-21, C-24, C-26
21	-	134.9		
22	7.28 d (8.4)	110.6	H-23	C-24, C-26
23	7.03 td (7.5, 1.3)	120.4	H-22, H-24	
24	6.81 td (7.5, 1.3)	118.3	H-23, H-25	C-22, C-23, C-25, C-26
25	7.05 d (8.4)	118.6	H-24	C-18, C-21, C-24, C-26
26	-	129.2		
27	-	40.4		
28	6.22 dd (17.4, 10.5)	146.5	H-29	C-19, C-27, C-30, C-31

(Continued on next page)

Pos.	δ_H (ppm) multi. J (Hz)	δ_C	COSY	HMBC
29	5.09 dd (17.4, 1.3)	111.5	H-28	C-19, C-27, C-28
	5.07 dd (10.5, 1.3)			
30	1.51 s	28.0		C-19, C-27, C-28, C-29, C-31
31	1.49 s	27.9		C-19, C-27, C-28, C-29, C-30
1′	-	-		
2′	7.09 d (1.3)	125.0		C-3′, C-8′, C-9′
3′	-	109.2		
4′	7.48 d (8.2)	118.9	H-5′	C-3′, C-6′, C-8′, C-9′
5′	7.04 td (7.5, 1.3)	120.7	H-4′	C-7′, C-9′
6′	6.90 td (7.5, 1.3)	121.3	H-5′, H-7′	C-4′, C-8′
7′	6.54 d (8.2)	111.9	H-6′	C-5′, C-9′
8′	-	134.7		
9′	-	129.4		
10′	2.45 dd (14.6, 8.8)	38.9	H-11′	C-2′, C-3′, C-9′
	3.02 dd (14.6, 9.3)			
11′	3.94 dd (8.8, 3.5)	55.1	H-10′	C-10′, C-13′
12′	7.62 d (3.0)	-	C-11′	C-14′, C-16′
13′	-	166.7		
14′	3.94 dd (7.8, 3.9)	56.3	H-17′	C-16′, C-18′
15′	8.05 d (2.7)	-	H-14′	C-11′, C-13′
16′	-	167.4		
17′	3.28 dd (14.5, 3.9)	30.3	H-14′	C-13′, C-14′, C-18′, C-19′, C-26′
	2.77 dd (14.5, 7.8)			
18′	-	104.4		
19′	-	141.4		
20′	10.67 s	-		C-18′, C-19′, C-21′, C-24′, C-26′
21′	-	134.8		
22′	7.34 d (8.0)	111.1	H-23′	C-23′, C-26′
23′	7.00 td (7.5, 1.3)	119.4	H-22′, H-24′	C-21′, C-25′
24′	6.96 td (7.5, 1.3)	118.7	H-23′, H-25′	C-22′, C-25′, C-26
25′	7.52 d (8.0)	118.0	H-24′	C-18′, C-21′, C-23′, C-26
26′	-	128.6		
27′	-	40.4		
28′	6.15 dd (17.4, 10.5)	146.3	H-29′	C-19′, C-27′, C-30′, C-31′
29′	5.05 dd (17.4, 1.3)	111.2	H-28′	C-19′, C-27′, C-28′
	5.00 dd (10.5, 1.3)			
30′	1.46 s	27.9		C-19′, C-27′, C-28′, C-29′, C-31′
31′	1.46 s	27.8		C-19′, C-27′, C-28′, C-29′, C-30′

Table S4. NMR data of compound **5a2** in DMSO-d_6

5a2

— COSY

⤴ Key HMBC

Pos.	δ_H (ppm) multi. J (Hz)	δ_C	COSY	HMBC
1	6.74 s	-		
2	5.55 s	75.9 [a]		
3	-	63.1		
4	6.52 m	123.9		110.1
5	6.52 m	117.9	H-6	118.0
6	6.99 m	129.1	H-5, H-7	129.7
7	6.52 m	108.6 [a]	H-6	122.2
8	-	151.3		
9	-	130.5		
10	2.55 m	39.0	H-11	
	2.30 m			
11	3.94 dd (9.9, 6.4)	57.1	H-10	
13	-	168.5		
14	4.33 dd (9.0, 4.3)	55.2	H-17	
15	6.23 s	-		C-11, C-13
16	-	169.4		
17	3.53 dd (15.4, 4.3)	24.7	H-14	C-13, C-14, C-18, C-19, C-26
	2.90 dd (15.4, 9.6)			
18	-	104.6		
19	-	141.5		
20	10.68 s	-		C-18, C-19, C-21, C-26
21	-	134.9		
22	7.34 d (7.9)	111.1	H-23	C-24, C-26
23	7.04 t (7.5)	120.8	H-22	C-21, C-25
24	6.94 t (7.5)	118.7	H-25	C-22, C-26
25	7.49 d (7.9)	117.9	H-24	C-18, C-21, C-23, C-26
26	-	128.8		
27	-	40.4		
28	6.17 dd (17.3, 10.5)	146.4	H-29	C-19, C-27, C-30, C-31
29	5.03 d (17.3)	111.4	H-28	C-27, C-28
	5.01 d (10.5)			

(Continued on next page)

126

Pos.	δ_H (ppm) multi. J (Hz)	δ_C	COSY	HMBC
30	1.49 s	27.9		C-19, C-27, C-28, C-29, C-31
31	1.49 s	27.9		C-19, C-27, C-28, C-29, C-30
1′	-	-		
2′	5.41 s	72.5		
3′	-	59.9		
4′	6.52 m	123.8		
5′	6.52 m	117.8	H-6′	
6′	6.99 m	128.5	H-5′, H-7′	
7′	6.52 m	108.3 [a]	H-6′	
8′	-	149.1		
9′	-	127.7		
10′	3.43 m	38.9	H-11′	
	3.28 dd (11.1, 5.7)			
11′	3.46 m	57.7	H-10′	
13′	-	165.2		
14′	4.33 dd (9.0, 4.3)	55.9	H-17′	
15′	6.17 s	-		
16′	-	167.9		
17′	3.53 dd (15.4, 4.3)	26.3	H-14′	C-13′, C-14′, C-18′, C-19′, C-26′
	2.99 dd (15.4, 9.6)			
18′	-	104.2		
19′	-	141.4		
20′	10.66 s	-		C-18′, C-19′, C-21 ′, C-26 ′
21′	-	134.8		
22′	7.34 d (7.9)	111.1	H-23′	C-24′, C-26′
23′	7.04 t (7.5)	120.8	H-22′	C-21′, C-25′
24′	6.94 t (7.5)	118.7	H-25′	C-22′, C-26′
25′	7.44 d (7.9)	117.8	H-24′	C-18′, C-21′, C-23′, C-26′
26′	-	128.6		
27′	-	40.4		
28′	6.17 dd (17.3, 10.5)	146.3	H-29′	C-19′, C-27′, C-30′, C-31′
29′	5.03 d (17.3)	111.3	H-28′	C-27′, C-28′
	5.01 d (10.5)			
30′	1.48 s	27.8		C-19′, C-27′, C-28′, C-29′, C-31′
31′	1.48 s	27.8		C-19′, C-27′, C-28′, C-29′, C-30′

[a] Signals were only detected in HSQC

Table S5. HRESIMS data of enzyme products

product	chemical formula	HRESIMS data		
		measured $[M + H]^+$	calculated $[M + H]^+$	deviation [ppm]
3a2	$C_{54}H_{54}N_8O_4$	879.4335	879.4341	1.38
4a1	$C_{49}H_{46}N_8O_4$	811.3713	811.3715	0.25
4a2	$C_{54}H_{54}N_8O_4$	879.4343	879.4341	0.23
5a2	$C_{54}H_{54}N_8O_4$	879.4337	879.4341	0.45

S12

Figure S1. LCMS analysis of the acceptance of aspergilazine A (**1**) by EchPT1, FgaPT2_R244L, FgaPT2_Y398F, 6-DMATS$_{Sa}$, and 7-DMATS. UV absorptions at 280 nm are illustrated in black. The chromatograms depicted in blue and red refer to EICs of $[M+H]^+$ for the monoprenylated at m/z 635.789 and those of diprenylated products at m/z 702.900, respectively. A tolerance range of $\pm\,0.005$ was used for ion detection.

Figure S2. LCMS analysis of the acceptance of naseseazine A (**2**) by EchPT1, FgaPT2_R244L, FgaPT2_Y398F, 6-DMATS_Sa, and 7-DMATS. UV absorptions at 280 nm are illustrated in black. The chromatograms depicted in blue and red refer to EICs of $[M+H]^+$ for the monoprenylated at *m/z* 607.735 and those of diprenylated products at *m/z* 674.846. A tolerance range of $\pm$ 0.005 was used for ion detection.
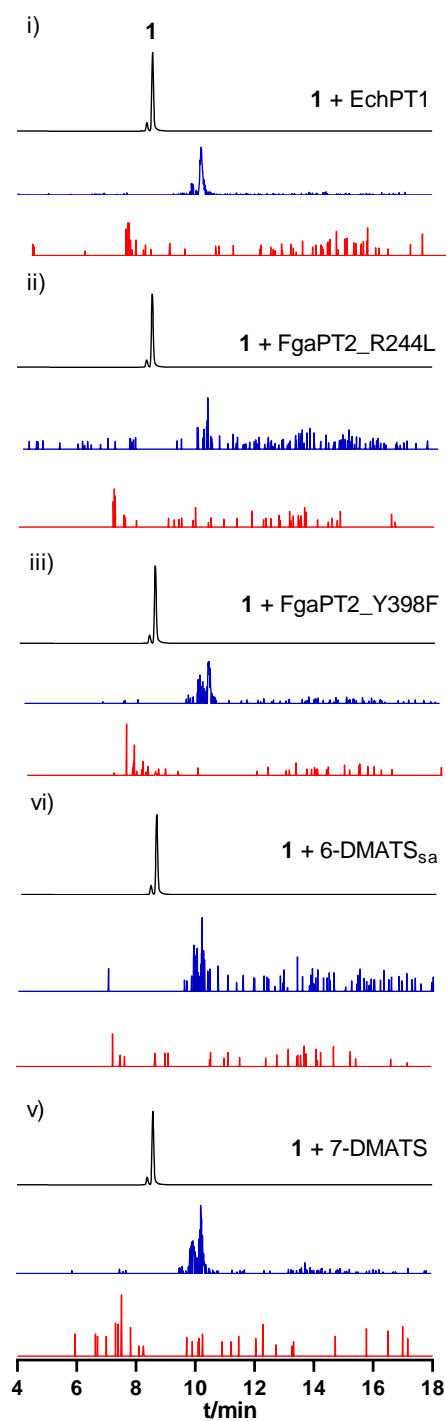
Figure S3. LCMS analysis of the acceptance of tetratryptomycin A (**3**) by EchPT1, FgaPT2_R244L, FgaPT2_Y398F, 6-DMATS_Sa, and 7-DMATS. UV absorptions at 280 nm are illustrated in black. The chromatograms depicted in blue and red refer to EICs of $[M+H]^+$ for the monoprenylated at *m/z* 811.372 and those of diprenylated products at *m/z* 879.434. A tolerance range of ± 0.005 was used for ion detection.
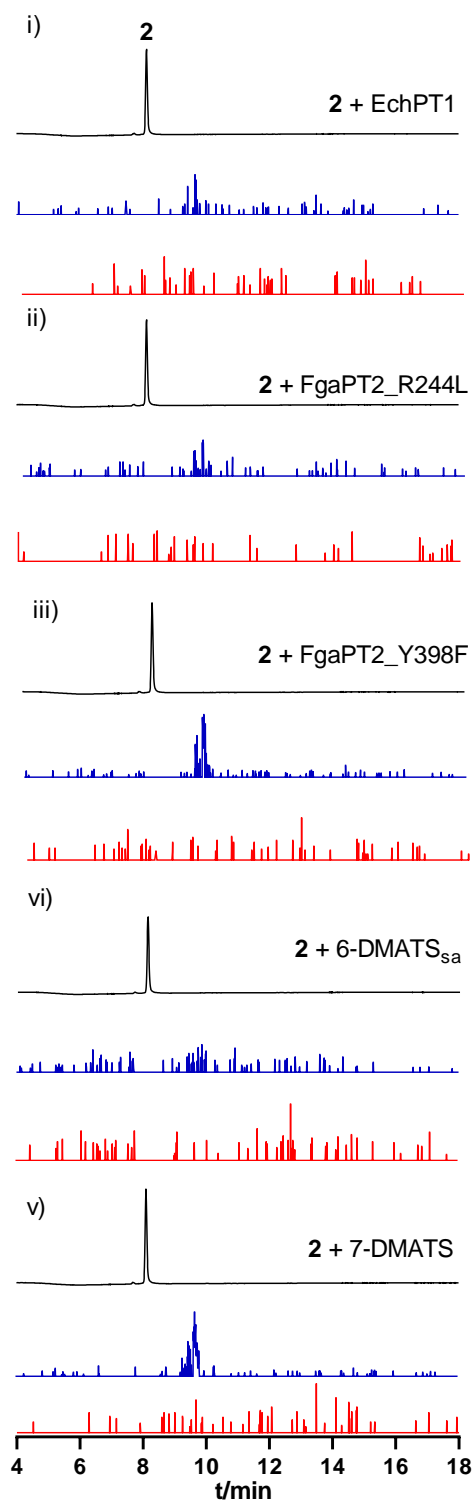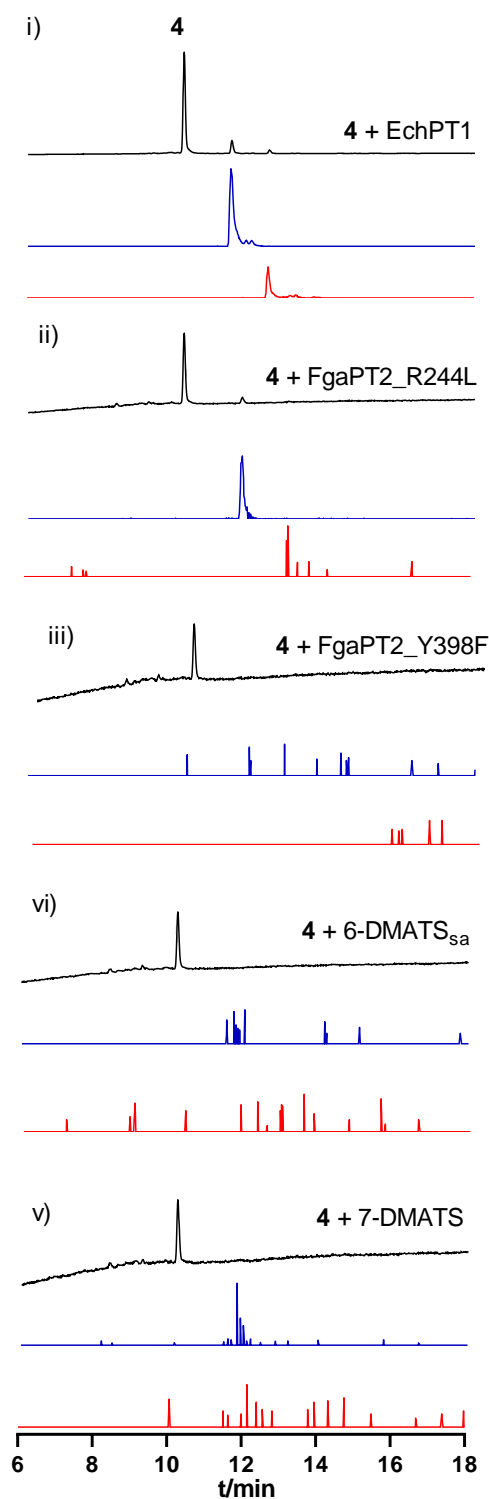
Figure S4. LCMS analysis of the acceptance of tetratryptomycin B (**4**) by EchPT1, FgaPT2_R244L, FgaPT2_Y398F, 6-DMATS_Sa, and 7-DMATS. UV absorptions at 280 nm are illustrated in black. The chromatograms depicted in blue and red refer to EICs of $[M+H]^+$ for the monoprenylated at *m/z* 811.372 and those of diprenylated products at *m/z* 879.434. A tolerance range of ± 0.005 was used for ion detection.
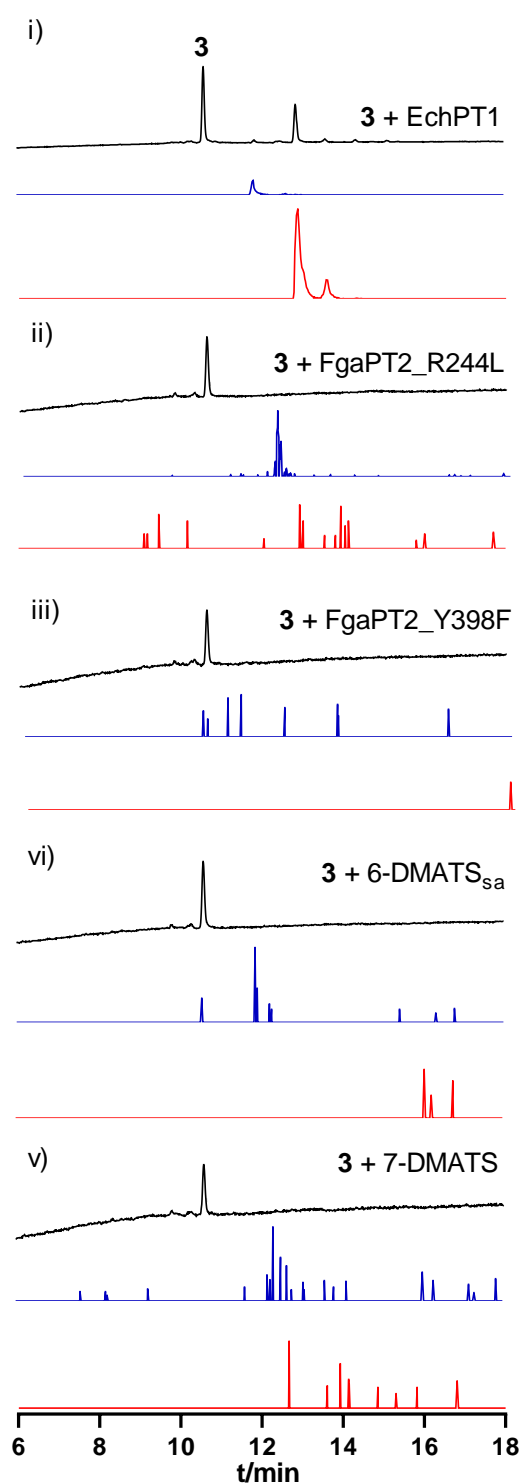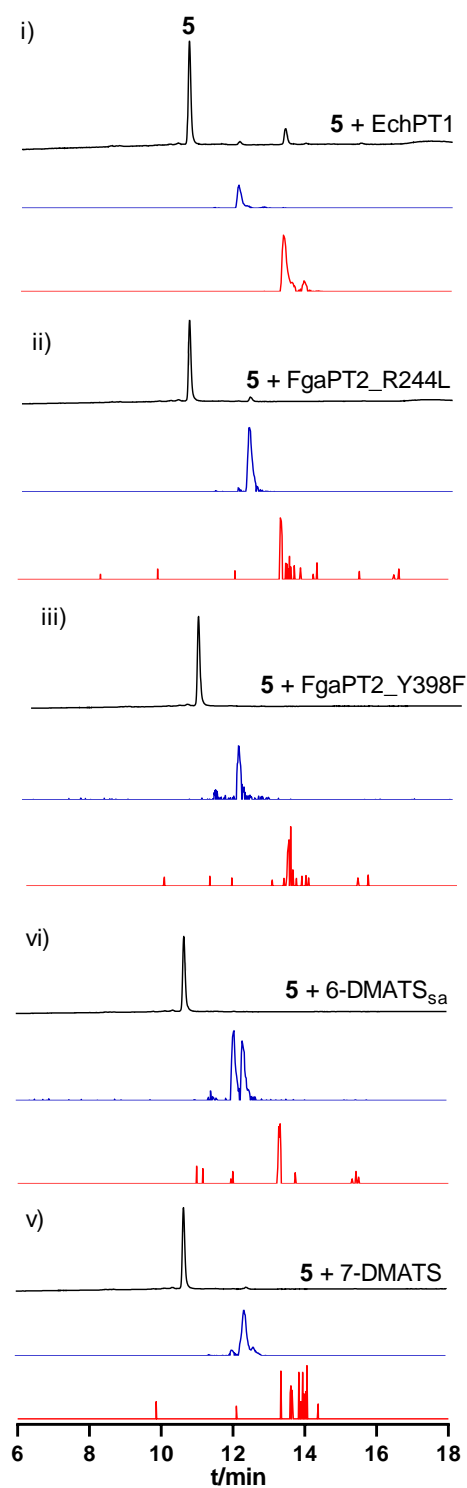
Figure S5. LCMS analysis of the acceptance of tetratryptomycin C (**5**) by EchPT1, FgaPT2_R244L, FgaPT2_Y398F, 6-DMATS_Sa, and 7-DMATS. UV absorptions at 280 nm are illustrated in black. The chromatograms depicted in blue and red refer to EICs of $[M+H]^+$ for the monoprenylated at *m/z* 811.372 and those of diprenylated products at *m/z* 879.434. A tolerance range of $\pm$ 0.005 was used for ion detection.
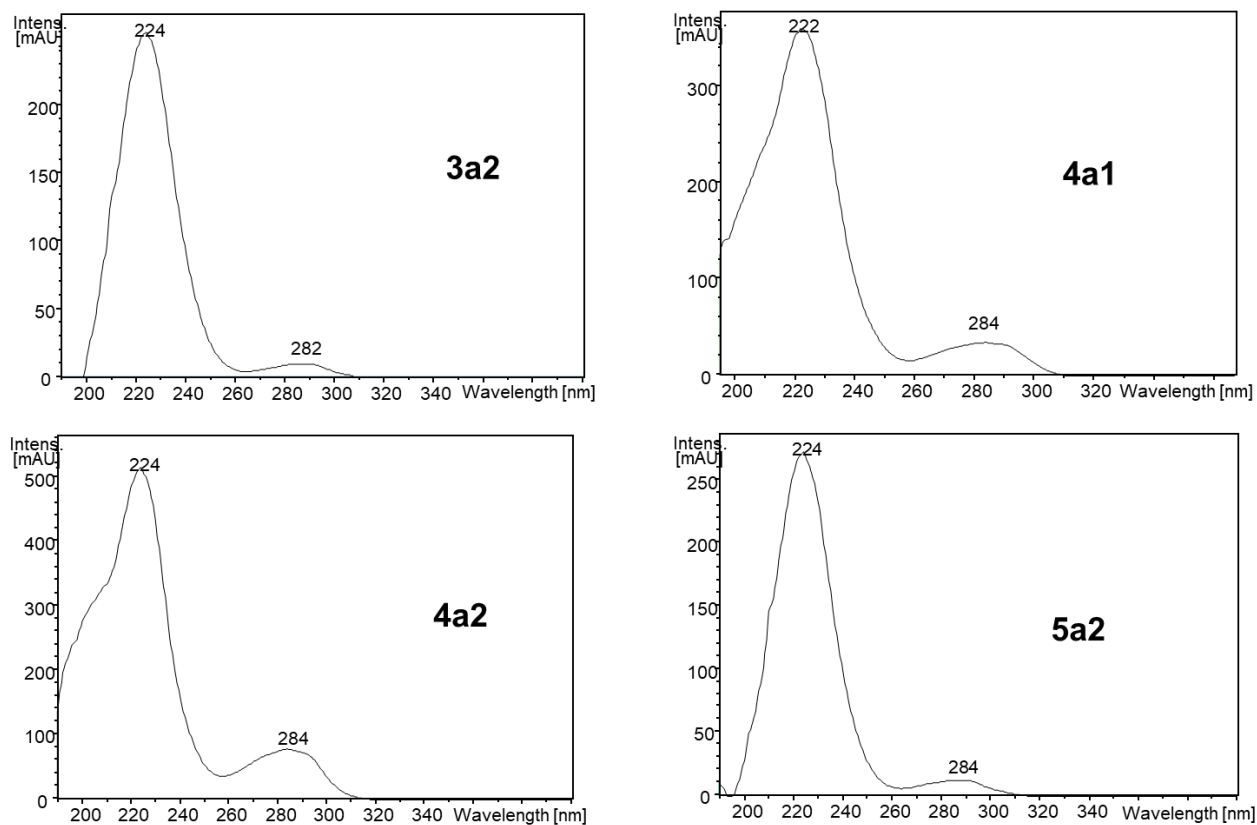
Figure S6. UV spectra of the prenylated compounds **3a2**, **4a1**, **4a2**, and **5a2**.
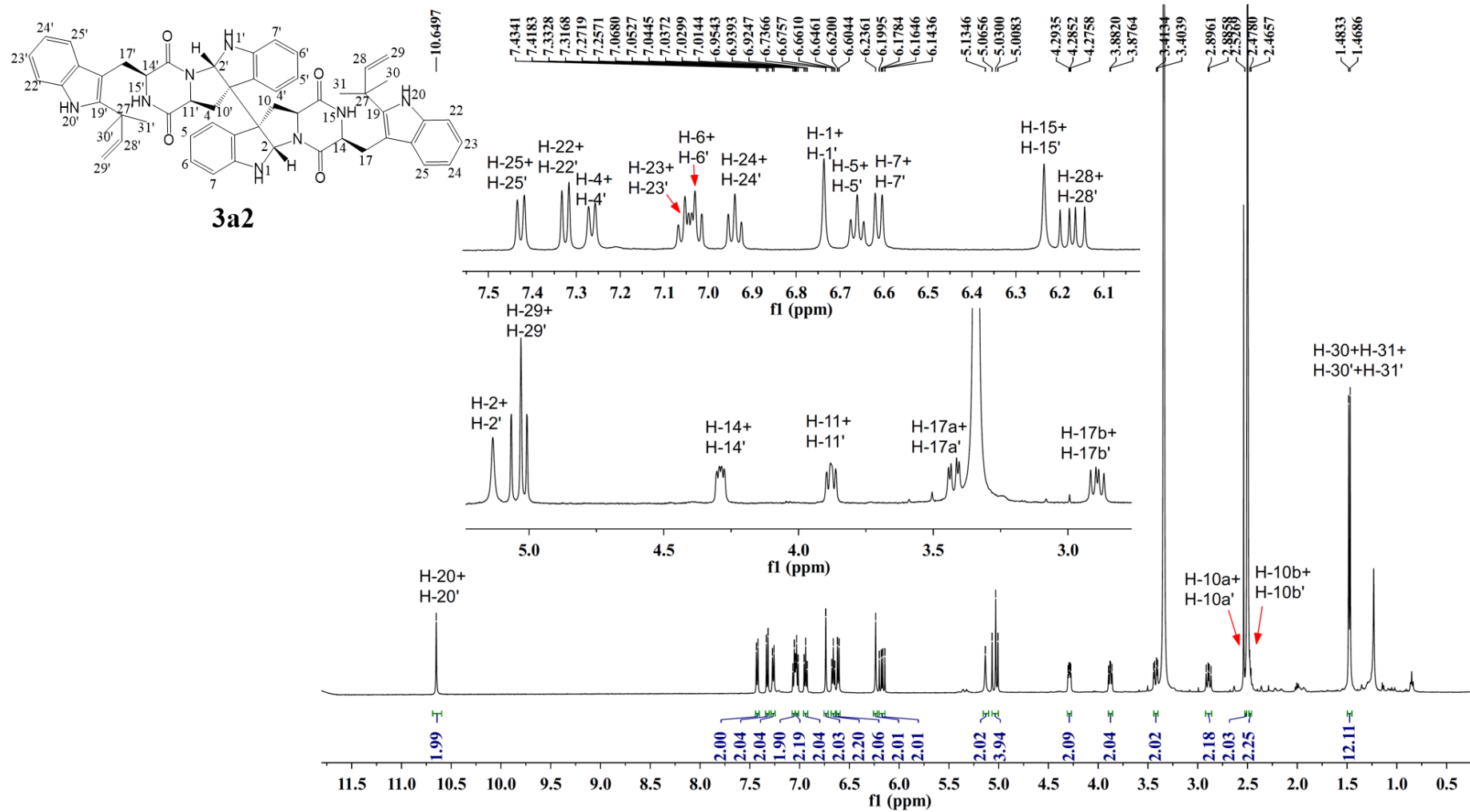
Figure S7. ^{1}H NMR spectrum of **3a2** in DMSO-d_6 (500 MHz).

S19

135
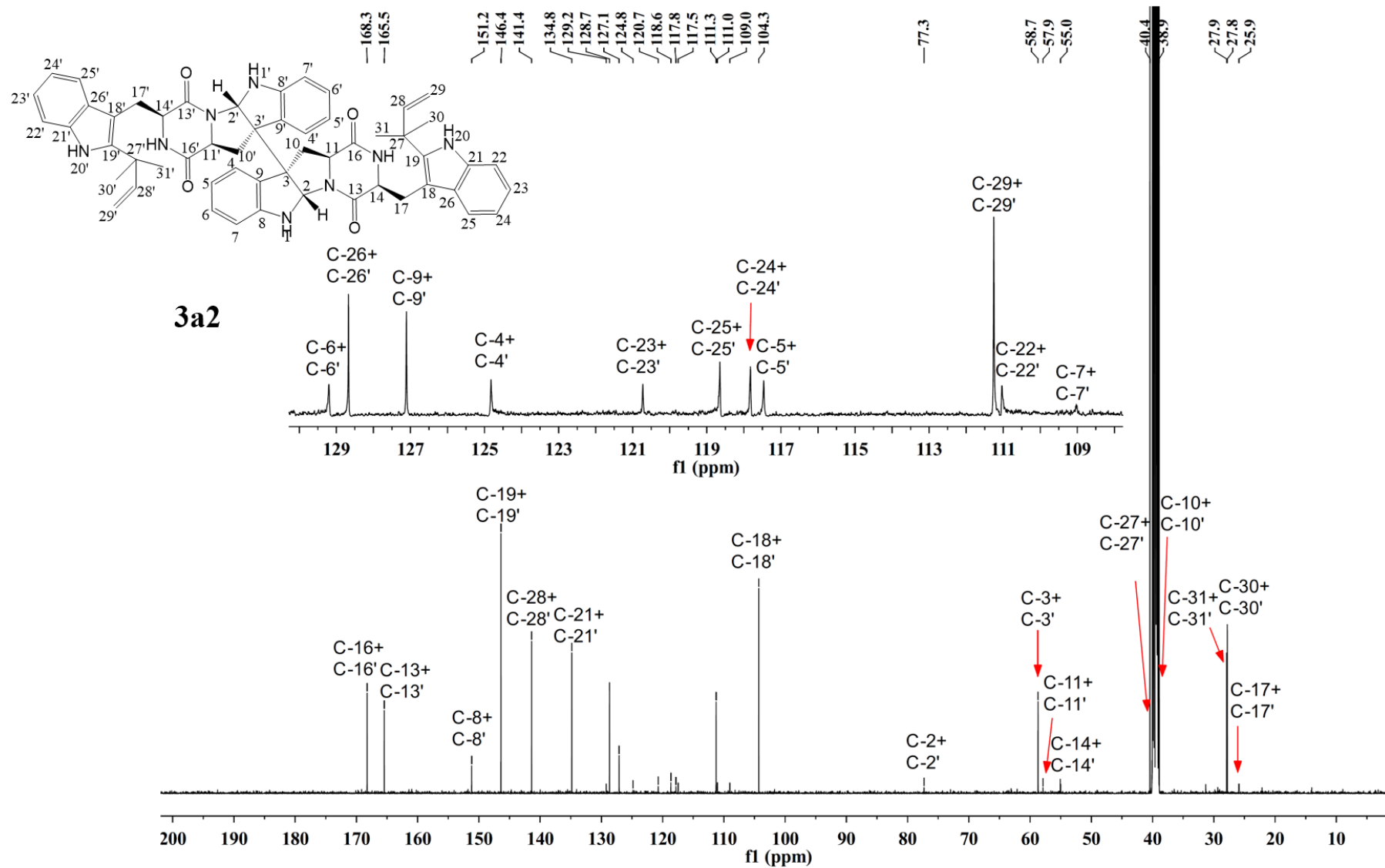
Figure S8. ^{13}C NMR spectrum of **3a2** in DMSO-d_6 (125 MHz).
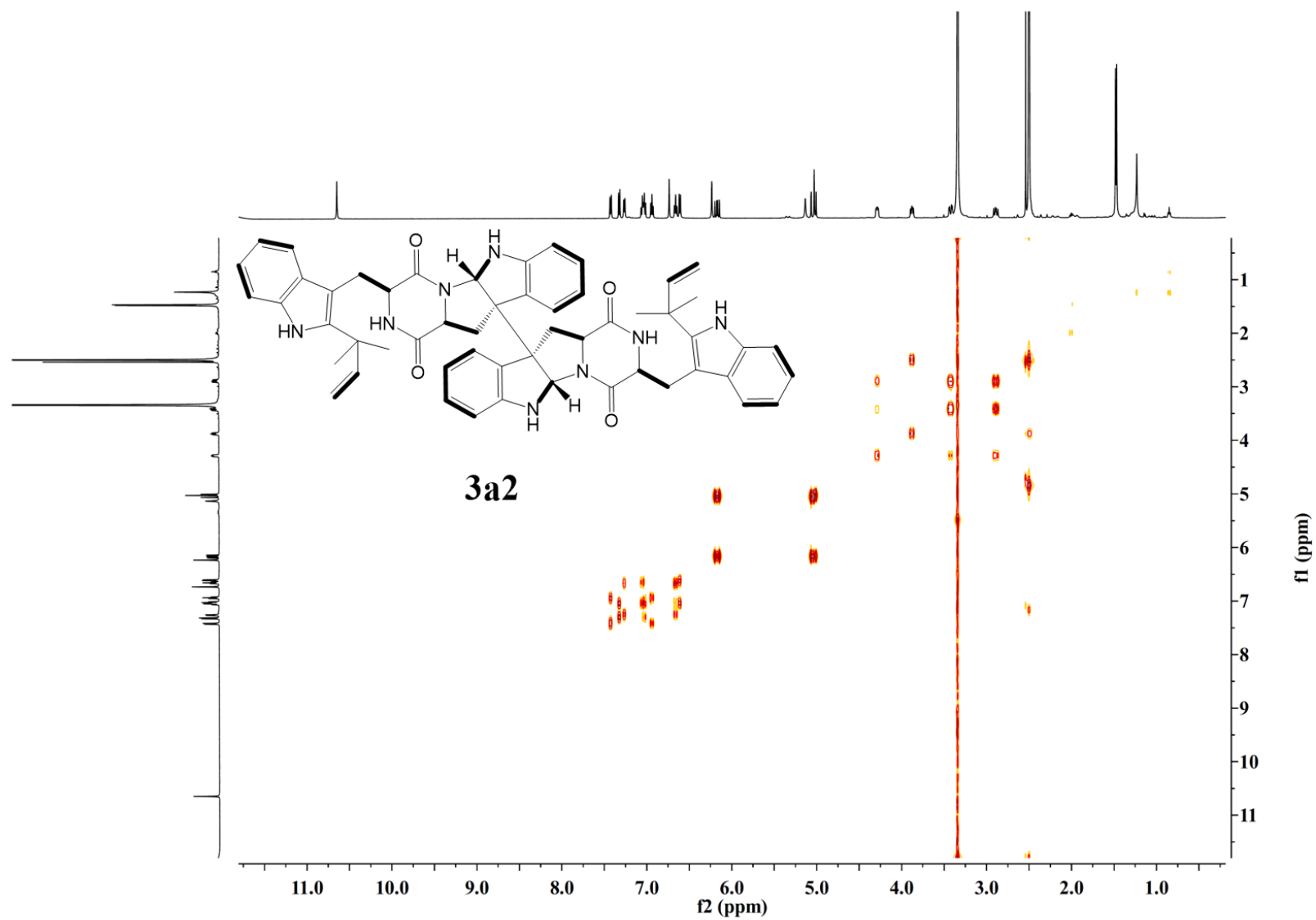
Figure S9. ^{1}H-^{1}H COSY spectrum of **3a2** in DMSO-d_6.

S21
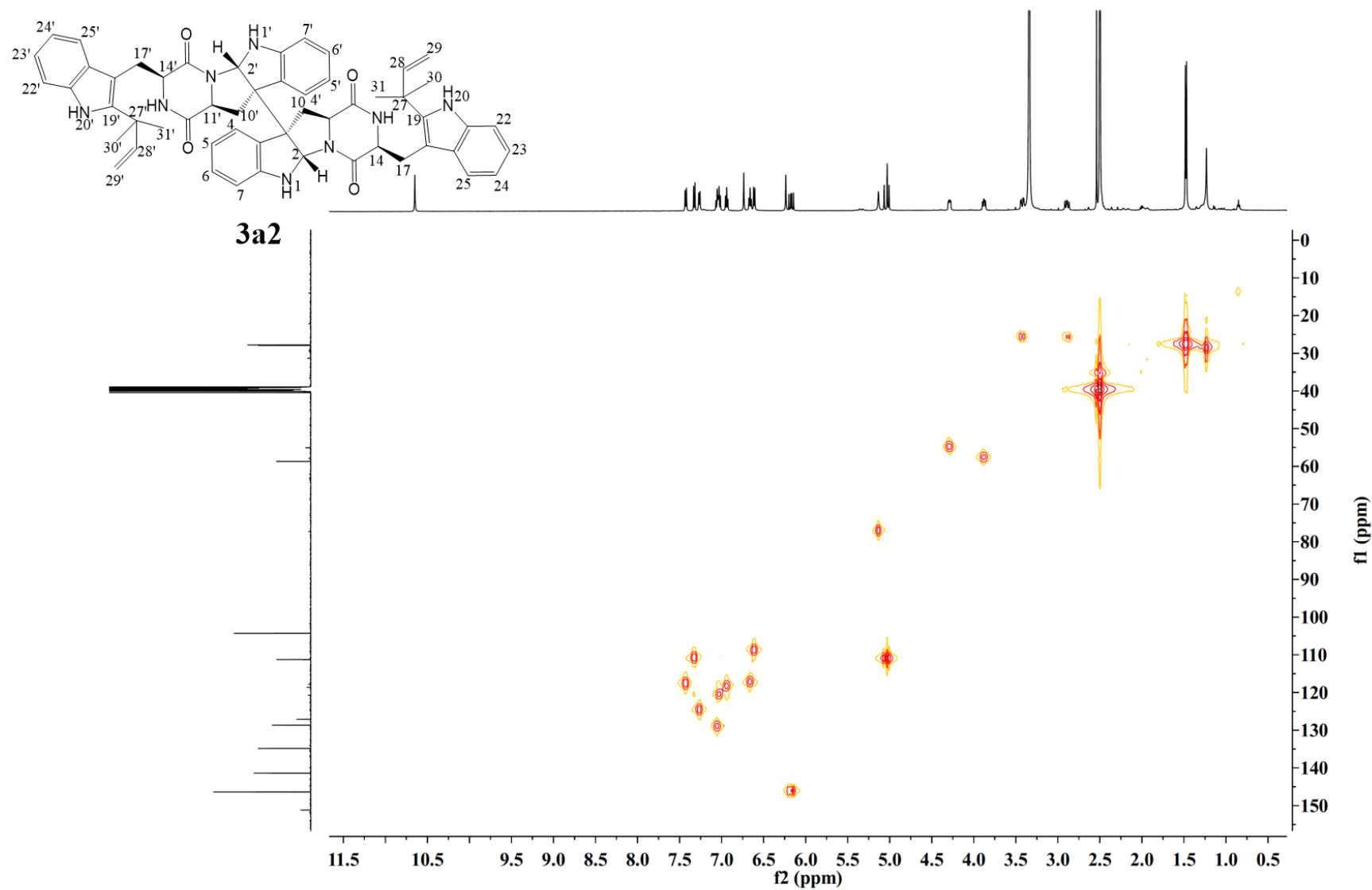
Figure S10. HSQC spectrum of **3a2** in DMSO-d_6.

S22
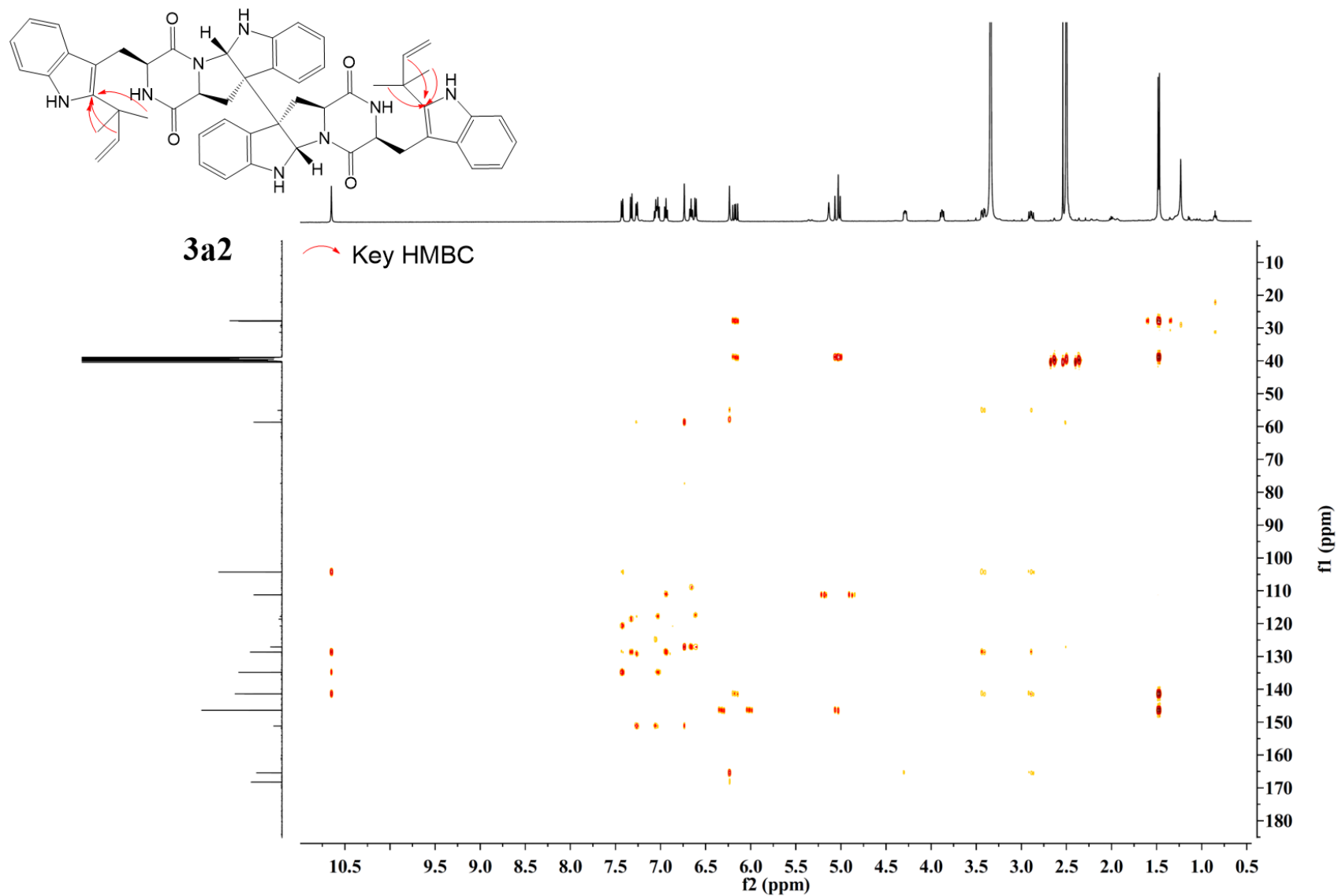
Figure S11. HMBC spectrum of **3a2** in DMSO-d_6.
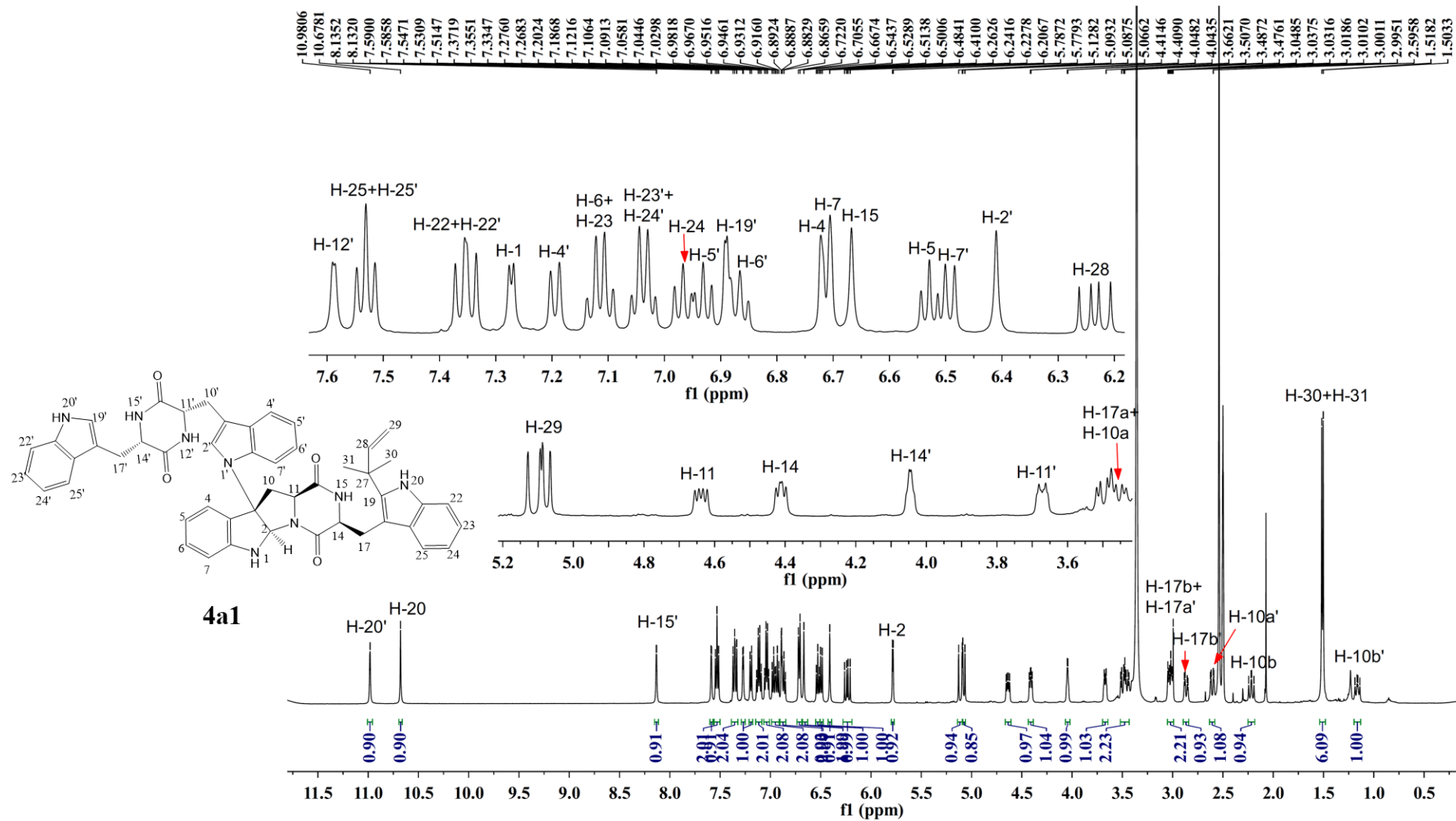
Figure S12. ^{1}H NMR spectrum of **4a1** in DMSO-d_6 (500 MHz).

S24

140
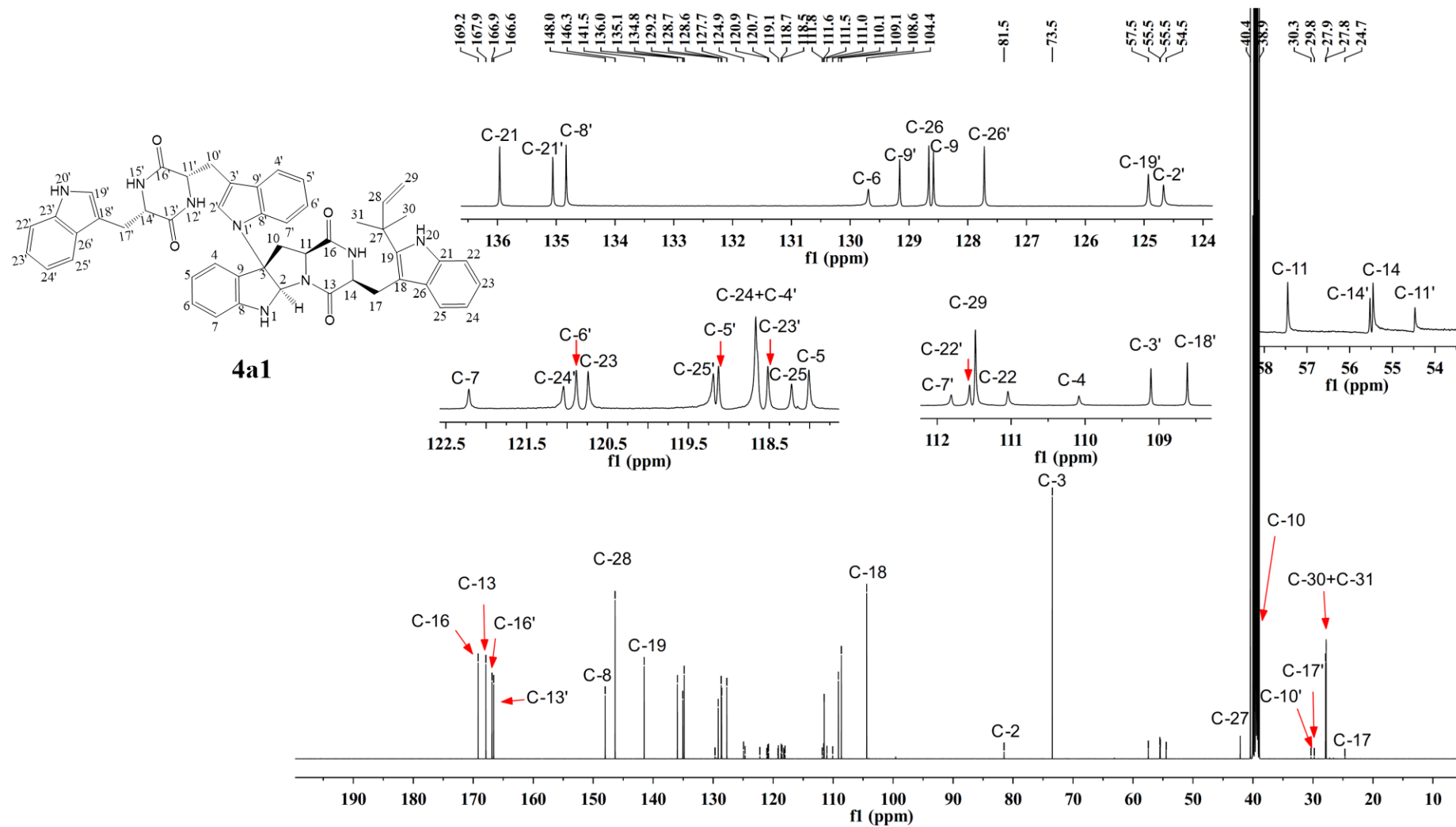
Figure S13. ^{13}C NMR spectrum of **4a1** in DMSO-d_6 (125 MHz).

S25

4a1
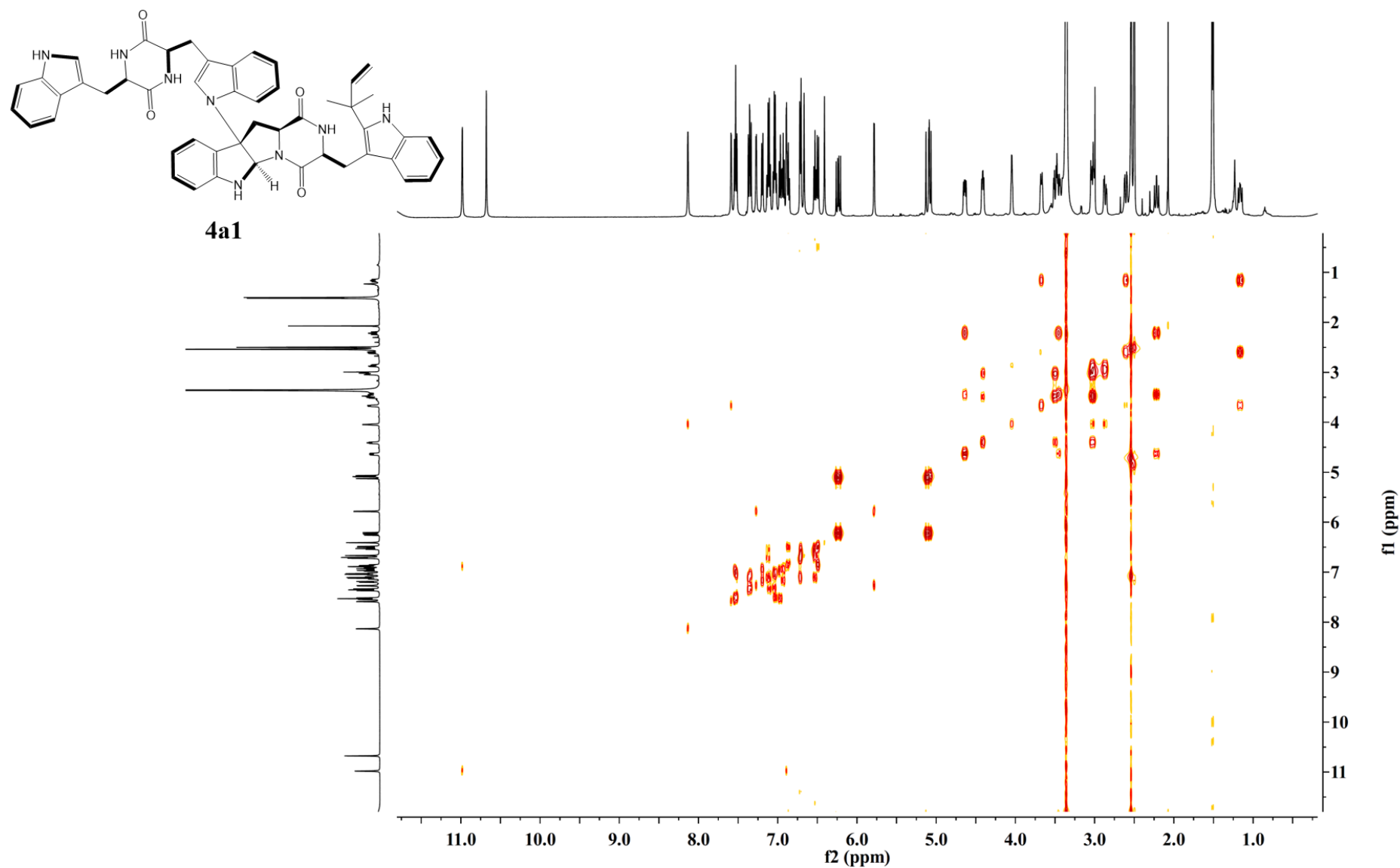
Figure S14. ^{1}H-^{1}H COSY spectrum of **4a1** in DMSO-d_6.

S26

142
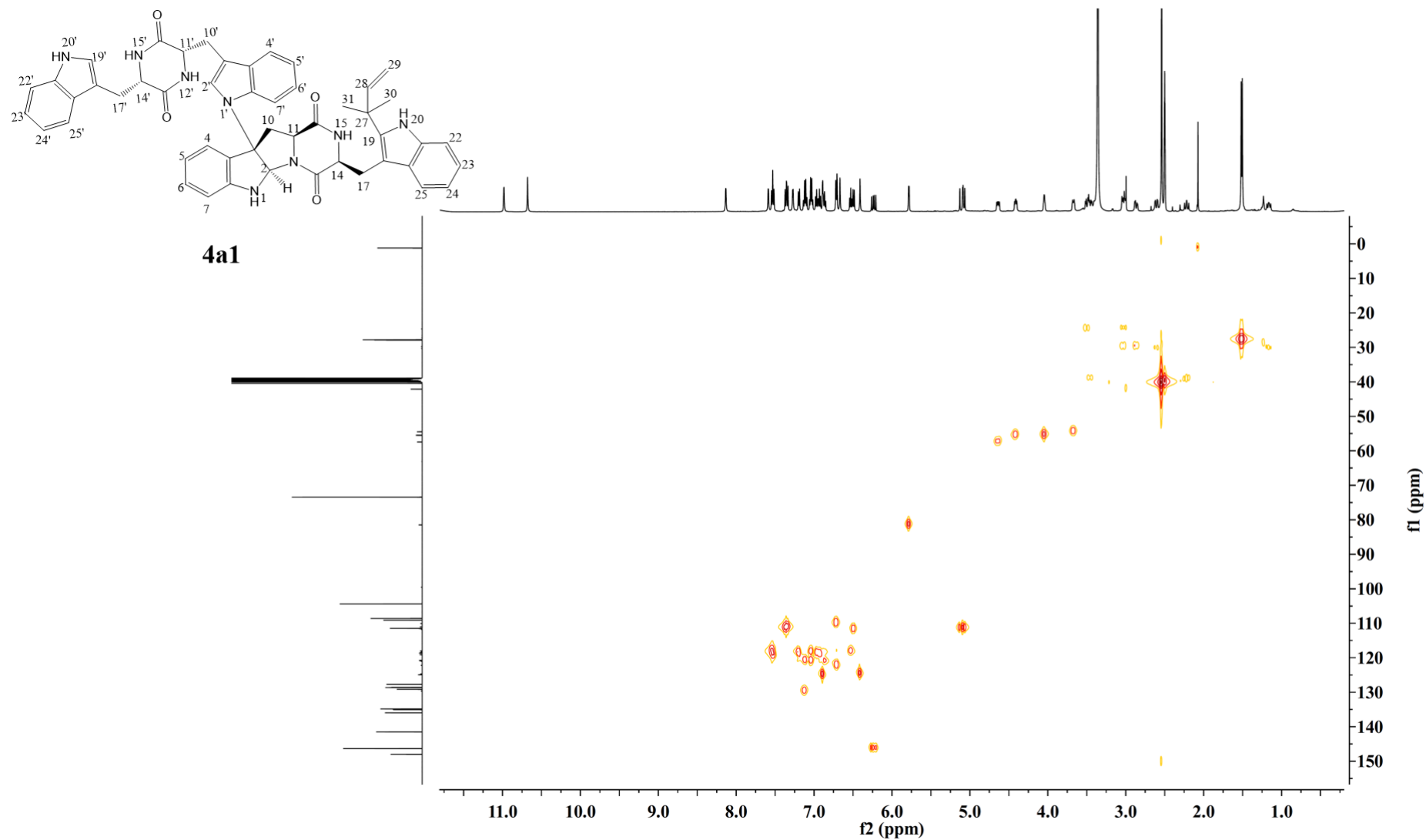
Figure S15. HSQC spectrum of **4a1** in DMSO-d_6.
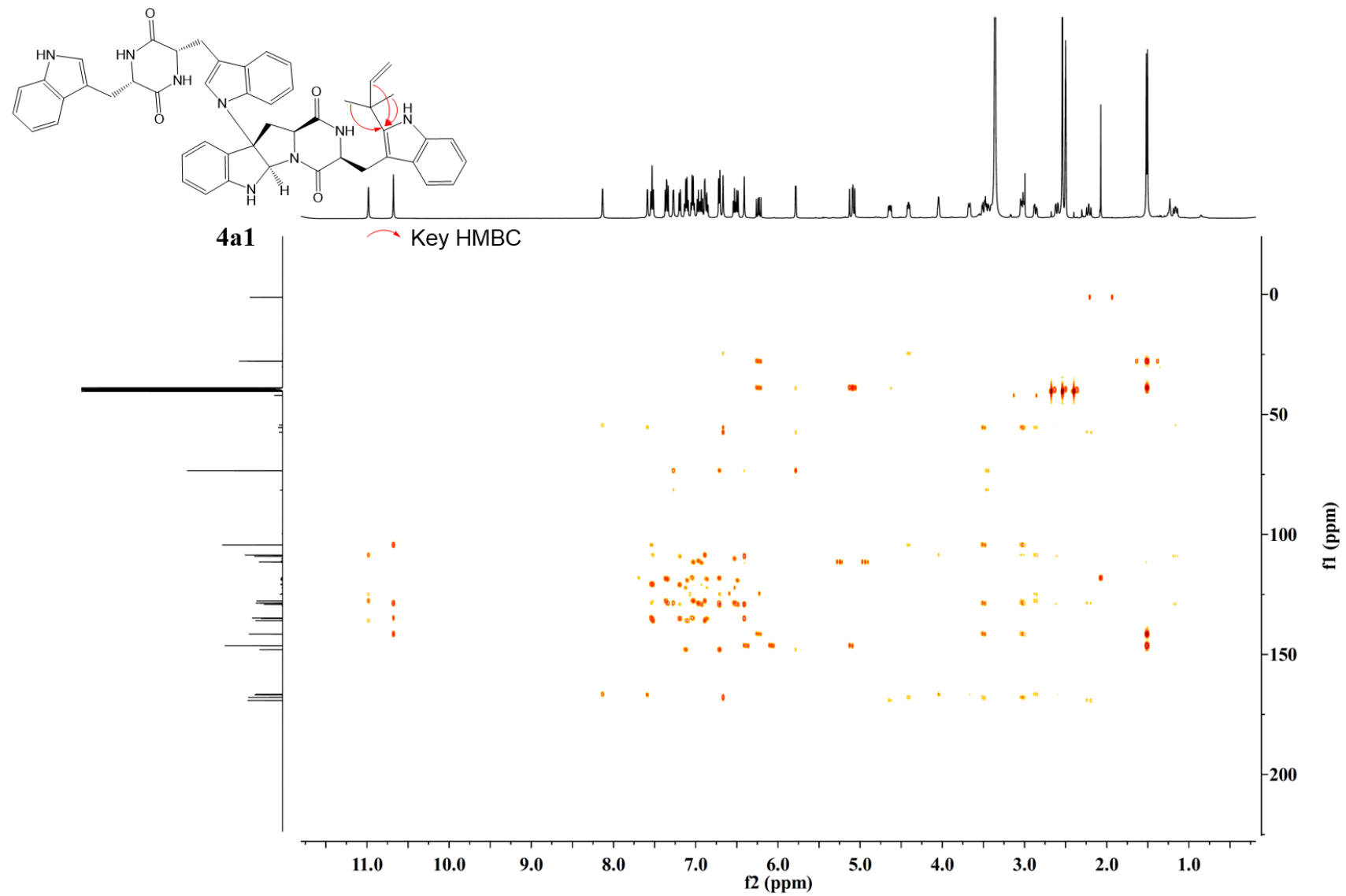
Figure S16. HMBC spectrum of **4a1** in DMSO-d_6.
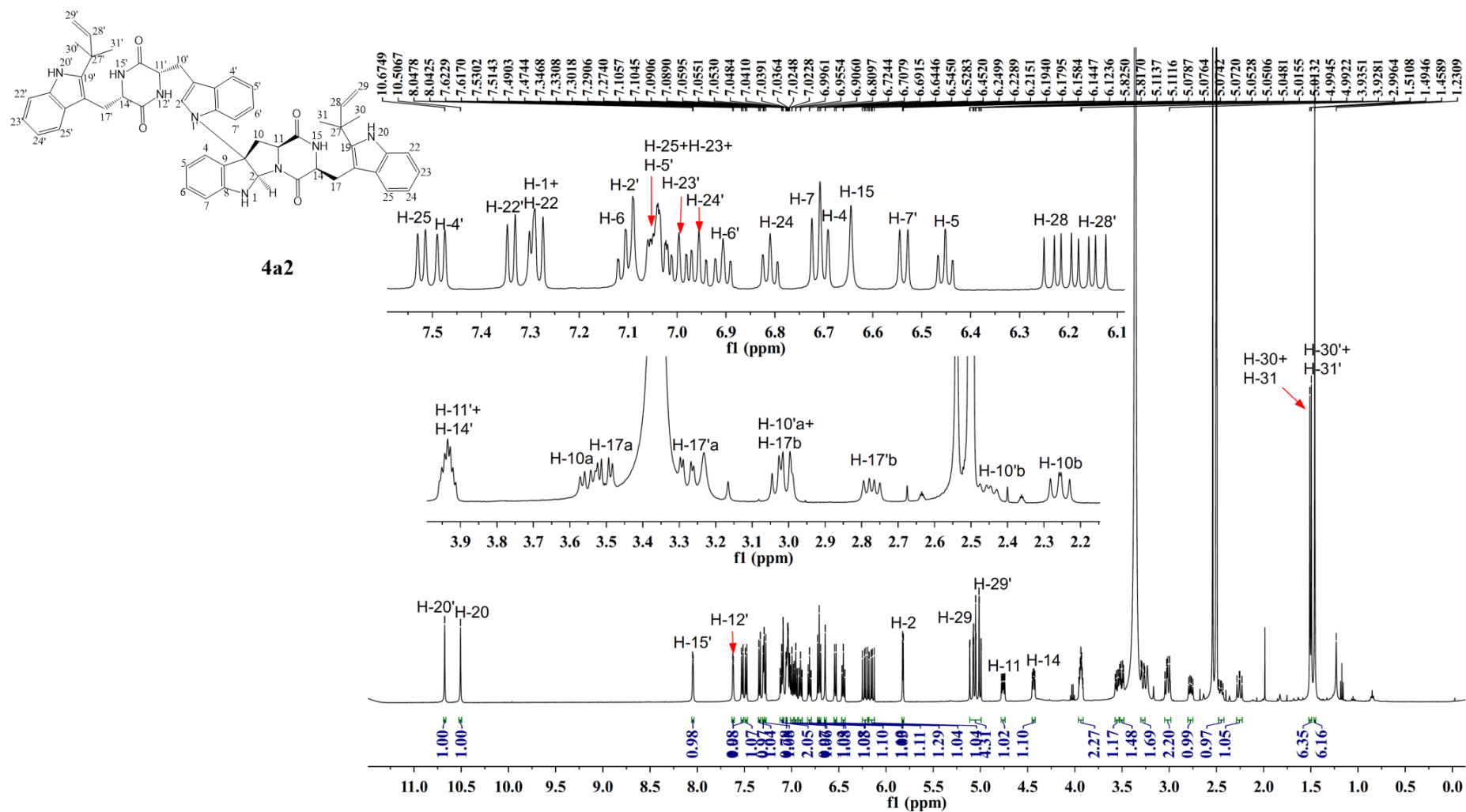
Figure S17. ^{1}H NMR spectrum of **4a2** in DMSO-d_6 (500 MHz).

S29

145
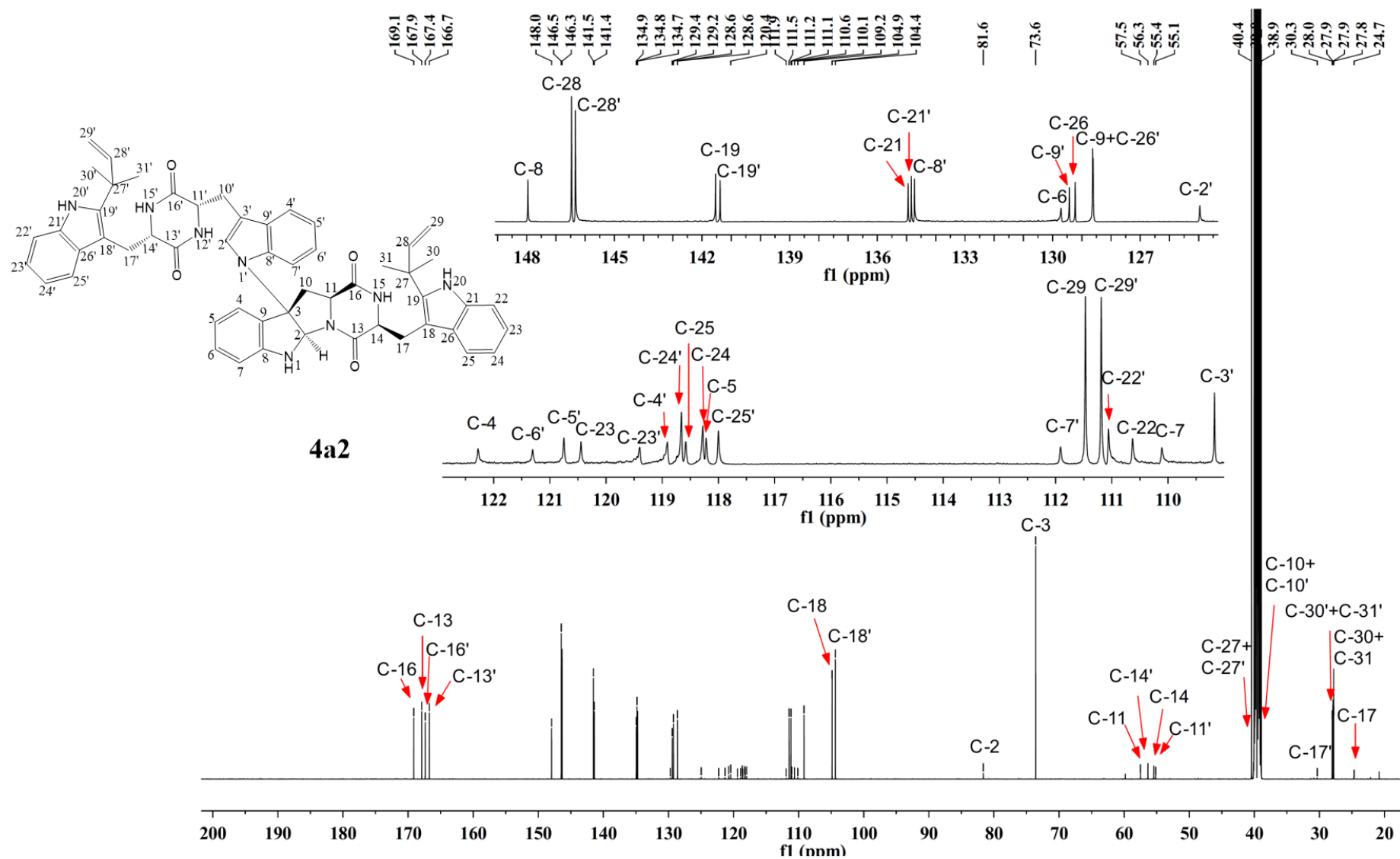
Figure S18. ^{13}C NMR spectrum of **4a2** in DMSO-d_6 (125 MHz).

S30

146
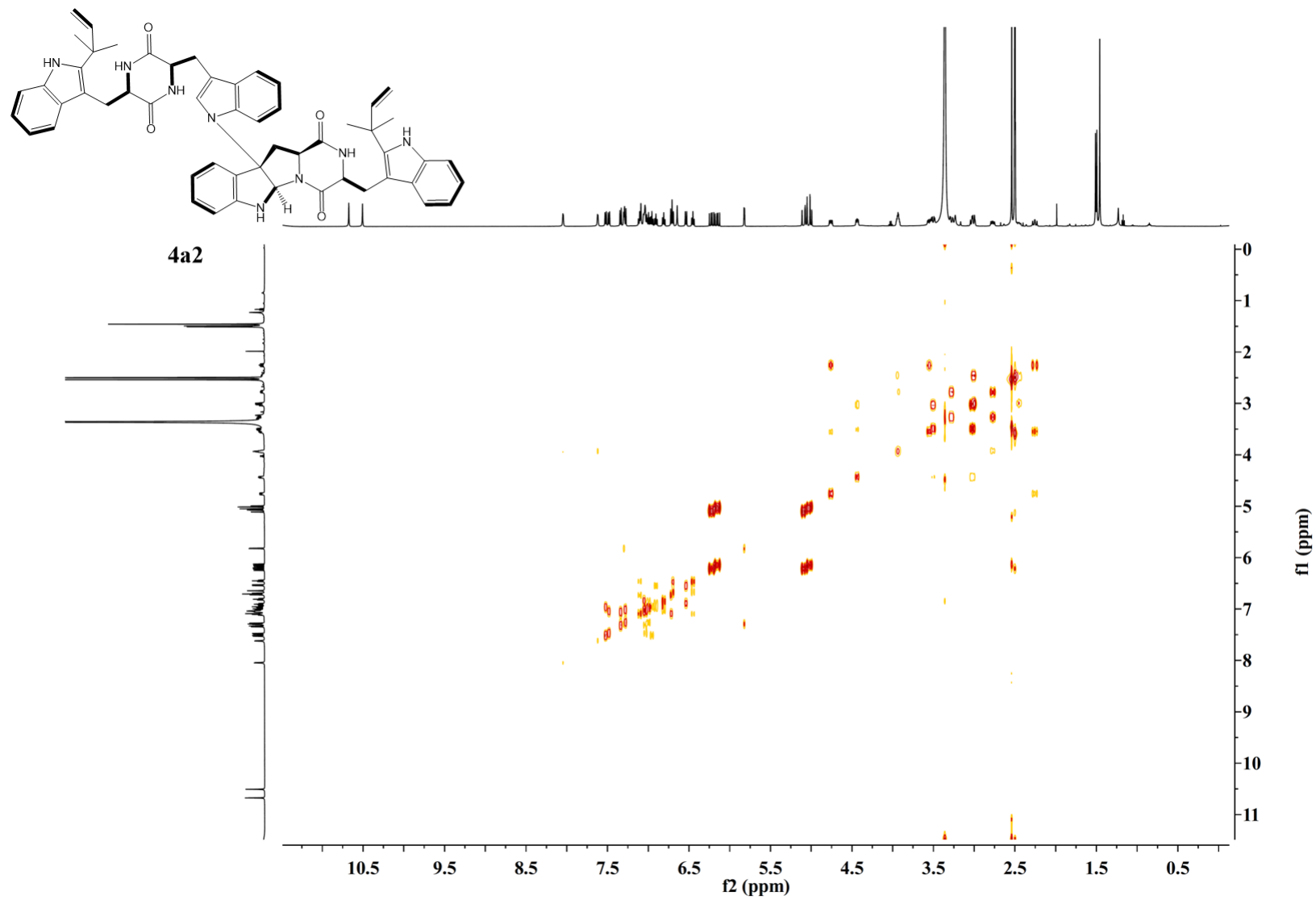
Figure S19. ^{1}H-^{1}H COSY spectrum of **4a2** in DMSO-d_6.

S31
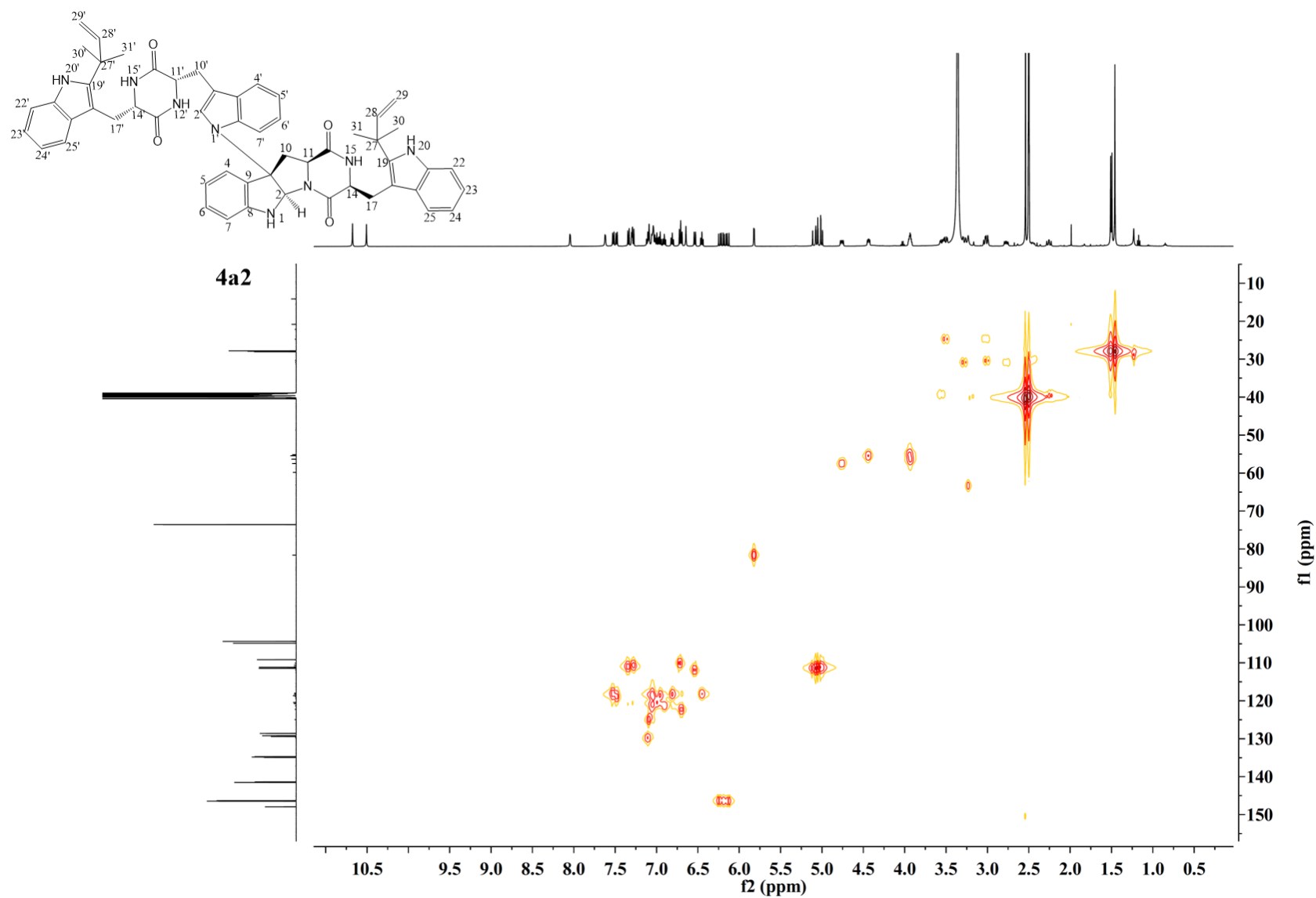
Figure S20. HSQC spectrum of **4a2** in DMSO-d_6.

S32

148
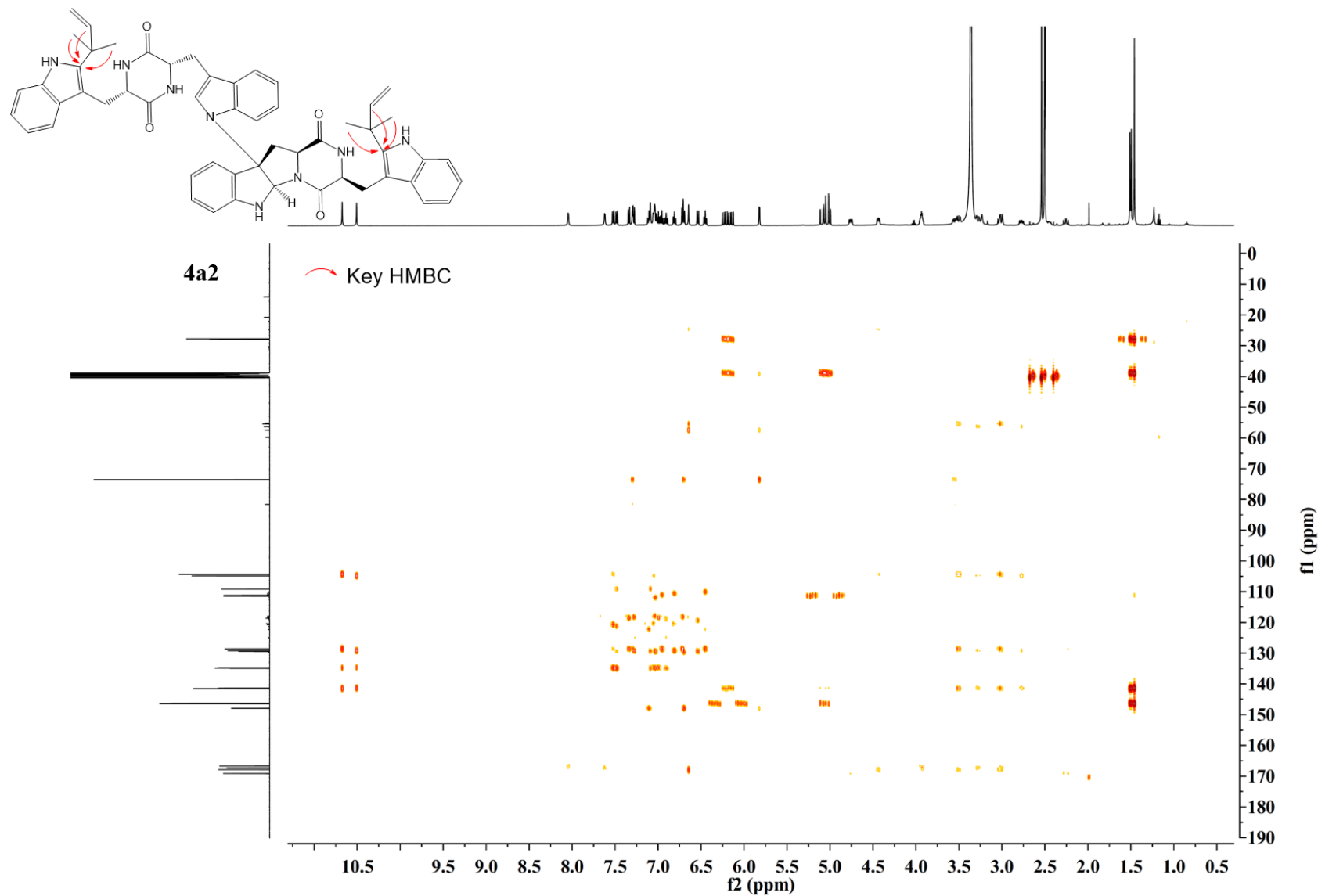
Figure S21. HMBC spectrum of **4a2** in DMSO-d_6.
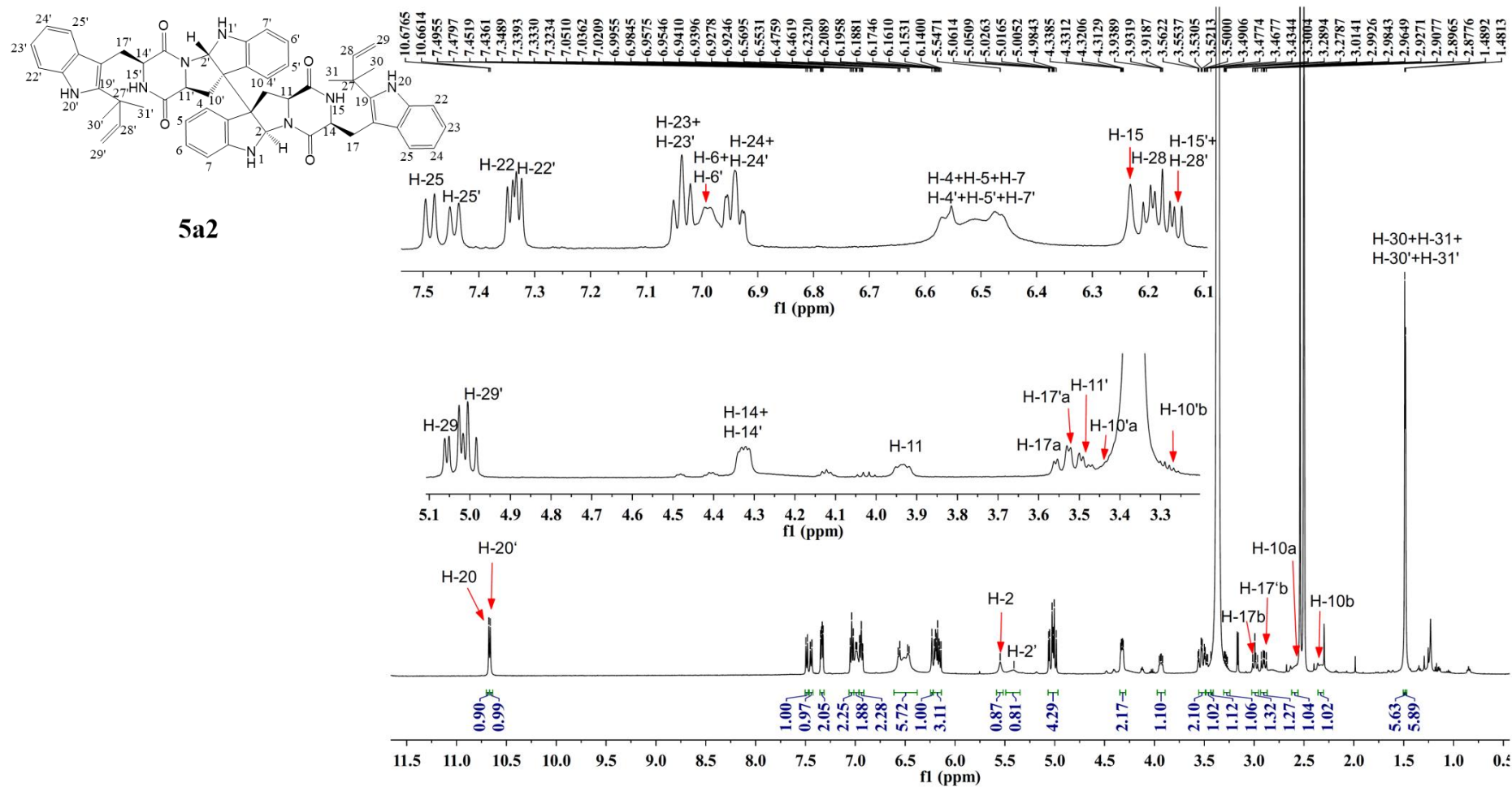
Figure S22. ^{1}H NMR spectrum of **5a2** in DMSO-d_6 (500 MHz).

S34

150
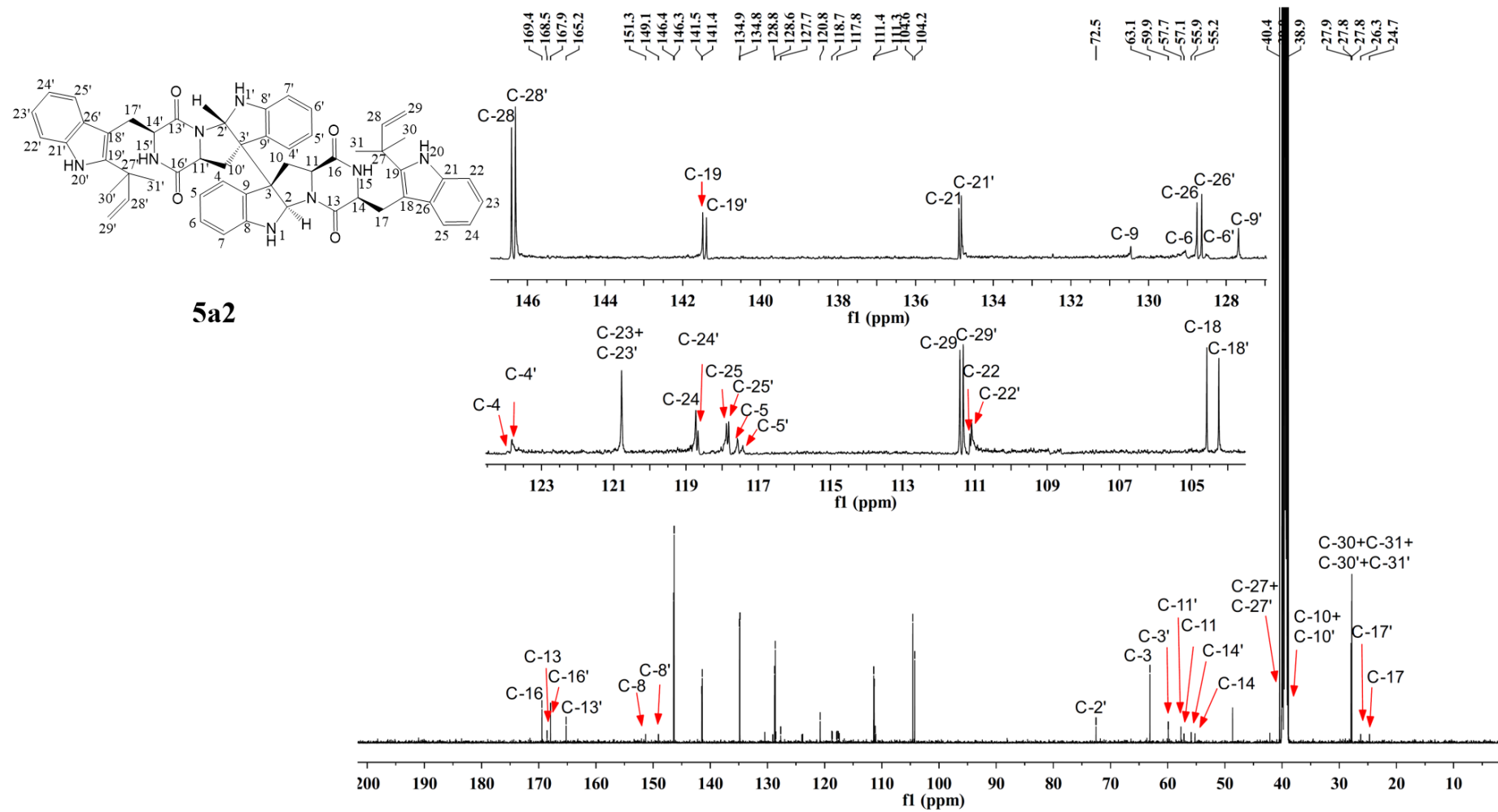
Figure S23. ^{13}C NMR spectrum of **5a2** in DMSO-d_6 (125 MHz).

S35
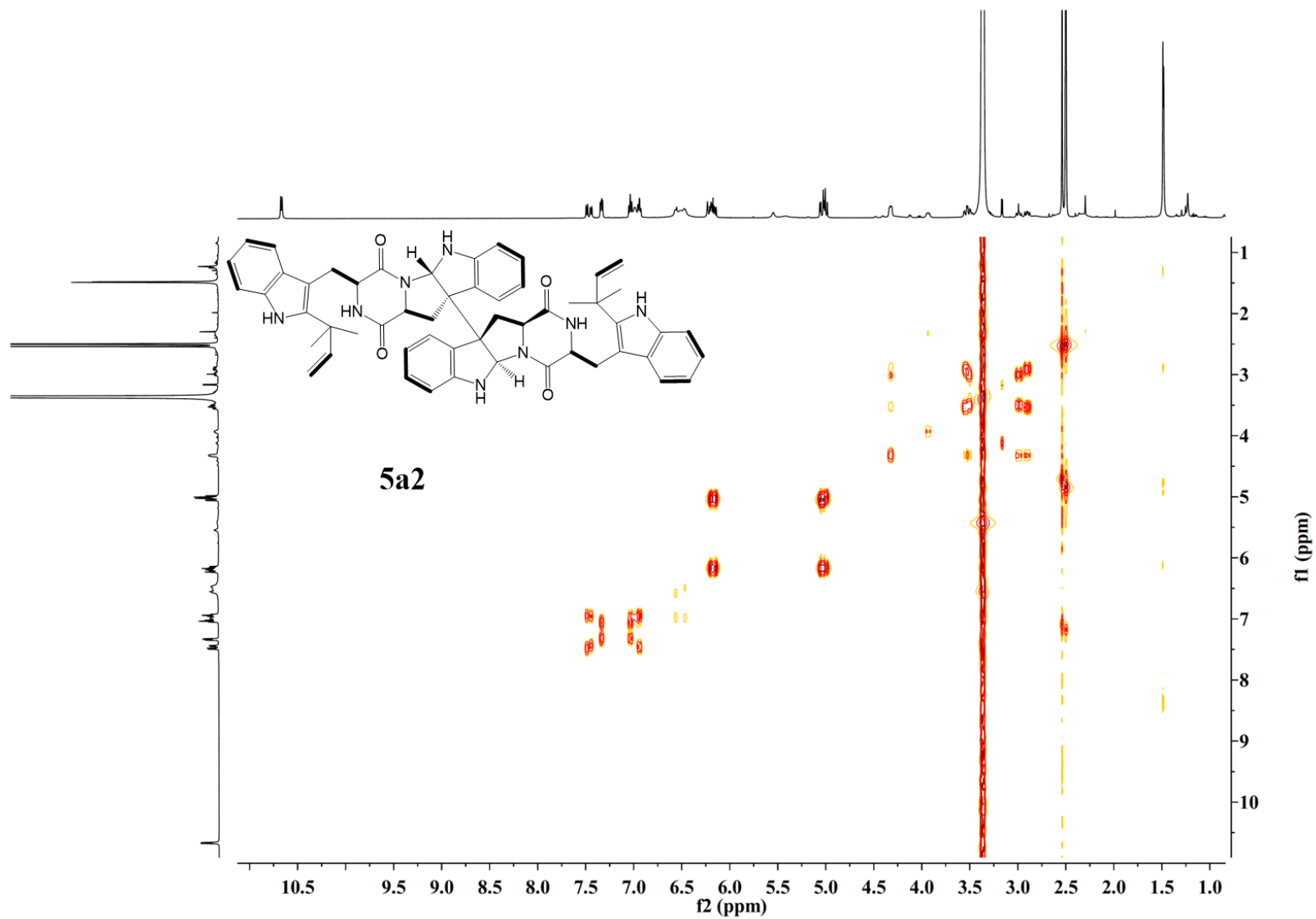
Figure S24. ^1H-^1H COSY spectrum of **5a2** in DMSO-d_6.

S36

152
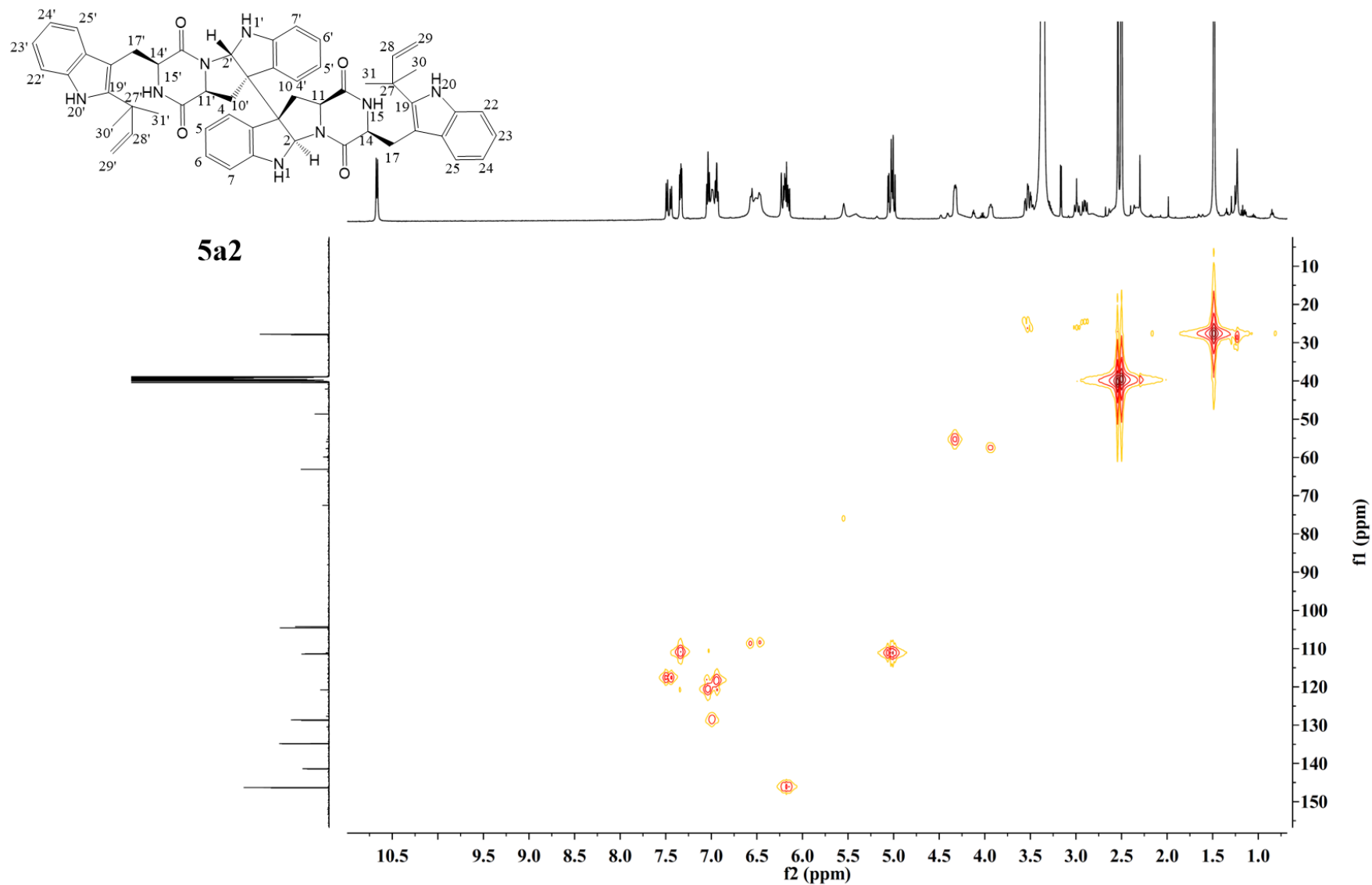
Figure S25. HSQC spectrum of **5a2** in DMSO-d_6.
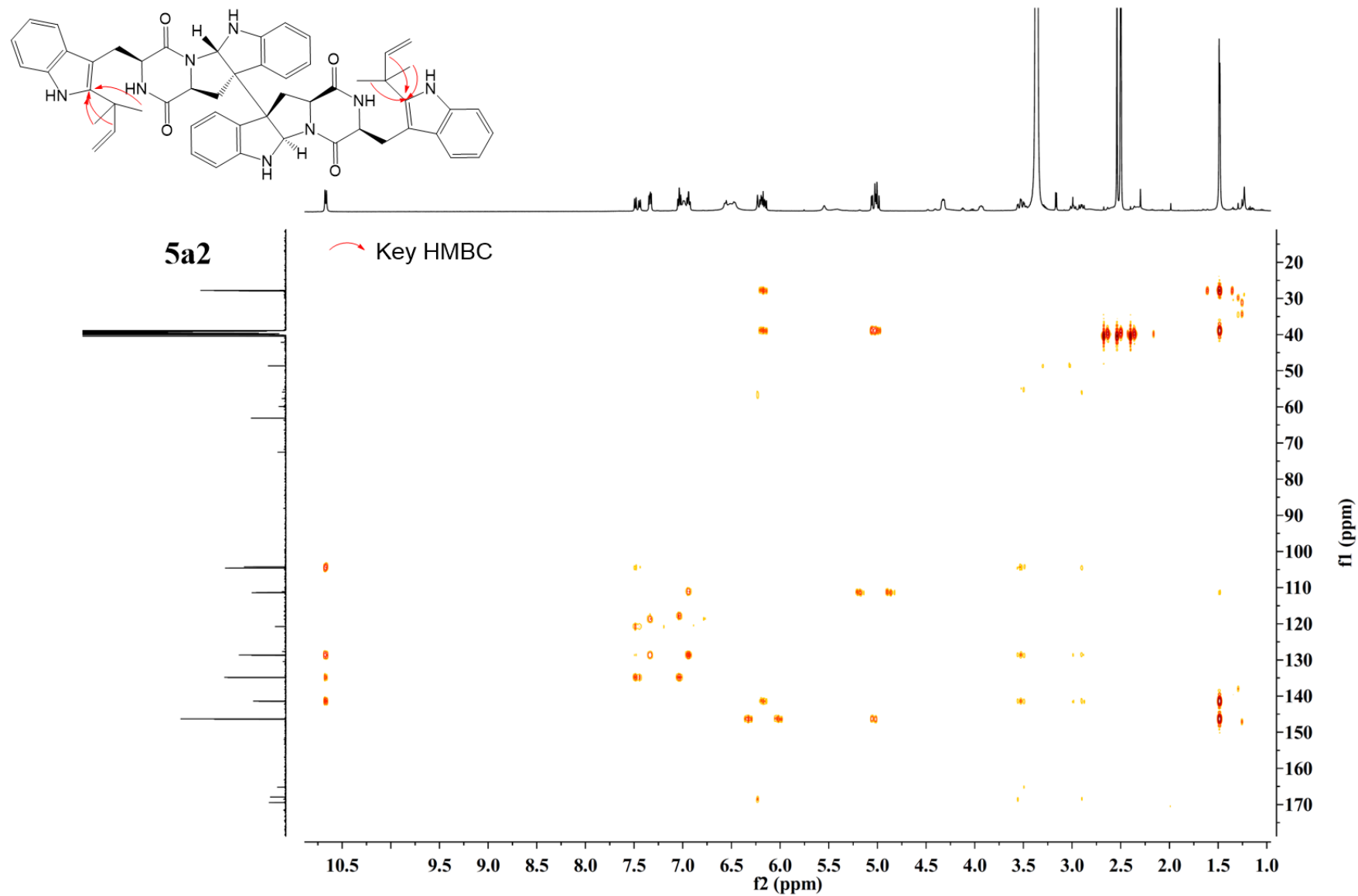
Figure S26. HMBC spectrum of **5a2** in DMSO-d_6.

S38

154
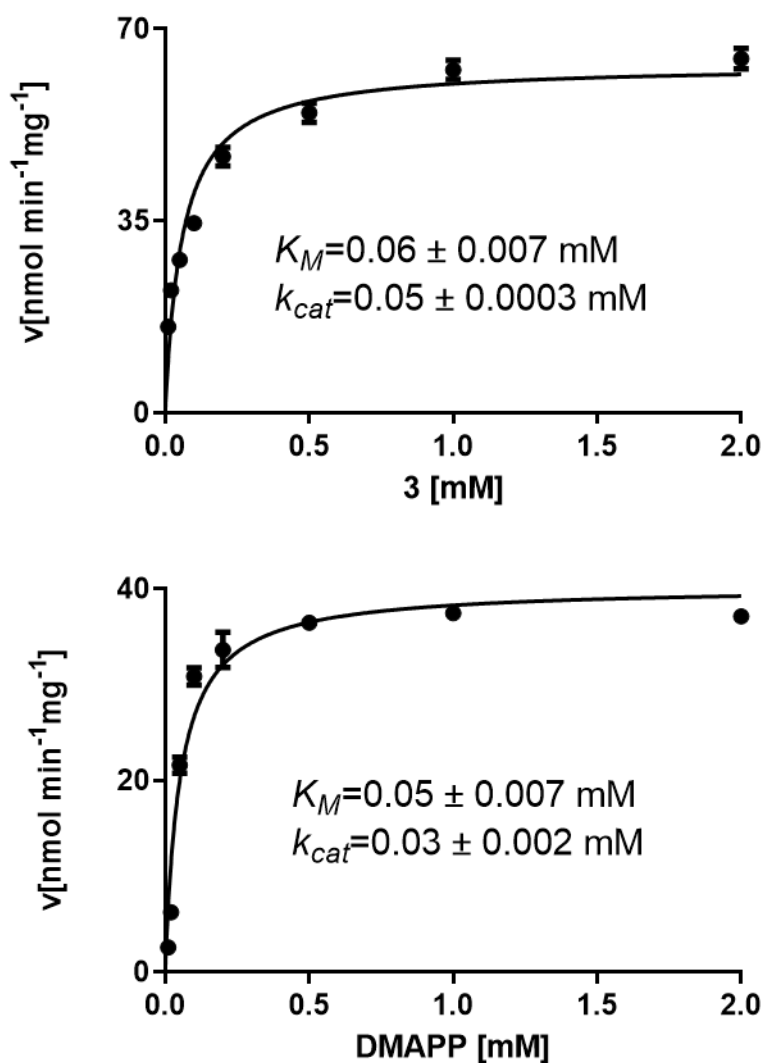
Figure S27. Determination of the kinetic parameters of EchPT1 for **3a2** formation toward **3** and DMAPP. The data were obtained from three independent measurements and the error bars represent the standard errors.
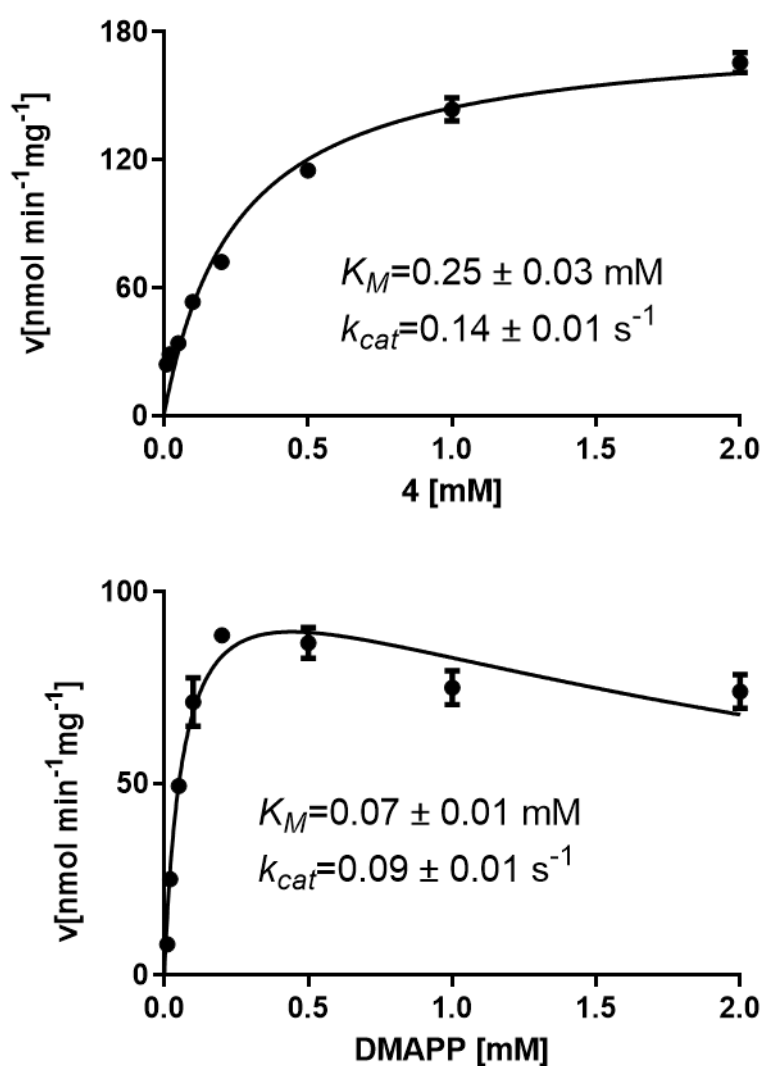
Figure S28. Determination of the kinetic parameters of EchPT1 for **4a1** formation toward **4** and DMAPP. The best curve fit for **4a1** formation toward DMAPP was achieved using a substrate inhibition model in GraphPad Prism 8.01. The data were obtained from three independent measurements and the error bars represent the standard errors.
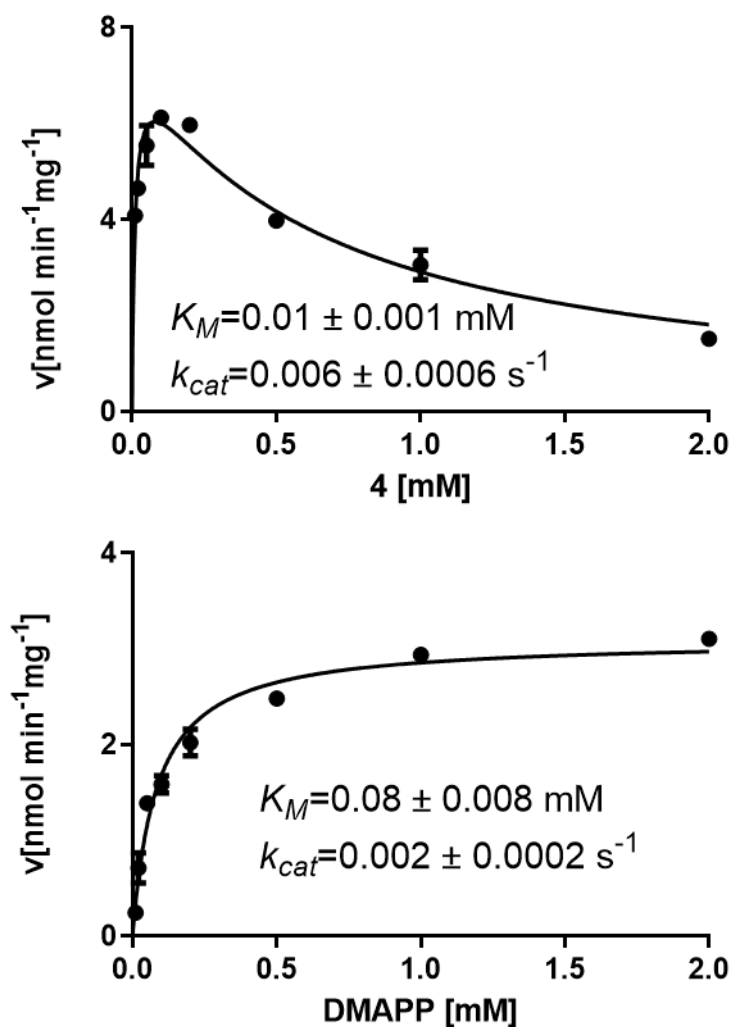
Figure S29. Determination of the kinetic parameters of EchPT1 for **4a2** formation toward **4** and DMAPP. The best curve fit for **4a2** formation toward **4** was achieved using a substrate inhibition model in GraphPad Prism 8.01. The data were obtained from three independent measurements and the error bars represent the standard errors.
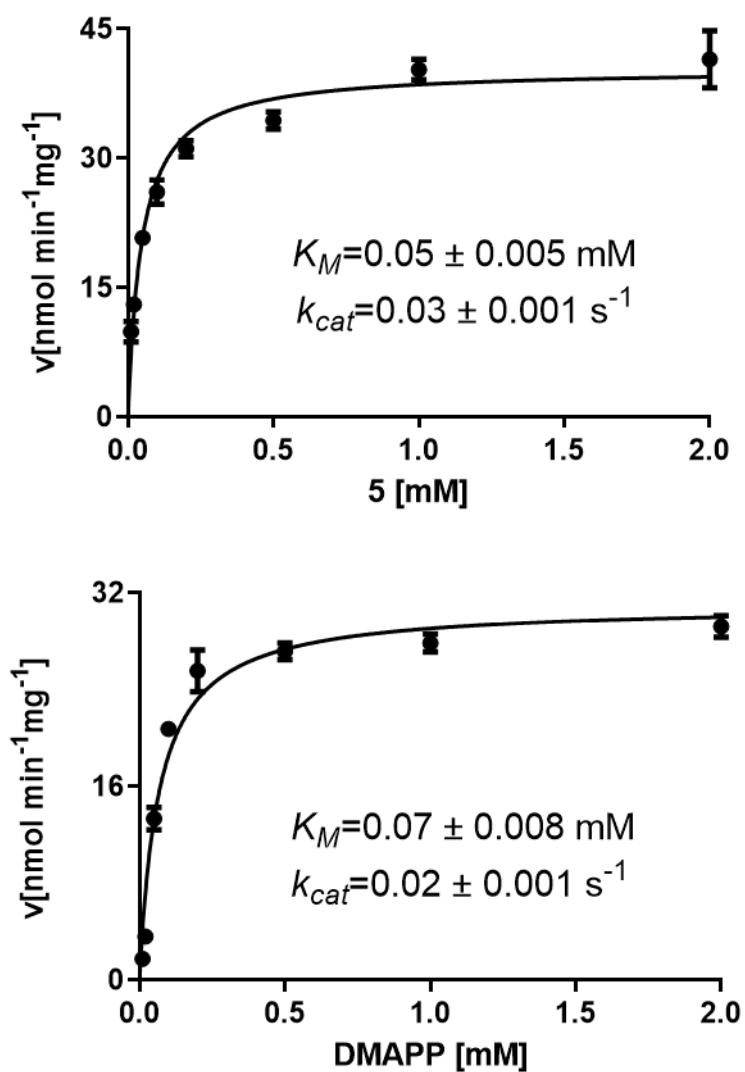
Figure S30. Determination of the kinetic parameters of EchPT1 for **5a2** formation toward **5** and DMAPP. The data were obtained from three independent measurements and the error bars represent the standard errors.

5 Conclusions and future prospects

In this thesis, the structural diversity of NPs was significantly increased by genome mining and chemoenzymatic synthesis. With the development of bioinformatic tools and genetic manipulation strategies, variety of novel BGCs remain to be explored. Investigation of the enzymes involved in the biosynthesis of NPs also provide another effective strategy for modification of NPs by using interesting biocatalysts. The three projects in this thesis were carried out based on the two strategies and each one has the highlight.

In the biosynthesis of novel NRPS-PKS in *Penicillium crustosum*, the function of hybrid gene *Pcr10109* was investigated by gene deletion and heterologous expression in *Aspergillus nidulans*. Compound isolation and structure elucidation proved its product as α-pyrone derivative 4-hydroxy-6-(4-hydroxyphenyl)-2*H*-pyran-2-one. Isotopic feeding experiments revealed that the A domain of *Pcr10109* can recognize PHBA as the start unit and then the KS domain assembles two acetate molecules for latter elongation. The product yield reached a maximum of 51 mg/kg rice after feeding with PHBA, which is five-fold than that obtained without feeding. This study provides another example for the less explored fungal NRPS-PKS hybrid enzymes and also helpful for product formation requiring special substrates supply.

Through chemoenzymatic synthesis, the spectra of prenyl CDP analogs were also expanded by using known PTs. In the production of diprenylated *cyclo*-L-Trp-L-Pro, we first followed the logic of the nature´s biosynthetic strategy to chemoenzymatic synthesis *C2,C4-*, *C2,C5-*, *C2,C6-*, and *C2,C7-*diprenylated derivatives. However, the *C2*-prenylated *cyclo*-L-Trp-L-Pro cannot be accepted by the tested *C4-*, *C5-*, *C6-*, and *C7*-PTs. After changing the reaction order and using *C2*-PT EchPT1 as the second biocatalyst, we successfully obtained the four target products including the unique *N1,C6-*diprenylated ones with significant product yields. This is the first report that EchPT1 can also catalyze the unusual *N1*-prenylation at the indole ring other than C2 position, which indicates the different active site(s) in EchPT1 toward *C6-*prenylated *cyclo*-L-Trp-L-Pro.

Inspired by the intriguing reactions by the promiscuous PTs, we intended to get prenylated dimeric CDPs by the soluble DMATS mentioned above. It was proven that the cWW dimers tetratryptomycins A − C can be well accepted by EchPT1 in the presence of DMAPP. Both monoprenylated and diprenylated products can be detected after shorter the incubation time for 1 h. What's more, tetratryptomycins A and C are better substrates of EchPT1 for prenylation

than tetratryptomycin B. The products catalyzed by EchPT1 were determined as *C2*- (and *C2´*-) prenylated tetratryptomycins, which is consistent with EchPT1 catalyzed *C2*-prenylation for its natural substrate cWA. Further kinetic parameters including K_M and k_{cat} determination proved that the values are in good consistence with the observed conversion yields and also in the range of EchPT1 reactions toward most CDPs.

For future prospects, the following works can be performed:

➢ In the first project, the final product of NRPS-PKS gene cluster in *Penicillium crustosum* remains to be elucidated. Therefore, investigation of its biosynthesis would be useful for better understanding the rare group enzymes in fungi.

➢ Targeted protein engineering of EchPT1 for understanding its catalytic mechanism toward *C6*-prenylated *cyclo*-L-Trp-L-Pro and dimeric *cyclo*-L-Trp-L-Trp.

➢ Co-expression of CDPS for production of tryptophan containing CDPs and the tailoring genes from different biosynthetic pathways such as PTs, P450s, and MTs in engineered heterologous expression host.

6 References

1. Atanasov, A. G.; Zotchev, S. B.; Dirsch, V. M.; Supuran, C. T. Natural products in drug discovery: advances and opportunities. *Nat. Rev. Drug Discov.* **2021,** *20* (3), 200-216.

2. Carter, G. T. Natural products and Pharma 2011: strategic changes spur new opportunities. *Nat. Prod. Rep.* **2011,** *28* (11), 1783-1789.

3. Vicente, M. F.; Basilio, A.; Cabello, A.; Peláez, F. Microbial natural products as a source of antifungals. *Clin. Microbiol. Infect.* **2003,** *9* (1), 15-32.

4. Gunatilaka, A. A. L. Natural products from plant-associated microorganisms: distribution, structural diversity, bioactivity, and implications of their occurrence. *J Nat. Prod.* **2006,** *69* (3), 509-526.

5. Harvey, A. Strategies for discovering drugs from previously unexplored natural products. *Drug Discov. Today* **2000,** *5* (7), 294-300.

6. Katz, L.; Baltz, R. H. Natural product discovery: past, present, and future. *J. Ind. Microbiol. Biotechn.* **2016,** *43* (2-3), 155-176.

7. Boruta, T. Uncovering the repertoire of fungal secondary metabolites: From Fleming's laboratory to the International Space Station. *Bioengineered* **2018,** *9* (1), 12-16.

8. Misiek, M.; Hoffmeister, D. Fungal genetics, genomics, and secondary metabolites in pharmaceutical sciences. *Planta Med.* **2007,** *73* (2), 103-115.

9. Weissman, K. J.; Müller, R. Myxobacterial secondary metabolites and modes-of-action. *Nat. Prod. Rep.* **2010,** *27* (9), 1276-1295.

10. Pickens, L. B.; Tang, Y.; Chooi, Y. H. Metabolic engineering for the production of natural products. *Annu. Rev. Chem. Biomol. Eng.* **2011,** *2*, 211-236.

11. Ram, V. J.; Kumari, S. Natural products of plant origin as anticancer agents. *Drug News Perspect.* **2001,** *14* (8), 465-482.

12. Keller, N. P.; Turner, G.; Bennett, J. W. Fungal secondary metabolism - from biochemistry to genomics. *Nat. Rev. Microbiol.* **2005,** *3* (12), 937-947.

13. Yan, W.; Ge, H. M.; Wang, G.; Jiang, N.; Mei, Y. N.; Jiang, R.; Li, S. J.; Chen, C. J.; Jiao, R. H.; Xu, Q.; Ng, S. W.; Tan, R. X. Pictet-Spengler reaction-based biosynthetic machinery in fungi. *Proc. Natl. Acad. Sci. U. S. A* **2014,** *111* (51), 18138-18143.

14. Bode, H. B.; Müller, R. The impact of bacterial genomics on natural product research. *Angew. Chem. Int. Ed Engl.* **2005,** *44* (42), 6828-6846.

15. Brakhage, A. A.; Schroeckh, V. Fungal secondary metabolites - strategies to activate silent gene clusters. *Fungal. Genet. Biol.* **2011,** *48* (1), 15-22.

16. Ikeda, H. Natural products discovery from micro-organisms in the post-genome era. *Biosci. Biotechnol. Biochem.* **2017,** *81* (1), 13-22.

17. He, X. M.; Liu, H. W. Formation of unusual sugars: Mechanistic studies and biosynthetic applications. *Annu. Rev. Biochem.* **2002,** *71,* 701-754.

18. Rahmat, E.; Kang, Y. Yeast metabolic engineering for the production of pharmaceutically important secondary metabolites. *Appl. Microbiol. Biotechnol.* **2020,** *104* (11), 4659-4674.

19. Blunt, J. W.; Copp, B. R.; Keyzers, R. A.; Munro, M. H.; Prinsep, M. R. Marine natural products. *Nat. Prod. Rep.* **2012,** *29* (2), 144-222.

20. Challis, G. L. Mining microbial genomes for new natural products and biosynthetic pathways. *Microbiology* **2008,** *154* (Pt 6), 1555-1569.

21. Asai, T.; Tsukada, K.; Ise, S.; Shirata, N.; Hashimoto, M.; Fujii, I.; Gomi, K.; Nakagawara, K.; Kodama, E. N.; Oshima, Y. Use of a biosynthetic intermediate to explore the chemical diversity of pseudo-natural fungal polyketides. *Nat. Chem.* **2015,** *7* (9), 737-743.

22. Hertweck, C. The biosynthetic logic of polyketide diversity. *Angew. Chem. Int. Ed.* **2009,** *48* (26), 4688-4716.

23. El-Elimat, T.; Raja, H. A.; Figueroa, M.; Al Sharie, A. H.; Bunch, R. L.; Oberlies, N. H. Freshwater fungi as a source of chemical diversity: A review. *J. Nat. Prod.* **2021,** doi: 10.1021/acs.jnatprod.0c01340.

24. Xue, Q.; Ashley, G.; Hutchinson, C. R.; Santi, D. V. A multiplasmid approach to preparing large libraries of polyketides. *Proc. Natl. Acad. Sci. U. S. A* **1999,** *96* (21), 11740-11745.

25. McDaniel, R.; Thamchaipenet, A.; Gustafsson, C.; Fu, H.; Betlach, M.; Ashley, G. Multiple genetic modifications of the erythromycin polyketide synthase to produce a library of novel "unnatural" natural products. *Proc. Natl. Acad. Sci. U. S. A* **1999,** *96* (5), 1846-1851.

26. Hobson, C.; Chan, A. N.; Wright, G. D. The antibiotic resistome: A guide for the discovery of natural products as antimicrobial agents. *Chem. Rev.* **2021,** doi: 10.1021/acs.chemrev.0c01214.

27. Zhou, Q.; Peng, S. Y.; Zhang, K.; Luo, G. C.; Han, L.; He, Q. L.; Tang, G. L. A flavin-dependent monooxygenase mediates divergent oxidation of rifamycin. *Org. Lett.* **2021,** *23* (6), 2342-2346.

28. Marcu, M. G.; Schulte, T. W.; Neckers, L. Novobiocin and related coumarins and depletion of heat shock protein 90-dependent signaling proteins. *J. Natl. Cancer Inst.* **2000,** *92* (3), 242-248.

29. Abdou, R.; Scherlach, K.; Dahse, H. M.; Sattler, I.; Hertweck, C. Botryorhodines A–D, antifungal and cytotoxic depsidones from *Botryosphaeria rhodina*, an endophyte of the medicinal plant *Bidens pilosa*. *Phytochemistry* **2010,** *71* (1), 110-116.

30. Huang, C.; Yang, C.; Zhang, W.; Zhang, L.; De, B. C.; Zhu, Y.; Jiang, X.; Fang, C.; Zhang, Q.; Yuan, C. S.; Liu, H. W.; Zhang, C. Molecular basis of dimer formation during the biosynthesis of benzofluorene-containing atypical angucyclines. *Nat. Commun.* **2018,** *9* (1), 2088.

31. Lackner, G.; Bohnert, M.; Wick, J.; Hoffmeister, D. Assembly of melleolide antibiotics involves a polyketide synthase with cross-coupling activity. *Chem. Biol.* **2013,** *20* (9), 1101-1106.

32. Frisvad, J.; Thrane, U. Standardized high-performance liquid chromatography of 182 mycotoxins and other fungal metabolites based on alkylphenone retention indexes and UV-VIS spectra (diode array detection). *J. Chromatogr.* **1987,** *404* (1), 195-214.

33. Kennedy, J.; Auclair, K.; Kendrew, S. G.; Park, C.; Vederas, J. C.; Hutchinson, C. R. Modulation of polyketide synthase activity by accessory proteins during lovastatin biosynthesis. *Science* **1999,** *284* (5418), 1368-1372.

34. Sorensen, J. L.; Auclair, K.; Kennedy, J.; Hutchinson, C. R.; Vederas, J. C. Transformations of cyclic nonaketides by *Aspergillus terreus* mutants blocked for lovastatin biosynthesis at the *lovA* and *lovC* genes. *Org. Biomol. Chem.* **2003,** *1* (1), 50-59.

35. Horinouchi, S. Combinatorial biosynthesis of non-bacterial and unnatural flavonoids, stilbenoids and curcuminoids by microorganisms. *J. Antibiot.* **2008,** *61* (12), 709-728.

36. Ames, B. D.; Walsh, C. T. Anthranilate-activating modules from fungal nonribosomal peptide assembly lines. *Biochemistry* **2010,** *49* (15), 3351-3365.

37. Felnagle, E. A.; Jackson, E. E.; Chan, Y. A.; Podevels, A. M.; Berti, A. D.; McMahon, M. D.; Thomas, M. G. Nonribosomal peptide synthetases involved in the production of medically relevant natural products. *Mol. Pharm.* **2008,** *5* (2), 191-211.

38. Stachelhaus, T.; Mootz, H. D.; Bergendahl, V.; Marahiel, M. A. Peptide bond formation in nonribosomal peptide biosynthesis. Catalytic role of the condensation domain. *J. Biol. Chem.* **1998,** *273* (35), 22773-22781.

39. Zhang, J.; Liu, N.; Cacho, R. A.; Gong, Z.; Liu, Z.; Qin, W.; Tang, C.; Tang, Y.; Zhou, J. Structural basis of nonribosomal peptide macrocyclization in fungi. *Nat. Chem Biol.* **2016,** *12* (12), 1001-1003.

40. Velkov, T.; Lawen, A. Mapping and molecular modeling of *S*-adenosyl-L-methionine binding sites in *N*-methyltransferase domains of the multifunctional polypeptide cyclosporin synthetase. *J. Biol. Chem* **2003,** *278* (2), 1137-1148.

41. Iacovelli, R.; Bovenberg, R. A. L.; Driessen, A. J. M. Nonribosomal peptide synthetases and their biotechnological potential in *Penicillium rubens*. *J. Ind. Microbiol. Biotechnol.* **2021,** *48* (7-8), kuab045.

42. Kries, H. Biosynthetic engineering of nonribosomal peptide synthetases. *J. Pept. Sci.* **2016,** *22* (9), 564-570.

43. Süssmuth, R. D.; Mainz, A. Nonribosomal peptide synthesis - Principles and prospects. *Angew. Chem. Int. Ed. Engl.* **2017,** *56* (14), 3770-3821.

44. Steiniger, C.; Hoffmann, S.; Mainz, A.; Kaiser, M.; Voigt, K.; Meyer, V.; Süssmuth, R. D. Harnessing fungal nonribosomal cyclodepsipeptide synthetases for mechanistic insights and tailored engineering. *Chem. Sci.* **2017,** *8* (11), 7834-7843.

45. Maiya, S.; Grundmann, A.; Li, S.-M.; Turner, G. The fumitremorgin gene cluster of *Aspergillus fumigatus*: identification of a gene encoding brevianamide F synthetase. *Chembiochem.* **2006,** *7* (7), 1062-1069.

46. Stack, D.; Neville, C.; Doyle, S. Nonribosomal peptide synthesis in *Aspergillus fumigatus* and other fungi. *Microbiology* **2007,** *153* (Pt 5), 1297-1306.

47. Newman, D. J.; Cragg, G. M. Natural products as sources of new drugs over the nearly four decades from 01/1981 to 09/2019. *J. Nat. Prod.* **2020,** *83*, 770-803.

48. Avalos, M.; Garbeva, P.; Vader, L.; Van Wezel, G. P.; Dickschat, J. S.; Ulanova, D. Biosynthesis, evolution and ecology of microbial terpenoids. *Nat. Prod. Rep.* **2022,** *39*, 249-272.

49. Liu, Y.; Ma, X.; Liang, H.; Stephanopoulos, G.; Zhou, K. Monoterpenoid biosynthesis by engineered microbes. *J. Ind. Microbiol. Biotechnol.* **2021,** kuab065.

50. Yuan, Y.; Cheng, S.; Bian, G.; Yan, P.; Ma, Z.; Dai, W.; Chen, R.; Fu, S.; Huang, H.; Chi, H.; Cai, Y.; Deng, Z.; Liu, T. Efficient exploration of terpenoid biosynthetic gene clusters in filamentous fungi. *Nature Catal.* **2022,** *5* (4), 277-287.

51. Zhao, L.; Chang, W. C.; Xiao, Y.; Liu, H. W.; Liu, P. Methylerythritol phosphate pathway of isoprenoid biosynthesis. *Annu. Rev. Biochem.* **2013,** *82*, 497-530.

52. Eisenreich, W.; Rieder, C.; Grammes, C.; Hessler, G.; Adam, K. P.; Becker, H.; Arigoni, D.; Bacher, A. Biosynthesis of a neo-epi-verrucosane diterpene in the liverwort *Fossombronia alaskana*. A retrobiosynthetic NMR study. *J. Biol. Chem.* **1999,** *274* (51), 36312-36320.

53. Knöss, W.; Reuter, B.; Zapp, J. Biosynthesis of the labdane diterpene marrubiin in *Marrubium vulgare* via a non-mevalonate pathway. *Biochem. J.* **1997,** *326* (Pt 2), 449-454.

54. Young, C. A.; Tapper, B. A.; May, K.; Moon, C. D.; Schardl, C. L.; Scott, B. Indole-diterpene biosynthetic capability of epichloe endophytes as predicted by ltm gene analysis. *Appl. Environ. Microbiol.* **2009,** *75* (7), 2200-2211.

55. Zhu, C.; Xu, B.; Adpressa, D. A.; Rudolf, J. D.; Loesgen, S. Discovery and biosynthesis of a structurally dynamic antibacterial diterpenoid. *Angew. Chem. Int. Ed. Engl.* **2021,** *60*, 14163-14170.

56. Liu, T.; Jiang, L.; Xiang, Z.; Li, J.; Zhang, Y.; Xiang, T.; Wang, W.; Li, X.; Jia, Y.; Huang, X.; Lu, X.; Xu, H.; Wang, X.; Sheng, J. Tereticornate A suppresses RANKL-induced osteoclastogenesis via the downregulation of c-Src and TRAF6 and the inhibition of RANK signaling pathways. *Biomed. Pharmacother.* **2022,** *151*, 113140.

57. Ouyang, C.; Ma, X.; Zhao, J.; Li, S.; Liu, C.; Tang, Y.; Zhou, J.; Chen, J.; Li, X.; Li, W. Oleanolic acid inhibits mercury chloride induced-liver ferroptosis by regulating ROS/iron overload. *Ecotoxicol. Environ. Saf* **2023,** *258*, 114973.

58. Cheng, J. Z.; Coyle, C. M.; Panaccione, D. G.; O'Connor, S. E. A role for old yellow enzyme in ergot alkaloid biosynthesis. *J. Am. Chem. Soc.* **2010,** *132* (6), 1776-1777.

59. Lindsay, A. C.; Kim, S. H.; Sperry, J. Non-monoterpenoid azepinoindole alkaloids. *Nat. Prod. Rep.* **2018**.

60. McCabe, S. R.; Wipf, P. Total synthesis, biosynthesis and biological profiles of clavine alkaloids. *Org. Biomol. Chem* **2016,** *14* (25), 5894-5913.

61. Cheng, J. Z.; Coyle, C. M.; Panaccione, D. G.; O'Connor, S. E. Controlling a structural branch point in ergot alkaloid biosynthesis. *J Am. Chem. Soc.* **2010,** *132*, 12835-12837.

62. Kim, J.; Movassaghi, M. Biogenetically-inspired total synthesis of epidithiodiketopiperazines and related alkaloids. *Acc. Chem. Res.* **2015,** *48* (4), 1159-1171.

63. Belofsky, G. N.; Gloer, J. B.; Wicklow, D. T.; Dowd, P. F. Antiinsectan alkaloids: Shearinines A-C and a new paxilline derivative from the ascostromata of *Eupenicillium shearii*. *Tetrahedron* **1995,** *51* (14), 3959-3968.

64. Cassady, J. M.; Li, G. S.; Spitzner, E. B.; Floss, H. G.; Clemens, J. A. Ergot alkaloids. Ergolines and related compounds as inhibitors of prolactin release. *J. Med. Chem.* **1974,** *17* (3), 300-307.

65. Chen, M.; Shao, C. L.; Fu, X. M.; Xu, R. F.; Zheng, J. J.; Zhao, D. L.; She, Z. G.; Wang, C. Y. Bioactive indole alkaloids and phenyl ether derivatives from a marine-derived *Aspergillus* sp. fungus. *J. Nat. Prod.* **2013,** *76*, 547-553.

66. Genovese, S.; Curini, M.; Epifano, F. Chemistry and biological activity of azoprenylated secondary metabolites. *Phytochemistry* **2009,** *70* (9), 1082-1091.

67. Ruiz-Sanchis, P.; Savina, S. A.; Albericio, F.; Alvarez, M. Structure, bioactivity and synthesis of natural products with hexahydropyrrolo[2,3-b]indole. *Chemistry.* **2011,** *17* (5), 1388-1408.

68. Sunazuka, T.; Hirose, T.; Omura, S. Efficient total synthesis of novel bioactive microbial metabolites. *Acc Chem. Res.* **2008,** *41* (2), 302-314.

69. West, E. G.; McDermott, C.; Chess-Williams, R.; Sellers, D. J. Mirabegron and solifenacin are effective for the management of the increased urinary frequency induced by psychological stress in female mice. *Sci Rep.* **2022,** *12* (1), 12365.

70. Kosilov, K.; Kuzina, I.; Kuznetsov, V.; Barabash, O.; Fedorishcheva, E. Efficacy of a combination of dutasteride, tadalafil, and solifenacin in the treatment of previously unsuccessful patients. *Asian J. Urol.* **2022,** *9* (1), 42-50.

71. Valipour, M.; Irannejad, H.; Emami, S. Papaverine, a promising therapeutic agent for the treatment of COVID-19 patients with underlying cardiovascular diseases (CVDs). *Drug Dev. Res.* **2022,** *83* (6), 1246-1250.

72. Cochrane, R. V.; Vederas, J. C. Highly selective but multifunctional oxygenases in secondary metabolism. *Acc. Chem. Res.* **2014,** *47* (10), 3148-3161.

73. Liu, B.; Chen, N.; Chen, Y. X.; Shen, J. J.; Xu, Y.; Ji, Y. B. A new benzophenone with biological activities purified from Aspergillus fumigatus SWZ01. *Nat. Prod. Res.* **2021,** *35* (24), 5710-5719.

74. Ostry, V.; Toman, J.; Grosse, Y.; Malir, F. Cyclopiazonic acid: 50th anniversary of its discovery. *World Mycotoxin J.* **2018,** *11*, 135-148.

75. Volckaert, G.; Jou, W. M.; Fiers, W. Analysis of 32P-labeled bacteriophage MS2 RNA by a mini-fingerprinting procedure. *Anal. Biochem.* **1976,** *72*, 433-446.

76. Fiers, W.; Contreras, R.; Duerinck, F.; Haegeman, G.; Iserentant, D.; Merregaert, J.; Min, J. W.; Molemans, F.; Raeymaekers, A.; Van den Berghe, A.; Volckaert, G.; Ysebaert, M. Complete nucleotide sequence of bacteriophage MS2 RNA: primary and secondary structure of the replicase gene. *Nature* **1976,** *260* (5551), 500-507.

77. Gross, H.; Stockwell, V. O.; Henkels, M. D.; Nowak-Thompson, B.; Loper, J. E.; Gerwick, W. H. The genomisotopic approach: a systematic method to isolate products of orphan biosynthetic gene clusters. *Chem Biol.* **2007,** *14* (1), 53-63.

78. Medema, M. H.; Cimermancic, P.; Sali, A.; Takano, E.; Fischbach, M. A. A systematic computational analysis of biosynthetic gene cluster evolution: lessons for engineering biosynthesis. *PLoS. Comput. Biol.* **2014,** *10* (12), e1004016.

79. Pfannenstiel, B. T.; Keller, N. P. On top of biosynthetic gene clusters: How epigenetic machinery influences secondary metabolism in fungi. *Biotechnol. Adv.* **2019,** *37* (6), 107345.

80. Chen, H.; Walsh, C. T. Coumarin formation in novobiocin biosynthesis: ß-hydroxylation of the aminoacyl enzyme tyrosyl-S-NovH by a cytochrome P450 NovI. *Chem. Biol.* **2001,** *8* (4), 301-312.

81. Mishra, A. K.; Choi, J.; Choi, S. J.; Baek, K. H. Cyclodipeptides: An overview of their biosynthesis and biological activity. *Molecules* **2017,** *22* (10), E1796.

82. Ding, Y.; Bojja, R. S.; Du, L. C. Fum3p, a 2-ketoglutarate-dependent dioxygenase required for C-5 hydroxylation of fumonisins in *Fusarium verticillioides*. *Appl. Environ. Microbiol.* **2004,** *70* (4), 1931-1934.

83. Ibrahim, R. K.; Bruneau, A.; Bantignies, B. Plant *O*-methyltransferases: molecular analysis, common signature and classification. *Plant Mol. Biol.* **1998,** *36* (1), 1-10.

84. Giessen, T. W.; Marahiel, M. A. The tRNA-dependent biosynthesis of modified cyclic dipeptides. *Int. J. Mol. Sci.* **2014,** *15* (8), 14610-14631.

85. Giessen, T. W.; von Tesmar, A. M.; Marahiel, M. A. A tRNA-dependent two-enzyme pathway for the generation of singly and doubly methylated ditryptophan 2,5-diketopiperazines. *Biochemistry* **2013,** *52* (24), 4274-4283.

86. Liu, J.; Harken, L.; Yang, Y.; Xie, X.; Li, S.-M. Widely distributed bifunctional bacterial cytochrome P450 enzymes catalyze both intramolecular C-C bond formation in *cyclo*-L-Tyr-L-Tyr and its coupling with nucleobases. *Angew. Chem. Int. Ed. Engl.* **2022,** *61* (21), e202200377.

87. Turkez, H.; Cacciatore, I.; Arslan, M. E.; Fornasari, E.; Marinelli, L.; Di, S. A.; Mardinoglu, A. Histidyl-proline diketopiperazine isomers as multipotent anti-Alzheimer drug candidates. *Biomolecules* **2020,** *10* (5), 737.

88. Poullennec, K. G.; Kelly, A. T.; Romo, D. Highly diastereoselective desymmetrizations of cyclo(Pro,Pro): an enantioselective strategy toward phakellstatin and phakellin. *Org. Lett.* **2002,** *4* (16), 2645-2648.

89. Salman, M.; Tariq, A.; Mustafa, G.; Javed, M. R.; Naheed, S.; Qamar, S. A. Cyclo(L-Leucyl-L-Prolyl) from Lactobacillus coryniformis BCH-4 inhibits the proliferation of Aspergillus flavus: an in vitro to in silico approach. *Arch. Microbiol.* **2022,** *204* (5), 267.

90. Bhargava, H. N.; Ritzmann, R. F. Inhibition of neuroleptic-induced dopamine receptor supersensitivity by cyclo (Leu-Gly). *Pharmacol. Biochem. Behav.* **1980,** *13* (5), 633-636.

91. Prasad, C. Bioactive cyclic dipeptides. *Peptides* **1995,** *16* (1), 151-164.

92. Yin, S.; Yu, X.; Wang, Q.; Liu, X. Q.; Li, S.-M. Identification of a brevianamide F reverse prenyltransferase BrePT from *Aspergillus versicolor* with a broad substrate specificity towards tryptophan-containing cyclic dipeptides. *Appl. Microbiol. Biotechnol.* **2013,** *97*, 1649-1660.

93. Bowden, C. R.; Karkanias, C. D.; Bean, A. J. Re-evaluation of histidyl-proline diketopiperazine [cyclo(His-Pro)] effects on food intake in the rat. *Pharmacol. Biochem. Behav.* **1988,** *29* (2), 357-363.

94. McCleland, K.; Milne, P. J.; Lucieto, F. R.; Frost, C.; Brauns, S. C.; Van, D., V; Du, P. J.; Dyason, K. An investigation into the biological activity of the selected histidine-containing diketopiperazines cyclo(His-Phe) and cyclo(His-Tyr). *J. Pharm. Pharmacol.* **2004,** *56* (9), 1143-1153.

95. Borgman, P.; Lopez, R. D.; Lane, A. L. The expanding spectrum of diketopiperazine natural product biosynthetic pathways containing cyclodipeptide synthases. *Org. Biomol. Chem.* **2019,** *17*, 2305-2314.

96. Honda-Uezono, A.; Kaida, A.; Michi, Y.; Harada, K.; Hayashi, Y.; Hayashi, Y.; Miura, M. Unusual expression of red fluorescence at M phase induced by anti-microtubule agents in HeLa cells expressing the fluorescent ubiquitination-based cell cycle indicator (Fucci). *Biochem. Biophys. Res. Commun.* **2012,** *428* (2), 224-229.

97. Balibar, C. J.; Walsh, C. T. GliP, a multimodular nonribosomal peptide synthetase in *Aspergillus fumigatus*, makes the diketopiperazine scaffold of gliotoxin. *Biochemistry* **2006,** *45* (50), 15029-15038.

98. Igarashi, Y.; Yabuta, Y.; Sekine, A.; Fujii, K.; Harada, K.; Oikawa, T.; Sato, M.; Furumai, T.; Oki, T. Directed biosynthesis of fluorinated pseurotin A, synerazol and gliotoxin. *J. Antibiot. (Tokyo)* **2004,** *57* (11), 748-754.

99. Patteson, J. B.; Cai, W.; Johnson, R. A.; Santa Maria, K. C.; Li, B. Identification of the biosynthetic pathway for the antibiotic bicyclomycin. *Biochemistry* **2017,** *57* (1), 61-65.

100. James, E. D.; Knuckley, B.; Alqahtani, N.; Porwal, S.; Ban, J.; Karty, J. A.; Viswanathan, R.; Lane, A. L. Two distinct cyclodipeptide synthases from a marine actinomycete catalyze biosynthesis of the same diketopiperazine natural product. *ACS Synth. Biol.* **2016,** *5* (7), 547-553.

101. Raju, R.; Piggott, A. M.; Huang, X. C.; Capon, R. J. Nocardioazines: a novel bridged diketopiperazine scaffold from a marine-derived bacterium inhibits p-glycoprotein. *Org. Lett.* **2011,** *13* (10), 2770-2773.

102. Liu, J.; Xie, X.; Li, S.-M. Guanitrypmycin biosynthetic pathways imply cytochrome P450-mediated regio- and stereospecific guaninyl transfer reactions. *Angew. Chem. Int. Ed. Engl.* **2019,** *58*, 11534-11540.

103. Song, F.; Liu, X.; Guo, H.; Ren, B.; Chen, C.; Piggott, A. M.; Yu, K.; Gao, H.; Wang, Q.; Liu, M.; Liu, X.; Dai, H.; Zhang, L.; Capon, R. J. Brevianamides with antitubercular potential from a marine-derived isolate of *Aspergillus versicolor*. *Org. Lett.* **2012,** *14* (18), 4770-4773.

104. Cai, R.; Jiang, H.; Xiao, Z.; Cao, W.; Yan, T.; Liu, Z.; Lin, S.; Long, Y.; She, Z. (-)-and (+)-Asperginulin A, a pair of indole diketopiperazine alkaloid dimers with a 6/5/4/5/6 pentacyclic skeleton from the mangrove endophytic fungus *Aspergillus* sp. SK-28. *Org. Lett.* **2019,** *21* (23), 9633-9636.

105. Geng, C. A.; Huang, X. Y.; Ma, Y. B.; Hou, B.; Li, T. Z.; Zhang, X. M.; Chen, J. J. (+/-)-Uncarilins A and B, dimeric isoechinulin-type alkaloids from *Uncaria rhynchophylla*. *J. Nat. Prod.* **2017,** *80* (4), 959-964.

106. Croitoru, A.; Babin, M.; Myllykallio, H.; Gondry, M.; Aleksandrov, A. Cyclodipeptide synthases of the NYH subfamily recognize tRNA using an α-helix enriched with positive residues. *Biochemistry* **2021,** *60* (1), 64-76.

107. Yang, K.; Li, S.-M.; Liu, X.; Fan, A. Reinvestigation of the substrate specificity of a reverse prenyltransferase NotF from *Aspergillus* sp. MF297-2. *Arch. Microbiol.* **2020,** *202*, 1419-1424.

108. Finking, R.; Marahiel, M. A. Biosynthesis of nonribosomal peptides. *Annu. Rev. Microbiol.* **2004,** *58*, 453-488.

109. Shah, G. R.; Wesener, S. R.; Cheng, Y. Q. Engineered production of ryprostatins in *E. coli* through reconstitution of a partial ftm biosynthetic gene cluster from *Aspergillus* sp. *Jacobs. J. Biotechnol. Bioeng.* **2014,** *2* (1), 009.

110. Bellezza, I.; Peirce, M. J.; Minelli, A. Cyclic dipeptides: from bugs to brain. *Trends Mol. Med.* **2014,** *20* (10), 551-558.

111. Jacques, I. B.; Moutiez, M.; Witwinowski, J.; Darbon, E.; Martel, C.; Seguin, J.; Favry, E.; Thai, R.; Lecoq, A.; Dubois, S.; Pernodet, J. L.; Gondry, M.; Belin, P. Analysis of 51 cyclodipeptide synthases reveals the basis for substrate specificity. *Nat. Chem Biol.* **2015,** *11* (9), 721-727.

112. Canu, N.; Moutiez, M.; Belin, P.; Gondry, M. Cyclodipeptide synthases: a promising biotechnological tool for the synthesis of diverse 2,5-diketopiperazines. *Nat. Prod. Rep.* **2020,** *37*, 312-321.

113. Bonitz, T.; Alva, V.; Saleh, O.; Lupas, A. N.; Heide, L. Evolutionary relationships of microbial aromatic prenyltransferases. *PLoS One* **2011,** *6* (11), e27336.

114. Gunera, J.; Kindinger, F.; Li, S.-M.; Kolb, P. PrenDB: A substrate prediction database to enable biocatalytic use of prenyltransferases. *J. Biol. Chem.* **2017**.

115. Liang, P. H.; Ko, T. P.; Wang, A. H. Structure, mechanism and function of prenyltransferases. *Eur. J. Biochem.* **2002,** *269* (14), 3339-3354.

116. Awakawa, T.; Mori, T.; Nakashima, Y.; Zhai, R.; Wong, C. P.; Hillwig, M. L.; Liu, X.; Abe, I. Molecular insight into the Mg^{2+}-dependent allosteric control of indole prenylation by aromatic prenyltransferase AmbP1. *Angew. Chem Int. Ed Engl.* **2018,** *57*, 6810-6813.

117. White, M. D.; Payne, K. A.; Fisher, K.; Marshall, S. A.; Parker, D.; Rattray, N. J.; Trivedi, D. K.; Goodacre, R.; Rigby, S. E.; Scrutton, N. S.; Hay, S.; Leys, D. UbiX is a flavin prenyltransferase required for bacterial ubiquinone biosynthesis. *Nature* **2015,** *522*, 502-506.

118. Fiesel, T.; Gaid, M.; Muller, A.; Bartels, J.; El-Awaad, I.; Beuerle, T.; Ernst, L.; Behrends, S.; Beerhues, L. Molecular cloning and characterization of a xanthone prenyltransferase from *Hypericum calycinum* cell cultures. *Molecules.* **2015,** *20* (9), 15616-15630.

119. Botta, B.; Monache, G. D.; Menendez, P.; Boffi, A. Novel prenyltransferase enzymes as a tool for flavonoid prenylation. *Trends Pharmacol. Sci.* **2005,** *26* (12), 606-608.

120. Haug-Schifferdecker, E.; Arican, D.; Brueckner, R.; Heide, L. A new group of aromatic prenyltransferases in fungi, catalyzing a 2,7-dihydroxynaphthalene dimethylallyltransferase reaction. *J. Biol. Chem.* **2010,** *285*, 16487-16494.

121. Ostertag, E.; Zheng, L.; Broger, K.; Stehle, T.; Li, S.-M.; Zocher, G. Reprogramming substrate and catalytic promiscuity of tryptophan prenyltransferases. *J. Mol. Biol.* **2021,** *433* (2), 166726.

122. Zou, H.; Zheng, X.; Li, S.-M. Substrate promiscuity of the cyclic dipeptide prenyltransferases from *Aspergillus fumigatus*. *J. Nat. Prod.* **2009,** *72*, 44-52.

123. Yu, X.; Xie, X.; Li, S.-M. Substrate promiscuity of secondary metabolite enzymes: prenylation of hydroxynaphthalenes by fungal indole prenyltransferases. *Appl. Microbiol. Biotechnol.* **2011,** *92* (4), 737-748.

124. Chen, R.; Gao, B.; Liu, X.; Ruan, F.; Zhang, Y.; Lou, J.; Feng, K.; Wunsch, C.; Li, S.-M.; Dai, J.; Sun, F. Molecular insights into the enzyme promiscuity of an aromatic prenyltransferase. *Nat. Chem. Biol.* **2017,** *13*, 226-234.

125. Couillaud, J.; Rico, J.; Rubini, A.; Hamrouni, T.; Courvoisier-Dezord, E.; Petit, J. L.; Mariage, A.; Darii, E.; Duquesne, K.; de Berardinis, V.; Iacazio, G. Simplified in vitro and in vivo bioaccess to prenylated compounds. *ACS Omega* **2019,** *4* (4), 7838-7849.

126. Bräuer, L.; Brandt, W.; Schulze, D.; Zakharova, S.; Wessjohann, L. A structural model of the membrane-bound aromatic prenyltransferase UbiA from *E. coli. Chembiochem* **2008,** *9* (6), 982-992.

127. Bayse, C. A.; Merz, K. M. Mechanistic insights into Mg^{2+}-independent prenylation by CloQ from classical molecular mechanics and hybrid quantum mechanics/molecular mechanics molecular dynamics simulations. *Biochemistry* **2014,** *53* (30), 5034-5041.

128. Yu, X.; Li, S.-M. Prenyltransferases of the dimethylallyltryptophan synthase superfamily. *Methods Enzymol.* **2012,** *516*, 259-278.

129. Yang, Y.; Ke, N.; Liu, S.; Li, W. Methods for structural and functional analyses of intramembrane prenyltransferases in the UbiA superfamily. *Methods Enzymol.* **2017,** *584*, 309-347.

130. Li, W. Bringing bioactive compounds into membranes: The UbiA superfamily of intramembrane aromatic prenyltransferases. *Trends Biochem. Sci.* **2016,** *41* (4), 356-370.

131. Nakagawa, K.; Hirota, Y.; Sawada, N.; Yuge, N.; Watanabe, M.; Uchino, Y.; Okuda, N.; Shimomura, Y.; Suhara, Y.; Okano, T. Identification of UBIAD1 as a novel human menaquinone-4 biosynthetic enzyme. *Nature* **2010,** *468*, 117-121.

132. Araya-Cloutier, C.; Martens, B.; Schaftenaar, G.; Leipoldt, F.; Gruppen, H.; Vincken, J. P. Structural basis for non-genuine phenolic acceptor substrate specificity of *Streptomyces roseochromogenes* prenyltransferase CloQ from the ABBA/PT-barrel superfamily. *PLoS. One.* **2017,** *12* (3), e0174665.

133. Johnson, B. P.; Scull, E. M.; Dimas, D. A.; Bavineni, T.; Bandari, C.; Batchev, A. L.; Gardner, E. D.; Nimmo, S. L.; Singh, S. Acceptor substrate determines donor specificity of an aromatic prenyltransferase: expanding the biocatalytic potential of NphB. *Appl. Microbiol. Biotechnol.* **2020,** *104*, 4383-4395.

134. Yang, Y.; Miao, Y.; Wang, B.; Cui, G.; Merz, K. M., Jr. Catalytic mechanism of aromatic prenylation by NphB. *Biochemistry* **2012,** *51* (12), 2606-2618.

135. Liebhold, M.; Xie, X.; Li, S.-M. Expansion of enzymatic Friedel-Crafts alkylation on indoles: Acceptance of unnatural beta-unsaturated allyl diphospates by dimethylallyl-tryptophan synthases. *Org. Lett.* **2012,** *14* (18), 4884-4885.

136. Li, S.-M. Applications of dimethylallyltryptophan synthases and other indole prenyltransferases for structural modification of natural products. *Appl. Microbiol. Biotechnol.* **2009,** *84* (4), 631-639.

137. Li, S.-M. Evolution of aromatic prenyltransferases in the biosynthesis of indole derivatives. *Phytochemistry* **2009,** *70,* 1746-1757.

138. Liang, P. H. Reaction kinetics, catalytic mechanisms, conformational changes, and inhibitor design for prenyltransferases. *Biochemistry* **2009,** *48*, 6562-6570.

139. Luk, L. Y. P.; Tanner, M. E. Mechanism of dimethylallyltryptophan synthase: evidence for a dimethylallyl cation intermediate in an aromatic prenyltransferase reaction. *J. Am. Chem. Soc.* **2009,** *131* (39), 13932-13933.

140. Tsai, H. F.; Wang, H.; Gebler, J. C.; Poulter, C. D.; Schardl, C. L. The *Claviceps purpurea* gene encoding dimethylallyltryptophan synthase, the committed step for ergot alkaloid biosynthesis. *Biochem. Biophys. Res. Commun.* **1995,** *216* (1), 119-125.

141. Yu, X.; Liu, Y.; Xie, X.; Zheng, X.-D; Li, S.-M. Biochemical characterization of indole prenyltransferases: Filling the last gap of prenylation positions by a 5-dimethylallyltryptophan synthase from *Aspergillus clavatus*. *J. Biol. Chem.* **2012,** *287* (2), 1371-1380.

142. Mai, P.; Zocher, G.; Ludwig, L.; Stehle, T.; Li, S.-M. Actions of tryptophan prenyltransferases toward fumiquinazolines and their potential application for the generation of prenylated derivatives by combining chemical and chemoenzymatic syntheses. *Adv. Synth. Catal.* **2016,** *358*, 1639-1653.

143. Takahashi, S.; Takagi, H.; Toyoda, A.; Uramoto, M.; Nogawa, T.; Ueki, M.; Sakaki, Y.; Osada, H. Biochemical characterization of a novel indole prenyltransferase from *Streptomyces* sp. SN-593. *J. Bacteriol.* **2010,** *192*, 2839-2851.

144. Kremer, A.; Westrich, L.; Li, S.-M. A 7-dimethylallyltryptophan synthase from *Aspergillus fumigatus*: overproduction, purification and biochemical characterization. *Microbiology* **2007,** *153* (Pt 10), 3409-3416.

145. Grundmann, A.; Li, S.-M. Overproduction, purification and characterization of FtmPT1, a brevianamide F prenyltransferase from *Aspergillus fumigatus*. *Microbiology* **2005,** *151* (Pt 7), 2199-2207.

146. Zou, H.-X.; Xie, X.-L.; Linne, U.; Zheng, X.-D.; Li, S.-M. Simultaneous *C7-* and *N1-*prenylation of cyclo-L-Trp-L-Trp catalyzed by a prenyltransferase from *Aspergillus oryzae. Org. Biomol. Chem.* **2010,** *8* (13), 3037-3044.

147. Mundt, K.; Li, S.-M. CdpC2PT, a reverse prenyltransferase from *Neosartorya fischeri* with distinct substrate preference from known *C2*-prenyltransferases. *Microbiology* **2013,** *159*, 2169-2179.

148. Liu, J.; Yang, Y.; Harken, L.; Li, S.-M. Elucidation of the streptoazine biosynthetic pathway in *Streptomyces aurantiacus* reveals the presence of a promiscuous prenyltransferase/cyclase. *J. Nat. Prod.* **2021,** *84*, 3100-3109.

149. Pockrandt, D.; Sack, C.; Kosiol, T.; Li, S.-M. A promiscuous prenyltransferase from *Aspergillus oryzae* catalyses *C*-prenylations of hydroxynaphthalenes in the presence of different prenyl donors. *Appl. Microbiol. Biotechnol.* **2014,** *98*, 4987-4994.

150. Xu, Y.; Li, D.; Tan, G.; Zhang, Y.; Li, Z.; Xu, K.; Li, S.-M.; Yu, X. A single amino acid switch alters the prenyl donor specificity of a fungal aromatic prenyltransferase toward biflavonoids. *Org. Lett.* **2021,** *23*, 497-502.

151. Steffan, N.; Li, S.-M. Increasing structure diversity of prenylated diketopiperazine derivatives by using a 4-dimethylallyltryptophan synthase. *Arch. Microbiol.* **2009,** *191* (5), 461-466.

152. Wohlgemuth, V.; Kindinger, F.; Li, S.-M. Convenient synthetic approach for tri- and tetraprenylated cyclodipeptides by consecutive enzymatic prenylations. *Appl. Microbiol. Biotechnol.* **2018,** *102* (6), 2671-2681.

153. He, B. B.; Bu, X. L.; Zhou, T.; Li, S.-M.; Xu, M. J.; Xu, J. Combinatory biosynthesis of prenylated 4-hydroxybenzoate derivatives by overexpression of the substrate-promiscuous prenyltransferase XimB in engineered *E. coli*. *ACS Synth. Biol.* **2018,** *7*, 2094-2104.

154. Malit, J. J. L.; Wu, C.; Tian, X.; Liu, W.; Huang, D.; Sung, H. H.; Liu, L. L.; Williams, I. D.; Qian, P. Y. Griseocazines: Neuroprotective multiprenylated cyclodipeptides identified through targeted genome mining. *Org. Lett.* **2022,** *24* (16), 2967-2972.

155. Kato, H.; Yoshida, T.; Tokue, T.; Nojiri, Y.; Hirota, H.; Ohta, T.; Williams, R. M.; Tsukamoto, S. Notoamides A-D: prenylated indole alkaloids isolated from a marine-derived fungus, *Aspergillus* sp. *Angew. Chem Int. Ed Engl.* **2007,** *46* (13), 2254-2256.

156. Steffan, N.; Grundmann, A.; Afiyatullov, A.; Ruan, H.; Li, S.-M. FtmOx1, a non heme Fe(II) and alpha-ketoglutarate-dependent dioxygenase, catalyses the endoperoxide formation of verruculogen in *Aspergillus fumigatus*. *Org. Biomol. Chem.* **2009,** *7* (19), 4082-4087.

157. Wohlgemuth, V.; Kindinger, F.; Xie, X.; Wang, B. G.; Li, S.-M. Two prenyltransferases govern a consecutive prenylation cascade in the biosynthesis of echinulin and neoechinulin. *Org Lett.* **2017,** *19* (21), 5928-5931.

158. Cox, R. J. Polyketides, proteins and genes in fungi: programmed nano-machines begin to reveal their secrets. *Org. Biomol. Chem.* **2007,** *5* (13), 2010-2026.

159. Bergmann, S.; Schumann, J.; Scherlach, K.; Lange, C.; Brakhage, A. A.; Hertweck, C. Genomics-driven discovery of PKS-NRPS hybrid metabolites from *Aspergillus nidulans*. *Nat. Chem Biol* **2007,** *3* (4), 213-217.

160. Boettger, D.; Hertweck, C. Molecular diversity sculpted by fungal PKS-NRPS hybrids. *Chembiochem.* **2013,** *14* (1), 28-42.

161. Sigrist, R.; Luhavaya, H.; McKinnie, S. M. K.; Ferreira da, S. A.; Jurberg, I. D.; Moore, B. S.; Gonzaga de, O. L. Nonlinear biosynthetic assembly of alpiniamide by a hybrid cis/trans-AT PKS-NRPS. *ACS Chem. Biol.* **2020,** *15*, 1067-1077.

162. Yu, F.; Zaleta-Rivera, K.; Z, X. C.; Huffman, J.; Millet, J. C.; Harris, S. D.; Yuen, G.; Li, X. C.; Du, L. C. Structure and biosynthesis of heat-stable antifungal factor (HSAF), a broad-spectrum antimycotic with a novel mode of action. *Antimicrob. Agents Chemother.* **2007,** *2006/10/30* (1), 64-72.

163. Burdock, G. A.; Flamm, W. G. Safety assessment of the mycotoxin cyclopiazonic acid. *Int. J. Toxicol.* **2000,** *19* (3), 195-218.

164. Song, Z.; Cox, R. J.; Lazarus, C. M.; Simpson TJ, T. J. Fusarin C biosynthesis in Fusarium moniliforme and *Fusarium venenatum. Chembiochem.* **2004,** *5* (9), 1196-1203.

165. Xu, W.; Cai, X.; Jung, M. E.; Tang, Y. Analysis of intact and dissected fungal polyketide synthase-nonribosomal peptide synthetase in vitro and in *Saccharomyces cerevisiae. J. Am. Chem. Soc.* **2010,** *132*, 13604-13607.

166. Amnuaykanjanasin, A.; Punya, J.; Paungmoung, P.; Rungrod, A.; Tachaleat, A.; Pongpattanakitshote, S.; Cheevadhanarak, S.; Tanticharoen, M. Diversity of type I polyketide synthase genes in the wood-decay fungus *Xylaria* sp. BCC 1067. *FEMS Microbiol. Lett.* **2005,** *251* (1), 125-136.

167. Theobald, S.; Vesth, T. C.; Andersen, M. R. Genus level analysis of PKS-NRPS and NRPS-PKS hybrids reveals their origin in Aspergilli. *BMC Genom.* **2019,** *20* (1), 847.

168. Yun, C. S.; Motoyama, T.; Osada, H. Biosynthesis of the mycotoxin tenuazonic acid by a fungal NRPS-PKS hybrid enzyme. *Nat. Commun.* **2015,** *6*, 8758.

169. Luo, F. F.; Hong, S.; Chen, B.; Yin, Y.; Tang, G.; Hu, F. L.; Zhang, H. Z.; Wang, C. S. Unveiling of swainsonine biosynthesis via a multibranched pathway in fungi. *ACS Chem. Biol.* **2020,** *15* (9), 2476-2484.

170. Cook, D.; Donzelli, B. G. G.; Creamer, R.; Baucom, D. L.; Gardner, D. R.; Pan, J.; Moore, N.; Krasnoff, S. B.; Jaromczyk, J. W.; Schardl, C. L. Swainsonine biosynthesis genes in diverse symbiotic and pathogenic fungi. *G3. (Bethesda.)* **2017,** *7* (6), 1791-1797.

171. Oba, Y.; Suzuki, Y.; Martins, G. N. R.; Carvalho, R. P.; Pereira, T. A.; Waldenmaier, H. E.; Kanie, S.; Naito, M.; Oliveira, A. G.; Dorr, F. A.; Pinto, E.; Yampolsky, I. V.; Stevani, C. V. Identification of hispidin as a bioluminescent active compound and its recycling biosynthesis in the luminous fungal fruiting body. *Photochem. Photobiol. Sci* **2017,** *16* (9), 1435-1440.

172. Hai, Y.; Huang, A.; Tang, Y. Biosynthesis of amino acid derived α-pyrones by an NRPS-NRPKS hybrid megasynthetase in fungi. *J. Nat. Prod.* **2020,** *83*, 593-600.

173. Chen, L.; Tang, J. W.; Liu, Y. Y.; Matsuda, Y. Aspcandine: A pyrrolobenzazepine alkaloid synthesized by a fungal nonribosomal peptide synthetase-polyketide synthase hybrid. *Org. Lett.* **2022,** *24* (26), 4816-4819.

174. Cooney, J. M.; Vanneste, J. L.; Lauren, D. R.; Hill, R. A. Quantitative determination of the antifungal compound 6-pentyl-alpha-pyrone (6PAP) using a simple plate bioassay. *Lett. Appl. Microbiol.* **1997,** *24* (1), 47-50.

175. Zhao, Q.; Wang, C. X.; Yu, Y.; Wang, G. Q.; Zheng, Q. C.; Chen, G. D.; Lian, Y. Y.; Lin, F.; Guo, L. D.; Gao, H. Nodulisporipyrones A-D, new bioactive alpha-pyrone derivatives from *Nodulisporium* sp. *J. Asian Nat. Prod. Res.* **2015,** *17* (5), 567-575.

176. Bumpus, S. B.; Evans, B. S.; Thomas, P. M.; Ntai, I.; Kelleher, N. L. A proteomics approach to discovering natural products and their biosynthetic pathways. *Nat. Biotechnol.* **2009,** *27* (10), 951-956.

177. Yun, C. S.; Nishimoto, K.; Motoyama, T.; Shimizu, T.; Hino, T.; Dohmae, N.; Nagano, S.; Osada, H. Unique features of the ketosynthase domain in a non-ribosomal peptide synthetase-polyketide synthase hybrid enzyme, tenuazonic acid synthetase 1. *J. Biol. Chem.* **2020,** *295* (33), 11602-11612.

178. Nambudiri, A. M.; Vance, C. P.; Towers, G. H. Effect of light on enzymes of phenylpropanoid metabolism and hispidin biosynthesis in Polyporus hispidus. *Biochem. J.* **1973,** *134* (4), 891-897.

179. Maiya, S.; Grundmann, A.; Li, X.; Li, S.-M.; Turner, G. Identification of a hybrid PKS/NRPS required for pseurotin A biosynthesis in the human pathogen *Aspergillus fumigatus*. *Chembiochem* **2007,** *8* (14), 1736-1743.

180. Simunovic, V.; Zapp, J.; Rachid, S.; Krug, D.; Meiser, P.; Müller, R. Myxovirescin A biosynthesis is directed by hybrid polyketide synthases/nonribosomal peptide synthetase, 3-hydroxy-3-methylglutaryl-CoA synthases, and trans-acting acyltransferases. *Chembiochem.* **2006,** *7* (8), 1206-1220.

181. Kirk, P. M.; Cannon, P. F.; Minter, D. W.; Stalpers, J. A. *Dictionary of fungi;* 10th ed.; CABI: Wallinford, 2008.

182. Xiao, Y.; Li, H. X.; Li, C.; Wang, J. X.; Li, J.; Wang, M. H.; Ye, Y. H. Antifungal screening of endophytic fungi from *Ginkgo biloba* for discovery of potent anti-phytopathogenic fungicides. *FEMS Microbiol. Lett.* **2013,** *339* (2), 130-136.

183. Gauthier, G. M.; Keller, N. P. Crossover fungal pathogens: The biology and pathogenesis of fungi capable of crossing kingdoms to infect plants and humans. *Fungal Genet. Biol.* **2013,** *61*, 146-157.

184. Matuschek, M. Molecular biological and biochemical investigations on the biosynthesis of mycotoxins from Ascomycetes. *Dissertation Universität Marburg* **2012**.

185. Chung, D.; Kim, H.; Choi, H. S. Fungi in salterns. *J. Microbiol.* **2019,** *57* (9), 717-724.

186. Kawai, K.; Nozawa, K.; Yamaguchi, T.; Nakajima, S.; Udagawa, S. Two chemotypes of *Penicillium crustosum* based on the analysis of indolic components. *Mycotoxins* **1992,** *36*, 19-24.

187. Kindinger, F.; Nies, J.; Becker, A.; Zhu, T.; Li, S.-M. Genomic locus of a *Penicillium crustosum* pigment as an integration site for secondary metabolite gene expression. *ACS Chem. Biol.* **2019,** *14* (6), 1227-1234.

188. Richard, J. L.; Bacchetti, P.; Arp, L. H. Moldy walnut toxicosis in a dog, caused by the mycotoxin, penitrem A. *Mycopathologia* **1981,** *76* (1), 55-58.

189. Liu, C.; Tagami, K.; Minami, A.; Matsumoto, T.; Frisvad, J. C.; Suzuki, H.; Ishikawa, J.; Gomi, K.; Oikawa, H. Reconstitution of biosynthetic machinery for the synthesis of the highly elaborated indole diterpene penitrem. *Angew. Chem Int. Ed Engl.* **2015,** *54* (19), 5748-5752.

190. Stierle, S. A.; Li, S.-M. Biosynthesis of xylariolide D in *Penicillium crustosum* implies a chain branching reaction catalyzed by a highly reducing polyketide synthase. *J. Fungi* **2022,** *8*, 493.

191. Xiang, P.; Li, S.-M. Formation of 3-orsellinoxypropanoic acid in *Penicillum crustosum* is catalyzed by a bifunctional nonreducing polyketide synthase. *Org. Lett.* **2022,** *24* (1), 462-466.

192. Sonjak, S.; Frisvad, J. C.; Gunde-Cimerman, N. Comparison of secondary metabolite production by *Penicillium crustosum* strains, isolated from Arctic and other various ecological niches. *FEMS Microbiol. Ecol.* **2005,** *53* (1), 51-60.

193. Finoli, C.; Vecchio, A.; Galli, A.; Dragoni, I. Roquefortine C occurrence in blue cheese. *J. Food Prot.* **2001,** *64* (2), 246-251.

194. Fan, J.; Liao, G.; Ludwig-Radtke, L.; Yin, W.-B.; Li, S.-M. Formation of terrestric acid in *Penicillium crustosum* requires redox-assisted decarboxylation and stereoisomerization. *Org. Lett.* **2020,** *22* (1), 88-92.

195. Fan, J.; Liao, G.; Kindinger, F.; Ludwig-Radtke, L.; Yin, W.-B.; Li, S.-M. Peniphenone and penilactone formation in *Penicillium crustosum via* 1,4-Michael additions of *ortho*-quinone methide from hydroxyclavatol to γ-butyrolactones from crustosic acid. *J. Am. Chem. Soc.* **2019,** *141*, 4225-4229.

196. Tilburn, J.; Scazzocchio, C.; Taylor, G. G.; Zabicky-Zissman, J. H.; Lockington, R. A.; Davies, R. W. Transformation by integration in *Aspergillus nidulans*. *Gene* **1983,** *26* (2-3), 205-221.

197. Galagan, J. E.; Calvo, S. E.; Cuomo, C.; Ma, L. J.; Wortman, J. R.; Batzoglou, S.; Lee, S. I.; Basturkmen, M.; Spevak, C. C.; Clutterbuck, J.; Kapitonov, V.; Jurka, J.; Scazzocchio, C.; Farman, M.; Butler, J.; Purcell, S.; Harris, S.; Braus, G. H.; Draht, O.; Busch, S.; d'Enfert, C.; Bouchier, C.; Goldman, G. H.; Bell-Pedersen, D.; Griffiths-Jones, S.; Doonan, J. H.; Yu, J.; Vienken, K.; Pain, A.; Freitag, M.; Selker, E. U.; Archer, D. B.; Penalva, M. A.; Oakley, B. R.; Momany, M.; Tanaka, T.; Kumagai, T.; Asai, K.; Machida, M.; Nierman, W. C.; Denning, D. W.; Caddick, M.; Hynes, M.; Paoletti, M.; Fischer, R.; Miller, B.; Dyer, P.; Sachs, M. S.; Osmani, S. A.; Birren, B. W. Sequencing of *Aspergillus nidulans* and comparative analysis with *A. fumigatus* and *A. oryzae*. *Nature* **2005,** *438* (7071), 1105-1115.

198. Nierman, W. C.; May, G.; Kim, H. S.; Anderson, M. J.; Chen, D.; Denning, D. W. What the *Aspergillus* genomes have told us. *Med. Mycol.* **2005,** *43 Suppl 1*, S3-S5.

199. van Dijk, J. W.; Wang, C. C. Heterologous expression of fungal secondary metabolite pathways in the *Aspergillus nidulans* host system. *Methods Enzymol.* **2016,** *575*, 127-142.

200. Brakhage, A. A.; Andrianopoulos, A.; Kato, M.; Steidl, S.; Davis, M. A.; Tsukagoshi, N.; Hynes, M. J. HAP-Like CCAAT-binding complexes in filamentous fungi: implications for biotechnology. *Fungal Genet. Biol* **1999,** *27* (2-3), 243-252.

201. Niu, K.; Wu, X. P.; Fu, Q.; Lang, K. P.; Zou, S. P.; Hu, Z. C.; Liu, Z. Q.; Zheng, Y. G. Effects of lipids and surfactants on the fermentation production of echinocandin B by Aspergillus nidulans. *J. Appl. Microbiol.* **2021,** *131* (6), 2849-2860.

202. Hof, H.; Dietz, A. Antifungal activity of anidulafungin, a product of Aspergillus nidulans, against Aspergillus nidulans. *Int. J. Antimicrob Agents* **2009,** *33* (3), 285-286.

203. Chiang, Y. M.; Ahuja, M.; Oakley, C. E.; Entwistle, R.; Asokan, A.; Zutz, C.; Wang, C. C.; Oakley, B. R. Development of genetic dereplication strains in *Aspergillus nidulans* results in the discovery of aspercryptin. *Angew. Chem. Int. Ed. Engl.* **2016,** *55* (5), 1662-1665.

204. Nielsen, M. T.; Nielsen, J. B.; Anyaogu, D. C.; Holm, D. K.; Nielsen, K. F.; Larsen, T. O.; Mortensen, U. H. Heterologous reconstitution of the intact geodin gene cluster in Aspergillus nidulans through a simple and versatile PCR based approach. *PLoS One* **2013,** *8* (8), e72871.

205. Chiang, Y. M.; Szewczyk, E.; Davidson, A. D.; Keller, N.; Oakley, B. R.; Wang, C. C. A gene cluster containing two fungal polyketide synthases encodes the biosynthetic pathway for a polyketide, asperfuranone, in *Aspergillus nidulans*. *J. Am. Chem Soc.* **2009,** *131* (8), 2965-2970.

206. Wiemann, P.; Soukup, A. A.; Folz, J. S.; Wang, P. M.; Noack, A.; Keller, N. P. CoIN: co-inducible nitrate expression system for secondary metabolites in *Aspergillus nidulans*. *Fungal Biol. Biotechnol.* **2018,** *5*, 6.

207. Yin, W. B.; Chooi, Y. H.; Smith, A. R.; Cacho, R. A.; Hu, Y.; White, T. C.; Tang, Y. Discovery of cryptic polyketide metabolites from dermatophytes using heterologous expression in *Aspergillus nidulans*. *ACS Synth. Biol.* **2013,** *2* (11), 629-634.

208. Cantwell, C. A.; Beckmann, R. J.; Dotzlaf, J. E.; Fisher, D. L.; Skatrud, P. L.; Yeh, W. K.; Queener, S. W. Cloning and expression of a hybrid Streptomyces clavuligerus cefE gene in Penicillium chrysogenum. *Curr Genet.* **1990,** *17* (3), 213-221.

209. Okorafor, I. C.; Chen, M.; Tang, Y. High-titer production of olivetolic acid and analogs in engineered fungal host using a nonplant biosynthetic pathway. *ACS Synth. Biol.* **2021,** *10* (9), 2158-2166.

210. Hoefgen, S.; Lin, J.; Fricke, J.; Stroe, M. C.; Mattern, D. J.; Kufs, J. E.; Hortschansky, P.; Brakhage, A. A.; Hoffmeister, D.; Valiante, V. Facile assembly and fluorescence-

based screening method for heterologous expression of biosynthetic pathways in fungi. *Metab Eng* **2018,** *48*, 44-51.

211. Newman, D. J.; Cragg, G. M. Natural products as sources of new drugs over the 30 years from 1981 to 2010. *J. Nat. Prod.* **2012,** *75* (3), 311-335.

212. Yan, Y.; Liu, Q.; Zang, X.; Yuan, S.; Bat-Erdene, U.; Nguyen, C.; Gan, J.; Zhou, J.; Jacobsen, S. E.; Tang, Y. Resistance-gene-directed discovery of a natural-product herbicide with a new mode of action. *Nature* **2018**.

213. Gqaleni, N.; Smith, J. E.; Lacey, J.; Gettinby, G. Production of the mycotoxin cyclopiazonic acid by *Penicillium commune* on solid agar media: Effects of water activity, temperature, and incubation time. *J. Food Protection* **1996,** *59* (8), 864-868.

214. Nielsen, P. V.; Beuchat, L. R.; Frisvad, J. C. Growth of and fumitremorgin production by *Neosartorya fischeri* as affected by temperature, light, and water activity. *Appl. Environ. Microbiol.* **1988,** *54* (6), 1504-1510.

215. Arora, D.; Gupta, P.; Jaglan, S.; Roullier, C.; Grovel, O.; Bertrand, S. Expanding the chemical diversity through microorganisms co-culture: Current status and outlook. *Biotechnol. Adv.* **2020,** *40*, 107521.

216. Halder, M.; Sarkar, S.; Jha, S. Elicitation: a biotechnological tool for enhanced production of secondary metabolites in hairy root cultures. *Eng. Life Sci.* **2019,** *19* (12), 880-895.

217. Ochi, K. Insights into microbial cryptic gene activation and strain improvement: principle, application and technical aspects. *J. Antibiot.* **2017,** *70* (1), 25-40.

218. Ren, H.; Wang, B.; Zhao, H. Breaking the silence: new strategies for discovering novel natural products. *Curr. Opin. Biotechnol.* **2017,** *48*, 21-27.

219. Zazopoulos, E.; Huang, K.; Staffa, A.; Liu, W.; Bachmann, B. O.; Nonaka, K.; Ahlert, J.; Thorson, J. S.; Shen, B.; Farnet, C. M. A genomics-guided approach for discovering and expressing cryptic metabolic pathways. *Nat. Biotechnol.* **2003,** *21* (2), 187-190.

220. Giessen, T. W.; Marahiel, M. A. Ribosome-independent biosynthesis of biologically active peptides: Application of synthetic biology to generate structural diversity. *FEBS Lett.* **2012,** *586* (15), 2065-2075.

221. Jamieson, C. S.; Misa, J.; Tang, Y.; Billingsley, J. M. Biosynthesis and synthetic biology of psychoactive natural products. *Chem Soc. Rev.* **2021,** *50* (12), 6950-7008.

222. Ziemert, N.; Alanjary, M.; Weber, T. The evolution of genome mining in microbes - a review. *Nat. Prod. Rep.* **2016,** *33* (8), 988-1005.

223. Blin, K.; Shaw, S.; Kloosterman, A. M.; Charlop-Powers, Z.; Van Wezel, G. P.; Medema, M. H.; Weber, T. antiSMASH 6.0: improving cluster detection and comparison capabilities. *Nucleic Acids Res.* **2021,** *49*, W29-W35.

224. Medema, M. H.; de, R. T.; Moore, B. S. Mining genomes to illuminate the specialized chemistry of life. *Nat. Rev. Genet.* **2021,** *22*, 553-571.

225. Floss, H. G. Combinatorial biosynthesis--potential and problems. *J. Biotechnol.* **2006,** *124* (1), 242-257.

226. Liu, K. I.; Ramli, M. N.; Woo, C. W.; Wang, Y.; Zhao, T.; Zhang, X.; Yim, G. R.; Chong, B. Y.; Gowher, A.; Chua, M. Z.; Jung, J.; Lee, J. H.; Tan, M. H. A chemical-inducible CRISPR-Cas9 system for rapid control of genome editing. *Nat. Chem Biol.* **2016,** *12* (11), 980-987.

227. Lubertozzi, D.; Keasling, J. D. Marker and promoter effects on heterologous expression in *Aspergillus nidulans*. *Appl. Microbiol. Biotechnol.* **2006,** *72* (5), 1014-1023.

228. Chater, K. F. Genetic regulation of secondary metabolic pathways in *Streptomyces*. *Ciba Found. Symp.* **1992,** *171*, 144-156.

229. Zhang, J. J.; Tang, X.; Moore, B. S. Genetic platforms for heterologous expression of microbial natural products. *Nat. Prod. Rep.* **2019,** *36* (9), 1313-1332.

230. Ongley, S. E.; Bian, X.; Neilan, B. A.; Muller, R. Recent advances in the heterologous expression of microbial natural product biosynthetic pathways. *Nat. Prod. Rep.* **2013,** *30* (8), 1121-1138.

231. Itoh, T.; Tokunaga, K.; Matsuda, Y.; Fujii, I.; Abe, I.; Ebizuka, Y.; Kushiro, T. Reconstitution of a fungal meroterpenoid biosynthesis reveals the involvement of a novel family of terpene cyclases. *Nat. Chem.* **2010,** *2* (10), 858-864.

232. Malit, J. J. L.; Liu, W.; Cheng, A.; Saha, S.; Liu, L. L.; Qian, P. Y. Global genome mining reveals a cytochrome P450-catalyzed cyclization of crownlike cyclodipeptides with neuroprotective activity. *Org. Lett.* **2021,** *23* (17), 6601-6605.

233. Li, L.; Liu, X.; Jiang, W.; Lu, Y. Recent advances in synthetic biology approaches to optimize production of bioactive natural products in actinobacteria. *Front Microbiol.* **2019,** *10*, 2467.

234. Siddiqui, M. S.; Thodey, K.; Trenchard, I.; Smolke, C. D. Advancing secondary metabolite biosynthesis in yeast with synthetic biology tools. *FEMS Yeast Res.* **2012,** *12* (2), 144-170.

235. Sánchez, C.; Zhu, L.; Braña, A. F.; Salas, A. P.; Rohr, J.; Méndez, C.; Salas, J. A. Combinatorial biosynthesis of antitumor indolocarbazole compounds. *Proc. Natl. Acad. Sci. U. S. A* **2005,** *102* (2), 461-466.

236. Marchand, J. A.; Neugebauer, M. E.; Ing, M. C.; Lin, C. I.; Pelton, J. G.; Chang, M. C. Y. Discovery of a pathway for terminal-alkyne amino acid biosynthesis. *Nature* **2019**.

237. Weist, S.; Süssmuth, R. D. Mutational biosynthesis--a tool for the generation of structural diversity in the biosynthesis of antibiotics. *Appl. Microbiol. Biotechnol.* **2005,** *68* (2), 141-150.

238. Williams, G. J. Engineering polyketide synthases and nonribosomal peptide synthetases. *Curr. Opin. Struct. Biol.* **2013,** *23* (4), 603-612.

239. Mori, T. Enzymatic studies on aromatic prenyltransferases. *J. Nat. Med.* **2020,** *74*, 501-502.

240. Li, S.-M. Prenylated indole derivatives from fungi: structure diversity, biological activities, biosynthesis and chemoenzymatic synthesis. *Nat. Prod. Rep.* **2010,** *27* (1), 57-78.

241. Fan, A.; Winkelblech, J.; Li, S.-M. Impacts and perspectives of prenyltransferases of the DMATS superfamily for use in biotechnology. *Appl. Microbiol. Biotechnol.* **2015,** *99* (18), 7399-7415.

242. Fan, A.; Zocher, G.; Stec, E.; Stehle, T.; Li, S.-M. Site-directed mutagenesis switching a dimethylallyl tryptophan synthase to a specific tyrosine *C3*-prenylating enzyme. *J. Biol. Chem.* **2015,** *290*, 1364-1373.

243. Zhao, W.; Fan, A.; Tarcz, S.; Zhou, K.; Yin, W. B.; Liu, X. Q.; Li, S.-M. Mutation on Gly115 and Tyr205 of the cyclic dipeptide *C2*-prenyltransferase FtmPT1 increases its catalytic activity toward hydroxynaphthalenes. *Appl. Microbiol. Biotechnol.* **2017**.

244. Liao, G.; Mai, P.; Fan, J.; Zocher, G.; Stehle, T.; Li, S.-M. Complete decoration of the indolyl residue in *cyclo*-L-Trp-L-Trp with geranyl moieties by using engineered dimethylallyl transferases. *Org. Lett.* **2018,** *20*, 7201-7205.

245. Xu, K.; Yang, C.; Xu, Y.; Li, D.; Bao, S.; Zou, Z.; Kang, F.; Tan, G.; Li, S.-M.; Yu, X. Selective geranylation of biflavonoids by *Aspergillus terreus* aromatic prenyltransferase (AtaPT). *Org. Biomol. Chem.* **2019,** *18* (1), 28-31.

246. Zhou, K.; Wunsch, C.; Dai, J.; Li, S.-M. *gem*-Diprenylation of acylphloroglucinols by a fungal prenyltransferase of the dimethylallyltryptophan synthase superfamily. *Org. Lett* **2017,** *19*, 388-391.

247. Fan, A.; Li, S.-M. One substrate - seven products with different prenylation positions in one-step reactions: prenyltransferases make it possible. *Adv. Synth. Catal.* **2013,** *355*, 2659-2666.

248. Liebhold, M.; Xie, X.; Li, S.-M. Breaking cyclic dipeptide prenyltransferase regioselectivity by unnatural alkyl donors. *Org. Lett.* **2013,** *15*, 3062-3065.

249. Horsman, M. E.; Hari, T. P.; Boddy, C. N. Polyketide synthase and non-ribosomal peptide synthetase thioesterase selectivity: logic gate or a victim of fate? *Nat. Prod. Rep.* **2016,** *33*, 183-202.

250. Gressler, M.; Zaehle, C.; Scherlach, K.; Hertweck, C.; Brock, M. Multifactorial induction of an orphan PKS-NRPS gene cluster in *Aspergillus terreus*. *Chem Biol.* **2011,** *18*, 198-209.

251. Tang, S.; Zhang, W.; Li, Z.; Li, H.; Geng, C.; Huang, X.; Lu, X. Discovery and characterization of a PKS-NRPS hybrid in *Aspergillus terreus* by genome mining. *J. Nat. Prod.* **2020,** *83* (2), 473-480.

252. Yin, W. B.; Chooi, Y. H.; Smith, A. R.; Cacho, R. A.; Hu, Y.; White, T. C.; Tang, Y. Discovery of cryptic polyketide metabolites from dermatophytes using heterologous expression in *Aspergillus nidulans*. *ACS Synth. Biol.* **2013**, *2* (11), 629-634.

253. Weber, V.; Coudert, P.; Duroux, E.; Leal, F.; Couquelet, J.; Madesclaire, M. Synthesis and in vitro studies of pyrone derivatives as scavengers of active oxygen species. *Arzneim. -Forsch.* **2001**, *51* (11), 877-884.

254. Lin, H. C.; Chiou, G.; Chooi, Y. H.; McMahon, T. C.; Xu, W.; Garg, N. K.; Tang, Y. Elucidation of the concise biosynthetic pathway of the communesin indole alkaloids. *Angew. Chem. Int. Ed Engl.* **2015**, *54*, 3004-3007.

255. Yazaki, K.; Sasaki, K.; Tsurumaru, Y. Prenylation of aromatic compounds, a key diversification of plant secondary metabolites. *Phytochemistry* **2009**, *70* (15-16), 1739-1745.

256. Uhlig, S.; Botha, C. J.; Vralstad, T.; Rolen, E.; Miles, C. O. Indole-diterpenes and ergot alkaloids in *Cynodon dactylon* (Bermuda Grass) infected with *Claviceps cynodontis* from an outbreak of tremors in cattle. *J. Agric. Food Chem.* **2009**, *57*, 11112-11119.

257. Ding, Y.; Wet, J. R.; Cavalcoli, J.; Li, S.; Greshock, T. J.; Miller, K. A.; Finefield, J. M.; Sunderhaus, J. D.; McAfoos, T. J.; Tsukamoto, S.; Williams, R. M.; Sherman, D. H. Genome-based characterization of two prenylation steps in the assembly of the stephacidin and notoamide anticancer agents in a marine-derived *Aspergillus* sp. *J. Am. Chem. Soc.* **2010**, *132* (36), 12733-12740.

258. Fraley, A. E.; Caddell, H. K.; Ye, Y.; Kelly, S. P.; Newmister, S. A.; Yu, F.; Williams, R. M.; Smith, J. L.; Houk, K. N.; Sherman, D. H. Molecular basis for spirocycle formation in the paraherquamide biosynthetic pathway. *J. Am. Chem. Soc.* **2020**, *142* (5), 2244-2252.

259. Knaus, H. G.; Mcmanus, O. B.; Lee, S. H.; Schmalhofer, W. A.; Garciacalvo, M.; Helms, L. M. H.; Sanchez, M.; Giangiacomo, K.; Reuben, J. P.; Smith, A. B.; Kaczorowski, G. J.; Garcia, M. L. Tremorgenic indole alkaloids potently inhibit smooth-muscle high-conductance calcium-activated potassium channels. *Biochemistry* **1994**, *33* (19), 5819-5828.

260. von Nussbaum, F. Stephacidin B-A new stage of complexity within prenylated indole alkaloids from fungi. *Angew. Chem. , Int. Ed. Engl.* **2003**, *42* (27), 3068-3071.

261. Zhang, Q.; Wang, S. Q.; Tang, H. Y.; Li, X. J.; Zhang, L.; Xiao, J.; Gao, Y. Q.; Zhang, A. L.; Gao, J. M. Potential allelopathic indole diketopiperazines produced by the plant endophytic *Aspergillus fumigatus* using the one strain-many compounds method. *J. Agric. Food Chem.* **2013**, *61* (47), 11447-11452.

262. Xu, W.; Gavia, D. J.; Tang, Y. Biosynthesis of fungal indole alkaloids. *Nat. Prod. Rep.* **2014**, *31* (10), 1474-1487.

263. Winkelblech, J.; Fan, A.; Li, S.-M. Prenyltransferases as key enzymes in primary and secondary metabolism. *Appl. Microbiol. Biotechnol.* **2015**, *99* (18), 7379-7397.

264. Nies, J.; Li, S.-M. Prenylation and dehydrogenation of a *C2*-reversely prenylated diketopiperazine as a branching point in the biosynthesis of echinulin family alkaloids in *Aspergillus ruber*. *ACS Chem. Biol.* **2021,** *16*, 185-192.

265. Kuramochi, K.; Ohnishi, K.; Fujieda, S.; Nakajima, M.; Saitoh, Y.; Watanabe, N.; Takeuchi, T.; Nakazaki, A.; Sugawara, F.; Arai, T.; Kobayashi, S. Synthesis and biological activities of neoechinulin A derivatives: new aspects of structure-activity relationships for neoechinulin a. *Chem Pharm Bull (Tokyo)* **2008,** *56* (12), 1738-1743.

266. Talapatra, S. K.; Mandal, S. K.; Bhaumik, A.; Mukhopadhyay, S.; Kar, P.; Patra, A.; Talapatra, B. Echinulin, a novel cyclic dipeptide carrying a triprenylated indole moiety from an Anacardiaceae, a Cucurbitaceae and two Orchidaceae plants: detailed high resolution 2D-NMR and mass spectral studies. *J. Indian Chem. Soc.* **2001,** *78* (10-12), 773-777.

267. Winkelblech, J.; Li, S.-M. Biochemical investigations of two 6-DMATS enzymes from *Streptomyces* revealing novel features of L-tryptophan prenyltransferases. *Chembiochem.* **2014,** *15*, 1030-1039.

268. Fan, A.; Li, S.-M. Saturation mutagenesis on Arg244 of the tryptophan C4-prenyltransferase FgaPT2 leads to enhanced catalytic ability and different preferences for tryptophan-containing cyclic dipeptides. *Appl. Microbiol. Biotechnol.* **2016,** *100*, 5389-5399.

269. Yu, H.; Li, S.-M. Two cytochrome P450 enzymes from *Streptomyces* sp. NRRL S-1868 catalyze distinct dimerization of tryptophan-containing cyclodipeptides. *Org. Lett.* **2019,** *21*, 7094-7098.

270. Liu, J.; Xie, X.; Li, S.-M. Increasing cytochrome P450 enzyme diversity by identification of two distinct cyclodipeptide dimerases. *Chem. Commun.* **2020,** *56* (75), 11042-11045.

Statutory Declaration

Ich, Wen Li, versichere, dass ich meine Dissertation

„ Genomics-driven and biochemical approaches to expand the spectrum of natural products "

selbständig ohne unerlaubte Hilfe angefertigt und mich dabei keiner anderen als der von mir ausdrücklich bezeichneten Quellen bedient habe. Alle vollständig oder sinngemäß übernommenen Zitate sind als solche gekennzeichnet.

Die Dissertation wurde in der jetzigen oder einer ähnlichen Form noch bei keiner anderen Hochschule eingereicht und hat noch keinen sonstigen Prüfungszwecken gedient.

Marburg, den..........................

....
Wen Li

Acknowledgements

Curriculum Vitae

Personal Information

Name: Wen Li

Date of Birth: 10.08.1991

Place of Birth: Zhumadian, Henan Province, P. R. China

Nationality: Chinese

Address: Robert-Koch-Str. 4, 35037, Marburg

Email: liwen@staff.uni-marburg.de

Education ＆ Research

PhD candidate: 10.2018 － now

Philipps-University Marburg, Germany

Institute for Pharmaceutical Biology and Biotechnology

Thesis title: "Genomics-driven and biochemical approaches to expand the spectrum of natural products"

Supervisor: Prof. Dr. Shu-Ming Li

Master of Science: 09.2015 － 06.2018

Shandong University, China

Microbiology, School of Life Science/State Key Laboratory of Microbial Technology

Thesis title: "Genome mining of four rare actinomycete strains for discovery of novel natural products"

Supervisor: Prof. Dr. Yuemao Shen

Bachelor of Science: 09.2011 － 06.2015

Henan Normal University, China

Biology, School of Life Science

Thesis title: "Development of an efficient method for production of various nutrients for bean seedlings growth"

Supervisor: Prof. Dr. Taixia Wang

High School: 09.2008 － 06.2011

Suiping Nr. 1 Middle School, China